

**SUPRAMOLECULAR SYNTHESIS OF AROMATIC
POLYCARBOXYLIC ACIDS**

A THESIS
SUBMITTED FOR THE DEGREE OF
DOCTOR OF PHILOSOPHY
(IN CHEMISTRY)

TO
UNIVERSITY OF PUNE

BY
Mr. Manishkumar Ramesh Shimpi

Dr. V. R. Pedireddi
(RESEARCH GUIDE)

DIVISION OF ORGANIC CHEMISTRY
NATIONAL CHEMICAL LABORATORY
DR. HOMI BHABHA ROAD

PUNE-411008

JULY-2010

Dedicated

To

MY

Parents





राष्ट्रीय रासायनिक प्रयोगशाला

(वैज्ञानिक तथा औद्योगिक अनुसंधान परिषद)

डॉ. होमी भाभा मार्ग पुणे - 411 008. भारत

NATIONAL CHEMICAL LABORATORY

(Council of Scientific & Industrial Research)

Dr. Homi Bhabha Road, Pune - 411 008. India.



CERTIFICATE

This is to certify that the work presented in this thesis entitled "SUPRAMOLECULAR SYNTHESIS OF AROMATIC POLYCARBOXYLIC ACIDS" submitted by Mr. Manishkumar R. Shimpi, has been carried out by the candidate at National Chemical Laboratory, Pune, India, under my supervision. Such materials as obtained from other sources have been duly acknowledged in the thesis. This work is original and has not been submitted for any other degree or diploma of this or any other university.

July 2010

Pune

V. R. Pedireddi

Dr. V. R. Pedireddi



Communication
Channels

+91-20-2590 2000
+91-20-2590 (DID)

FAX

+91-20-2590 2601(DIR)
+91-20-2590 2660 (COA)

WEBSITE

www.ncl-india.org

CANDIDATE'S DECLARATION

I hereby declare that the research work presented in the thesis entitled **“SUPRAMOLECULAR SYNTHESIS OF AROMATIC POLYCARBOXYLIC ACIDS”** was carried out by me at the National Chemical Laboratory, Pune, India, under the supervision of **Dr. V. R. Pedireddi**, Scientist, Division of Organic Chemistry, National Chemical Laboratory, Pune, India and submitted for the degree of Doctor of Philosophy in Chemistry to the University of Pune. This work is original and has not been submitted in part or full by me for any other degree or diploma of this or any other university.

July 2010
Pune

MANISHKUMAR R. SHIMPI

Acknowledgements

With deep sense of gratitude and profound respect, I express my sincere thanks to my mentor, Prof. V. R. Pedireddi for his inspiring guidance and constant encouragement throughout my Ph.D. He has been my source of inspiration in many aspects. I have been able to learn many things from him and consider my association with him a rewarding experience.

It is my privilege to thank Dr. K. N. Ganesh, former Head of the Division of Organic Chemistry, NCL, and currently director, IISER, Pune, for his constant support and encouragement during the progress of this work. I take this opportunity to thank Dr. Ganesh Pandey, for his continued support as present Head of the Division.

I thank Dr. S. Sivaram, Director NCL, Dr. B. D. Kulkarni, Deputy Director for giving infrastructure facilities and DST, CSIR, New Delhi for financial support.

My heartfelt thanks to Dr. C. V. V. Sathyanarayana for his assistance in powder X-ray diffraction analysis. I also thank Dr. Ramana, Dr. Srinivas Hotha, Dr. P. A. Joy, Dr. Avinash Kumbhar and Dr. C. G. Suresh for fruitful scientific discussions and support in many aspects.

I am grateful to Dr. Mohan Bhadbhade, Dr. Mrs. Vedavathi Puranik, Dr. Rajesh Gonnade and Dr. Manoj for their assistance in the single crystal X-ray diffraction. I would like to thank Prof. Udai Singh, Roorkee and Dr. E. Suresh, Bhavnagar, for his assistance in the collection of X-ray diffraction data.

My sincere thanks go to Prof. Judith Howard, University of Durham, for her invaluable contribution by supporting to visit University of Durham and also for granting to attend BCA/CCG 11th Intensive Course in X-ray Structure Analysis.

I am very much thankful to Prof. Willam Cleg, Prof. Peter Main, Dr. Claire Wilson, and Dr. Lehman the organizers of the BCA/CCG 11th Intensive Course-2007 for their support and wonderful hospitality during my visit to Durham.

I wish to thank my friendly and cooperative labmates, Prakash, Kapil, Sunil, Seetha, Marivel, Sathya, Amit, Deepika, Shreeja, Parul, Vandana, Yogesh, Ketaki, Manish, Nagarajan and Prince for their help in various capacities and providing me with an excellent working ambience.

I am thankful to all the teachers and lecturers, who taught me throughout my career. My sincere thanks to Bhadane, Dr. Nandini, Udavant, Dr. Depak Agrwal, Phathan, Dr. Nimablker, Dr. Talware, Dr. Khoshe and Dr. Bhavsar who ignited my interest in chemistry through excellent chemistry lectures.

It gives me great pleasure to thank my beloved parents, for their love, tremendous patience, trust and encouragement during many years of studies. They have been my constant source of strength and have brought a great deal of happiness to my life.

Special thank to my wife, Mayura who has provided me with that extra bit of inspiration when I really needed it.

Special thanks to my brother Vickey, elder sister Deepali, brother-in-law Satish Jiju, younger sister Monali, brother-in-law, Nitin pant and nephews; Mau, Trisha, and Soham (Love kids), grandmother and all my family members; for their expectations and hope, that kept me awake all along.

I would like to thank my parents-in-law, sister-in-law, Neha for their expectations and hope, that kept me awake all along.

I thank all my friends Pramod, Jayesh, Pradeep Chadrashkekhar, Deepak Gupta, Deepesh, Prashant, Rakesh, Rahul, Dharmesh Shah, Dyneshwar Deva, Bhavin, Sujata, Kavita, Jasmine, Parul, Harishchandra, Sachin Badgujar, Sachin, Umesh, Arvind, Vijay, Vishweshwar, Tushar, Tukarm, Swapnil Shimpi, Santosh Kadam, Vishwas, Swaroop, Rajendrea, Ashpaq Suleman, Abasheb, Manmat Patil, Sachin Malwadkar, Sudhir, Kalpesh Rana, Tanpreet and Gaurao for their cheerful environment.

The blessings and best wishes of my parents keep me active throughout my life. They made me what I am and I owe everything to them. Dedicating this thesis to them is a minor recognition for their invaluable support and encouragement.

I thank all of you once again for your kind support and cooperation.

Manishkumar

CONTENTS

Chapter 1

Dynamic supramolecular chemistry

1.1. Modern interdisciplinary organic chemistry	2
1.2. Intermolecular interactions	4
1.2.1. The hydrogen bond is the interaction of choice	5
1.2.2. Characterization of hydrogen-bonded supramolecular assemblies	9
1.2.3. Describing hydrogen-bonded motifs: Graph set	10
1.3. Self-assembly	11
1.4. Molecular recognition	13
1.5. Supramolecular synthesis	14
1.6. Carboxyl group in supramolecular synthesis	15
1.7. Metal coordination assemblies	20
1.8. Potential applications of organic and metal-organic assemblies	23
1.8.1. Photodimerization reactions	23
1.8.2. Pharmaceutical co-crystallization	26
1.8.3. Gas storage materials	28
1.8.4. Dynamic frameworks	32
1.8.5. Porous frameworks as a catalyst	36
1.9. References	38

Chapter 2

Molecular recognition studies of benzenepentacarboxylic acid with some azadonors

2.1. Introduction	51
2.2. Molecular complexes of 1,2,3,4,5-benzenepentacarboxylic acid (BPC)	55
2.2.1. Molecular complex of BPC and bpy (1a)	56
2.2.2. Molecular complex of BPC and bpyea (1b)	60
2.2.3. Molecular complex of BPC and bpyee (1c)	64
2.2.4. Molecular complex of BPC and dabco (1d)	67
2.2.5. Molecular complex of BPC and 110phe (1e)	69
2.2.6. Molecular complex of BPC and 47phe (1f)	72
2.2.7. Molecular complex of BPC and bpy (1g)	76
2.2.8. Molecular complex of BPC and 47phe (1h)	79
2.3. Conclusions	83

2.4. Experimental section	84
2.5. References	92

Chapter 3

Molecular adducts of benzenehexacarboxylic acid (mellitic acid) with various aza-donor compounds

3.1. Introduction	97
3.2. Supramolecular assemblies of mellitic acid (MA)	100
3.3. Molecular adducts of mellitic acid (MA)	102
3.3.1. Solid state structure of MA and bpy (1a)	103
3.3.2. Molecular complex of MA and bpyea (1b)	105
3.3.3. Molecular complex of MA and bpyee (1c)	108
3.3.4. Molecular complex of MA and bpypa (1d)	110
3.3.5. Molecular complex of MA and dabco (1e)	112
3.3.6. Molecular complex of MA and 47phe (1f)	114
3.3.7. Molecular complex of MA and bpy (1g)	117
3.4. Conclusions	120
3.5. Experimental section	121
3.6. References	127

Chapter 4

Coordination polymers of benzene penta and hexa carboxylic acids

4.1 Introduction	133
4.2.1 Coordination complex of Co(II) with BPC and bpy (1a)	136
4.2.2 Coordination complex of Cu(II) with BPC and bpy (1b)	138
4.2.3 Coordination complex of Cd(II) with BPC and bpy (1c)	141
4.2.4 Coordination polymer of Cu(II) with BPC and bpyea (1d)	144
4.2.5 Coordination polymer of Cd(II) with BPC and bpyea (1e)	146
4.3 Coordination assemblies of mellitic acid (MA)	149
4.3.1 Coordination polymer of Cu(II) with MA and bpy (2a)	150
4.3.2 Coordination assemblies of Cu(II) with MA and bpypa (2b)	152
4.4 Conclusion	156
4.5 Experimental section	158
4.6 References	167

The research work reported in the thesis entitled “**Supramolecular Synthesis of Aromatic Polycarboxylic Acids**” was carried out with a focus to evaluate the efficacy of the hydrogen bond in the creation of organic molecular complexes as well as coordination polymers, through ensembling of molecules possessing polycarboxylic groups and conformation flexibility. The thesis has been compiled into four chapters as describe below. Chapter-1 gives an introduction to the contemporary research in the areas of supramolecular chemistry, with an emphasis on the organic assemblies such as host-guest complexes and pharmaceutical co-crystallization as well as metal-organic frameworks. Chapter-2 describes molecular recognition studies of benzenepentacarboxylic acid with some aza-donor compounds through various types of hydrogen bonds. Similarly, molecular adducts of benzenehexacarboxylic acid (mellitic acid) with various aza-donor compounds, obtained by co-crystallization techniques, are described in Chapter-3. Finally, in Chapter-4, synthesis of various coordination polymers of benzene penta and hexa carboxylic acids with different transition metal ions, in conjunction with various aza-donor compounds, is illustrated through several metal-organic hybrid assemblies.

Chapter- 1

Lehn defined supramolecular chemistry as “*the chemistry of the intermolecular bond*”. Just as molecules are due to the connectivity between the atoms by covalent bonds, supramolecular compounds are formed by linking molecules through intermolecular interactions. Various types of interactions may be distinguished, that shows different degree of strength, directionality such as metal ion coordination, electrostatic forces, hydrogen bonding, van der Waals interactions, donor-acceptor interactions etc. Their strength ranging from strong to very strong for metal ion coordination, to weak or moderate as in hydrogen bonds. The ability of interactions with respective desired chemical design, specificity and molecular switching opened up the development of new molecular materials through self-assembly and molecular recognition. It has emerged as a powerful tool for the development of target assemblies of desired architectures, with tailor made properties that can be utilized in

different applications. For example, synthesis of non-centrosymmetric materials for non-linear optical properties, host-guest type lattices for catalytical studies, preparation of pharmaceutical co-crystals for the evaluation of bioactivity in different types of formulations, for altering physical properties etc.

A different approach for the formation of supramolecular species via spontaneous self-assembly of precursor building blocks is the use of metals and dative bonding. The coordination polymers, with channels in their three-dimensional structures, provide reactive sites within the nanoporous environment. Among a number of chemical properties sought in the nanoporous environment of the chiral coordination assemblies, size, shape and enantioselective separation and catalytic properties have proven to be the most challenging and exciting. Elaborate discussion of the contemporary research work in these areas is presented in Chapter-1.

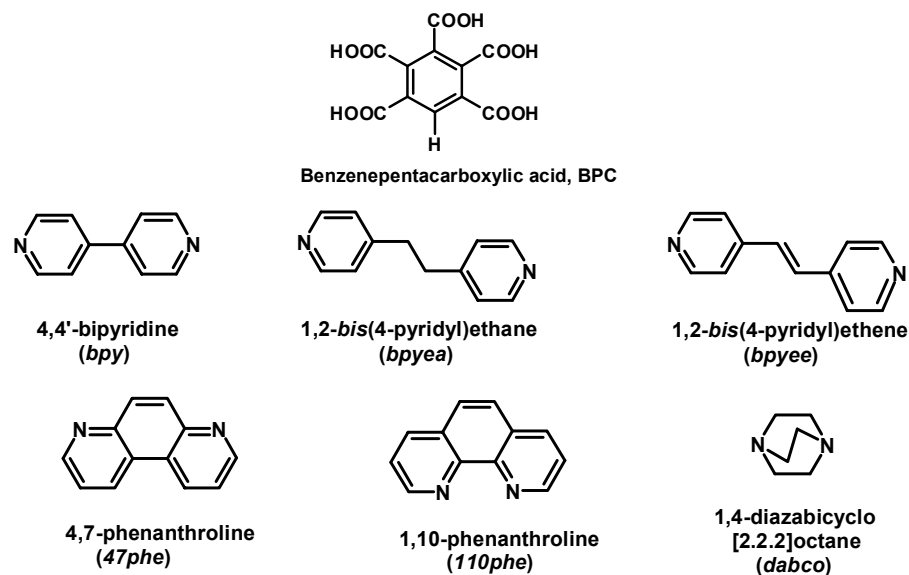
Chapter- 2

In Chapter 2, molecular recognition studies of benzenepentacarboxylic acid (**BPC**) with some aza-donor molecules are explored, in the solid state, with a focus to evaluate its hydrogen bond capabilities towards creating exotic architectures.

Carboxylic acids are well-known to form robust cyclic dimer as well as catemer motifs, and also either O–H \cdots N or O–H \cdots N/C–H \cdots O pair wise hydrogen bonds with several aza-donor compounds. Taking into account the availability of maximum number of carboxylic groups and the conformational flexibility, we are interested to explore the utilization of **BPC** with some aza-donor compounds (as illustrated in Chart 1) for the creation of supramolecular assemblies of excellence.

All the complexes were characterized by single crystal X-ray diffraction method. Structural analysis reveals that **BPC** form several of supramolecular networks such as zeolite-type network, host guest assemblies, ladders, planner sheets etc. depending upon the nature of aza-donor molecules, as exemplified below for some molecular complexes.

Chart 1



Molecular complexes of **BPC** with aza-donor molecules like 4,4'-bipyridine and 1,2-*bis*(4-pyridyl)ethene yield sheet structures in two dimensional arrangement, which are stacked in three dimensions (See Figure 1).

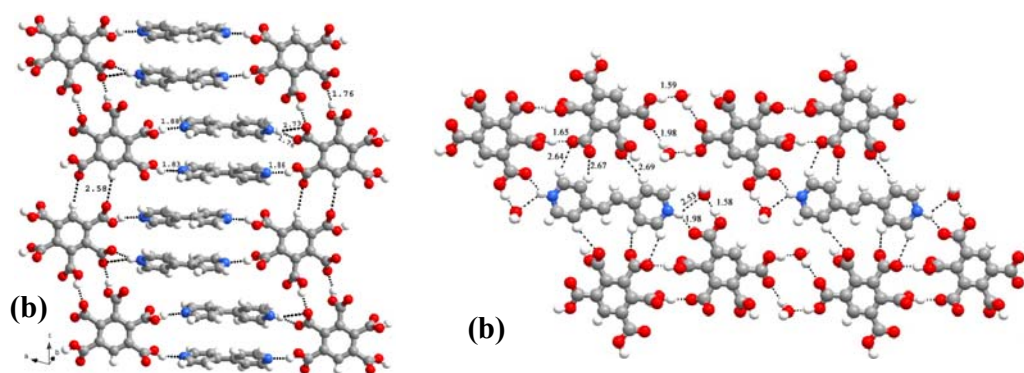


Figure 1. (a) Formation of ladder like structure in the complex of **BPC** and 4,4'-bipyridine.(b) Arrangement of molecules in a typical layer observed in the crystal structures of **BPC** and 1,2-*bis*(4-pyridyl)ethene.

In a typical layer of the complex between **BPC** and 4,4'-bipyridine adjacent **BPC** molecules are held together by O–H···O hydrogen bonds, form rods type geometry, which are being separated by 4,4'-bipyridine moiety, Thus, a ladder type

structure is formed as shown in Figure 1a. However, in the co-crystal of **BPC** and 1,2-*bis*(4-pyridyl)ethene, the **BPC** molecules forms infinite molecular tapes and 1,2-*bis*(4-pyridyl)ethene molecules are sandwiched in between the tapes as shown in Figure 1b.

In three-dimensional structure analysis of complex between **BPC** with 1,10-phenanthroline and 4,7-phenanthroline independently yielded a zeolite-type network with **BPC** molecules forming open frame network, with voids being filled by aza-donor molecules as shown in Figure 2. In these assemblies, water molecules play a crucial role in the formation of cavities in accordance with the dimension of the guest molecule. A detailed analysis of the structural features of these complexes would be discussed in Chapter 2.

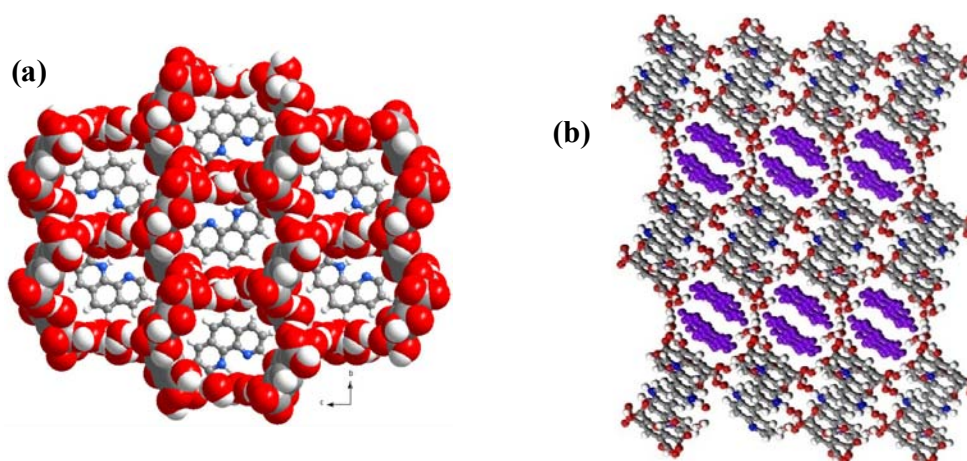
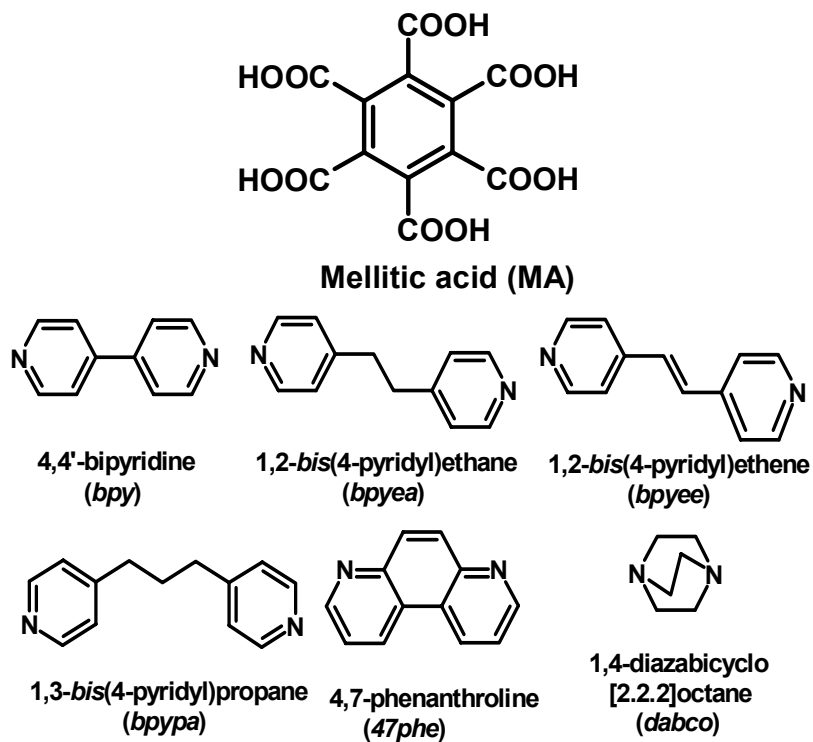


Figure 2. Three dimensional arrangement observed in the molecular complex of **BPC** with (a) 1,10-phenanthroline. (b) 4,7-phenanthroline, in the form of zeolite-type assembly.

Chapter- 3

Systematic literature search of chemical and crystallographic databases reveals that apart from benzenepentacarboxylic acid (**BPC**), its higher analogue benzenhexacarboxylic acid (mellitic acid, **MA**) is also not been well explored in molecular recognition studies, especially for the creation of exotic architectures. Thus, we have co-crystallized **MA** with various aza-donor molecules, as illustrate in Chart 2, anticipating supramolecular assemblies with exotic architectures.

Chart 2



Structure elucidation of mellitic acid (MA) and its co-crystals with 1,2-bis(4-pyridyl)ethane and 1,2-bis(4-pyridyl)ethane reveals stacked sheet structures in three-dimensional arrangement. The packing arrangements of molecules are shown Figure 3. In each sheet, either MA or aza-donor molecules are only present, thus, yielding only homomeric interactions.

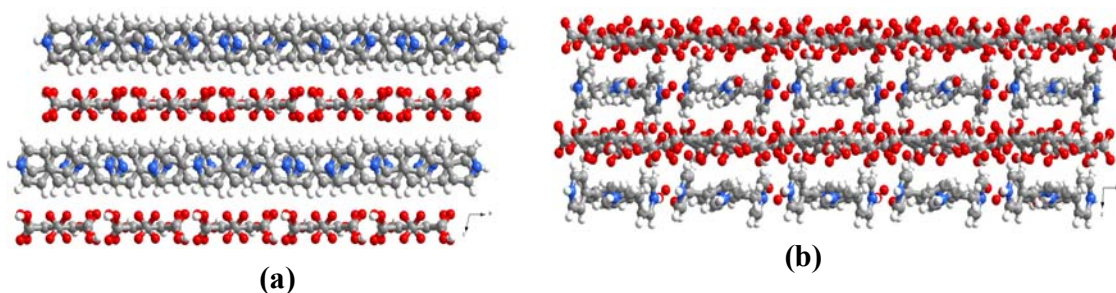


Figure 3. Three-dimension arrangements of sheets of MA are separated by sheets of aza-donor molecules. Aza-donor molecules, 1,2-bis(4-pyridyl)ethene and 1,2-bis(4-pyridyl)ethane respectively in (a) and (b).

Molecular adducts of MA and aza-donor compounds like 1,4-biazadicyclo[2.2.2]octane and 4,7-phenanthroline yield zeolite-type architectures as shown in Figure 4. Packing analysis reveals that complexes are host-guest type, in which host is being formed by MA and water molecules, while aza-donor molecules are being inserted as guest species, in the space available within the host lattice, as shown in Figure 4.

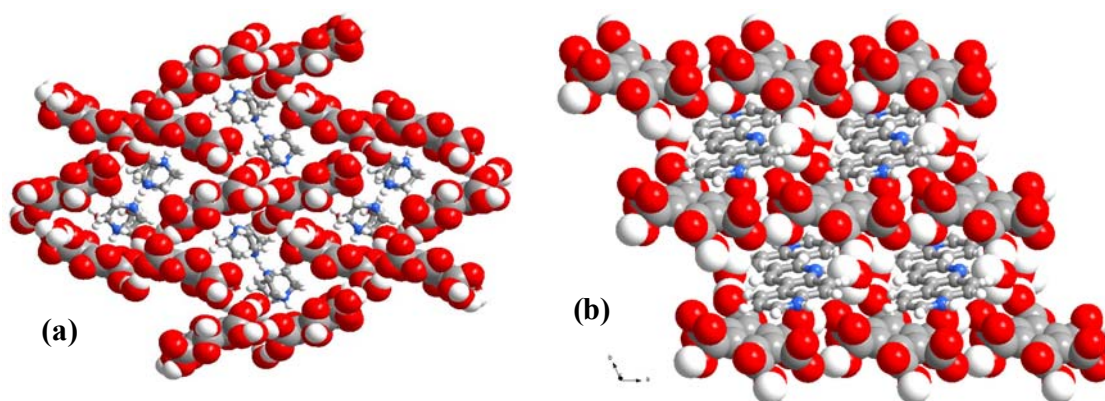


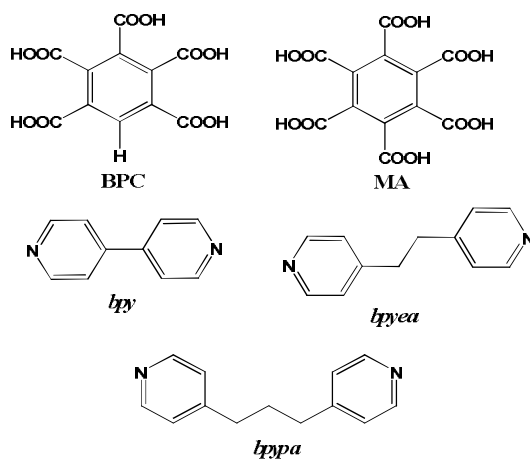
Figure 4. Host-guest complexes of MA with (a) 1,4-diazabicyclo[2.2.2]octane and (b) 4,7-phenanthroline.

Chapter- 4

While studies on coordination polymers have been largely focused on synthesizing the open framework structures, by making use of the coordinate bonds, formed between metal species like cobalt, copper and cadmium etc., and organic ligands, such as tri and tetra substituted benzene carboxylic acids, only a limited examples are known in the literature about the collective effect of intermolecular interactions and coordination mode of the ligands on the architecture of the resulting supramolecular assembly. For this purpose, to explore the impact of intermolecular interactions in coordination polymers, penta and hexa aromatic carboxylic acids have been chosen as prime substrates to obtain coordination polymers with different metal species. The assemblies, thus, obtained are discussed in Chapter 4, dividing it into two sections depending upon the polycarboxylic acid used.

The schematic diagram in Chart 3 shows the typical network structure of coordination polymers formed by M(II) [M= Co(II), Cu(II) and Cd(II)] species with **BPC** and **MA**, in the presence of aza-donor compounds 4,4'-bipyridine, 1,2-bis(4-pyridyl)ethane and 1,3-bis(4-pyridyl)propane.

Chart 3



1) Coordination polymers of benzenepentacarboxylic acid (BPC)

Coordination polymers of benzenepentacarboxylic acid with cobalt, copper and cadmium salts in the presence of various aza-donor molecules (Chart 1) have been prepared by either hydrothermal or slow evaporation methods.

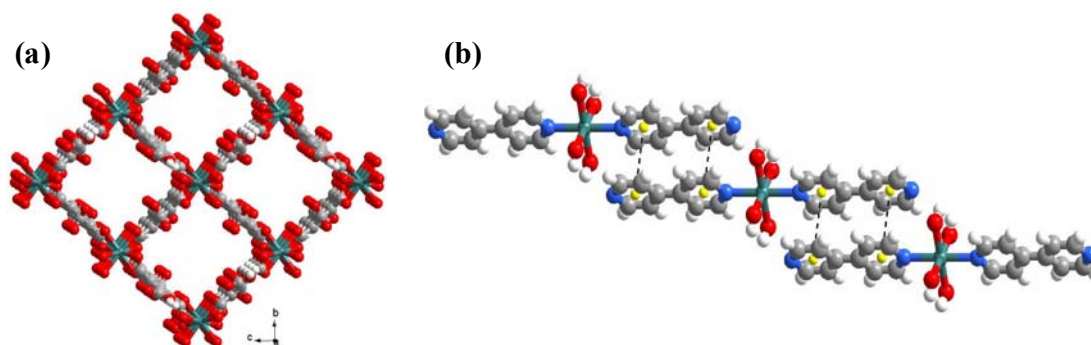


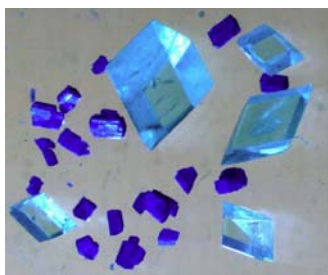
Figure 5. (a) A Three-dimension view of host ($\text{Cd}(\text{C}_{11}\text{H}_3\text{O}_{10})_4$) network along *a* axis. (b) Arrangement of guest species, $\text{Cd}(\text{C}_{10}\text{H}_8\text{N}_2)_2 \cdot 4\text{H}_2\text{O}$ molecules within channels interacting through $\pi \cdots \pi$ stacking.

The hydrothermal reaction of **BPC**, 4,4'-bipyridine and Cd(II) ions gave rise to a novel supramolecular host-guest framework, by two types of coordination motifs.

A three-dimensional architecture that comprises interesting square grid host networks formed by **BPC** and Cd(II), through dative bonds has been filled by Cd-4,4'-bipyridine polymer chains, as shown in Figure 5.

Coordination polymers of benzenhexacarboxylic acid (Mellitic acid, MA)

Two different types of crystals, differentiated by color (Prussian and Royal blue), as shown below, were obtained concomitantly, upon dissolving mellitic acid, 1,3-*bis*(4-pyridyl)propane and Cu(II) in water and evaporating the solution at ambient conditions. While both the crystals are coordination complexes of Cu(II), the compositions and coordination geometry are different in both the types of crystals.



Royal blue crystals, has an hexa coordination around each Cu(II) with two **MA** molecules, as monodentate ligands, and four coordinate water molecules, resulting in an octahedral geometry. Such species gave coordination sheets, which are arranged in three-dimensions separated by sheets of 1,3-*bis*(4-pyridyl)propane molecules (see Figure 6a). However, in Prussian blue crystals, Cu(II) form two different coordination spheres, octahedral and square-planar, through hexa and tetra coordination of mellitic acid moieties to metal centre. The two different coordination spheres lie in three-dimensional arrangement in alternate layers such that each of Cu(II) hexa hydrate, indeed, joins the tetra coordinated sheets through O–H···O

hydrogen bonds, creating cavities, which are in turn align to yield huge channels of dimension $16 \times 30 \text{ \AA}^2$, as shown in Figure 6b, which are being occupied by 1,3-*bis*(4-pyridyl)propane molecules and a cluster of water molecules.

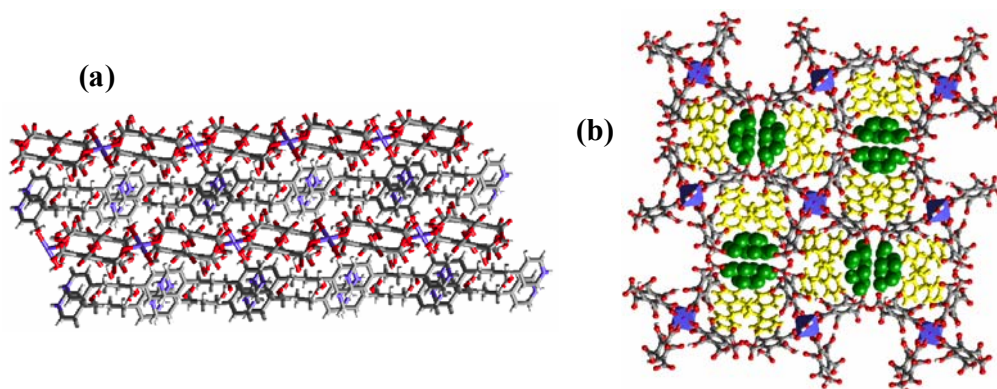


Figure 6. (a) Three-dimensional arrangement of coordination sheets of mellitic acid and Cu(II) separated by sheets of 1,3-*bis*(4-pyridyl)propane molecules observed in Royal blue crystals. (b) Arrangement of guest species, 1,3-*bis*(4-pyridyl)propane and water molecules within the channels observed in Prussian blue crystals.

Thus, it is interesting to note that in both the complexes, 1,3-*bis*(4-pyridyl)propane molecules do not form any coordinate bond with Cu(II). A detailed discussion of these assemblies would be presented in this section.

References:

- [1] a) J. -M. Lehn, *Supramolecular Chemistry: Concepts and Perspectives*; VCH: Weinheim, **1995**. b) S. R. Byrn; R. R. Pfeiffer; J. G. Stowell; *Solid state chemistry of Drugs, 2nd Edition, SSCI Inc.*, West Lafayette, Indiana, **1999**. c) J. W. Steed, J. L. Atwood, *Supramolecular Chemistry*, VCH, Weinheim, **1995**. d) G. R. Desiraju, *Crystal Engineering: The Design of Organic Solids Elsevier: Amsterdam* **1989**. e) MacGillivray, L. R.; Papaefstathiou, G. S.; Friscic, T.; Hamilton, T. D.; Bucar, D. K.; Chu, Q.; Varshney, D. B.; Georgiev, I. G. *Acc. Chem. Res.* **2008**, *41*, 280–291 f) Perumalla, S. R.; Suresh, E.; Pedireddi, V. R. *Angew. Chem., Int. Ed.* **2005**, *44*, 7752–7757.

- [2] a) Etter, M. C. *Acc. Chem. Res.* **1990**, *23*, 120–126. b) Duchamp, D. J.; Marsh, R. E. *Acta Crystallogr.* **1969**, *B25*, 5–19. c) Kolotuchin, S. V.; Rhiessen, P. A.; Fenlon, E. E.; Wilson, S. R.; Loweth, C. J.; Zimmerman, S. C. *Chem. Eur. J.*, **1999**, *5*, 2537–2547. d) e) Marivel, S.; Shimpi, M. R.; Pedireddi, V. R. *Cryst. Growth Des.* **2007**, *7*, 1791–1796. f) Leiserowitz, L. *Acta Cryst.* **1976**, *B32*, 775–802. g) Shan, N.; Jones, W. *Tetrahedron Lett.*, **2003**, *44*, 3687–3689.
- [3] a) Arora, K. K.; Pedireddi, V. R. *J. Org. Chem.* **2003**, *68*, 9177–9185. b) Shimpi, M. R.; SeethaLekshmi, N.; Pedireddi, V. R. *Cryst. Growth Des.* **2007**, *7*, 1958–1963. c) Biradha, K.; Zaworotko, M. J. *Crystal Engineering*, **1998**, *1*, 67–78. d) Shattock, T. R.; Vishweshwar, P.; Wang, Z.; Zaworotko, M. J. *Cryst. Growth Des.*, **2005**, *5*, 2046–2049. e) Delori, A.; Suresh, E.; Pedireddi, V. R. *Chem. Eur. J.* **2008**, *14*, 6967–6977.
- [4] a) Zhao, X.; Xiao, B.; Fletcher, A. J.; Thomas, K. M.; Bradshaw, D.; Rosseinsky, M. J. *Science*, **2004**, *306*, 1012–1015. b) Pedireddi, V. R.; Shimpi, M. R.; Yakhmi, J. V. *Micromol. Symp.* **2006**, *241*, 83–87. c) Kitagawa, S.; Kitaura, R.; Noro, S. *Angew. Chem., Int. Ed.* **2004**, *43*, 2334–2375. d) Yaghi, O. M.; Li, H. *J. Am. Chem. Soc.* **1996**, *118*, 295–296. f) Rowsell, J. L. C.; Yaghi, O. M. *Angew. Chem., Int. Ed.* **2005**, *44*, 4670–4679.

CHAPTER 1

Dynamic Supramolecular Chemistry

“The chemist finds illustration, inspiration, and stimulation in natural processes, as well as confidence and reassurance since they are proof that such highly complex systems can indeed be achieved on the basis of molecular components.”

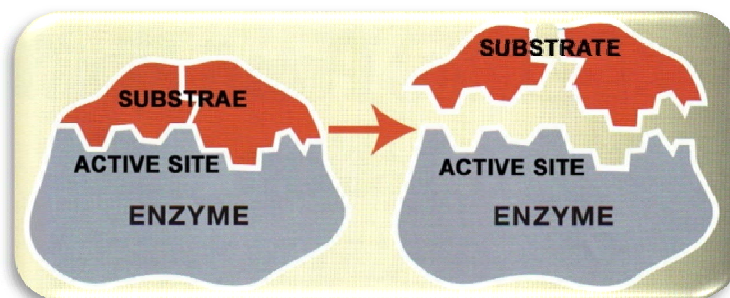
Jean-Marie Lehn, 1995

1.1. Modern interdisciplinary organic chemistry

Organic chemistry, traditionally known for the synthesis of exotic molecules by challenging and innovative methods of functional group transformations expanded now into various frontier areas of research excellence. Of which, one of the contemporary themes is the organic materials for the sustainability. The current advancements in this directions have transformed the materials of everyday life, but this is merely a glimpse of tiny subset of a materials in the form of molecular devices that conduct electricity, self-reproducing organic compounds, singly and multiply configurable solid-state switching devices that are based upon electrochemically switchable molecular and supramolecular systems, molecules that work (nano-engineering), and even molecules that think may transform our world in ways not yet imagined, etc.

On the other hand, the recent advancements in science and technology indeed alarm the necessity of new approaches for the rapid handling of vast amounts of information at the molecular scale. To meet such challenges, Richard Feynman¹ proposed a “*bottom-up*” approach, starting from atoms and molecules, as early as in the 1960s, which originated of *supramolecular chemistry*²– a discipline that exploits fundamental concepts such as self-assembly,³ self-organization and self-replication that are central to the natural functions, establishing on union of chemistry, biology and physics. In fact, Emil Fischer laid a foundation for the of chemistry-biology-physics interfaces, with the narration of enzyme-substrate interaction as lock and key process⁴, as illustrated below pictorially. This elegant mechanism is indeed the focal

point for the evolution of new frontier area of research, based on two principles, molecular recognition and supramolecular function.⁵




An organic molecule is usually understood as a stable collection of atoms, connected by well defined network of covalent bonds. Development of different strategies and methods for constructing these networks is the central focus in many frontier research areas of organic chemistry. However, in recent times for the construction of large and intricate, yet highly ordered, functioning materials of molecular and supramolecular entities, noncovalent synthesis has become integral part of the organic synthesis.


The term supramolecular chemistry was coined in 1969 by Nobel Laureate Jean-Marie Lehn in his study of inclusion compounds and cryptands⁶ along with other Nobel Laureates Charles Pedersen, Donald Cram. Lehn defined supramolecular chemistry as “*the chemistry of the intermolecular bond*”. Just as the molecules are built by connecting atoms with covalent bonds, supramolecular compounds are built by linking molecules with intermolecular interactions. If the utilization of intermolecular interactions is taken as the paradigm of supramolecular chemistry, and periodicity as the paradigm of the crystalline state, the exploitation of periodically distributed intermolecular interactions is the paradigm of crystal engineering. On this

basis, molecular crystals can be viewed as periodic supermolecules, *solid supermolecules*, in which approximately Avogadro's number of molecules interact via a plethora of noncovalent interactions which generate *collective* physical and chemical properties via self-recognition and self-organization.

1.2. Intermolecular interactions

Knowledge of the various types of intermolecular interactions involved in supramolecular assembly is, of course, of fundamental importance to the design of new supramolecular systems; it is also necessary for understanding the structural interplays that control the assembly of known systems both in the solid state and in solution. In broad terms, interactions may be considered to fall into two main classes:

 **Short-range** - these are mainly of the coulombic and exchange-type that include also covalent bonds and result from orbital overlap. They can be attractive or repulsive and in particular instances may represent the strongest interactions present in a molecular system.

 **Long-range** - these consist of those interactions that may be broadly characterized as being proportional to internuclear distance; these include electrostatic (including hydrogen bonding), π - π interactions and van der Waals forces. Long-range interactions are those that contribute primarily towards supramolecular complexation.

The understanding of intermolecular interactions is as important to supramolecular chemistry as the understanding of covalent bond to molecular chemistry. This novel synthetic approach, also referred in the literature as noncovalent synthesis/supramolecular synthesis is well explored with applications in various

disciplines (such as in biology, physics, materials preparation) making supramolecular synthesis as an interdisciplinary area of research.⁷ The progress in the last several decades demonstrate that noncovalent interactions have an enormous potential for the construction of chemical structures exhibiting a high degree of structural complexity. Various types of interactions may be distinguished, that shows different degree of strength, directionality, metal ion coordination, electrostatic forces, hydrogen bonding, van der Waals interactions, donor-acceptor interactions etc., depending upon the strength. Hydrogen bonding with a moderate strength compared to covalent and coordinate bonds has been described as the ‘master key interaction in supramolecular chemistry’,⁸ and systematically utilized in crystal engineering⁹ studies.

1.2.1. The hydrogen bond is the interaction of choice

Weak interactions between molecules containing hydroxyl groups were noted as early as in 1892 by Nernst. And also, Werner highlighted the weak interactions in his concept of “Nebenvaleanz” (minor valence), which was in fact a proper description of the phenomenon of hydrogen bonding. Based on the fact that hydrogen atom is the center of weak interactions, Bernal and Huggins proposed the actual term ‘hydrogen bond’, which has become generally adopted to describe this phenomenon. Since then, H-bonding interactions fascinate the researchers from all the sections of science spectrum.¹⁰

Hydrogen bonds can be considered to represent a special type of electrostatic interaction and impart special properties to the systems. The properties of the various polymorphic forms of ice, resulting from hydrogen bond aggregation of water

molecules, are different from those of an isolated water molecule in the vapor phase, which, in turn, is different from those of liquid water. In fact, even the morphology is predominantly being influenced by noncovalent interactions as it could be observed in the snowflakes shown in Figure 1.1

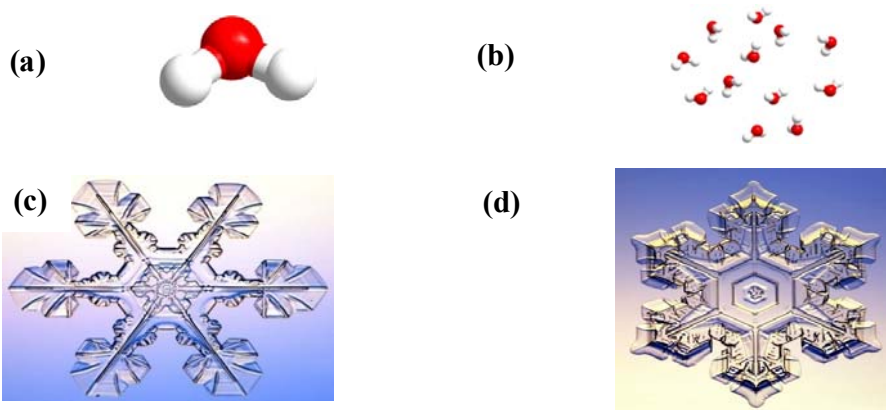


Figure 1.1. Ball and stick representation of (a) A water molecule and (b) aggregated water molecules. (c) and (d) the elegant supramolecular arrangement of water molecules via O–H···O hydrogen bond in a snowflake.

In recent times, with the growing interest in the studies of understanding the nature of noncovalent interactions, in detail, hydrogen bonds have been addressed so much, taken into account mainly the bonding parameters. The modern definition, thus, in circulation is an attractive interaction between a proton donor and a proton acceptor. In this direction, Pimentel and McClellan defined hydrogen bond as:

*A hydrogen bond exists between a functional group **D–H** and an atom or a group of atoms in the same or a different molecule when:*

(a) There is an evidence of bond formation (association or chelation).

*(b) There is an evidence that this new bond linking **D–H** and **A** specifically involves the hydrogen atom already bonded to **D**.*

Both the donor (**D**) and acceptor (**A**) atoms have electronegative character, with the proton involved in the hydrogen bond being shared between the electron pairs on **D** and **A**. Hydrogen bonding is the attraction between hydrogen attached to an electronegative atom (**D**) and a second species (**A**) bearing a lone pair, as shown below.

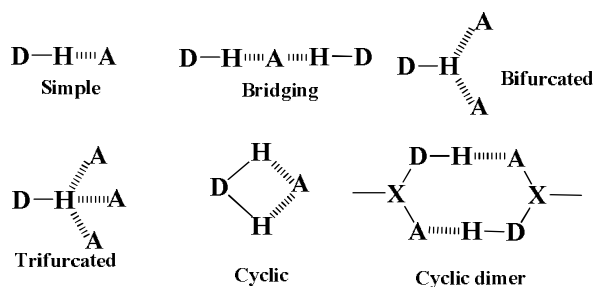


Where **D** = C, N, O, S, F, Cl, etc.

A = N, O, S, F, Cl, etc.

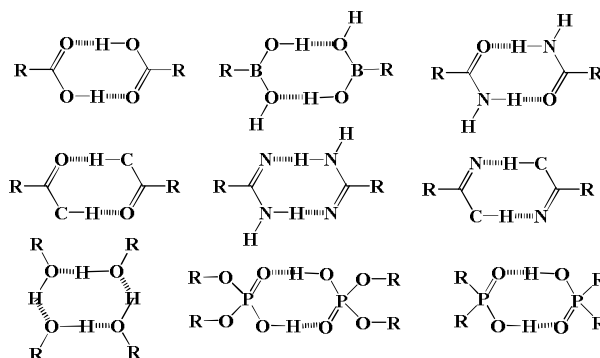
Topology of the hydrogen bonds may be described as *simple* (this type is often bent rather than linear), *bifurcated*, *trifurcated*, *bridging* or *cyclic* (Scheme 1.1). The most common hydrogen bond donor groups are C–H, N–H, O–H, S–H, F–H and Cl–H while acceptor groups include N, O, P, S, F, and Cl as well as alkenes, alkynes, aromatic π -clouds and transition metals.

The strength and directionality of the hydrogen bond, as compared with other intermolecular forces, account for its significance and has made it the most important interaction in the molecular recognition studies. Many design strategies for supramolecular synthesis rely on the complementarity of hydrogen-bond interactions.



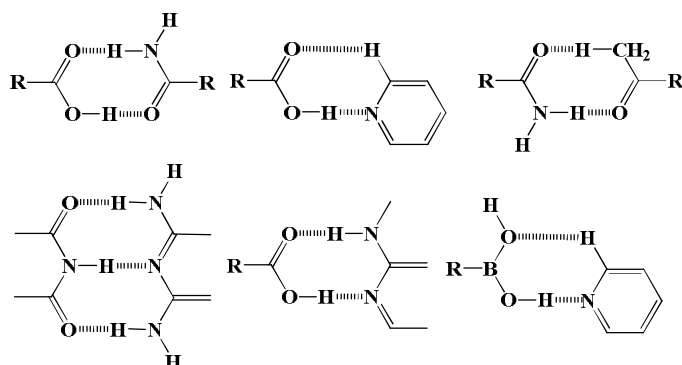
Scheme 1.1

The complementarity can involve both geometric factors and a suitable balance between the number of hydrogen-bond donors and hydrogen-bond acceptors. Some of the self-complementary (or *homomeric*) interactions that have been well studied extensively, are shown in Scheme 1.2.



Scheme 1.2. Examples of self-complementary (*homomeric*) hydrogen bond interactions.

Not only do these complementary moieties bring molecules and ions together, they also constrain the relative orientation of those components in much the same way as carbon-carbon double bonds impart specific stereochemistry to individual molecules. More recently, many *heteromeric* (but still complementary) hydrogen-bond interactions (Scheme 1.3) have been employed in supramolecular synthesis.



Scheme 1.3. Examples of complementary (*heteromeric*) hydrogen bond interactions.

The reliability and competition between various types of aggregations are most effectively determined through systematic database studies, not through detailed analyses of individual structures. Etter and coworkers¹¹ pioneered in this area, and after extensive studies of preferential hydrogen-bond patterns in organic crystals the following empirical ‘rules’ are formulated as a guide to the deliberate design of hydrogen-bonded solids;

- (i) All good proton donors and acceptors are involved in hydrogen bonding.
- (ii) Six-membered ring intramolecular hydrogen bonds form in preference to intermolecular hydrogen bonds.
- (iii) The best proton donor and acceptor remaining after intramolecular hydrogen bond formation will form intermolecular hydrogen bonds.

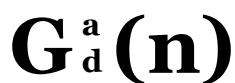
1.2.2. Characterization of hydrogen-bonded supramolecular Assemblies.

Hydrogen bonds occur between atoms, molecules, or ions (positive or negative) in the gas, liquid, solid or supercritical phases. Hydrogen bonds may be simple (involving only one donor and one acceptor), bifurcated (three-centre), or trifurcated (four-centre) (See Scheme 1.1). Hydrogen bonds can vary in strength from being very weak to being the strongest (and most directing) of the intermolecular interactions. The identification of hydrogen-bonded dimers is relatively simple. However, for large multicomponent assemblies held together by weak forces the characterization is far from straightforward and is currently one of the major challenges in this field. *So, how a hydrogen bond detected?* Its net effect, in the

system D–H···A is to weaken the D–H bond (compared with D–H in an isolated system), and this is the basis of the Zeegers-Huyskens and Huyskens definition. Spectroscopic tools, such as IR, MALDI and NMR have been widely employed to investigate hydrogen-bonded assemblies. Furthermore, 2D NMR techniques, such as NOESY, COSY and TOCSY have greatly facilitated the characterization of hydrogen bonded assemblies with sizes approaching that of biological assemblies. Although there are a considerable number of neutron diffraction studies on hydrogen bonded crystals, X-ray diffraction studies remain one of the most commonly applied techniques.

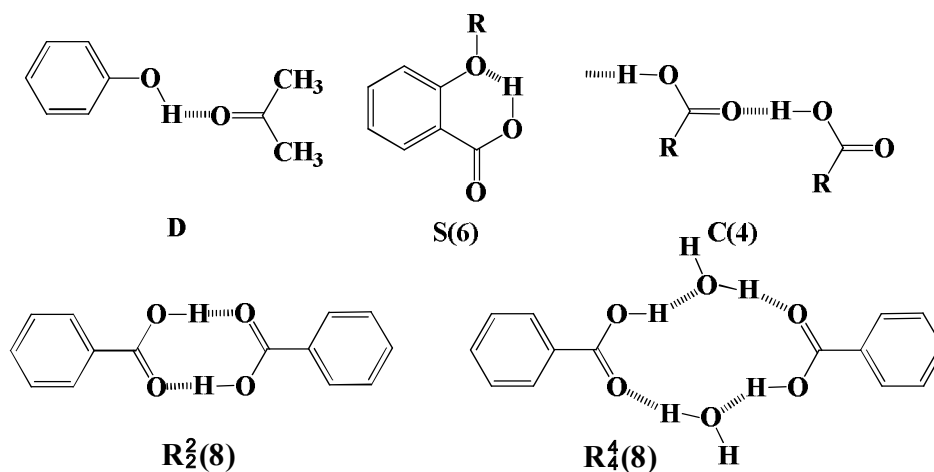
1.2.3. Describing hydrogen-bonded motifs: Graph Sets

An important contribution by Etter, Bernstein and coworkers has been the introduction of a language, based upon graph theory, for describing and analyzing hydrogen-bonded networks in the three-dimensional (3-D) structures.¹² The process of assigning a graph set (Scheme 1.4) begins by identifying the number of different types of hydrogen bonds present in the structure, and then by defining the bonds by the nature of its donors and acceptors.



Scheme 1.4. A generic graph-set descriptor.

A set of molecules connected by hydrogen bonds in a repeat unit, a motif is characterized by one of the four designators, C (chain), R (ring), D (dimer), or S (self, for intramolecular hydrogen bond).



Scheme 1.5. Graph-set assignments for some hydrogen-bond motifs.

The numbers of donors and acceptors used in each motif are assigned as subscripts and superscripts respectively, and the total number of atoms in the repeat unit is denoted in brackets (Scheme 1.5). A benefit of using graph sets is that it brings the focus onto the hydrogen-bonded pattern, and not simply on the geometrical constraints of non-covalent interactions.

1.3. Self-assembly

Self-assembly,¹³ is a process of aggregation of molecules, especially is organic molecules, by noncovalent bonds like hydrogen bonds. It plays a significant role in understanding of many structures as well as facile synthetic routes that are of important in the studies of chemistry and biology for the construction of larger molecules.

Self-assembly may be defined as the process by which supramolecular species are formed spontaneously from its components. In the majority of systems, it appears to be a beautifully simple convergent process, giving rise to the assembled target in a

straight forward manner.¹⁴ Thus, it can be taken to designate the evolution towards spatial confinement through spontaneous connection of a few/many components resulting in the formation of discrete/extended entities at molecular, covalent or supramolecular, non-covalent level. Self-assembly required molecular components containing two or more interaction sites and thus capable of establishing multiple connections. The self-assembly of a supramolecular architecture is multistep process, implying information and instruct components of one or several types.

The growth of the crystal,¹⁵ the formation of liquid crystals,¹⁶ the spontaneous generation of synthetic lipid bilayer, the synthesis of metal co-ordination complexes,¹⁷ and the alignment of molecules on existing surfaces¹⁸ are some of the many manifestations of self-assembly in chemical systems. A system that self-assembles can do so either reversibly or irreversibly.

Self-assembly can thus be described by a series of principles that are often obeyed:

- 1) Self-assembly is an association of many weak and reversible interactions yielding a structure that represents a thermodynamic minimum.
- 2) In general, only a finite number of molecules are involved in the modular self-assembly.
- 3) Self-assembly proceed through positive cooperativity.
- 4) Complimentarity in molecular shape provides the foundation for the association between the components. Shape-dependent association based on van der Waals forces and hydrophobic interactions can be made more specific and stronger by the additional forces like hydrogen bonding and electrostatic interactions.

Static self-assembly does not dissipate energy and it may be a global or local equilibrium. For example, atomic, ionic, and molecular crystals, liquid and colloidal crystals are formed by static self-assembly.

In dynamic self-assembly, the interactions which are responsible for the formation of structures or patterns between the components occur only if the system is dissipating energy. The porous of a cell replication and transformation into another cell during mitosis, bacteria swarm etc., are well known examples of dynamic self-assembly, with the other noted examples being oscillating reactions in solution and on the surface of catalysts, Rayleigh-Bernard convection cells, patterns that form in fluidized beds of particles and storm cells in the atmosphere, etc.

1.4. Molecular recognition

The formulation of fundamental principles of molecular recognition goes back to the early 20th century, when Emil Fischer and Paul Ehrlich introduced the terms “lock and key principle” (Fischer 1894) and “receptor/substrate” (Ehrlich 1906),¹⁹ as already discussed earlier in this chapter. Thus, molecular recognition is the specific interaction between two molecules of complimentary in nature, in their geometric and electronic features.

The selective binding of a substrate by a molecular receptor to form a supermolecule, proceed through molecular recognition rests on the molecular information stored in the interacting partners. Molecular recognition events represent the basis of information processing at the supramolecular level. It refers to the specific interactions established between two or more molecules, by making use of the various

non-covalent forces. The importance of molecular recognition was realized around the middle of the nineteenth century, when Pasteur noticed the existence of tartaric acid in two different kinds of crystals.

Molecular recognition is the fundamental concept in supramolecular chemistry, which is originated from the studies of host–guest chemistry of simple crown ether or cryptand-type molecules.²⁰ It plays a role at several key levels: (1) the building up of the device from its components; (2) its incorporation into supramolecular arrays; (3) the selective operation on given species (e.g., ions); (4) the response to external physical or chemical stimuli (light, electrons, ions, molecules, etc.) that may regulate the operation of the device and switch it on or off; (5) the nature of the signals generated and signal conversion effected (photon/photon, photon/electron, electron/electron, electron/ion, ion/ion, etc).

1.5. Supramolecular synthesis

Molecules are the collection of atoms that are connected by a continuous network of strong chemical bonds. Molecules in a confined medium interact further through much weaker and kinetically labile noncovalent interactions (electrostatic and van der Waals forces or hydrophobic effects, π - π stacking interactions, metal coordination and hydrogen bonding). In biology, such interactions are responsible for the transduction of signals, the selective transport of ions and small molecules across membranes, enzymatic reactions, or the formation of larger aggregates. In chemistry, such weak noncovalent interactions determine the physical properties of molecules,

e.g., the properties of liquids, the solubility of solids, or the organization of amphiphilic molecules in larger aggregates such as membranes, micelles, and vesicles.

In supramolecular chemistry,²¹ molecules are designed and synthesized to interact specifically with other complimentary molecules to form larger aggregates. The concepts developed in supramolecular chemistry are increasingly used in various fields like material science, surface science, sensor technology and nanotechnology.

1.6. Carboxyl group in supramolecular synthesis

Self-assembly, driven by hydrogen bonds formed by carboxylic groups is extensively studied and it play a key role in the development of exotic supramolecular assemblies.²² It is mainly because $-\text{COOH}$ has dual character with the oxygen atoms present in it can act as acceptors as well as donors. Thus, with regard to hydrogen bonds formation, carboxylic groups are self-complimentary (i.e., two carboxylic groups can form a cyclic dimer interconnected by two equivalent hydrogen bonds). Common binding arrangements for carboxylic acids in molecular crystals²³ are cyclic dimers, trimers and catemeric motifs as depicted in Figure 1.2.

The most economical and efficient approach in designing a self-assembling aggregate is through the employment of the self-complimentary molecule. This has been the approach used in the preparation of a vast ensemble of supramolecular assemblies, with the examples vary from the simple dimeric assemblies to stable porous three-dimensional networks obtained from various molecular building units. Thus, benzoic acid forms zero-dimensional units, isophthalic acid forms zigzag tapes, terephthalic acid forms one dimensional tapes, trimesic acid with its three fold

symmetry forms a two-dimensional chicken wire network and adamantane tetracarboxylic acid group forms a diamondoid network in three-dimension, by utilizing robust dimeric hydrogen bonds, as shown in Figure 1.3.²⁴

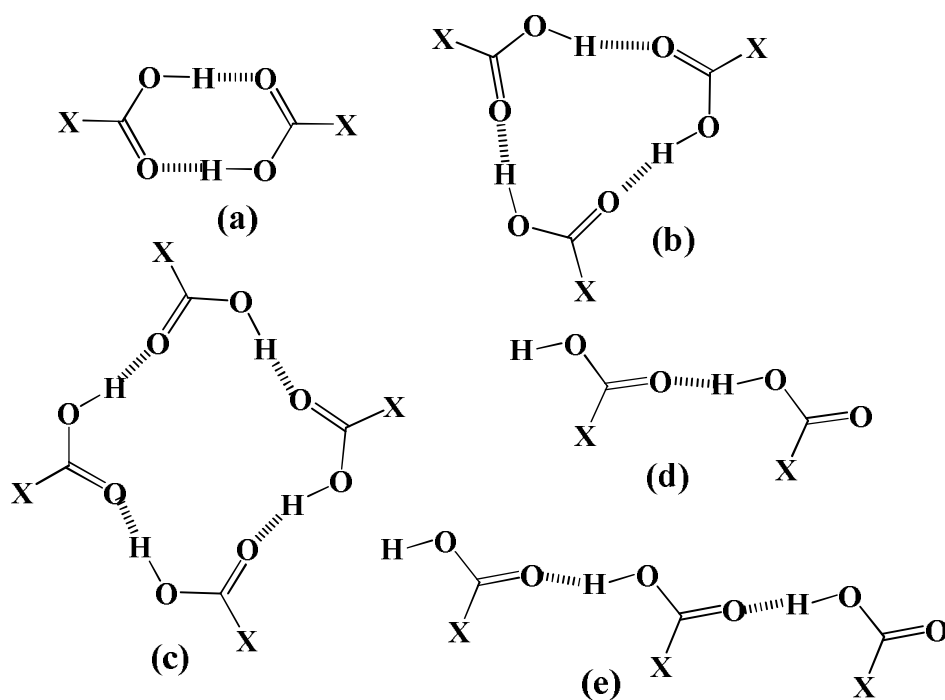


Figure 1.2. Most common modes of carboxylic acid self-association: (a) cyclic dimer (b) cyclic trimer (c) cyclic tetramer (d) linear dimer (e) chain.

Also, carboxylate groups are known to be strong acceptors that often bond to multiple donors. For example, Gorbitz and Etter has shown that carboxylate groups typically form hydrogen bonds with three different donors and can accommodate as many as five in the solid state.²⁵ The hydrogen bonding networks and molecular structure organization in crystalline carboxylic acids have been exhaustively investigated by Leiserowitz.^{24a}

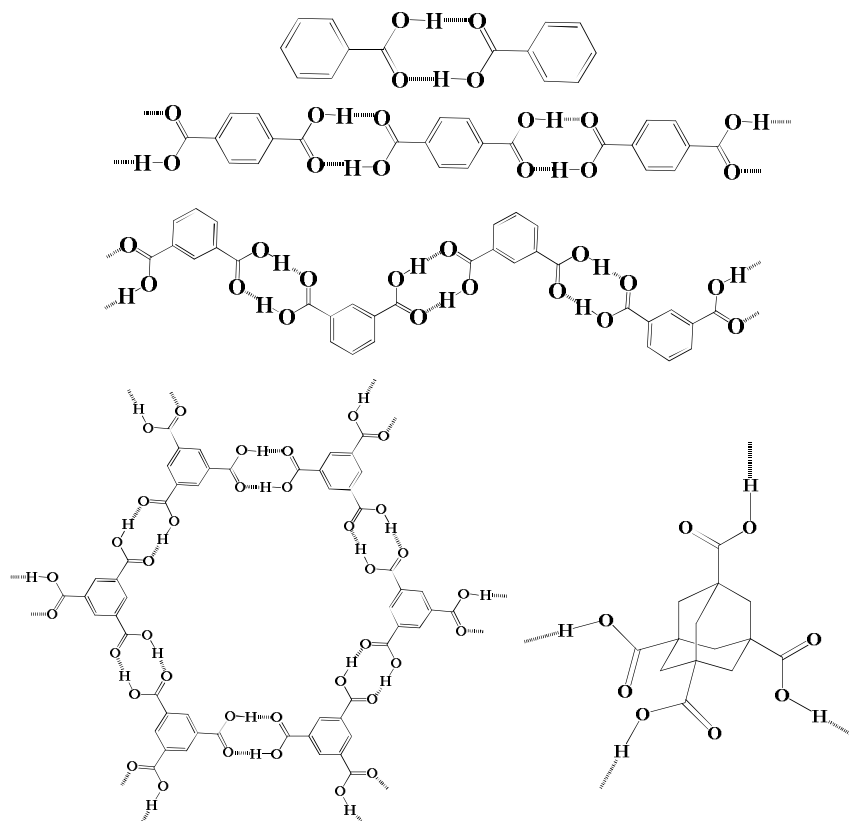


Figure 1.3. Construction of supramolecular assemblies through dimeric hydrogen bonds from different molecular building units, formed by $-\text{COOH}$.

The strong and directional nature of *homomeric* hydrogen bonds is well exploited in the organized self-assembly of molecules in solution and the solid-state. However, the understanding of factors that direct hydrogen bonding motifs between hetero functional groups is still evolving. For a successful outcome, understanding of the synergy, interplay and competition between different functional groups during self-assembly are so essential. In this directions, $\text{O}-\text{H}\cdots\text{N}$ or $\text{O}-\text{H}\cdots\text{N}/\text{C}-\text{H}\cdots\text{O}$ pairwise hydrogen bonds,²⁶ especially being formed between organic acids and bases are well explored in the different areas of supramolecular chemistry. Some of the exotic

examples, observed from the literature, are discussed below as representative examples.



Figure 1.4. Space filling mode of a hexagonal host network of **TMA** and ethanol molecules to accommodate the guest species.

Zimmerman *et al.* reported an exotic hexagonal network of benzene-1,3,5-tricarboxylic acid (trimesic acid, **TMA**).²⁷ In this case **TMA** and pyrene were co-crystallized from ethanol and the resulting assembly forms a host guest complex. The hexagonal host network is formed by the **TMA** and ethanol molecules, creating voids, which are being occupied by pyrene and ethanol molecules as shown in Figure 1.4.

Zaworotko *et al.*²⁸ reported a 2:3 cocrystal of **TMA** and 4,4'-bipyridine (**bpy**) demonstrating a prototypical (6,3) honeycomb network, formed by two molecular components. The co-crystal is sustained by a pair wise hydrogen bonds and in effect the **bpy** molecules act as spacers between acid dimers, thereby expanding the $14 \times 14 \text{ \AA}^2$ **TMA** cavity to ca. $35 \times 26 \text{ \AA}^2$, as shown in Figure 1.5a. This hexagonal cavity is filled by 3-fold interpenetration. Similarly co-crystallization reaction of **TMA** and *trans*-1,2-bis(4-pyridyl)ethane (**bpyea**) exhibit expanded hexagonal (6,3) networks of

cavity of $41 \times 35 \text{ \AA}^2$ (See Figure 1.5b) dimensions with effective close packing by 3-fold parallel interpenetration. Further, Nangia et al. shown the efficacy of unsaturated carboxylic acids through 1,3,5-cyclohexane-tricarboxylic acid.²⁹

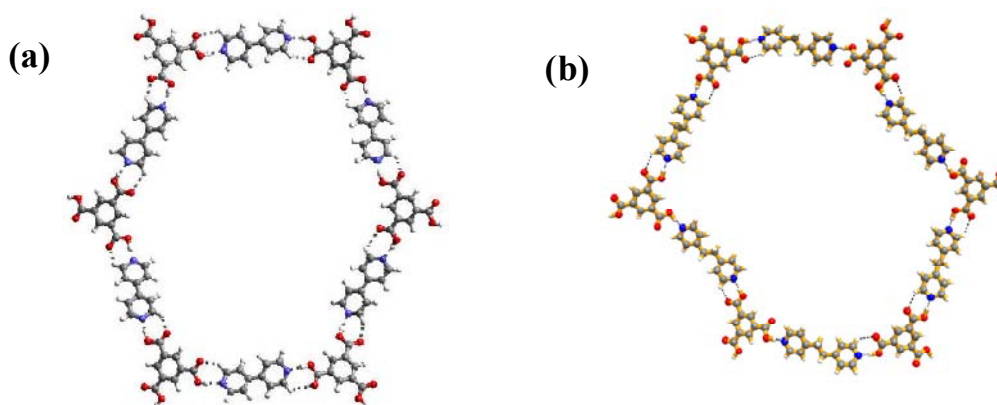


Figure 1.5. Super honeycomb (6,3) network in the molecular complex of **TMA** with *bpy* (a) and with *bpyea* (b).

Similarly, Coppens and co-workers³⁰ have illustrated the formation of a host-guest complex through co-crystallization of tridentate ligand 1,3,5-tri(4-pyridyl)-2,4,6-triazine (**TPT**) and **TMA** in the presence of pyrene, which forms a honeycomb framework. The observed three-dimensional structure, with four pyrene molecules in each channel, is shown in Figure 1.6.

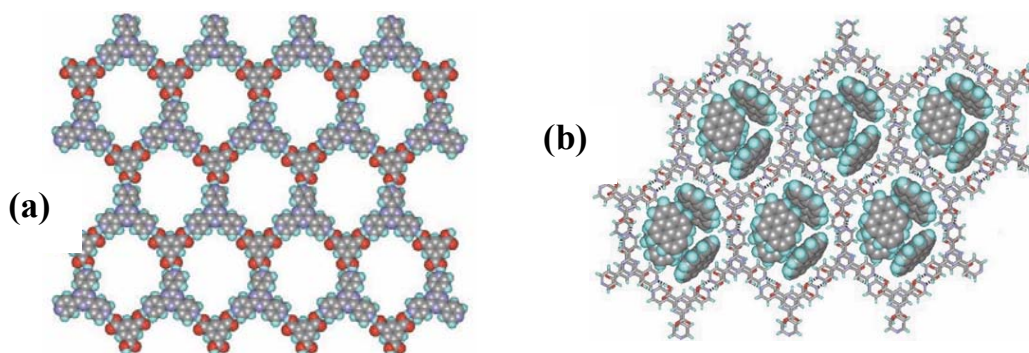


Figure 1.6. (a) Honeycomb framework formed by **TMA** and **TPT** in space filling model (b) Arrangement of four pyrene molecules in the honeycomb network.

Pedireddi *et al.* reported numerous supramolecular assemblies that primarily possess -COOH and aza-donor moieties to deduce the salient features of recognition patterns in terms of the pK_a of the constituents,³¹ through co-crystallization of 2,4-diamino-6-methyl-1,3,5-triazine (**DMT**) with various aliphatic dicarboxylic acids, such as malonic, succinic, or adipic acid, etc. The highlight of this contribution is that the observed differences in the host-guest networks are correlated to the pK_a of the acids employed in specific assembly. Thus, it was shown that acids with $pK_a < 3.0$ give host networks that consist of only **DMT** (Figure 1.7a), while the acid in the study occupies the positions as guests. But with the acids having $pK_a > 3.0$, host is being constituted by both **DMT** and the acid molecules, as shown in Figure 1.7b, with the channels being filled by solvent of crystallization.

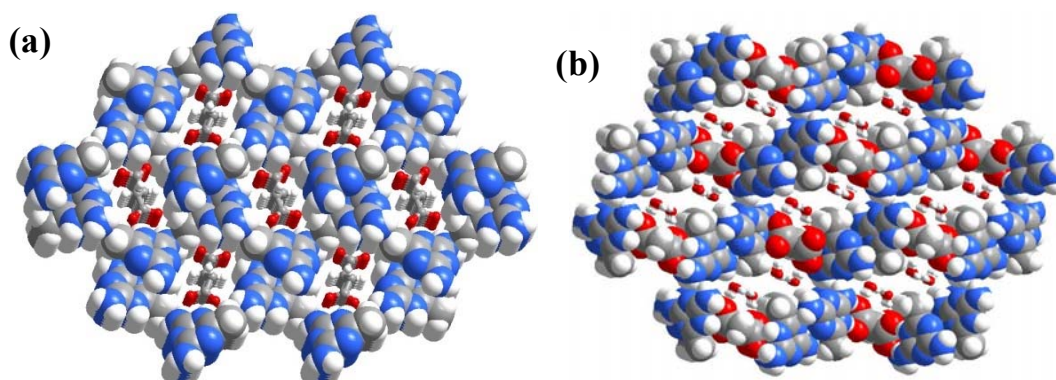
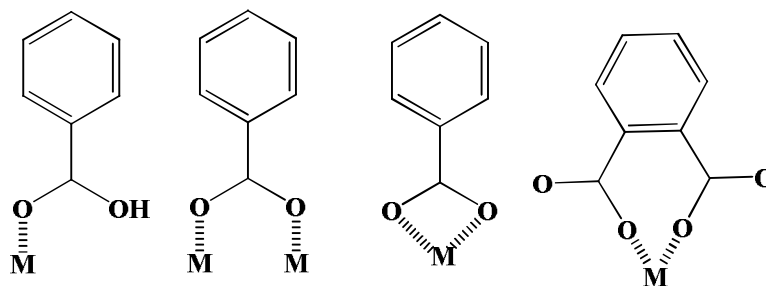


Figure 1.7. (a) Host-guest network observed in complex, **DMT**-Succinic acid, with the host being formed by the molecules of **DMT** and succinate molecules occupying the channels. (b) Host-guest network observed in complex **DMT**-malonic acid, with the channels being filled by guest water molecules.

1.7. Metal Coordination assemblies

Metal Organic Frameworks (MOFs) are metal clusters interconnected by organic linker groups, a design that endows the materials with large pores, open

channels, and huge internal surface areas for adsorbing molecules. By mixing and matching metal oxide nodes with a wide variety of organic struts, Yaghi,³² Zaworotko,³³ Braga,³⁴ Kitagawa,³⁵ Ferey,³⁶ Rosseinsky³⁷ and several other researchers reported myriad of MOFs. Construction of MOFs using dative bonds is not only well known for their fascinating, esthetic architectures but also due to the potential applications in catalysis, ion-exchange, molecular sensing, gas storage, chiral separation, etc. In addition, a wide range of functional groups utilized using crystal engineering concept for novel metal organic frameworks. A carboxylate group is known as a good functional group of metal coordination. In this direction multidentate linkers such as carboxylates allow for the formation of more rigid frameworks due to their ability to aggregate metal ions into M–O–C clusters that refers to as secondary building units (SBUs). There are several bonding modes of the carboxylate group in metal coordination as shown in Scheme 1.7. The SBUs are sufficiently rigid because the metal ions are locked into their positions by the carboxylates; thus, instead of having one metal ion at a network vertex, the SBUs serve as large rigid vertices that can be joined by rigid organic links to produce extended frameworks of high structural stability.



Scheme 1.7.

Recently, Champness and co-workers³⁸ synthesized a robust metal-organic framework, by hydrothermal reaction of ZnCl_2 and 4,4'-bipyridine-2,6,2',6'-tetracarboxylic acid (H_4L) (See Figure 1.8a). It crystallizes in a chiral space group, with the chirality generated by the helical chains of hydrogen-bonded guest water molecules. However, the removal of the guest water molecules from the crystal, gave a porous material, which has very high thermal stability and is chemically inert.

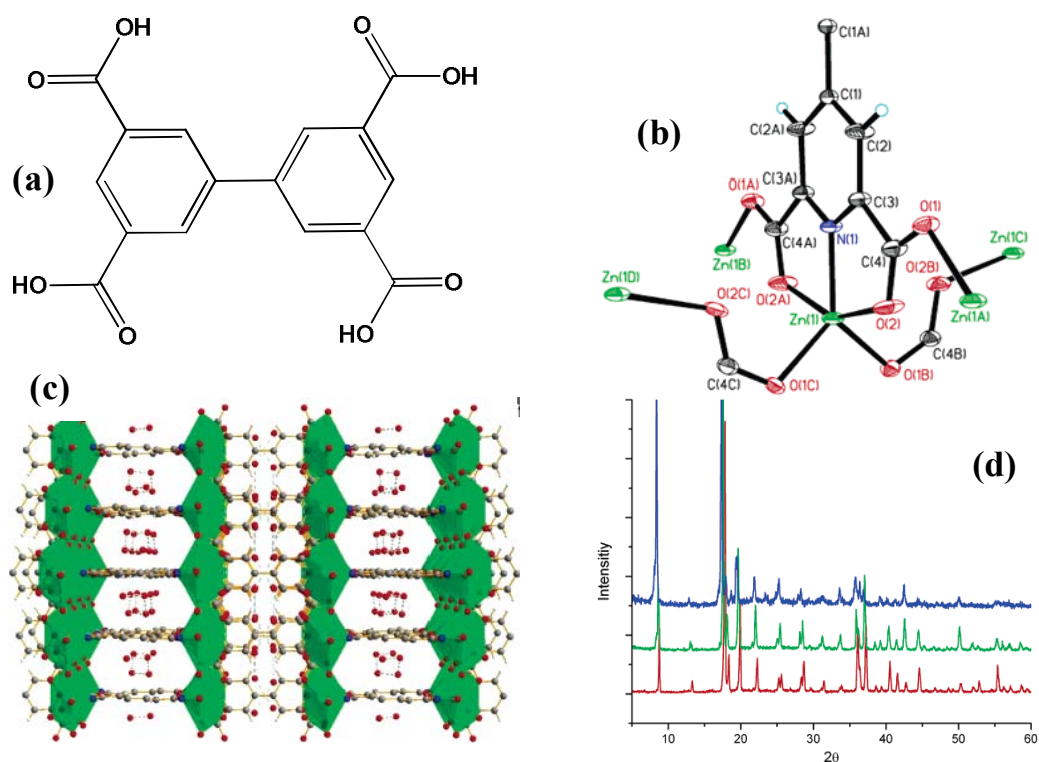


Figure 1.8. (a) Molecular structure of the carboxylic acid ligand, H_4L . (b) Coordination sphere around $\text{Zn}(\text{II})$ in the crystal structure of $\{[\text{Zn}_2(\text{L})]\infty 4\text{H}_2\text{O}\}$ (**I**). (c) Framework structure of $\{[\text{Zn}_2(\text{L})]\infty 4\text{H}_2\text{O}\}$ (**I**), in which $\text{Zn}(\text{II})$ coordination spheres are represented by green polyhedron and channel occupied by guest water molecules (d) Powder XRD patterns of at different temperatures, showing the stability without any change in peak positions.

The framework is constructed from Zn(II) ions and anionic ligands, $L^{\cdot-}$. Zn(II) is coordinated by a tridentate array comprising two O-donors from 2,6-dicarboxylate groups and one pyridyl N-donor, all from the same ligand (Figure 1.8b). The crystal structure of the above complex shows a three-dimensional host framework with interconnecting pore cavities containing water molecules, as shown in Figure 1.8c. Further, based on TGA and DSC data, it is concluded that, no phase change was recorded after the removal of the water molecules from the channels up to 250 °C in air or 450 °C under a nitrogen atmosphere, above which the framework starts to decompose. Variable temperature XRPD confirms that considerable crystallinity remains, even after the sample has been heated to 500 °C in a TGA experiment, with only marginal peak broadening observed (Figure 1.8d).

1.8. Potential applications of organic and metal-organic assemblies.

1.8.1. Photodimerization reactions

For a [2 + 2] cycloaddition reaction to occur in the solid state, the adjacent olefinic bonds should conform to geometry criteria outlined by Schmidt.³⁹ Specifically, following crystal structure studies involving cinnamic acids, Schmidt forwarded that the adjacent unsaturated bonds should be aligned parallel and separated by $<4.2 \text{ \AA}$. Understanding the efficacy of intermolecular interactions in the organization of molecular entities, MacGillivray and co-workers demonstrated that compounds like 1,8-naphthalenedicarboxylic acid (**1,8-nap**), resorcinol, etc., can serve as a templates,⁴⁰ to induce 2+2 photochemical cycloaddition reaction in the

compounds like *trans*-1,2-bis(4-pyridyl)ethylene⁴¹ which is otherwise photostable because of unfavorable packing of molecules for photochemical reaction. Thus, co-crystallization of 1,8-naphthalenedicarboxylic acid with *trans*-1,2-bis(4-pyridyl)ethylene (*bpyee*) produced a four-component assembly, 2(**1,8-nap**)·2(*bpyee*), held together by four O–H···N hydrogen bonds (Figure 1.9a). In this arrangement, the twisted conformation of carboxylic acid groups, positioned the reactants for reaction with the pairs of C=C bonds to align parallel with a distance of separation 3.73 Å. Hence, UV-irradiation of the co-crystals produced *rctt*-tetrakis(4-pyridyl)cyclobutane in quantitative yield, as shown in Figure 1.9b.

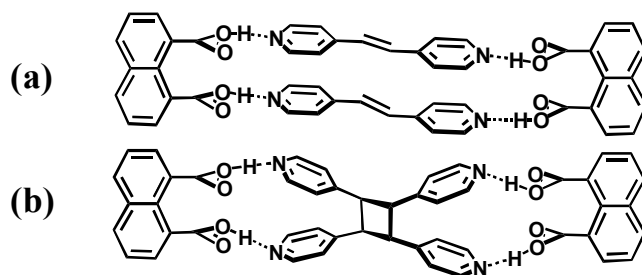


Figure 1.9. (a) Alignment of *bpyee* molecules in the crystal structure of 2(**1,8-nap**)·2(*bpyee*), (b) Cycloaddition product irradiated after UV-irradiation.

Similarly, Wolf and co-workers⁴² have also utilized the carboxylic acid and aza donor interactions for the preparation of cyclobutane tetracarboxylic acid as shown in Figure 1.10.

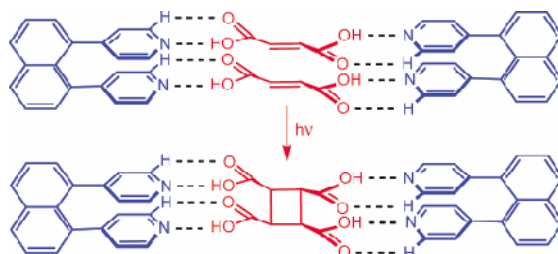


Figure 1.10. Schematic representation for the preparation of cyclobutane tetracarboxylic acid.

Jones and co-workers used polycarboxylic acid templates for the synthesis of [2+2] photodimerized product.⁴³ Irradiating the co-crystals of 1,2,4,5 benzenetetracarboxylic acid and *bpyee*, in which the adjacent molecules of aza-donor moieties are aligned for [2+2] photodimerization (Figure 1.11a), gave a product *rc*tt-tetrakis(4-pyridyl)cyclobutane (**tpcb**) in 100% yield. Further, the irradiated crude product upon co-crystallization from DMSO, gave a structure with a porous host network, as shown in Figure 1.11(b), with the voids being filled by the solvent of crystallization DMSO and water, as guest species.

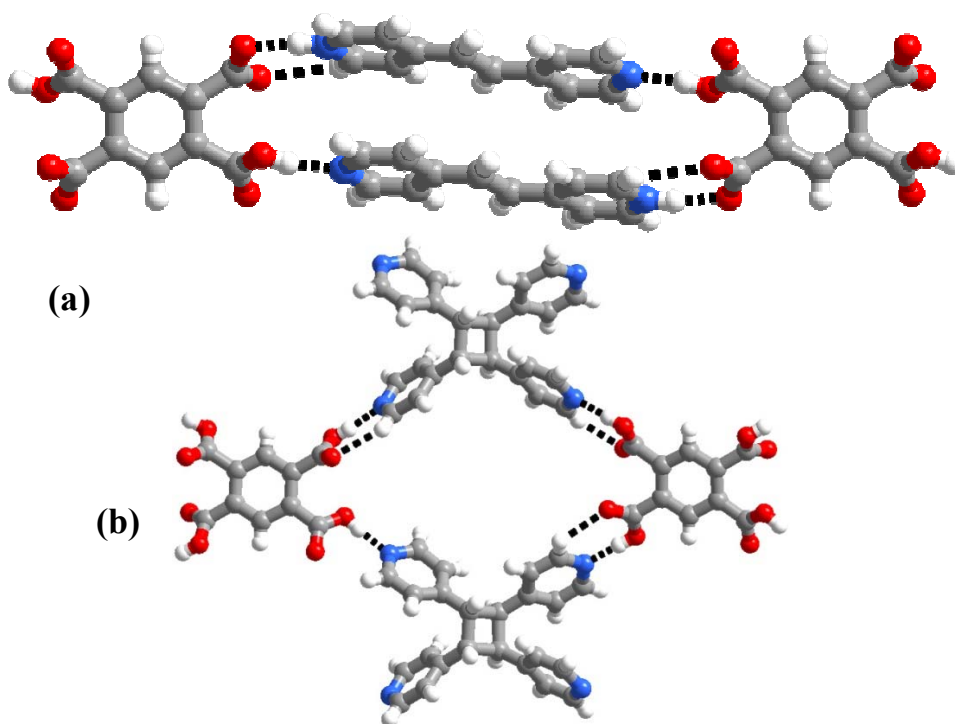


Figure 1.11. (a) Co-crystal formed between 1,2,4,5-benzenetetracarboxylic acid and 1,2-*bis*(4-pyridyl)ethene (b) Porous network formed by the irradiation of co-crystal of 1,2,4,5-benzenetetracarboxylic acid and 1,2-*bis*(4-pyridyl)ethene (solvent molecules are removed for clarity)

Apart from synthesis of various cyclobutane derivatives, in fact, the elegance of utilization of co-crystallization concept has been demonstrated by preparing complex molecules like cyclophanes, ladderanes by simple template processes.

1.8.2. Pharmaceutical co-crystallization

Pharmaceutical co-crystals extended the arms of supramolecular synthesis to control polymorphism in active pharmaceutical ingredients (APIs), patenting of new forms, drug formulations, delivery, etc.,⁴⁴⁻⁴⁶ as illustrated through numerous examples in the recent literature. For example, the cocrystals of *cis*-itraconazole, a triazole anti-fungal agent, and dicarboxylic acids (Figure 1.12) resulting from a high-throughput crystallization screen, reported by Remenar and co-workers,⁴⁷ have been shown to exhibit increased solubility of API than its native crystals/amorphous solid.

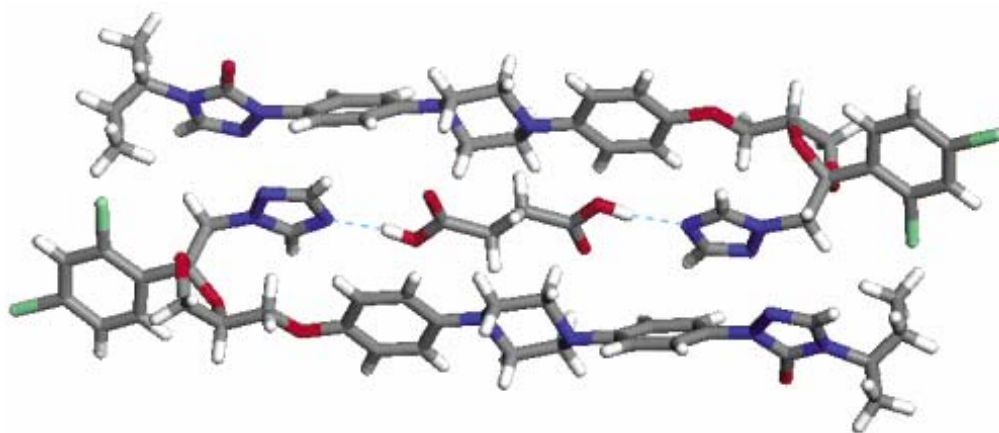


Figure 1.12. Supramolecular assembly formed by *cis*-itraconazole with succinic acid.

Zaworotko and co-workers recently reported preparation of a specific polymorph co-crystal using polymorphic active pharmaceutical ingredients (APIs), considering piracetam with gentisic acid and *p*-hydroxybenzoic acid, by solvent drop griding method (Figure 1.13).

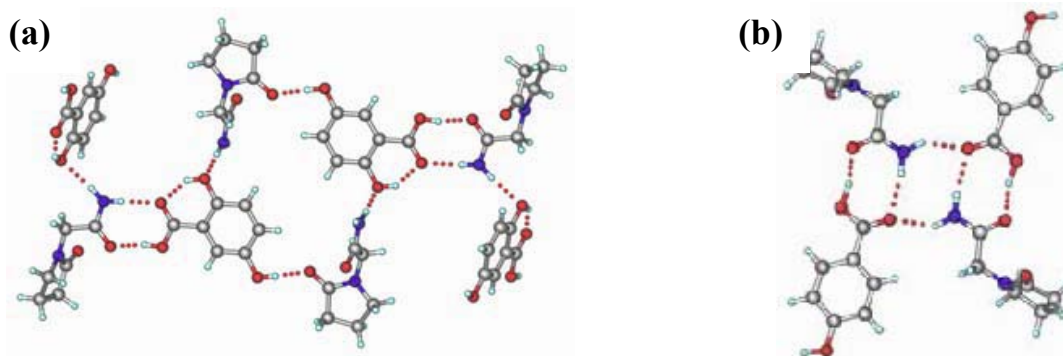


Figure 1.13. (a) Hydrogen bond network in the co-crystals of piracetam and gentisic acid. (b) Carboxylic acid-amide interaction in the form of tetrameric motif, in the co-crystals of piracetam and *p*-hydroxybenzoic acid.

Carbamazepine (**CBZ**) [5H-dibenzazepine-5-carboxamide], has been in use for over 30 years to treat epilepsy and trigeminal neuralgia even though it poses multiple challenges to oral drug delivery and dissolution limited bioavailability.⁴⁸ From a supramolecular perspective, **CBZ** has potential functional group to form co-crystals with carboxylic acids. Thus, several solvates are prepared⁴⁹ and to improve the bioproperties of **CBZ**, structural elucidation reveals that pair wise O–H \cdots O/N–H \cdots O hydrogen bonds and N–H \cdots O hydrogen bonds stabilized the assemblies, as shown in Figure 1.14.

Taken in to account the different types of architectures formed by a variety of chemical species, it is evident that the molecules containing –COOH groups are potential precursors for the synthesis of host-guest networks. In this connection we have noted that benzenepentacarboxylic acid (**BPC**) and mellitic acid (**MA**) molecules are not well utilized in the supramolecular synthesis. Thus, a study of the molecular complexes formed by the penta and hexa-substituted carboxylic acids employing

various aza-donor molecules have been proposed to study systematic variation, as described in chapters two and three.

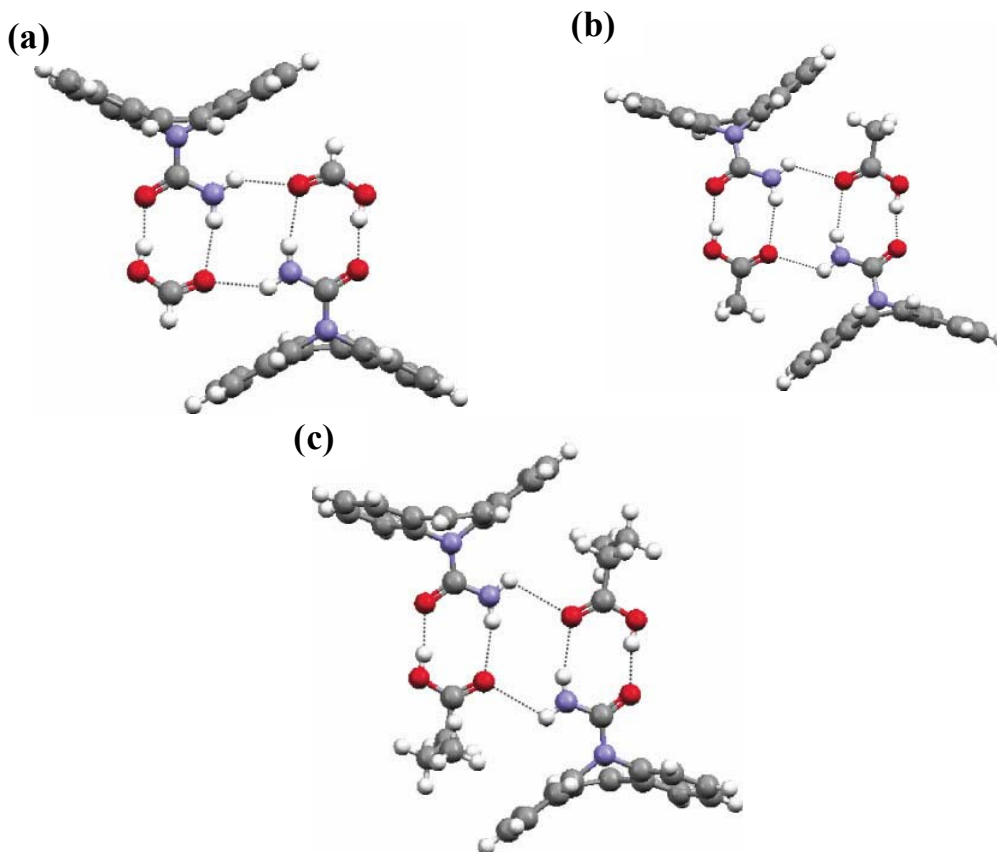


Figure 1.14. Illustrations of the supramolecular assemblies of **CBZ** with different carboxylic acid solvates.

1.8.3. Gas storage materials

Yaghi and coworkers reported a metal organic framework MOF-5 (Fig. 1.15a), in which inorganic $[\text{OZn}_4]^{6+}$ groups are joined to an octahedral array of $[\text{O}_2\text{C}-\text{C}_6\text{H}_4-\text{CO}_2]^{2-}$ (1,4-benzenedicarboxylate, **BDC**) to form a robust and highly porous cubic framework.⁵⁰ The results of hydrogen adsorption in MOF-5 demonstrate the importance of the organic linkers in determining H_2 uptake levels.

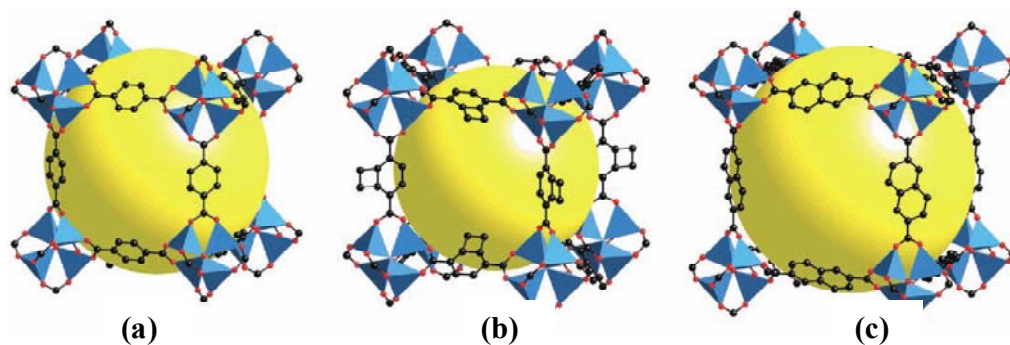


Figure 1.15. Single-crystal X-ray structure of (a) MOF-5, (b) IRMOF-6 and (c) IRMOF-8, showing a single cube fragment.

The nature of the binding sites is determined through Inelastic Neutron Scattering (INS) spectra on adsorbed hydrogen molecules, as shown in Figure 1.16, which demonstrates the influence of advanced characterization tools. Similarly, H₂ sorption in IRMOF-6⁵¹ and IRMOF-8⁵² were also carried out and reported in the literature as part of studies in the frontier area of ‘reticular synthesis’. A noteworthy highlight of MOF-5, IRMOF-6 and IRMOF-8 is the tunability of pore size from several angstroms to a few nanometers just by controlling the length of the organic ligands.

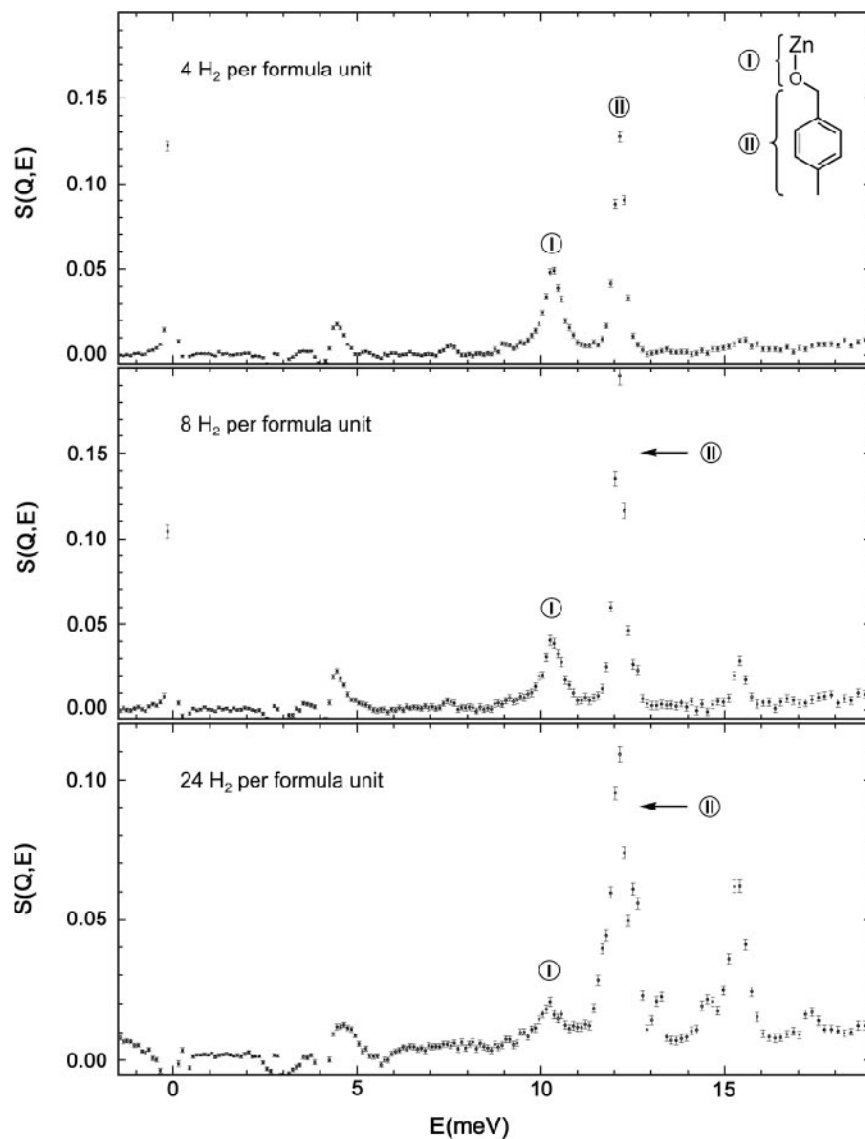
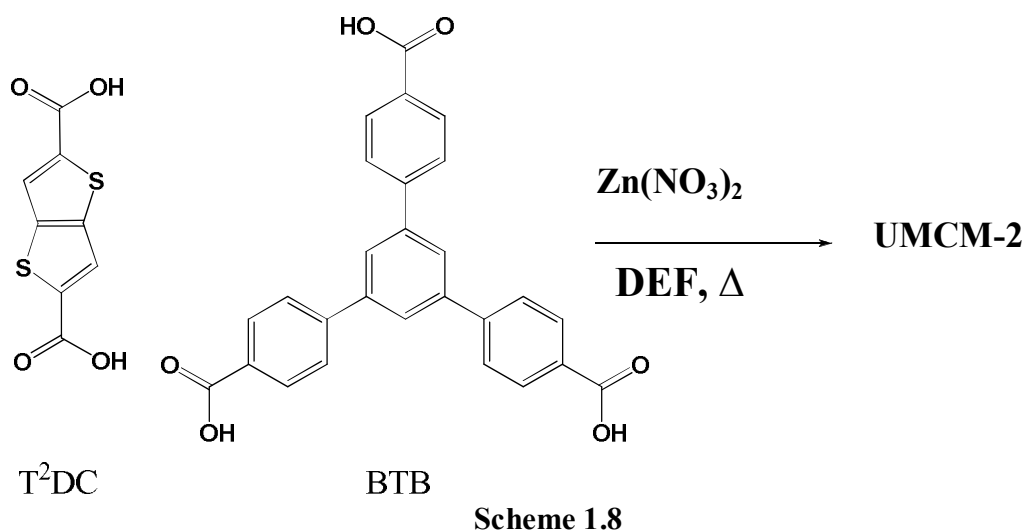


Figure 1.16. INS spectra ($T = 10$ K) for hydrogen adsorbed in MOF-5 with loadings of $4H_2$ (top), $8H_2$ (middle) and $24H_2$ (bottom) per formula unit [$Zn_4O(BDC)_3$] obtained on the QENS spectrometer.

Matzger and co-workers reported different process for the making MOFs,⁵³ by combining zinc with two different types of commonly used organic linker groups, like thieno[3,2-b]thiophene-2,5-dicarboxylate (**T²DC**) and 1,3,5-tris(4-carboxyphenyl)-benzene (**BTB**), as shown in Scheme 1.8.



X-ray diffraction study of hexagonal plate like crystals shows that the product crystallizes in a hexagonal space group, $P63/m$. The framework labeled as UMCM-2 consists of Zn_4O metal clusters linked together by two **T²DCs** and four **BTBs** arranged in an octahedral geometry, as shown in Figure 1.17, with a record surface area for a mesoporous channel material of $4160 \text{ m}^2/\text{g}$.

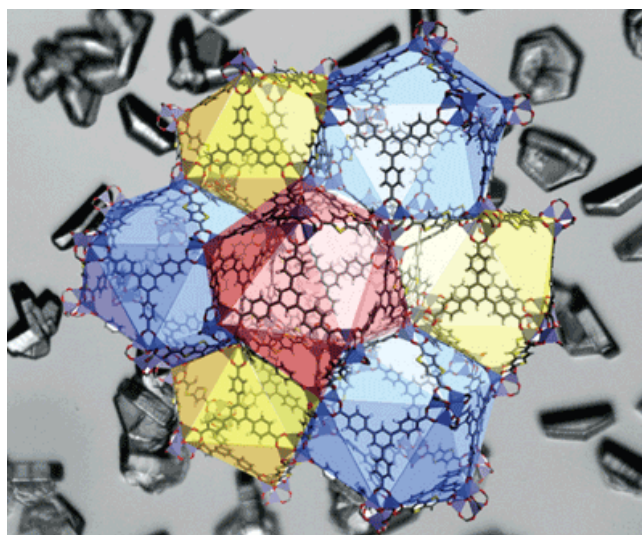


Figure 1.17. The structure of UMCM-2, composed of Zn_4O clusters coordinated to thiophene-based dicarboxylic acid and benzene-based tricarboxylic acid linkers; crystals of the material are shown in the background.

The N₂ sorption isotherm of UMCM-2 is shown in Figure 1.18. UMCM-2 exhibits exceptionally high N₂ uptake (ca. 1500 cm³/g), and by applying the Brunauer-Emmer-Teller (BET) model upto the first plateau ($P/P_0 \approx 0.1$), the apparent surface area is calculated to be 5200 m²/g (a similar treatment using the Langmuir model affords a surface area of 6060 m²/g). This value is significantly higher than that of any other porous material reported to date. UMCM-2 shows an excess gravimetric H₂ uptake of 68.8 mg/g (6.9 wt% based on MCP) at 46 bar.

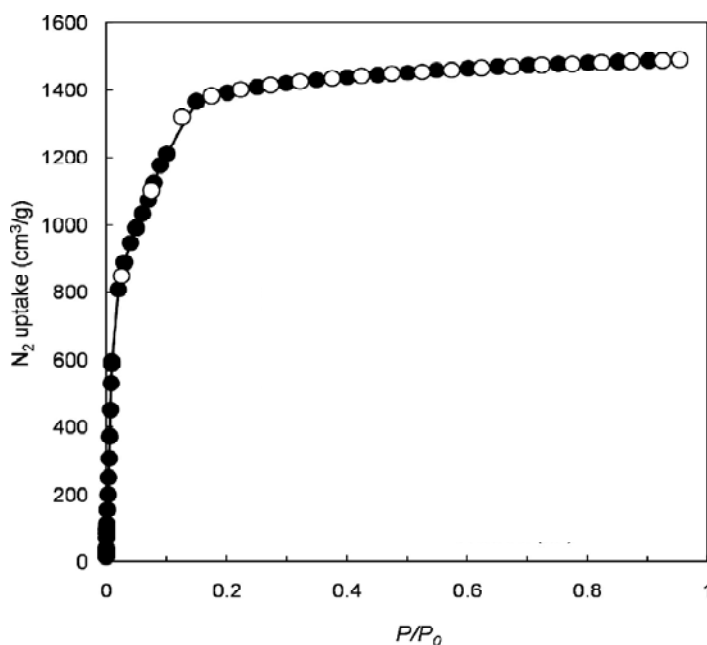


Figure 1.18. Nitrogen adsorption isotherm at 77 K for UMCM-2 (●, adsorption; ○, desorption).

1.8.4. Dynamic frameworks

Most of the porous materials have been synthesized with an aim of obtaining a robust structure. However, Kitagava and his group developed flexible frameworks that provide pore structures which are suited for a given guest molecule and are much

more useful for molecular recognition or selective guest inclusion than a robust porous structure.⁵⁴ The “shape-responsive fitting” properties afford a novel recognition system using crystalline materials. In this direction, a porous coordination polymer with pillared layer structure ($[\text{Cu}_2(\text{pzdc})_2(\text{bpy})]$, (**CPL-2**) (**pzdc** = pyrazine-2,3-dicarboxylate), **bpy** = 4,4'-bipyridine) was constructed from stiff motifs of **bpy** and the pyrazine ring in **pzdc**, that possess a flexible motif of the carboxyl groups with the rotational freedom.⁵⁵ The crystal structures of the **CPL-2 (apohost)** at 293 K and was determined from XRPD measurements and Rietveld analysis. The adsorption isotherm of benzene on the **apohost** was measured at 300 K and structure was determined from Rietveld analysis. The coordination environment is similar in the structure of **apohost** and **CPL-2/benzene**, as shown in Figure 1.19.

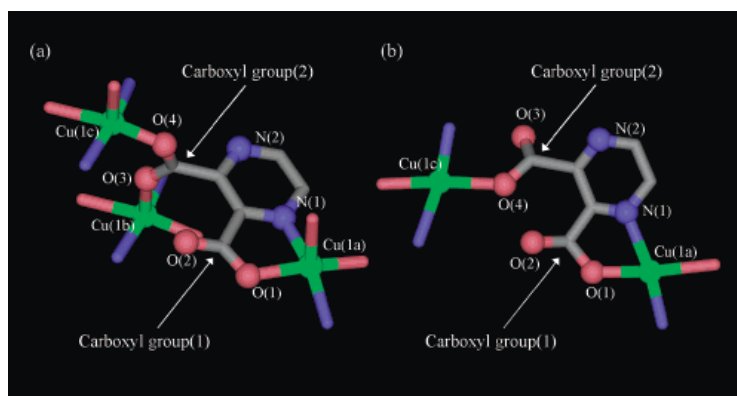


Figure 1.19. Crystal structures of (a) **apohost** and (b) **CPL-2 / benzene** (Cu, green; O, pink; N, blue; C, gray) of **pzdc** ligand and Cu(II). Hydrogen atoms are omitted for clarity.

Both the **CPL-2/benzene** and the **apohost** structures possess 1D channels running along a crystallographic axis. Interestingly, the pillared layer framework undergoes a deformation such that the channels dimension suit to get incorporate

benzene, as shown in Figure 1.20. Also, this study demonstrated the reversible structural change due to the adsorption/desorption of guest molecules and are monitored by X-ray diffraction patterns, which detected a “shape-responsive fitting” profile on guest molecule adsorption with large crystalline shrinking.

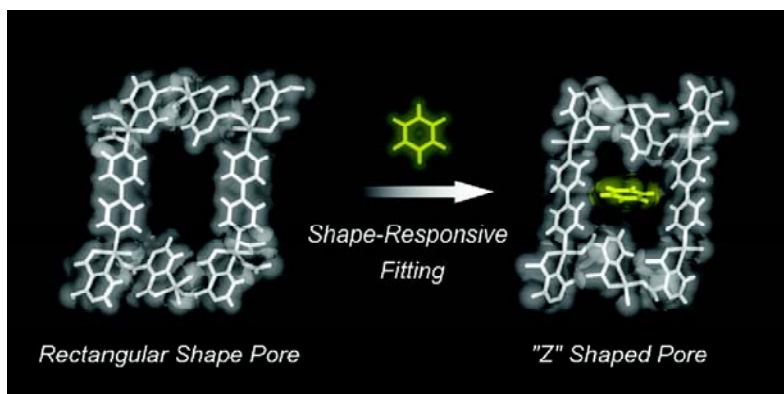


Figure 1.20. Representation of the pore structures of (a) **apohost** and (b) **CPL-2/benzene**.

A novel metal–organic framework with permanent porosity and a high surface area, which also shows unusual guest-dependent dynamic behavior is recently reported by kim et al.⁵⁶ The framework shrinks upon guest inclusion and expands upon guest release as proved unequivocally by single-crystal X-ray crystallography. These changes are fully reversible and depend on the nature of guests. The framework is composed of dinuclear Zn_2 units with a paddle wheel structure, which are bridged by **BDC** dianions to form a distorted 2D square-grid $\{Zn_2(\mathbf{BDC})_2\}$. The framework maintain single crystallinity even after the guest is removed completely, by heating in a vacuum for 1 day, which allowed to determine the guest-free structure by single-crystal X-ray crystallography. Crystal structure analysis reveals that it formed a perfect two dimensional square grid as shown in Figure 1.21a.

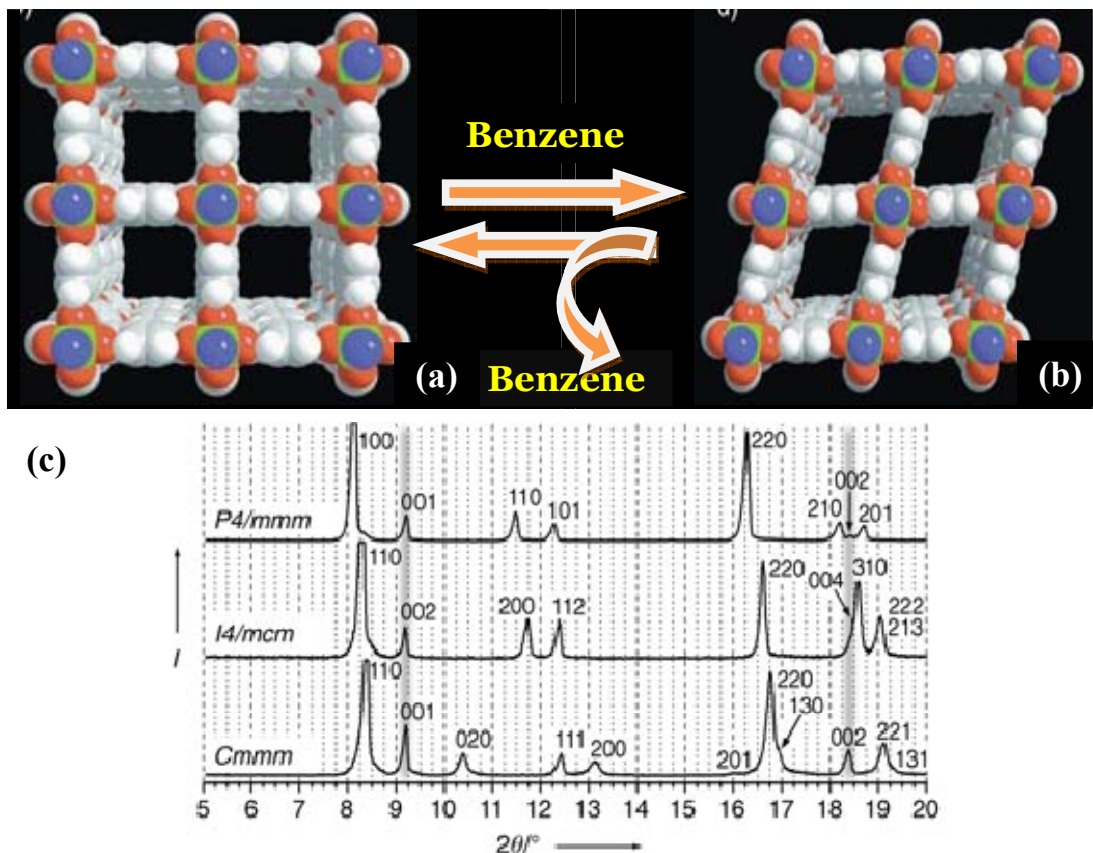


Figure 1.21. (a) Space-filling representation of evacuated framework, which emphasizes the open square channels; view along fourfold axis. (b) Space-filing representation of the benzene-inclusion framework structure, showing rhombic-grid motif of $\{Zn_2(BDC)_2\}$ layers. (c) Powder X-ray diffractograms of evacuated framework (top), as-synthesized (middle) and benzene-inclusion framework (bottom).

A different mode of the framework distortion leading to the shrinkage of pores was observed upon inclusion of benzene into the evacuated framework as confirmed by power XRD studies (Figure 1.21c). Once again, all the structural changes are reversible. The structure of the benzene-inclusion framework was also determined by single-crystal X-ray diffraction process (See Figure 1.21b). The overall framework

connectivity in $1 \cdot 2\text{C}_6\text{H}_6$ remains the same, but the Zn_2 paddle wheels and **BTC** linkers now form a 2D rhombic grid.

1.8.5. Porous frameworks as a catalyst

Kim et al. reported the synthesis of a homochiral metal organic porous material that allows the enantioselective inclusion of metal complexes in its pores and catalyses a transesterification reaction in an enantioselective manner.⁵⁷ The enantiopure chiral organic building block, methyl 2,2-dimethyl-5-[(4-pyridinylamino)carbonyl]-1,3-dioxolane-4-carboxylate, reacts with Zn^{2+} ions to produce a homochiral open-framework solid. In the crystal structure, there are six pyridyl groups per trinuclear unit and three of them are coordinated to the zinc ions of three neighboring trinuclear units while the other three extrude into the channel without any interactions with the framework as shown in Figure 1.22.

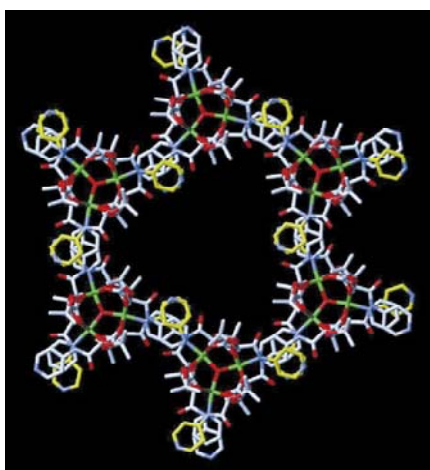


Figure 1.22. The hexagonal framework with large pores that is formed with the trinuclear secondary building units. The pyridyl groups those are exposed in the pore are shown in yellow.

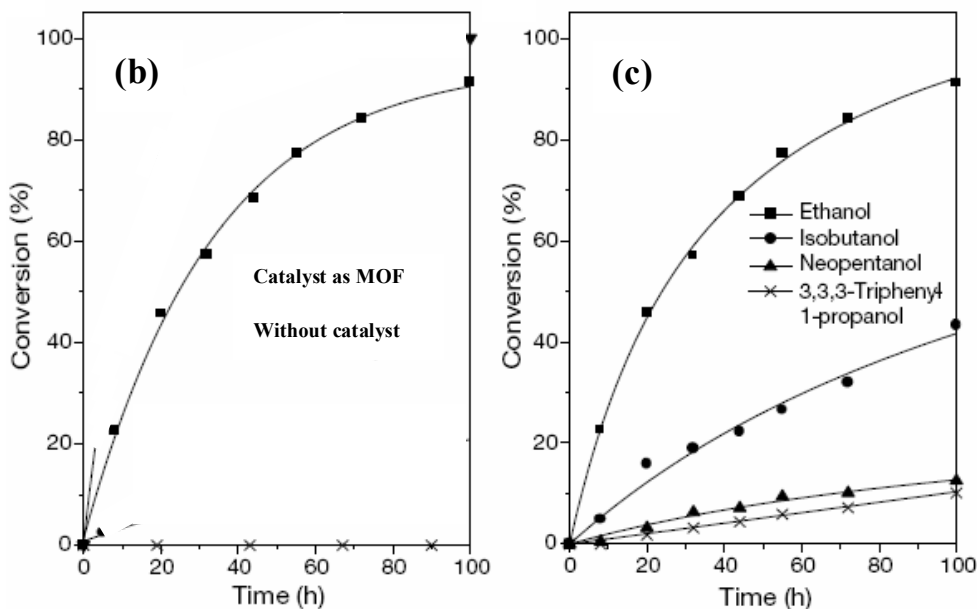
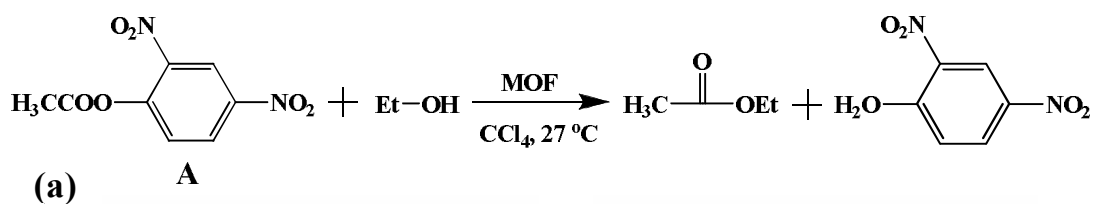


Figure 1.23. (a) Transesterification reaction scheme (b) Transesterification of **A** with ethanol in the presence of MOF. The reaction was carried out in carbon tetrachloride at 27 °C in the absence of MOF. (c) The reaction was carried out with ethanol, isobutanol, neopentanol or 3,3,3-triphenyl-1-propanol with same reaction condition.

The presence of the pyridyl groups exposed in the channels provide a unique opportunity in catalysis. Hence, catalytic activity study of transesterification reactions was carried out, in presence of this porous framework. The reaction profile is shown in Figure 1.23a. Treatment of compound **A** and ethanol with suspension of MOF (0.1 equivalents) in carbon tetrachloride for 55 h at 27 °C produced ethyl acetate in 77% yield. No or little transesterification occurs in absence of MOF (Figure 1.23b). Transesterification of compound **A** with bulkier alcohols such as isobutanol,

neopentanol and 3,3,3-triphenyl-1-propanol occurs with a much slower or even negligible rate under otherwise identical reaction conditions (Figure 1.23c). Such size selectivity suggests that the catalysis mainly occurs in the channels.

The numerous illustrations of various metal organic assemblies in the literature as exemplified in the above sections, demonstrate the potentials of the assemblies towards the development of materials of tailor-made properties. Thus, exploration of new assemblies is of great significance for various application studies. In this direction, as the carboxylates play a significant role in the several MOFs, coordination assemblies of benzene penta and hexa carboxylic acids have been considered to explore the structural features by deducing three dimensional structures, with the aid of single crystal X-ray diffraction methods. The results obtained and salient features of the assemblies are described in chapter 4.

1.9. References

1. Feynman, R. P. *Eng. Sci.* **1960**, *23*, 22–26.
2. Lehn, J. M. *Pure Appl. Chem.* **1978**, *50*, 871-892.
3. (a) Whitesides, G. M.; Mathias, J. P.; Seto, C. T. *Science* **1991**, *254*, 1312-1319. (b) Whitesides, G. M.; Grzybowski, B. *Science* **2002**, *295*, 2418-2421. (c) Philip, D.; Stoddart, J. F. *Angew. Chem., Int. Ed.* **1996**, *35*, 1154-1196. (d) Lehn, J.-M. *Angew. Chem., Int. Ed.* **1990**, *29*, 1304-1319. (e) Lehn, J. M. *Science* **2002**, *295*, 2400-2403. (f) Orr, G. M.; Barbour, L.; Atwood, J. L. *Science* **1999**, *285*, 1049-1051.
4. Fischer E. *Ber. Dt. Chem. Ges.* **1894**, *27*, 2985–2993.

5. (a) *Comprehensive Supramolecular Chemistry*; Eds. Atwood, J. L.; Davies, J. E. D.; MacNicol, D. D.; Vögtle, Pergamon: Oxford, 1996. (b) Lehn, J. -M. *Supramolecular chemistry: concepts and perspectives*; VCH: Weinheim, 1995. (c) Pedersen, C. J. *Angew. Chem., Int. Ed.* **1988**, *27*, 1021-1027. (d) Cram, D. *J. Angew. Chem., Int. Ed.* **1988**, *27*, 1009-1020.
6. Dietrich, B.; Lehn, J. M. *Tetrahedron Lett.* **1969**, *10*, 2885-2888.
7. (a) Rudkevich, D. M. *Angew. Chem., Int. Ed.* **2004**, *43*, 558-571. (b) Oshovsky, G. V.; Reinhoudt, D. N.; Verboom, W. *Angew. Chem., Int. Ed.* **2007**, *46*, 2366-2398. (c) Blake, A. J.; Champness, N. R.; Hubberstey, P.; Li, W.S.; Withersby, M. A.; Schröder, M. *Coord. Chem. Rev.* **1999**, *183*, 117-138. (d) Chae, H. K.; Siberio-Pérez, D. Y.; Kim, J.; Go, Y.; Eddaoudi, M.; Matzger, A. J.; O'Keeffe, M.; Yaghi, O. M. *Nature* **2004**, *427*, 523-527.
8. (a) Jeffrey, G. A.; Saenger, W. *Hydrogen Bonding in Biological Structures*; Springer-Verlag: Berlin, 1991. (b) Jeffrey, G. A. *An Introduction to Hydrogen Bonding*; Oxford University Press: New York, 1997. (c) Steiner, T. *Angew. Chem. Int. Ed.* **2002**, *41*, 48-76.
9. (a) *Comprehensive Supramolecular Chemistry, Solid-State Supramolecular Chemistry: Crystal Engineering*; MacNicol, D. D.; Toda, F.; Bishop, R. Eds.; Pergamon: New York; Vol. 6, 1996. (b) Moulton, B.; Zaworotko, M. J. *Chem. Rev.* **2001**, *101*, 1629-1658. (c) Desiraju, G. R. *Crystal Engineering: The Design of Organic Solids*; Elsevier: Amsterdam, 1989.
10. (a) Zerkowski, J. A.; Seto, C. T.; Whitesides, G. M. *J. Am. Chem. Soc.* **1992**, *114*, 5473-5475. (b) MacDonald, J. C.; Dorrestein, P. C.; Pilley, M. M. *Cryst.*

- Growth Des.* **2001**, *1*, 29-38. (c) Ma, Y.; Kolotuchin, S. V.; Zimmerman, S. C. *J. Am. Chem. Soc.* **2002**, *124*, 13757-13769. (d) Motherwell, W. D. S.; Ammon, H. L.; Dunitz, J. D.; Dzyabchenko, A.; Erk, P.; Gavezzotti, A.; Hofmann, D. W. M.; Leusen, F. J. J.; Lommerse, J. P. M.; Mooij, W. T. M.; Price, S. L.; Scheraga, H.; Schweizer, B.; Schmidt, M. U.; van Eijck, B. P.; Verwer, P.; Williams, D. E. *Acta Crystallogr., Sect. B: Struct. Crystallogr. Cryst. Chem.* **2002**, *58*, 647-661. (e) Du, M.; Zhang, Z.-H.; Zhao, X.-J. *Cryst. Growth Des.* **2005**, *5*, 1247-1254. (f) Zeng, H.; Miller, R. S.; Flowers, R. A., II; Gong, B. *J. Am. Chem. Soc.* **2000**, *122*, 2635-2644. (g) Rodriguez-Spong, B.; Price, C. P.; Jayasankar, A.; Matzger, A. J.; Rodriguez-Hornedo, N. *Adv. Drug Delivery Rev.* **2004**, *56*, 241-274.
11. Etter, M. C. *Acc. Chem. Res.* **1990**, *23*, 120-126.
12. (a) Etter, M. C.; MacDonald, J. C.; Bernstein, J. *Acta Crystallogr.* **1990**, *B46*, 256-263. (b) Etter, M. C. *J. Phys. Chem.* **1991**, *95*, 4601-4606. (c) Bernstein, J. *Acta Crystallogr.* **1991**, *B47*, 1004-1012. (d) Bernstein, J.; Davis, R. E.; Shimoni, L.; Chang, N. L. *Angew. Chem. Int. Ed.* **1995**, *34*, 1555-1573.
13. (a) Seto, C. T.; Whitesides, G. M. *J. Am. Chem. Soc.* **1990**, *112*, 6409-6411. (b) Whitesides, G. M.; Laibinis, P. E. *Langmuir* **1990**, *6*, 87-96. (c) Bain, C.D.; Whitesides, G. M. *Angew. Chem. Int. Ed.* **1989**, *101*, 522-528.
14. (a) Seto, C. T.; Whitesides, G. M. *J. Am. Chem. Soc.* **1990**, *112*, 6409-6411. (b) Ranganathan, A.; Pedireddi, V. R.; Rao, C. N. R. *J. Am. Chem. Soc.* **1999**, *121*, 1752-1753.

15. *The Crystal as a Supramolecular Entity*, ed. G.R. Desiraju, 1996, Wiley, Chichester, UK.
16. (a) Espinet, P.; Esteruelas, M. A.; Oro, L. A.; Serrano, J. L.; and Sola, E. *Coord. Chem. Rev.*, 1992, **117**, 215; (b) Bissell, R. and Boden, N. *Chem. Br.*, **1995**, 38.
17. (a) Férey, G.; Mellot-Draznieks, C.; Serre, C.; Millange, F.; Dutour, J.; Surblé, S.; Margiolaki, I. *Science* **2005**, *309*, 2040-2042. (b) Abourahma, H.; Moulton, B.; Kravtsov, V.; Zaworotko, M. J. *J. Am. Chem. Soc.* **2002**, *124*, 9990-9991. (c) Wang, X.; Qin, C.; Wang, E. *Cryst. Growth Des.* **2006**, *6*, 439-443. (d) Kitaura, R.; Kitagawa, S.; Kubota, Y.; Kobayashi, T. C.; Kindo, K.; Mita, Y.; Matsuo, A.; Kobayashi, M.; Chang, H.; Ozawa, T. C.; Suzuki, M.; Sakata, M.; Takata, M. *Science* **2002**, *298*, 2358-2361.
18. (a) Theobald, J. A.; Oxtoby, N. S.; Phillips, M. A.; Champness, N. R.; Beton, P. H. *Nature* **2003**, *424*, 1029. (b) Corso, M.; Auwarter, W.; Muntwiler, M.; Tamai, A.; Greber, T.; Osterwalder, J. *Science* **2004**, *303*, 217. (c) Stepanow, S.; Lingenfelder, M.; Dmitriev, A.; Spillmann, H.; Delvigne, E.; Lin, N.; Deng, X. B.; Cai, C. Z.; Barth, J. V.; Kern, K. *Nat. Mater.* **2004**, *3*, 229.
19. Fisher, E. *Ber. Deutsch. Chem. Gesell* **1894**, *27*, 2985.
20. (a) Lehn, J. -M. *Angew. Chem. Int. Ed.* **1988**, *27*, 89-112. (b) Cram, D. J. *Angew. Chem. Int. Ed.* **1988**, *27*, 1009-1112. (c) Pederson, C. J. *Angew. Chem. Int. Ed.* **1988**, *27*, 1021-1027.
21. (a) *Perspectives in Supramolecular Chemistry: The Crystal as a Supramolecular Entity*; Desiraju, G. R., Ed.; Wiley: Chichester, 1996; Vol. 2.

- (b) *Comprehensive Supramolecular Chemistry*; MacNicol, D. D., Toda, F., Bishop, R., Eds.; Pergamon: Oxford, 1996; Vol. 6, pp 1-16.
22. (a) Arora, K. K.; Pedireddi, V. R. *J. Org. Chem.* **2003**, *68*, 9177-9185. (b) Roy, S.; Singh, D. D.; Vijayan, M. *Acta Crystallogr.* **2005**, *B61*, 89-95. (c) Shattock, T.R.; Vishweshwar, P.; Wang, Z.; Zaworotko, M. J. *Cryst. Growth Des.* **2005**, *5*, 2046-2049. (d) MacDonald, J. C.; Dorrestein, P. C.; Pilley, M. M. *Cryst. Growth Des.* **2001**, *1*, 29-38. (e) Kato, T.; Ihata, O.; Ujiie, S.; Tokita, M.; Watanabe, J. *Macromolecules* **1998**, *31*, 3551-3555. (f) Aakeroy, C. B.; Beatty, A. M.; Helfrich, B. A. *Angew. Chem. Int. Ed.* **2001**, *40*, 3240-3242. (g) Butcher, R. J.; Bashir-Hashemi, A.; Gilardi, R. D. *J. Chem. Crystallogr.* **1997**, *27*, 99-107.
23. (a) Lazar, A.; Danylyuk, O.; Suwinska, K.; Perret, F.; Coleman, A. W. *Chem. Commun.* **2006**, 903-905. (b) Vishweshwar, P.; McMahon, J. A.; Oliveira, M.; Peterson, M. L.; Zaworotko, M. J. *J. Am. Chem. Soc.* **2005**, *127*, 16802-16803. (c) Gdaniec, M.; Jankowski, W.; Milewska, M. J.; Poonski *Angew. Chem. Int. Ed.* **2003**, *42*, 3903-3906. (d) Schmuck, C.; Lex, J. *Eur. J. Org. Chem.* **2001**, 1519-1523.
24. (a) Leiserowitz, L. *Acta Crystallogr.* **1976**, *B32*, 775. (b) Görbitz, C. H.; Etter, M. C. *J. Am. Chem. Soc.* **1992**, *114*, 627-631. (c) Beyer, T.; Price, S. L. *J. Phy. Chem. B* **2000**, *104*, 2647-2655. (d) Nangia, A.; Desiraju, G. R. *Top. Curr. Chem.* **1998**, *198*, 57. (e) Berkovitch-Yellin, Z.; Leiserowitz, L. *J. Am. Chem. Soc.* **1982**, *104*, 4052. (f) Bruno, G.; Randaccio, L. *Acta Crystallogr.* **1980**, *B36*, 1711-1712. (g) Bailey, M.; Brown, C. J.; *Acta Crystallogr.* **1967**, *22*, 387-

391. (h) Duchamp, C. J.; Marsh, R. E.; *Acta Crystallogr.* **1969**, *B25*, 5-19. (i) Ermer, O. *J. Am. Chem. Soc.* **1988**, *110*, 3747-3754.
25. Gorbitz, C. H.; Etter, M. C. *J. Am. Chem. Soc.* **1992**, *114*, 627-631.
26. (a) Shimpi, M. R.; SeethaLekshmi, N.; Pedireddi, V. R. *Cryst. Growth Des.* **2007**, *7*, 1958-1963. (b) Perumalla, S. R.; Suresh, E.; Pedireddi, V. R. *Angew. Chem., Int. Ed.* **2005**, *44*, 7752-7757 (c) Pedireddi, V. R.; Jones, W.; Chorlton, A. P.; Docherty, R. *Chem. Commun.* **1996**, 997-998. (d) Aaker□y, C. B.; Salmon, D. J. *CrystEngComm* **2005**, *7*, 439. (e) Shattock, T. R.; Vishweshwar, P.; Wang, Z.; Zaworotko, M. J. *Cryst. Growth Des.* **2005**, *5*, 2046. (f) Steed, J. W. *CrystEngComm* **2003**, *5*, 169. (g) Varughese, S.; Pedireddi, V. R. *Chem. Eur. J.* **2006**, *12*, 1597-1609. (h) Das, D.; Banerjee, R.; Mondal, R.; Howard, J. A. K.; Boese, R.; Desiraju, G. R. *Chem. Commun.* **2006**, 555. (i) Pedireddi, V. R.; Prakashreddy, J.; Arora, K. K. *Tetrahedron Lett.* **2003**, *44*, 4857-4860. (j) Anderson, K. M.; Goeta, A. E.; Hancock, K. S. B.; Steed, J. W. *Chem. Commun.* **2006**, 2138.
27. (a) Li, H.; Eddaoudi, M.; Groy, T. L.; Yaghi, O. M. *J. Am. Chem. Soc.*, **1998**, *120*, 8571; (b) Eddaoudi, M.; Li, H.; Yaghi, O. M. *J. Am. Chem. Soc.*, **2000**, *122*, 1391.
28. (a) McManus, G. J.; Wang, Z.; Zaworotko, M. J. *Cryst. Growth Des.* **2004**, *4*, 11-13 (b) Perry, J. J.; McManus, G. J.; Zaworotko, M. J. *Chem. Commun.* **2004**, *10*, 2534-2535.

29. (a) Braga, D.; Maini, L.; Polito, M.; Mirolo, L.; Grepioni, F. *Chem. Commun.* **2002**, 2960-2961. (b) Braga, D.; Grepioni, F.; Byrne, J. J.; Wolf, A. *J. Chem. Soc.-Chem. Commun.* **1995**, 1023-1024.
30. (a) Kitagawa, S.; Munakata, M. *Trends Inorg. Chem.* **1993**, 3, 437-462. (b) Kondo, M.; Shimamura, M.; Noro, S.; Minakoshi, S.; Asami, A.; Seki, K.; Kitagawa, S. *Chem. Mater.*, **2000**, 12, 1288. (c) Kitagawa, S.; Kondo, M. *Bull. Chem. Soc. Jpn.* **1998**, 71, 1739-1753. (d) Kitagawa, S.; Kitaura, R. *Inorg. Chem.* **2002**, 23, 101-126. (e) Kitagawa, S.; Kawata, S. *Coord. Chem. Rev.* **2002**, 224, 11-34.
31. (a) Vimont, Goupil, J. M.; Lavalley, J. C.; Daturi, M.; Surblo, S.; Serre, C.; Millange, F.; Ferey, G.; Audebrand, N. *J. Am. Chem. Soc.* **2006**, 128, 3218-3227; (g) Surble, S.; Serre, C.; Mellot-Draznieks, C.; Millange, F.; Ferey, G. *Chem. Commun.* **2006**, 284-286.
32. Prior, T. J.; Rosseinsky, M. J. *Chem. Commun.* **2001**, 495-496.
33. Kolotuchin, S. V.; Fenion, E. E.; Wilson, S. R.; Loweth, C. J.; Zimmerman, S.C. *Angew. Chem. Int. Ed.* **1995**, 34, 2654-2657.
34. Sharma, C. V. K.; Zaworotko, M. J. *Chem. Commun.* **1996**, 2655-2656.
35. Bhogala, B. R.; Nangia, A. *Cryst. Growth Des.* **2003**, 3, 547-554.
36. Ma, B. Q.; Coppens, P. *Chem. Commun.* **2003**, 2290-2291.
37. Delori, A.; Suresh, E.; Pedireddi, V. R. *Chem. Eur. J.* **2008**, 14, 6967-6977.
38. Lin, X.; Blake, A. J.; Wilson, C.; Sun, X. Z.; Champness, N. R.; George, M. W.; Hubberstey, P.; Mokaya, R.; Schröder, M. *J. Am. Chem. Soc.* **2006**, 128, 10745-10753.

39. Schmidt, G. M. J. *Pure Appl. Chem.* **1971**, *27*, 647-678.
40. Papaefstathiou, G. S.; Kipp, A. J.; MacGillivray, L. R. *Chem. Commun.* **2001**, 2462-2463.
41. (a) MacGillivray, L. R. *CrystEngComm* **2002**, *4*, 37-41. (b) Friscic, T.; MacGillivray, L. R. *Chem. Commun.* **2005**, 5748-5750. (c) Gao, X.; Friscic, T.; MacGillivray, L. R. *Angew. Chem. Int. Ed.* **2004**, *43*, 232-236.
42. Mei, X.; Liu, S.; Wolf, C. *Org. Lett.*, **2007**, *9*, 2729-2732.
43. Shan, N.; Jones, W. *Tetrahedron Lett.* **2003**, *44*, 3687-3689.
44. (a) Caira, M. R.; Nassimbeni, L. R.; Wildervanck, A. F. *J. Chem. Soc., Perkin Trans.* **1995**, 2213-2216. (b) Stanton, M. K.; Bak, A. *Cryst. Growth Des.* **2008**, *8*, 3856-3862. (c) Hörter, D.; Dressman, J. B. *Adv. Drug. Deliv. Rev.* **1997**, *25*, 3-14. (d) Hancock, B. C.; Parks, M. *Pharm. Res.* **2000**, *17*, 397-404. (e) Bettinetti, G.; Caira, M. R.; Callegari, A.; Merli, M.; Sorrenti, M.; Tadini, C. *J. Pharm. Sci.* **2000**, *89*, 478-489. (f) Fleischman, S. G.; Kuduva, S. S.; McMahon, J. A.; Moulton, B.; Bailey Walsh, R. D.; Rodríguez-Hornedo, N.; Zaworotko, M. J. *Cryst. Growth Des.* **2003**, *3*, 909-919. (g) Almarsson, Ö.; Hickey, M. B.; Peterson, M. L.; Morissette, S. L.; Soukasene, S.; McNulty, C.; Tawa, M.; MacPhee, J. M.; Remenar, J. F. *Cryst. Growth Des.* **2003**, *3*, 927-933. (h) Remenar, J. F.; MacPhee, J. M.; Larson, B. K.; Tyagi, V. A.; Ho, J. H.; McIlroy, D. A.; Hickey, M. B.; Shaw, P. B.; Almarsson, Ö. *Org. Process Res. Dev.* **2003**, *7*, 990-996. (i) Roy, S.; Alexander, K. S.; Riga, A. T.; Chatterjee, K. *J. Pharm. Sci.* **2003**, *92*, 747-759.

45. (a) Almarsson, Ö.; Zaworotko, M. J. *Chem. Commun.* **2004**, *10*, 1889-1896. (b) Morissette, S. L.; Almarsson, Ö.; Peterson, M. L.; Remenar, J. F.; Read, M. J.; Lemmo, A. V.; Ellis, S.; Cima, M. J.; Gardner, C. R. *Adv. Drug. Deliv. Rev.* **2004**, *56*, 275-300. (c) Vishweshwar, P.; McMahon, J. A.; Peterson, M. L.; Hickey, M. B.; Shattock, T. R.; Zaworotko, M. J. *Chem. Commun.* **2005**, 4601-4603. (d) Bis, J. A.; McLaughlin, O. L.; Vishweshwar, P.; Zaworotko, M. J. *Cryst. Growth Des.* **2006**, *6*, 2648-2650. (e) McNamara, D. P.; Childs, S. L.; Giordano, J.; Iarriccio, A.; Cassidy, J.; Shet, M. S.; Mannion, R.; O'Donnell, E.; Park, A. *Pharm. Res.* **2006**, *23*, 1888-1897. (f) Govindarajan, R.; Zinchuk, A.; Hancock, B.; Shalaev, E.; Suryanarayanan, R. *Pharm. Res.* **2006**, *23*, 2454-2468. (g) Friščić, T.; Trask, A. V.; Jones, W.; Motherwell, W. D. S. *Angew. Chem., Int. Ed.* **2006**, *45*, 7546-7550.
46. (a) Vishweshwar, P.; McMahon, J. A.; Bis, J. A.; Zaworotko, M. J. *J. Pharm. Sci.* **2006**, *95*, 499-516. (b) Patel, U.; Haridas, M.; Singh, T. P. *Acta crystallogr.*, **1988** *C44*, 1264-1267. (c) Oswald, I. D. H.; Allan, D. R.; MaGregor, P. A.; Motherwell, W. D.; Parsons, S.; Pulham, C. R. *Acta Crystallogr.*, **2002**, *B58*, 1057-1066. (d) Berge, S. M.; Bighley, L. D.; Monkhouse, D. C. *J. Pharma. Sci.* **1977**, *66*, 1-19. (e) Fleischman, S. G.; Kuduva, S. S.; McMahon, J. A.; Moulton, B.; Bailey Walsh, R. D.; Rodríguez-Hornedo, N.; Zaworotko, M. J. *Cryst. Growth Des.* **2003**, *3*, 909-919. (f) Bhatt, P. M.; Azim, Y.; Thakur, T. S.; Desiraju, G. R. *Cryst. Growth Des.* **2009**, *9*, 951-957. (g) Trask, A. V.; Van De Streek, J.; Motherwell, W. D. S.; Jones, W.

- Cryst. Growth Des.* **2005**, *5*, 2233-2241. (h) Haynes, D. A.; Jones, W.; Motherwell, W. D. S. *J. Pharm. Sci.* **2005**, *94*, 2111-2120.
47. Remenar, J. F.; Morissette, S. L.; Peterson, M. L.; Moulton, B.; MacPhee, J. M.; Guzmán, H. R.; Almarsson, Ö. *J. Am. Chem. Soc.* **2003**, *125*, 8456-8457.
48. Viertelhaus, M.; Hilfiker, R.; Blatter, F.; Moulton, B.; Bailey Walsh, R. D.; Rodríguez-Hornedo, N.; Zaworotko, M. J. *Cryst. Growth Des.* **2009**, *9*, 2220-2228.
49. Fleischman, S. G.; Kuduva, S. S.; McMahon, J. A.; Moulton, B.; Walsh, R. B.; Rodriguez-Horenedo, N.; Zaworotko, M. J. *Cryst. Growth Des.* **2003**, *3*, 909-919.
50. (a) Eddaoudi, M.; Moler, D. B.; Li, H.; Chen, B.; Reineke, T. M.; O'Keeffe, M.; Yaghi, O. M. *Acc. Chem. Res.* **2001**, *34*, 319-330. (b) Yaghi, O. M.; O'Keeffe, M.; Ockwig, N. W.; Chae, H. K.; Eddaoudi, M.; Kim, J. *Nature* **2003**, *423*, 705-714. (c) Fujita, M.; Tominaga, M.; Hori, A.; Therrien, B. *Acc. Chem. Res.* **2005**, *38*, 369-378.
51. (a) Lin, X.; Blake, A. J.; Wilson, C.; Sun, X. Z.; Champness, N. R.; George, M. W.; Hubberstey, P.; Mokaya, R.; Der, M. *J. Am. Chem. Soc.* **2006**, *128*, 10745-10753. (b) Wang, S.; Xing, H.; Li, Y.; Bai, J.; Pan, Y.; Scheer, M.; You, X. *Eur. J. Inorg. Chem.* **2006**, 3041-3053. (c) Wan, Y.; Yang, H.; Zhao, D. *Acc. Chem. Res.* **2006**, *39*, 423-432. (d) Li, Y.; Yang, R. T. *J. Am. Chem. Soc.* **2006**, *128*, 8136-8137. (e) Mueller, U.; Schubert, M.; Teich, F.; Puetter, H.; Schierle-Arndt, K.; Pastre, J. *J. Mater. Chem.* **2006**, *16*, 626-636.

52. (a) Tominaga, M.; Suzuki, K.; Kawano, M.; Kusukawa, T.; Ozeki, T.; Sakamoto, S.; Yamaguchi, K.; Fujita, M. *Angew. Chem. Int. Ed.* **2004**, *43*, 5621-5625. (b) Leininger, S.; Olenyuk, B.; Stang, P. J. *Chem. Rev.* **2000**, *100*, 853-907. (c) Zaworotko, M. J. *Chem. Commun.* **2001**, 1-9. (d) James, S. L. *Chem. Soc. Rev.* **2003**, *32*, 276-288. (e) Batton, S. R.; Robson, R. *Angew. Chem. Int. Ed.* **1998**, *37*, 1460-1494. (f) Ferey, G. *Chem. Commun.* **2003**, 2976-2977. (g) Papaefstathiou, G. S.; MacGillivray, L. R. *Coord. Chem. Rev.* **2003**, *246*, 169-184. (h) James, S. L. *Chem. Soc. Rev.* **2003**, *32*, 276-288. (i) Beatty, A. M. *Coord. Chem. Rev.* **2003**, *246*, 131-143.
53. (a) Matsuda, R.; Kitaura, R.; Kitagawa, S.; Kubota, Y.; Belosludov, R. V.; Kobayashi, T. C.; Sakamoto, H.; Chiba, T.; Takata, M.; Kawazoe, Y.; Mita, Y. *Nature* **2005**, *436*, 238-241. (b) Rosseinsky, M. J. *Microporous Mesoporous Mater.* **2004**, *73*, 15-30. (c) Gomez-Lor, B.; Gutierrez-Puebla, E.; Iglesias, M.; Monge, M. A.; Ruiz-Valero, C.; Snejko, N. *Chem. Mater.* **2005**, *17*, 2568-2573.
54. (a) Kitagawa, S.; Kitaura, R.; Noro, S. I. *Angew. Chem. Int. Ed.* **2004**, *43*, 2334-2375. (b) Ouyang, X. M.; Li, Z. W.; Okamura, T. A.; Li, Y. Z.; Sun, W. Y.; Tang, W. X.; Ueyama, N. *J. Solid State Chem.* **2004**, *177*, 350-360. (c) Batten, S. R.; Murray, K. S. *Coord. Chem. Rev.* **2003**, *246*, 103-130.
55. Li, M. Eddaoudi, M. O'Keeffe, O. M. Yaghi, *Nature* **402**, 276 (1999).
56. Eddaoudi, M.; Kim, J.; Rosi, N.; Vodak, D.; Wachter, J.; O'Keeffe, M.; Yaghi, O. M. *Science* **2002**, *295*, 469-472.

57. Rosi, N. L.; Eckert, J.; Eddaoudi, M.; Vodak, D. T.; Kim, J.; O'Keeffe, M.; Yaghi, O. M. *Science* **2003**, *300*, 1127-1129.
58. Koh, K.; Wong-Foy, A.; Matzger, A. J. *J. Am. Chem. Soc.* **2009**, *131*, 4184-4185.
59. (a) Kitagawa, S.; Kitaura, S.; Noro, S. I. *Angew. Chem. Int. Ed.* **2004**, *116*, 2388–2430 (b) Kitagawa, S.; Uemura, M. *Chem. Soc. Rev.* **2005**, *34*, 109–119; (c) A. J. Fletcher, K. M. Thomas, M. J. Rosseinsky, *J. Solid State Chem.* **2005**, *178*, 2491 – 2510; (d) S. Kitagawa, S. I. Noro, T. Nakamura, *Chem. Commun.* **2006**, 701–707.
60. Matsuda, R.; Kitaura, R.; Kitagawa, S.; Kubota, Y.; Kobayashi, T. C.; Horike, S.; Takata, M. *J. Am. Chem. Soc.* **2004**, *126*, 14063-14070.
61. Dybtsev, D. N.; Chun, H.; Kim, K. *Angew. Chem. Int. Ed.* **2004**, *43*, 5033-5036.
62. Seo, J. S.; Whang, D.; Lee, H.; Jun, S. I.; Oh, J.;Yeon, Y. J. Kim, K. *Nature* **2000**, *404*, 982-986.

**CHAPTER
2**

**Molecular Recognition
Studies of
Benzenepentacarboxylic
Acid with Some Aza-donors**

2.1. Introduction

The crystal is a representation of free energy minimum of a molecule, resulting from the optimization of attractive and repulsive noncovalent interactions, with varying strengths, directional preferences, distance-dependence properties, etc. Hence, understanding the nature and strength of noncovalent interactions is of fundamental importance in supramolecular chemistry.¹ Noncovalent interactions² include charged as well as neutral hydrogen bonds ($\text{O}-\text{H}\cdots\text{O}^-$, $\text{N}^+-\text{H}\cdots\text{O}^-$, $\text{O}-\text{H}\cdots\text{O}$, $\text{N}-\text{H}\cdots\text{O}$, etc.), generally known as strong hydrogen bonds, hydrogen bonds formed by weak donors in the form $\text{C}-\text{H}\cdots\text{X}$, (where X is a oxygen, halogen, sulfur etc.), referred as weak hydrogen bonds, as well as heteroatom interactions such as halogen \cdots halogen, nitrogen \cdots halogen, sulfur \cdots halogen and so on.³ Statistical analysis of a particular type of an interaction in a group of crystal structures lead to useful chemical conclusions. Implicit in the statistical approach to supramolecular chemistry is an insight into the various ways in which the interactions can be grouped together to form sub-structural units. These sub-structural units have been variously termed as motifs,⁴ synthons,⁵ building blocks⁶ or supramolecular patterns.⁷ Knowledge about supramolecular patterns is clearly important to supramolecular synthesis, as understanding of reaction mechanisms and reagents in covalent synthesis. Supramolecular pattern is the smallest structural unit containing the maximum structural information. Accordingly, the supramolecular patterns consist of chemical and geometrical information necessary for the molecular recognition⁸ and for the generation of supermolecules. Thus, in a broader sense, it can be suggested that, supramolecular synthesis of organic ensembles

employing two or more components is a two step process, formation of a supermolecule between the constituents through the recognition of the complimentary functional groups followed by self-assembly⁹ or packing of the supermolecules in the three-dimensional space.

In the supramolecular synthesis, hydrogen bonding interactions¹⁰ are widely used in the design of various assemblies as these intermolecular interactions are highly directional and reproducible. Thus, several studies of systematic analysis of hydrogen bonding patterns have been carried out.¹¹ In this respect, carboxylic acid (–COOH) moieties represent perhaps the most widely studied functional group in terms of understanding of the hydrogen bonding not only in the solid state but in solution as well.¹² Supramolecular assemblies based on the carboxylic group are very well-known because of its ability to form robust hydrogen bonds on its own (*homomeric*)¹³ in the form of dimers as well as catemers and also with complimentary function groups (*hetromeric*)¹⁴ such as aza-donor compounds through O–H···N or O–H···N/C–H···O pair-wise hydrogen bonds. In this process, the design of materials with desired physical, chemical or biological properties is dependent of the geometry, position and conformation of the juxtaposed complimentary hydrogen bonding functional groups. Hence, symmetrically substituted molecule like trimesic acid¹⁵ forms a honeycomb network (Figure 2.1a) by hydrogen-bonding interactions. However, in the presence of 1,2-*bis*(4-pyridyl)ethane, which has potential to form O–H···N hydrogen bonds with –COOH, the trimesic acid forms a super-honeycomb structure as shown in Figure 2.1a.¹⁶ In this direction, a systematic study of synthesis of a variety of supramolecular assemblies, employing other polycarboxylic acids, for example 1,2,4,5-

benzenetetracarboxylic acid and different types of aza-donors as reported by Arora *et al.*,¹⁷ demonstrate the significance of the volume of the aza-donors in the formation of a specific assembly. Pictorial representation of the assemblies is given in the Figure 2.1b. Thus, the carboxylic acid–aza-donor recognition is one of the most reliable supramolecular patterns to obtain desirable architectures.

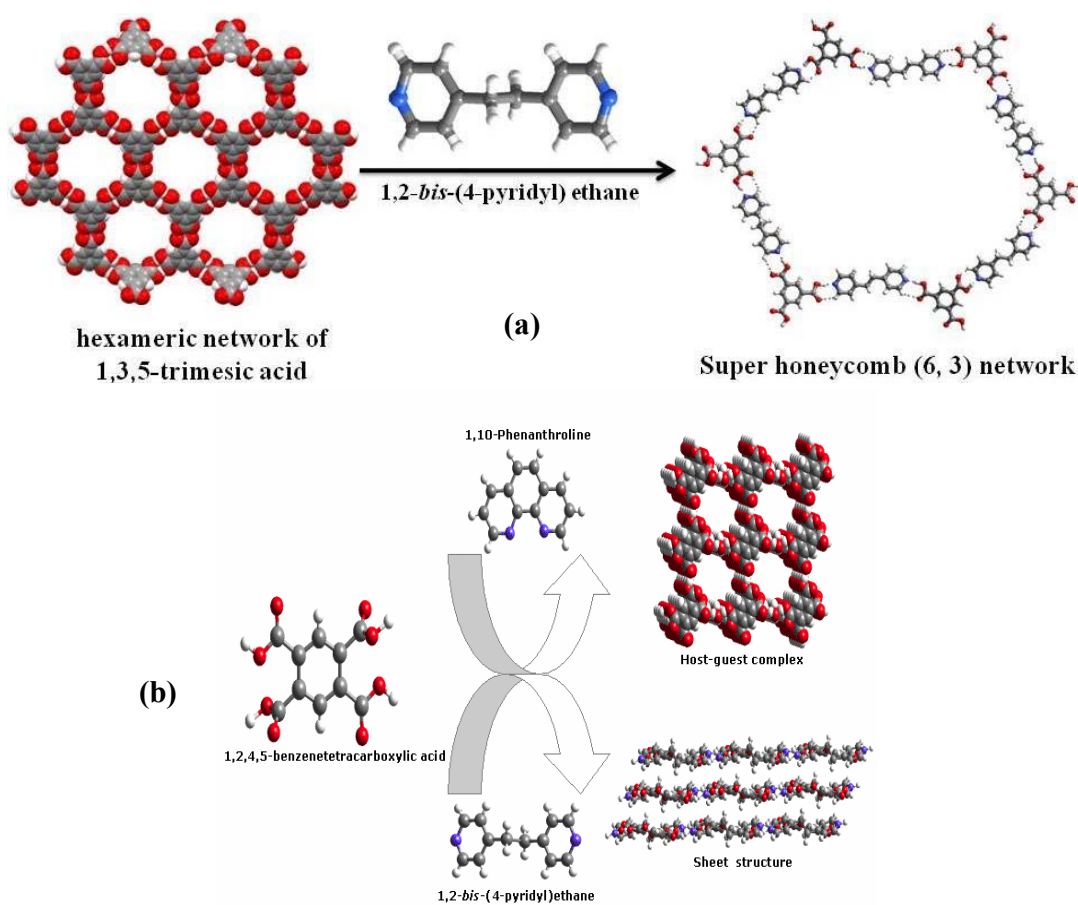


Figure 2.1. (a) Honeycomb network formed by trimesic acid and super-honeycomb network in the molecular complex of trimesic acid and 1,2-bis(4-pyridyl)ethane. (b) Different supramolecular architectures observed in the complexes of 1,2,4,5-benzenetetracarboxylic acid, with different aza-donors.

Analysis of Cambridge Structural Database (CSD)¹⁸ further reveals that molecular complexes of polycarboxylic acids, such as 1,2,3,4,5-benzenepentacarboxylic acid (**BPC**) are not known in the literature except the native crystal structure.¹⁹ In the crystal structure of **BPC**, the molecules are arranged in a sheet form, with each molecule is connected to five neighbours through $R_2^2(8)$ type hydrogen bonding pattern. Interestingly, all the five -COOH groups are involved in such hydrogen bonding patterns, as shown in Figure 2.2.

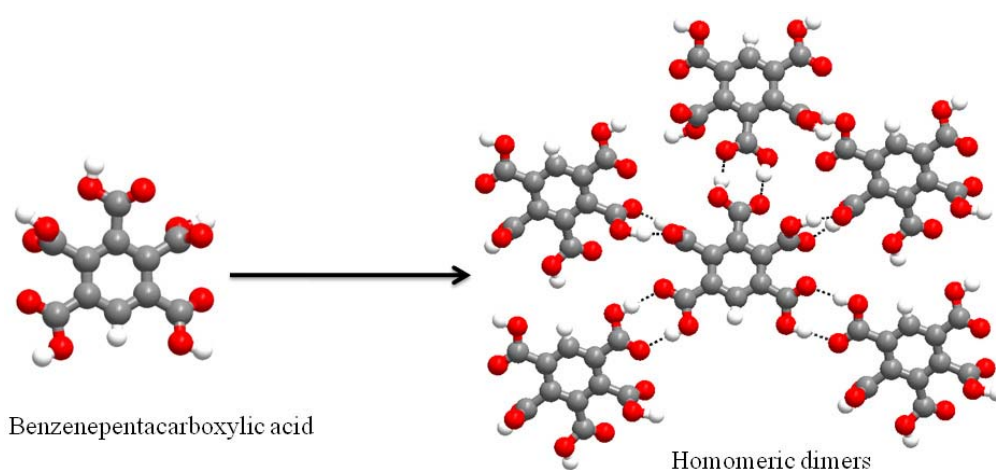


Figure 2.2. Homomeric hydrogen bonds via $R_2^2(8)$ patterns in 1,2,3,4,5-benzenepentacarboxylic acid, (**BPC**).

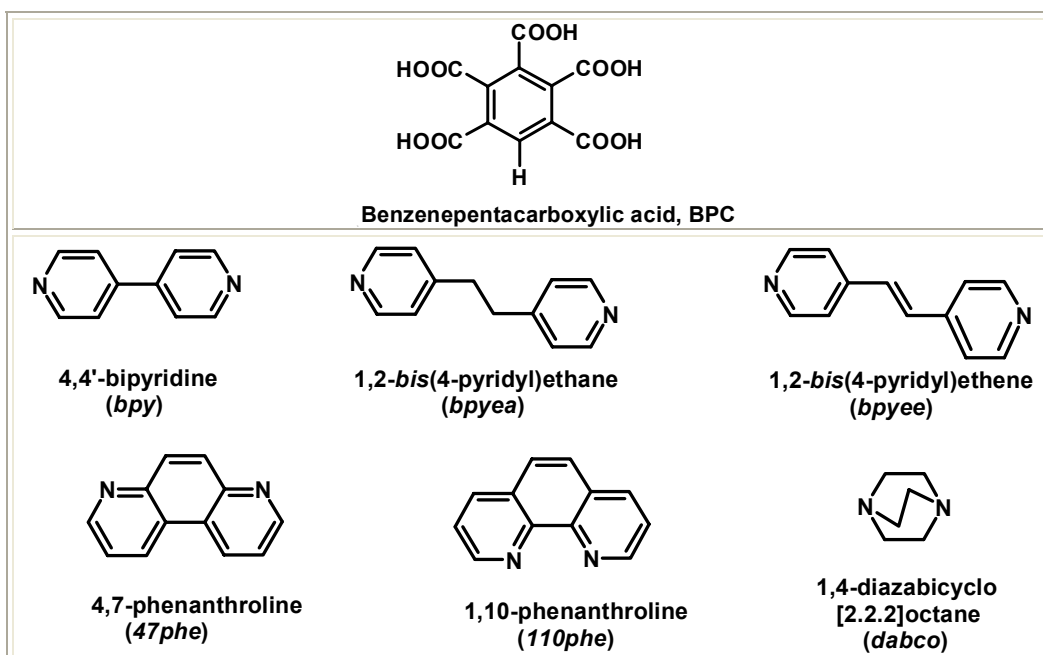
Taking into account the availability of maximum number of carboxylic groups as well as their conformational flexibility, it may be possible to create a myriad of exotic supramolecular assemblies, thus to explore the utilization of **BPC** in supramolecular synthesis, co-crystallization of **BPC** with various aza derivatives as listed in Chart 2.1, has been carried out. Structure determination of all the complexes

reveals several common features as well as distinctly unique features, as discussed in following sections.

2.2. Molecular complexes of 1,2,3,4,5 benzenepentacarboxylic acid, BPC

The synthesis of molecular complexes of **BPC** with various aza-donor compounds, 4,4'-bipyridine (*bpy*), 1,2-bis(4-pyridyl)ethane (*bpyea*), 1,2-bis(4-pyridyl)ethene (*bpyee*), 1,4-diazabicyclo[2.2.2]octane (*dabco*), 1,10-phenanthroline (*110phe*) and 4,7-phenanthroline (*47phe*), as listed in Chart 2.1, has been carried out by following different types of crystallization processes.

Chart 2.1.



In all the cases, good quality single crystals of molecular complexes were obtained, either from slow evaporation at room temperature or hydrothermal method. All the experiments were carried out in a 1:1 ratio of **BPC** and the respective aza-

donor compound, but depending upon the reaction conditions, the molecular complexes were obtained in variable ratios. The resulting molecular complexes are listed in Table 2.1.

Table 2.1. Details of co-crystals formed by **BPC** with different aza-donor compounds.

Reactants	Reactants ratio	Solvent used	Reaction condition	Product and composition (including solvent molecules)
BPC + bpy	1:1	H ₂ O	RT	1a (2:1:7)
BPC + bpyea	1:1	H ₂ O	RT/HT	1b (1:1:4)
BPC + bpyee	1:1	H ₂ O	RT/HT	1c (2:1:2)
BPC + dabco	1:1	H ₂ O	RT/HT	1d (1:1:1)
BPC + 110phe	1:1	H ₂ O	RT/HT	1e (1:2:5)
BPC + 47phe	1:1	H ₂ O	RT	1f (1:2:5)
BPC + bpy	1:1	H ₂ O	HT	1g (1:2)
BPC + 47phe	1:1	H ₂ O	HT	1h (1:1:4)

RT = Room temperature, 4 days; HT = Hydrothermal, 140 °C, 4 days.

2.2.1. Molecular complex of **BPC** and 4,4'-bipyridine (*bpy*), **1a**

Co-crystallization of **BPC** with 4,4'-bipyridine (*bpy*) in a 1:1 ratio, from water, by slow evaporation process, gave good quality crystals, **1a**, suitable for structure determination by X-ray diffraction methods, while other common organic solvents like methanol, chloroform etc., gave only a precipitate. Structure analysis of **1a** reveals that **BPC** and *bpy* co-crystallize as a heptahydrate of 2:1 complex. The complete crystallographic details are given in Table. 2.2 and ORTEP is shown in Figure 2.3.

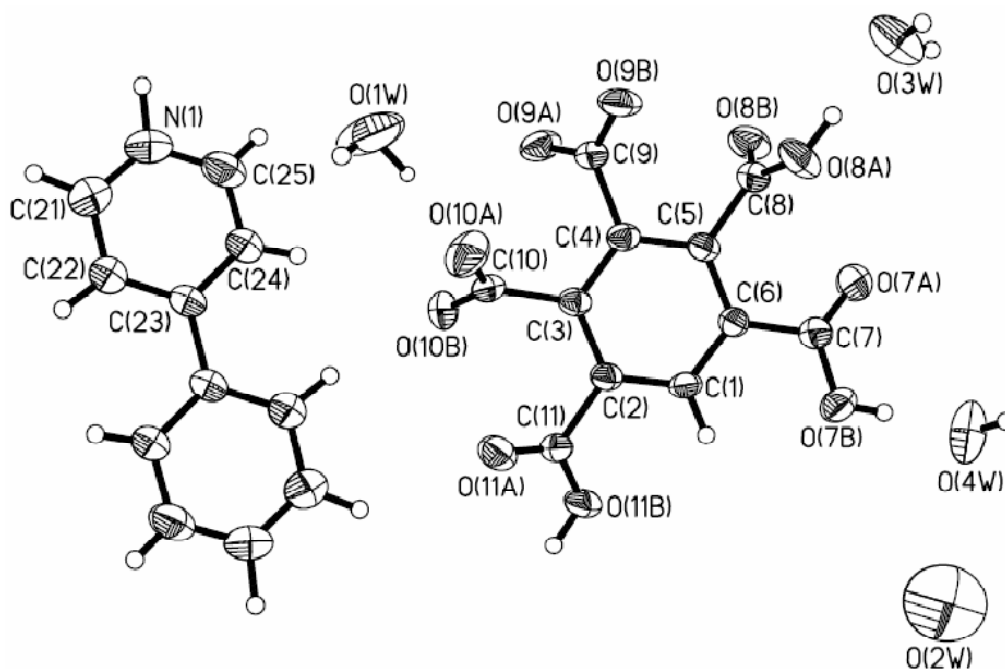


Figure 2.3. ORTEP (50% probability level) of complex **1a**.

In three-dimensional arrangement, the molecules in the complex **1a** form a zeolite-type network (Figure 2.4a) with **BPC** molecules creating an open frame network with voids, which are being filled by *bpy* and water molecules. A detailed analysis reveals that the void space is being created with the aggregation of each of four molecules of **BPC** and water molecules (see Figure 2.4b) that are held together by series of O–H \cdots O (H \cdots O, 1.69, 1.91 Å) hydrogen bonds with H \cdots O distances in the range 1.69–1.91 Å. Molecules of *bpy* interact with such host network of acids, through C–H \cdots O (H \cdots O, 2.38, 2.56 Å) hydrogen bonds (Figure 2.4b). Indeed such a network is realized due to the stacking of layers, with the channels being occupied by *bpy* skewed across the adjacent layers as shown in Figure 2.4c. Further analysis of

intermolecular interactions within a layer is quite intriguing. A typical layer structure is shown in Figure 2.5.

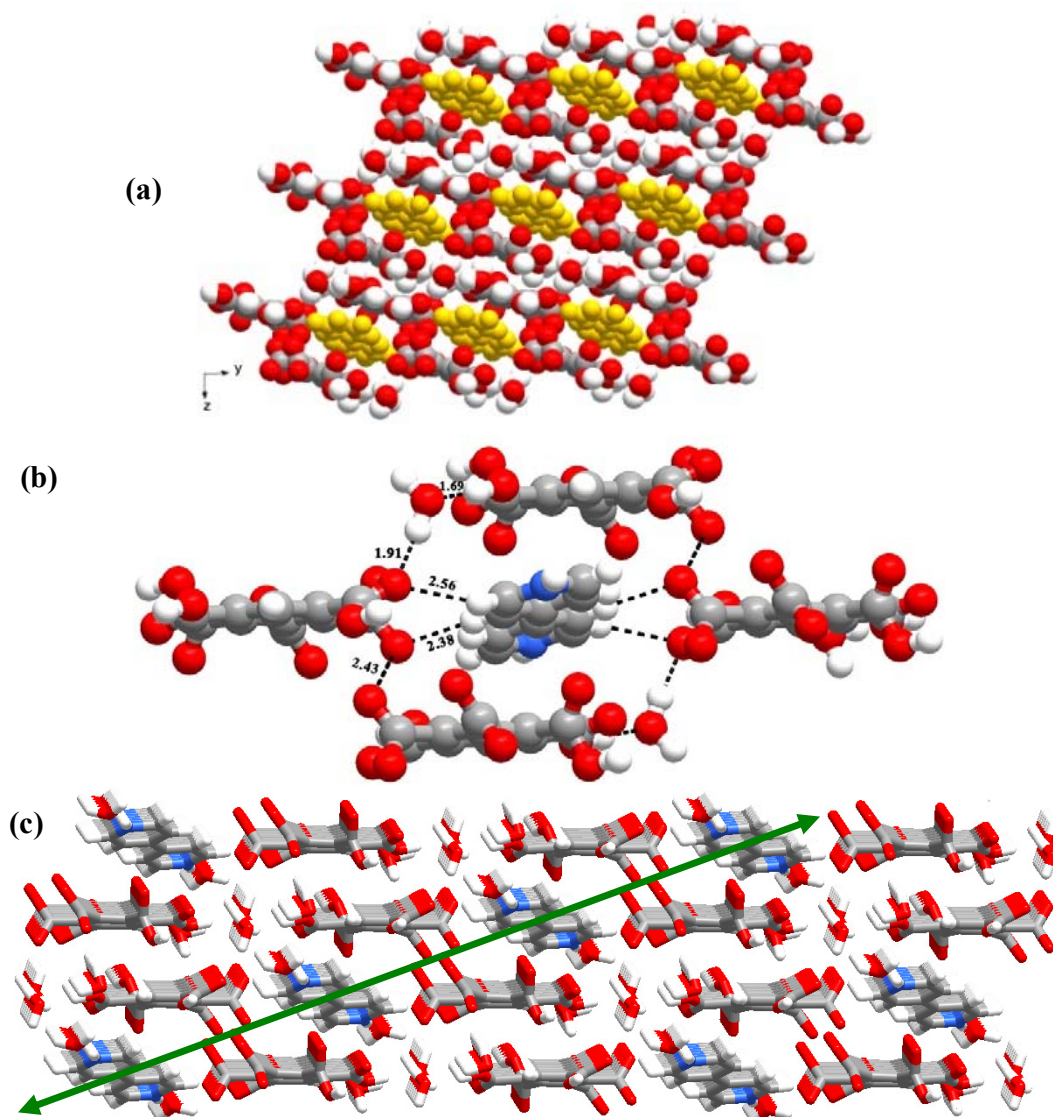


Figure 2.4. (a) Three-dimensional arrangement of molecules in the crystal structure of **1a**. (b) Host-guest type network observed in complex **1a**. (c) An arrangement of stacked layers with *bpy* molecules skewed across the layers in the crystal structure of **1a**.

In each layer, the acid molecules form chains through catemeric $\text{O}-\text{H}\cdots\text{O}^-$ ($\text{H}\cdots\text{O}$, 1.77 Å) hydrogen bonds formed between carboxyl and carboxylates moieties.

Such adjacent acid chains are further held together through water molecules by O–H···O hydrogen bonds, with H···O interaction of 1.69, 1.91 Å. In between such ensembles *bpy* molecules which are glued to other water molecules by O–H···O (H···O, 1.64 Å) hydrogen bonds are inserted. Within this arrangement *bpy* molecules interact with the acid molecules through C–H···O (H···O, 2.38, 2.56 Å) hydrogen bonds as shown in Figure 2.5.

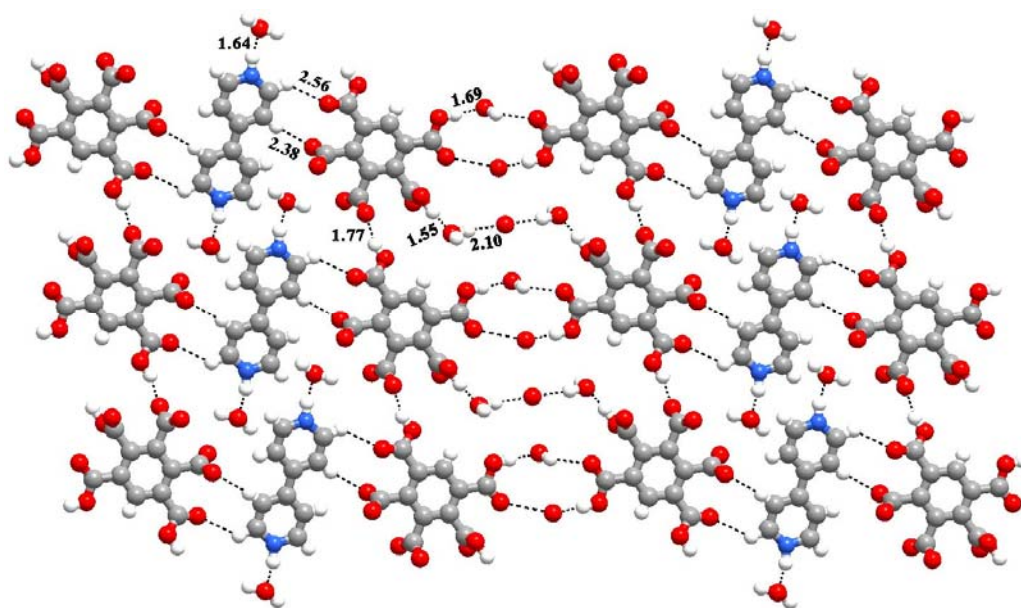


Figure 2.5. A typical layer structure in the complex **1a**.

Taken into account the presence of water molecules and also zeolite type topological network, it is essential to understand the stability of the complex for any further application studies. Thus, a thermogravimetric analysis (TGA) was carried out in the range 25–450 °C, by heating the sample under nitrogen atmosphere. The obtained thermogram curve is shown in Figure 2.6. A noteworthy feature is the observation of weight loss of 14.32% between 60 to 210 °C, which can be correlated

to the release of seven water molecules per formula unit (calcd, 14.37%). It is also apparent from Figure 2.6 that complex **1a** shows to decomposition around 210 °C.

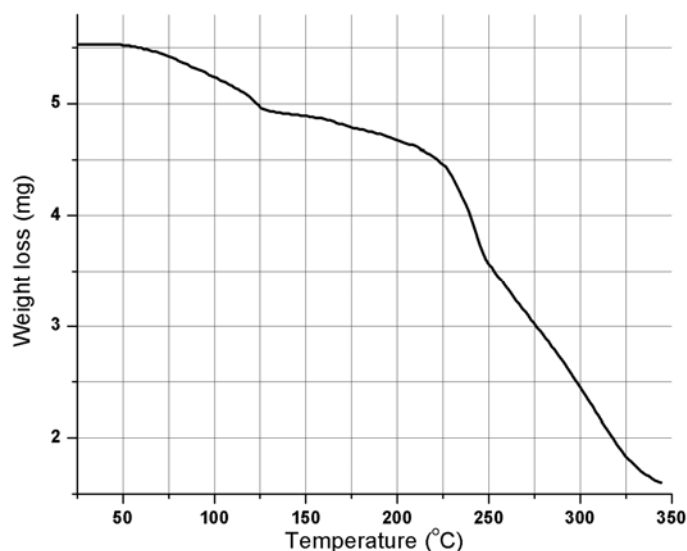


Figure 2.6. Thermogravimetric analysis of complex **1a**.

2.2.2. Molecular complex of BPC and *bpyea*, **1b**

Co-crystallization of **BPC** and 1,2-*bis*(4-pyridyl)ethane (*bpyea*), from water in a 1:1 ratio, by slow evaporation of the solution, gave single crystals of appreciable quality, which were characterized by X-ray diffraction method. Structure analysis reveals that as observed in **1a**, a hydrate of 1:1 complex of **BPC** and *bpyea* is formed which is labeled as **1b**. In the complex **1b**, the asymmetric unit consists of one molecule of **BPC** and two molecules of *bpyea* along with four water molecules, as shown in Figure 2.7. It has been observed that during data collection, at first instance crystal bend in the middle and also crystallinity was lost at ambient laboratory conditions.

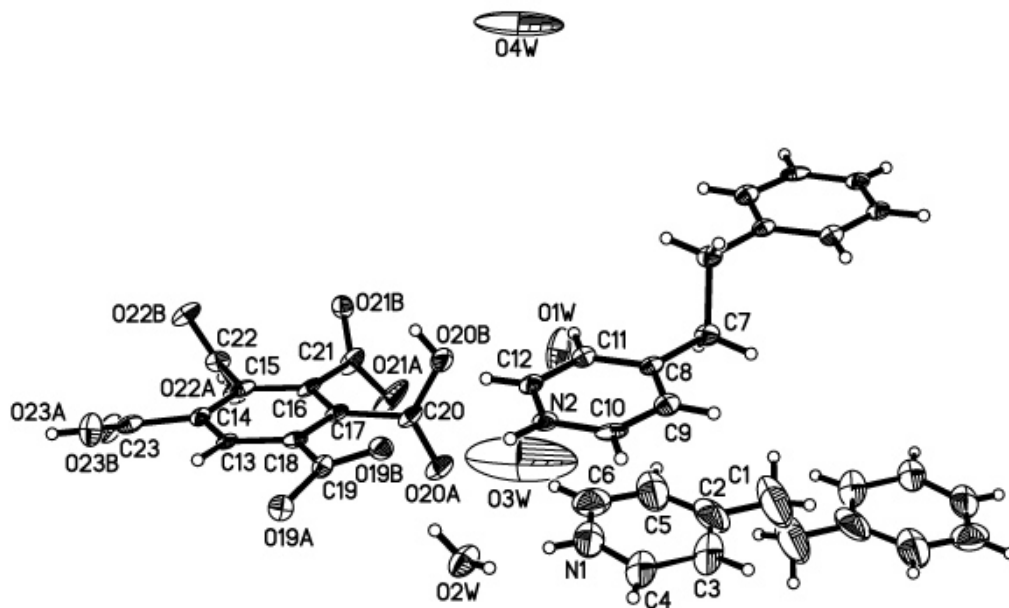


Figure 2.7. ORTEP (50% probability level) of the molecular complex, **1b**, of **BPC** and *bpyea*.

To obtain accurate and good intensity data, the experiment was repeated by smearing the crystals in paraffin oil and also data was collected at lower temperature (100K). Nevertheless, the final data obtained was still not of good quality, but appreciable structure solution could be obtained with *R*-factor being 14.54%, which is, however, relatively higher than generally known for organic assemblies. The complete crystallographic details are given in Table 2.2. The structural analysis reveals that two *bpyea* molecules in the asymmetric unit exist in different conformations.

In three-dimensional arrangement, as found in **1a**, the molecules in the complex **1b** also form a zeolite type network (See Figure 2.8) such that the host is being created by molecules of **BPC**, *bpyea* and water together. A detailed analysis reveals that the host, in the form of four molecular entities, is being created by $N^+ \cdots H \cdots O$ ($H \cdots O$, 1.96 Å) and $O-H \cdots O$ ($H \cdots O$, 2.12 Å) formed by **BPC** and *bpyea* through

water molecules, as depicted in Figure 2.8b. Such adjacent entities are further held together by second *bpyea* molecules through $N^+ \cdots H \cdots O^-$ ($H \cdots O^-$, 1.90 Å) hydrogen bonds formed directly with the $-COO^-$ moieties of **BPC** molecules (Figure 2.8b). It is noteworthy to mention that the channels observed in the complex **1b** are occupied by four water molecules which do not show any appreciable interaction among them as intermolecular distance between the adjacent water molecules is in the range 2.93-3.96 Å.

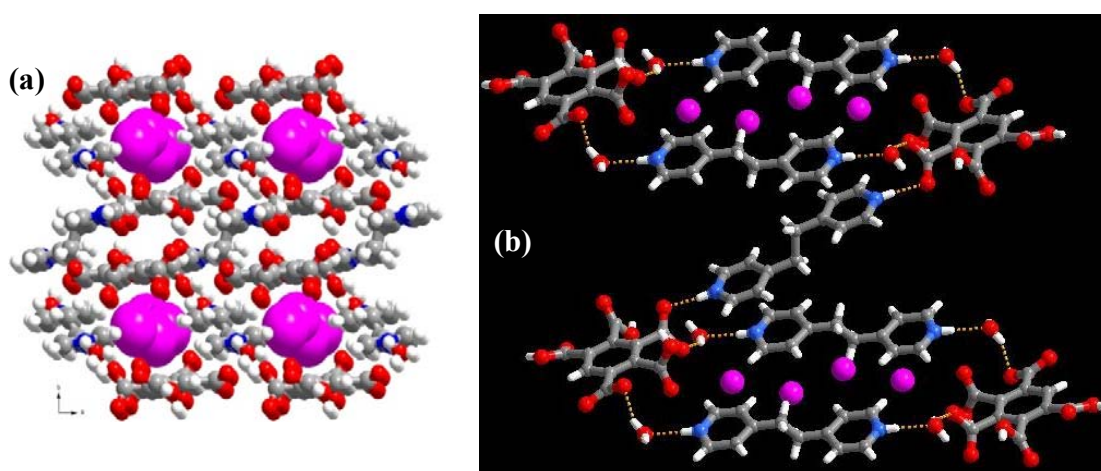


Figure 2.8. (a) A three-dimensional view of complex **1b** along a crystallographic direction, with water molecules in the channels shown in magenta. (b) Aggregation of molecules in two dimensional arrangement in the complex **1b**.

Further, to understand the robustness of the host network as well as stability of the complex, **1b**, thermogravimetric analysis is performed in an inert atmosphere in the range 25 °C to 350 °C. The thermogram plot is shown in Figure 2.9. In contrast to the observation in **1a**, steady weight loss is noted with 4.03% and 4.09% in two successive stages in the temperature range 60-120 °C. It may be correlated to the loss of water molecules exist in the crystal lattice in two environments (host network and

guest positions). Further, the complex is found to be thermally stable up to 180 °C and then decomposes, as shown in Figure 2.9.

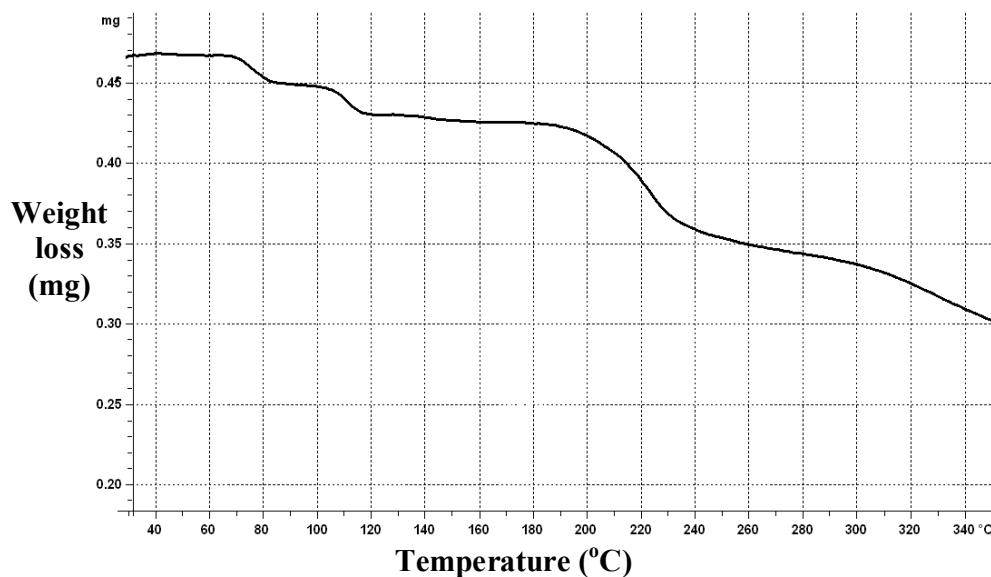


Figure 2.9. A plot of thermogravimetric analysis of complex, **1b**.

In supramolecular synthesis, often molecular dimension plays a significant role rather than hybridization of the carbon skeleton as long as the required acceptor/donor groups are available at desired geometrical positions. Thus, structural analogue of a specific ligand, in general, forms isostructural complexes. Since, in the complex **1b**, an exotic zeolite type network, which is also quite stable thermally, is observed, co-crystallization of **BPC** with, 1,2-*bis*(4-pyridyl)ethene (*bppee*), a structural analogue of the aza-donor employed in the preparation of **1b**, has been carried out.

2.2.3. Molecular complex of BPC and *bpyee*, **1c**

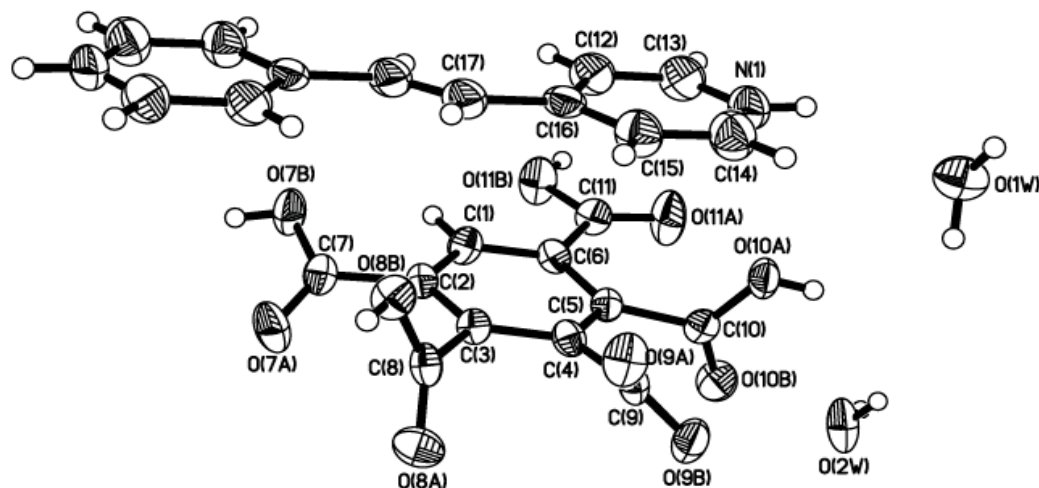


Figure 2.10. ORTEP of the solvated 2:1 complex of BPC with *bpyee*, **1c**. Displacement ellipsoids are at the 50% probability level.

BPC and 1,2-*bis*(4-pyridyl)ethene (*bpyee*) gave single crystals of a molecular complex, **1c**, as a hydrate in a 2:1 ratio by slow evaporation of the water solution at room temperature. The asymmetric unit is shown in the Figure 2.10.

Pictorial representation of three-dimensional arrangement is shown in Figure 2.11a. In contrast to anticipated iso-structurality with **1b**, in complex **1c**, three dimensional structure is observed in the form of stacked layers, known for numerous organic supramolecular assemblies, while interaction between the adjacent layers is exclusively formed by water molecules via O–H \cdots O (O \cdots H 1.87, 1.91 Å) hydrogen bonds as shown in Figure 2.11b. The arrangement of the molecules and recognition patterns, in a typical layer between the constituents is shown in Figure 2.12.

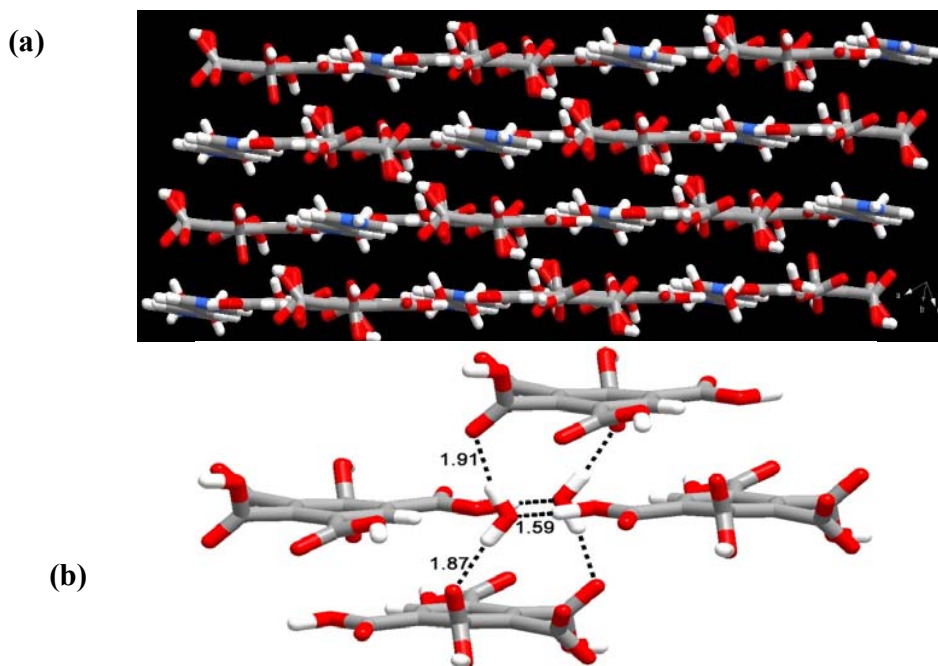


Figure 2.11. (a) Close packing of stacked layers in the crystal lattice. (b) Highlighting the O–H \cdots O hydrogen bonds formed between the sheets in complex **1c**.

Within the two dimensional arrangement, the adjacent **BPC** molecules are held together as dimers by O–H \cdots O (H \cdots O, 1.65 Å) hydrogen bonds. Such dimers are further connected to each other through water molecules by different hydrogen bonds with H \cdots O distances of 1.59 and 1.98 Å, thus, yielding infinite molecular tapes. Interestingly, *bpyee* molecules in the form of charged species are sandwiched along with the water molecules, in between the molecular tapes of **BPC** (Figure 2.12) and establish interaction with the tapes through N–H \cdots O (H \cdots O, 1.98 Å) and a varieties of C–H \cdots O hydrogen bonds.

The structural analysis further reveals that supramolecular assembly in complex **1c** may not be as stable as observed in **1a** and **1b** as the water molecules

played a direct role in the open framework network without participating as a space filling moieties.

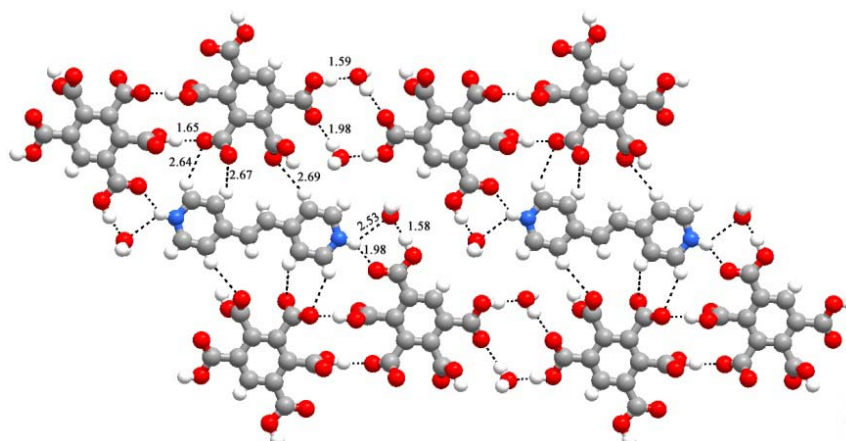


Figure 2.12. Arrangement of molecules within a typical layer observed in the structure, **1c**.

In fact, the thermogravimetric (TG) analysis, as given in Figure 2.13, shows that **1c** starts decomposing around 100 °C, soon after the release of water molecules, characterized by the rapid weight loss of 8.76%, coincident with estimated water content from the structural features.

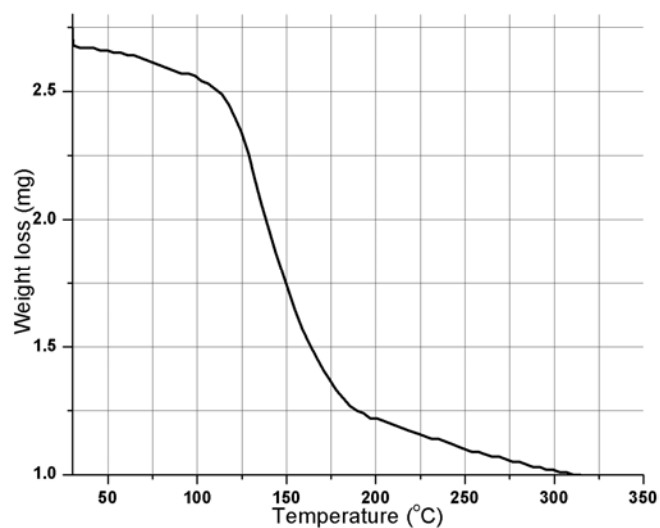


Figure 2.13. Thermogravimetric analysis of complex, **1c**.

2.2.4. Molecular complex of BPC and *dabco*, **1d**

Co-crystallization of **BPC** with 1,4-diazabicyclo[2.2.2]octane, *dabco*, in a 1:1 ratio, gave good quality crystals, **1d**, suitable for structure determination by X-ray diffraction methods, from water, by slow evaporation process. The ORTEP of the asymmetric unit is shown in the Figure 2.14a. Unlike in the complexes **1a-1c**, in **BPC** molecules, the carboxylic group at C₄ position is disordered. The complete crystallographic details and the characteristics of hydrogen bonds are given in Tables 2.2 and 2.3, respectively.

As observed in the structure of the molecular complex, **1c**, the three-dimensional structure of complex **1d** is also due to the stacking of planar layers, as shown in Figure 2.14b. A typical layer is shown in Figure 2.14c. Within each layers, the **BPC** molecules are held together in the form of molecular chains by catemeric O-H \cdots O hydrogen bonds with an H \cdots O distance of 1.69 Å. Further, such chains are connected to each other through water molecules by O-H \cdots O (H \cdots O, 1.75 Å) and O-H \cdots O⁻ (H \cdots O, 2.11 Å) hydrogen bonds. Such an association is left with void space of $8 \times 10 \text{ \AA}^2$, which is being occupied by *dabco* molecules, establishing N⁺-H \cdots O⁻ hydrogen bonds with the corresponding H \cdots O⁻ distance being 1.68 and 2.38 Å. In addition, *dabco* molecules form a variety of C-H \cdots O hydrogen bonds with the **BPC** molecules.

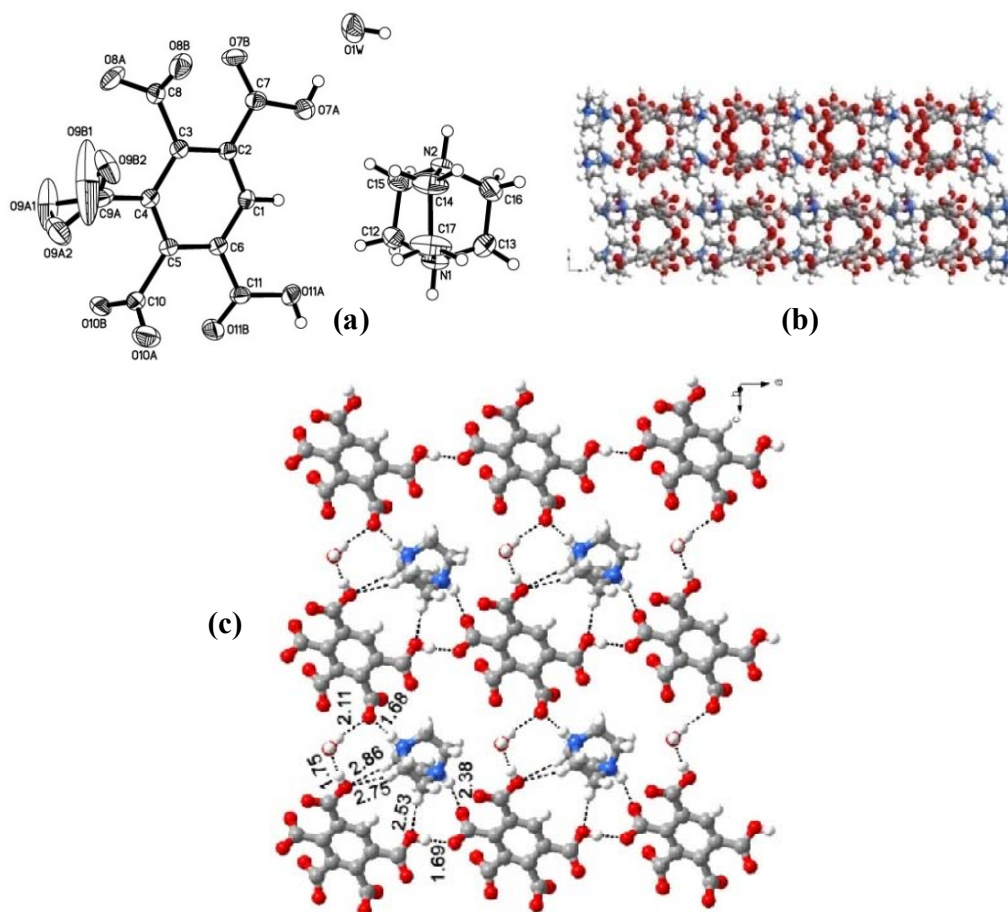


Figure 2.14. (a) ORTEP (50% probability level) of asymmetric unit in the molecular complex, **1d**. (b) Stacking of layers in the three-dimensional arrangement in the crystal structure of **1d**. (c) Arrangement of molecules in a typical layer noted in the complex **1d**.

Since the complex **1d** is also a hydrated ensemble, thermogravimetric analysis has been carried out as did in **1a-1c** to obtain further information to correlate the packing of molecules with stability and robustness of the network, etc.

Thermogravimetric analysis is performed in a nitrogen gas atmosphere in the temperature range of 25-350 °C, with heating rate of 10 °C per min and weight change that occurs is recorded against temperature as the crystal is heated. Thermographic plot is shown in Figure 2.15. It is noteworthy to mention that there is no appreciable

and measurable weight loss till 180 °C but the complex shows the decomposition feature directly from 180 °C onwards. This feature suggests that water molecules are strongly bound within the framework, unlike in the complexes **1a-1c**.

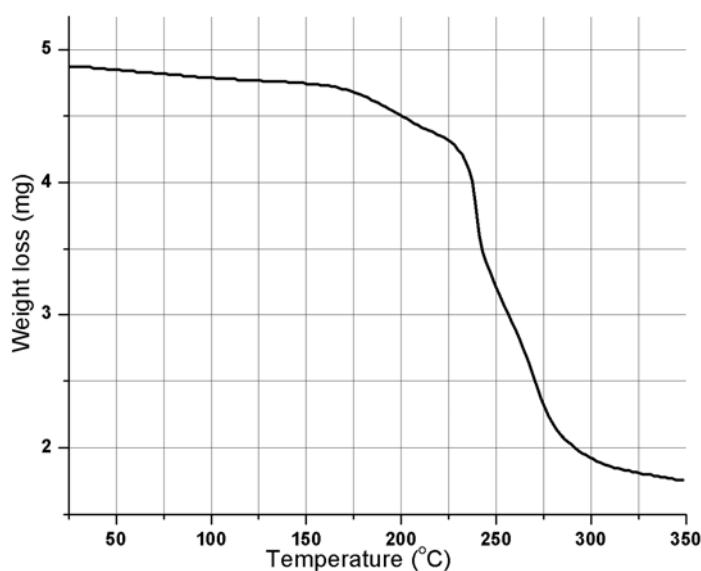


Figure 2.15. TGA plot illustrating variation in the weight loss against temperature rise, in complex **1d**.

2.2.5. Molecular complex of BPC and *110phe*, **1e**

A molecular complex of **BPC** and 1,10-phenanthroline (*110phe*), is prepared at room temperature by slow evaporation of water solution of the co-crystal formers in the form of single crystals. The X-ray structure determination of the single crystals, thus, obtained revealed the formation of a molecular complex, **1e**, as a pentahydrate of **BPC** and *110phe* in a 1:2 ratio and the asymmetric unit is shown in Figure 2.16. Pertinent crystallographic details are given in Table 2.2.

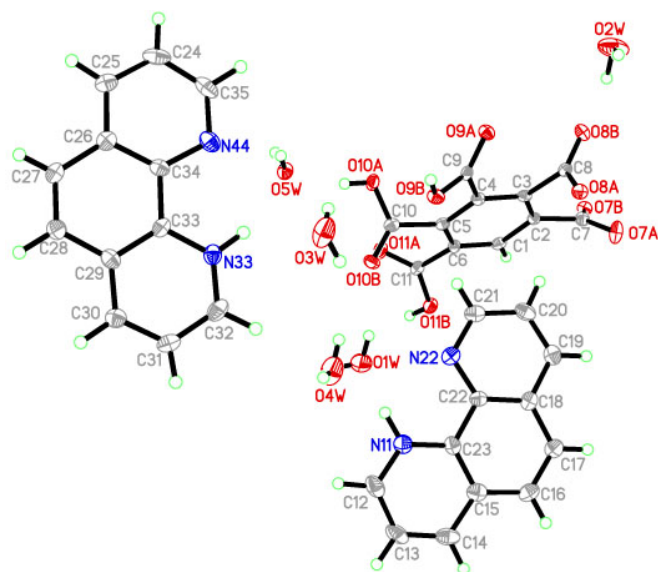


Figure 2.16. ORTEP (50% probability level) of the molecular complex, **1e** of **BPC** and 1,10 Phenanthroline, **110 phe**.

Analysis of molecular packing reveals that in complex, **1e**, the **BPC** molecules along with water molecules form a host network with channels of dimensions 10 x 14 Å², which are being occupied by **110phe** molecules, mimicking a zeolite type structure, as observed in the complex **1a**. The assembly is shown in Figure 2.17a. Further analysis, however, reveals that the channels are formed due to the interaction between the zig-zag molecular tapes of **BPC** through water molecules, as shown in Figure 2.17b. In a typical sheet, **BPC** molecules are held together in the form of chains by pair-wise O–H^{···}O[–]/C–H^{···}O (H^{···}O, 1.71, 2.55 Å) hydrogen bonds as shown in Figure 2.17c. Such chains are further connected to each other through water molecules by different type of O–H^{···}O hydrogen bonds. The details of the hydrogen bonds are given in Table 2.3.

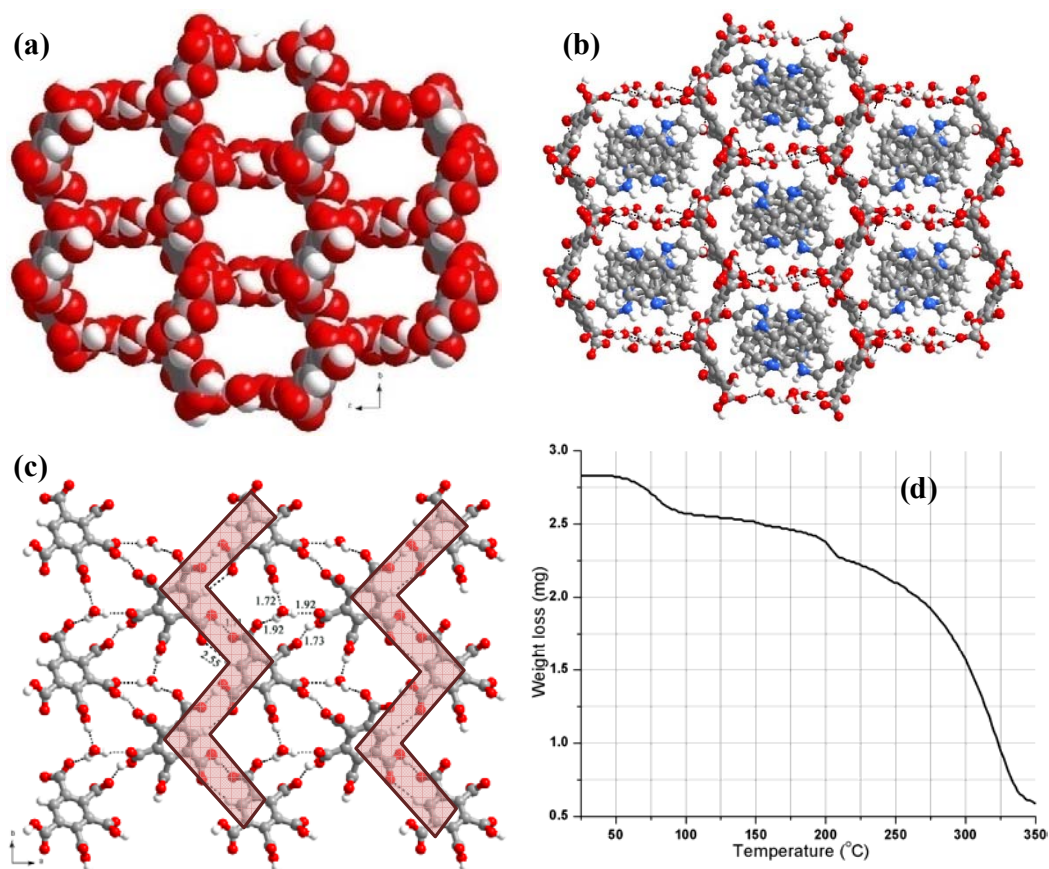


Figure 2.17. Three-dimensional host assembly (a) with the cavities of $10 \times 14 \text{ \AA}^2$ and (b) with guest molecules in complex **1e**. (c) Two dimensional arrangement of **BPC** molecules in complex **1e**. (d) TGA plot of complex **1e**.

In the complex, **1e**, since the water molecules are essentially involved in the formation of open frameworks, as observed in **1c**, the thermal stability of the complex **1e** also is expected to be low.

Thermogravimetric analysis performed in the range 25-350 °C, as shown in Figure 2.18d, indicates weight loss of 3.4% around 80 °C, corresponding to the total number of water molecules in the structure. In fact, **1e** shows decomposition soon after

the removal of water molecules and confirms the structure directive role of water in the formation of host network.

2.2.6. Molecular complex of BPC and 47phe, 1f

Co-crystallization of BPC and 4,7-phenanthroline (*47phe*), dissolved in water, gave single crystals, by slow evaporation process, as a pentahydrate of 1:2 molecular complex, **1f**. The contents of a symmetric unit are shown in Figure 2.18. In the complex **1f** also, two of the –COOH groups are deprotonated as observed in the complex, **1e**.

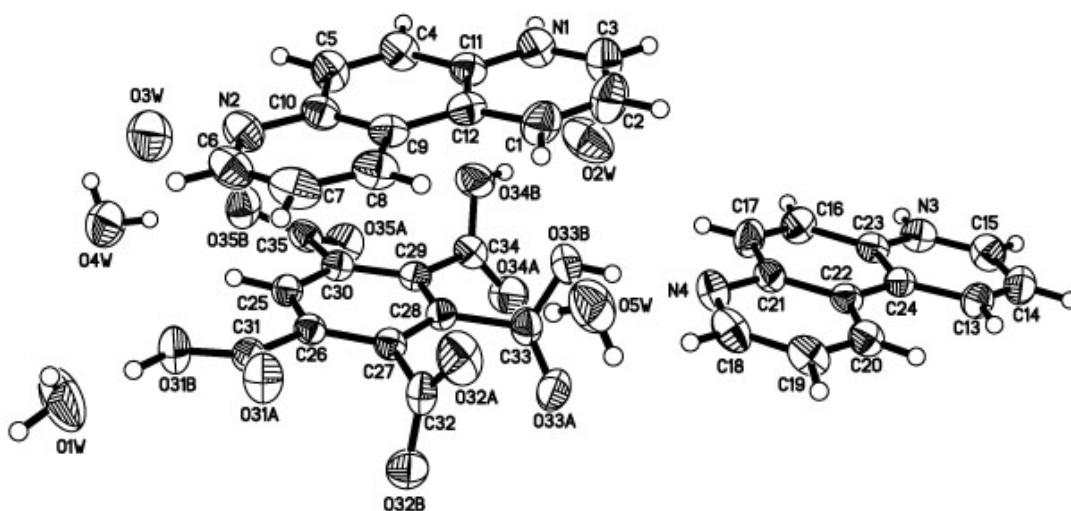


Figure 2.18. ORTEP of asymmetric unit in the crystal structure of **1f**.

Structural analysis of **1f**, shows several other similar features to that of complex **1e**. Firstly, in three dimensional arrangement, the molecules are packed mimicking zeolite type network consisting of host network with channels, which are filled by guest molecules, as shown in Figure 2.19a.

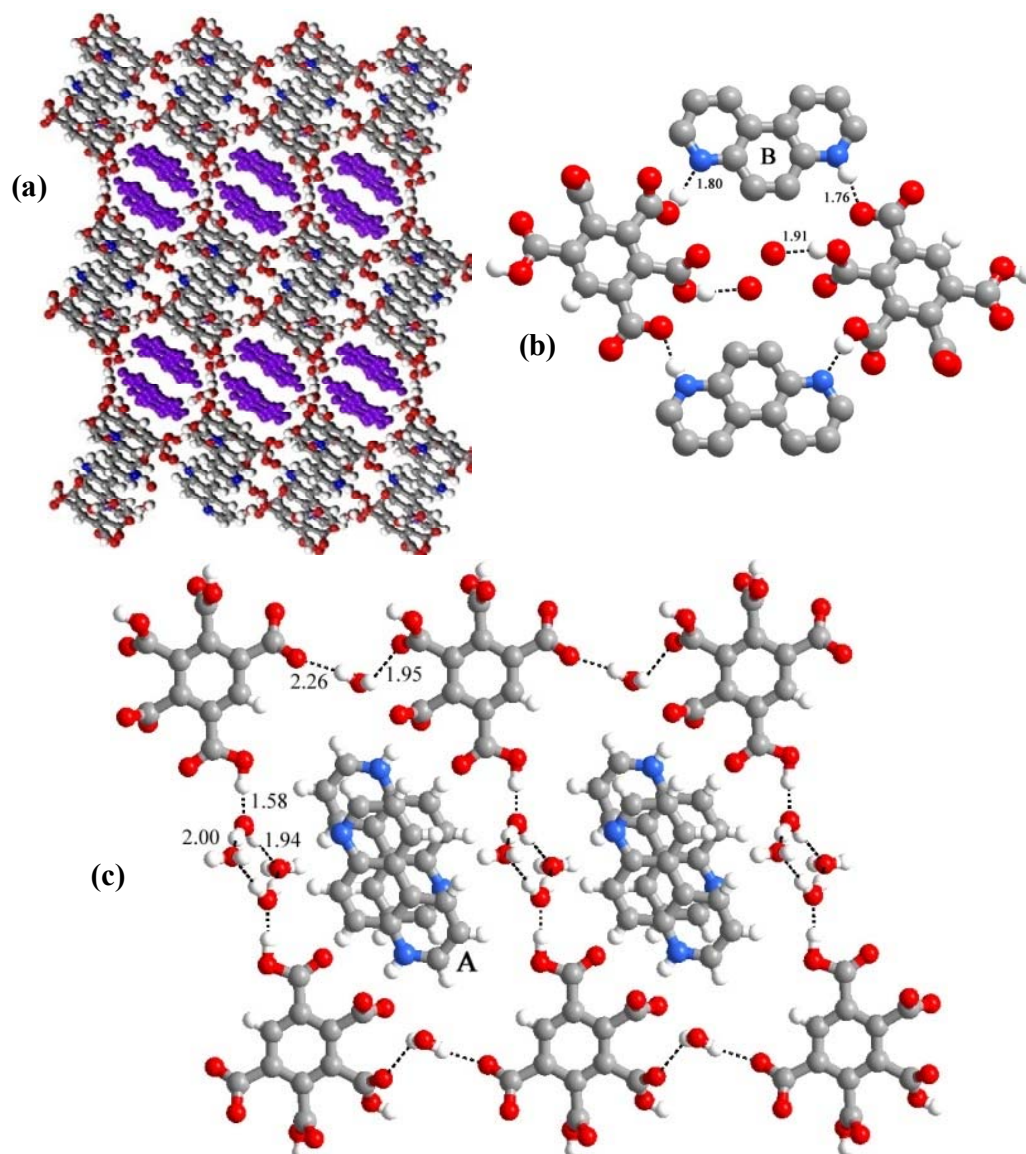


Figure 2.19. (a) Three dimensional arrangement observed in the complex, **1f** in the form of zeolite-type assembly. (b) Tetrameric unit formed between **BPC** and **47phe** (**B**-type) with guest water molecules. (c) Illustration of host-guest arrangement in the complex **1f**.

However, the nature of intermolecular interactions, the molecular arrangements and channels is quite different. For example, within two-dimensional arrangement **BPC** molecules interact with one of the **47phe** molecules (labeled **B**)

through O–H \cdots N (H \cdots O, 1.80 Å) and N $^+$ –H \cdots O $^-$ (H \cdots O, 1.76 Å) hydrogen bonds, creating small voids, that are occupied by water molecules as shown in Figure 2.19b. Further, such entities are propagated through interactions formed with another cyclic moieties, that are formed due to the association of molecules of **BPC** and water, with void space, which is being occupied by other *47phe* molecules. Such a cyclic network is shown in Figure 2.19c. In this network each of four **BPC** molecules connects to each other through different types of water molecules by several O–H \cdots O hydrogen bonds. The details are given in Table 2.3.

It is understood that as found in all other structures, described so far, in **1f** also water molecules play a crucial role in the formation of host network as well as guest species. In fact, this feature is well reflected in the thermogravimetric analysis as shown in Figure 2.20.

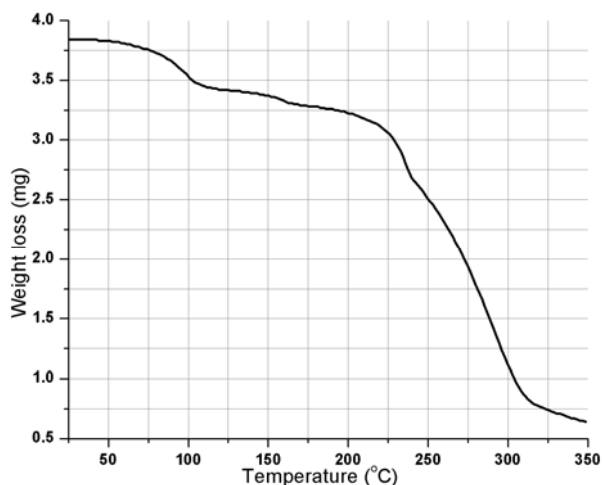


Figure 2.20. TGA plot illustrating weight loss in complex **1f**.

Thermogravimetric experiment was carried out by heating the sample of **1f** in the range 25–350 °C and the corresponding weight loss at every 10 °C variation in the

temperature is recorded. It was noted that all the five water molecules are lost below 120 °C with overall weight loss observed (~12%) matches with the estimated percentage from the structural analysis. And also the complete compound shows decomposition feature soon after losing the water as noted in **1e**.

In the further extension of exploring more assemblies of **BPC** with aza-donors, co-crystallization of it with 1, 7-phenanthroline was carried out as it is isostructural with the aza donors employed in **1e** and **1f** complexes. However, no single crystals were obtained from either water or any organic solvents. In fact, attempts even to crystallize by hydrothermal methods were also unsuccessful as in all the cases, only precipitates were obtained. However, the precipitates appear to be the adduct of **BPC** and *17phen* as X-ray powder diffraction patterns (XRPD) show significant differences with that of the co-crystal formers.

In recent years, crystallization/co-crystallization by following different routes, either by changing solvent of crystallization or method of crystallization gain much popularity as newer assemblies were found to be obtained even with the same co-crystal formers. Often, the obtained assemblies may be polymorphic form but sometimes complex of different composition or trapping of solvent of crystallization in varied ratios also been observed. Since the complexes **1a-1f** are hydrated complexes, it is expected that following different crystallization method may perturb the degree of hydration and possibly formation of assemblies of different types of architectures.

Hence, co-crystallization **BPC** with the aza-donors used in the preparation of **1a-1f**, 4,4'-bipyridine (*bpy*), 1,2-bis(4-pyridyl)ethane (*bpyea*), 1,2-bis(4-pyridyl)ethene

(*bpyee*), 1,4-diazabicyclo[2.2.2]octane (*dabco*), 1,10-phenanthroline (*110phe*), and 4,7-phenanthroline (*47phe*), has been carried out by hydrothermal co-crystallization method. It has been observed that while *bypea*, *bpyee*, *dabco* and *110phe* yielded the same molecular complex with **BPC** as obtained at room temperature conditions, interestingly in the case of *bpy* and *47phe*, **BPC** gave different molecular complexes characterized by single X-ray crystal diffraction methods. A detailed account of these results is given below.

2.2.7. Molecular complex of BPC and *bpy*, **1g**

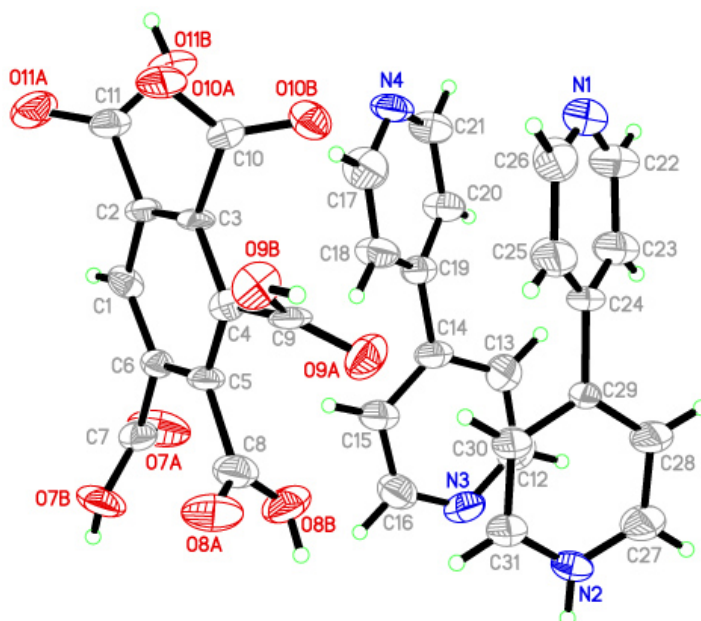


Figure 2.21. ORTEP drawing of asymmetric unit in the crystal structure of **1g**.

Treatment of **BPC** and *bpy* in a hydrothermal bomb at 140 °C for 4 days gave colorless block-type crystals, **1g**. The structure determination reveals that it is an

anhydrous complex of the co-crystal formers in 1:2 ratio (see Figure 2.21). Pertinent crystallographic details are given in Table 2.2.

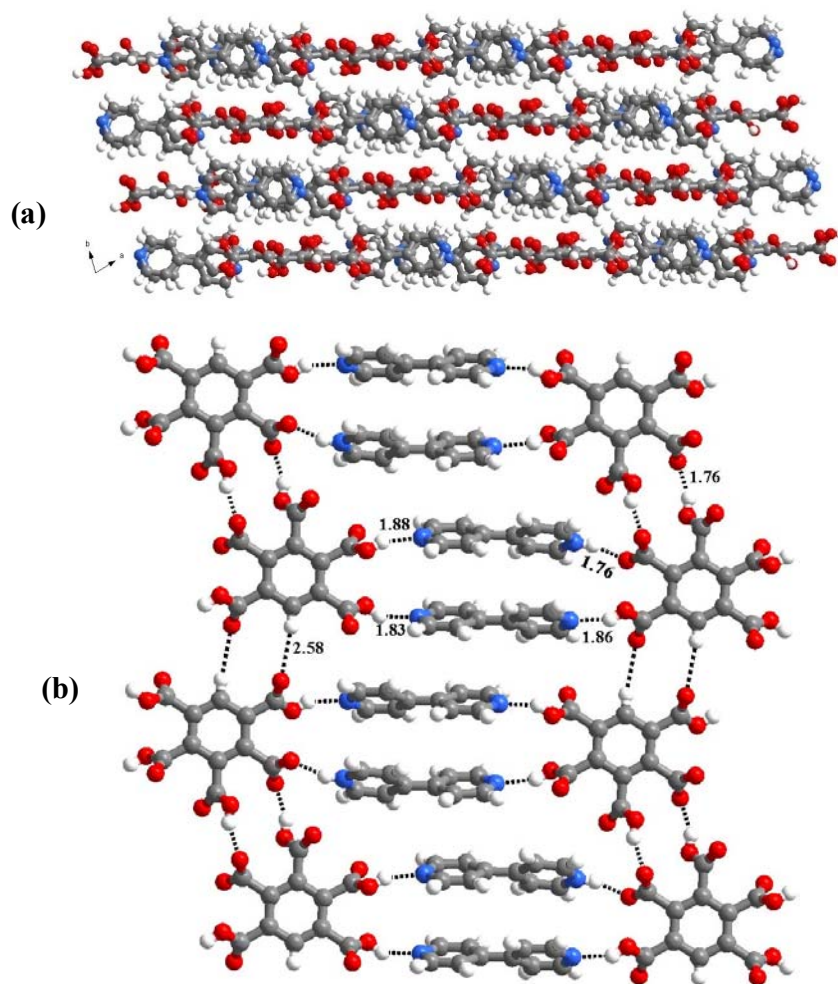


Figure 2.22. (a) Three-dimensional arrangement of molecules in the form of stacked layers observed in the crystal structure of **1g**. (b) Formation of ladder like structure by **BPC** and *bpy* in the complex **1g**.

It may be noted that one of the carboxylic group is deprotonated in the acid moiety. The three dimensional arrangement is in the form of stacked layers, as shown in Figure 2.22a. In a typical layer, the adjacent **BPC** molecules form rods type

geometry by two catemeric O–H \cdots O (H \cdots O, 1.76 Å) hydrogen bonds, through R $_2^2$ (14) motif, and also by two C–H \cdots O (H \cdots O, 2.58 Å) hydrogen bonds, through R $_2^2$ (10) pattern. Between such rods of **BPC**, *bpy* molecules get inserted and establish interaction with the **BPC** molecules by O–H \cdots N (H \cdots N, 1.83, 1.86, 1.88 Å) and N–H \cdots O (H \cdots O, 1.76 Å) hydrogen bonds. Thus, a ladder type structure is realized, with **BPC** molecule as rods, while *bpy* molecules being rungs, as shown in Figure 2.22b.

Since, this is an anhydrous complex, the stability is expected to be of different than **1a**, which is a hydrated complex. In fact, thermogravimetric analysis carried under nitrogen atmosphere in the range 25-350 °C shows that the complex **1g** is highly stable up to 210 °C (See Figure 2.23) without showing any significant weight loss, in agreement with the structural features.

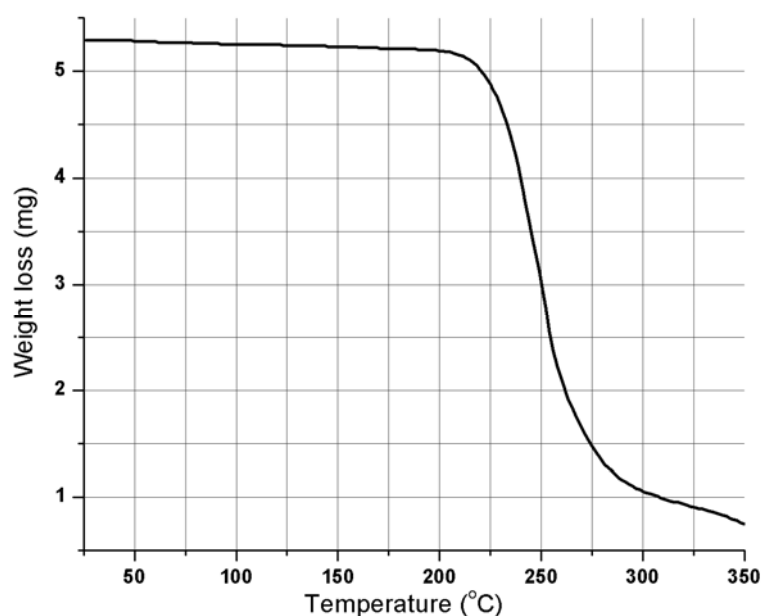


Figure 2.23. Thermogravimetric analysis (TGA) plot of molecular complex of **1g**.

2.2.8. Molecular complex of BPC and 47phe, 1h

Co-crystallization of BPC with 4,7-phenanthroline, (*47phe*) from hydrothermal method also gave block-like colorless crystals like in **1f**, suitable for X-ray diffraction studies. In contrast to **1f**, the structure determination reveals that BPC forms a hydrated molecular complex, **1h** with *47phe*, with the constituents in the asymmetric unit being in a 1:1:4 ratio of the reactants. The ORTEP of the asymmetric unit is shown in Figure 2.24. The complete crystallographic details are given in Table 2.2.

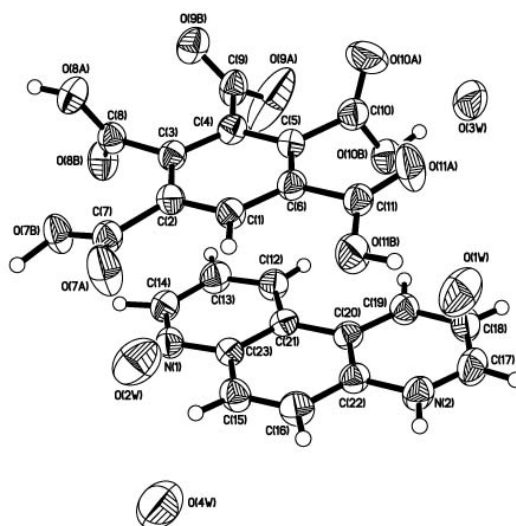


Figure 2.24. ORTEP (50% probability level) of the molecular complex **1h**.

The structural analysis reveals that three dimensional structure of the complex **1h** is the resultant of stacking of layers, constituted by BPC, aza-donor and water molecules (Figure 2.25a).

Within a typical layer, BPC and phenanthroline molecules are held together by a pair wise O–H···N (H···N, 1.54 Å)/C–H···O (H···O, 2.41 Å) hydrogen bonds as well as

single C–H \cdots O (H \cdots O, 2.54 Å) hydrogen bond, yielding chains. The arrangement is shown in Figure 2.25b. Further, each of two adjacent chains are connected to each other by N $^+$ –H \cdots O (H \cdots O, 1.71 Å) hydrogen bonds, as depicted in Figure 2.25b. These ensembles are in turn aggregated in the sheets, through water molecules by numerous hydrogen bonds (See Figure 2.25b).

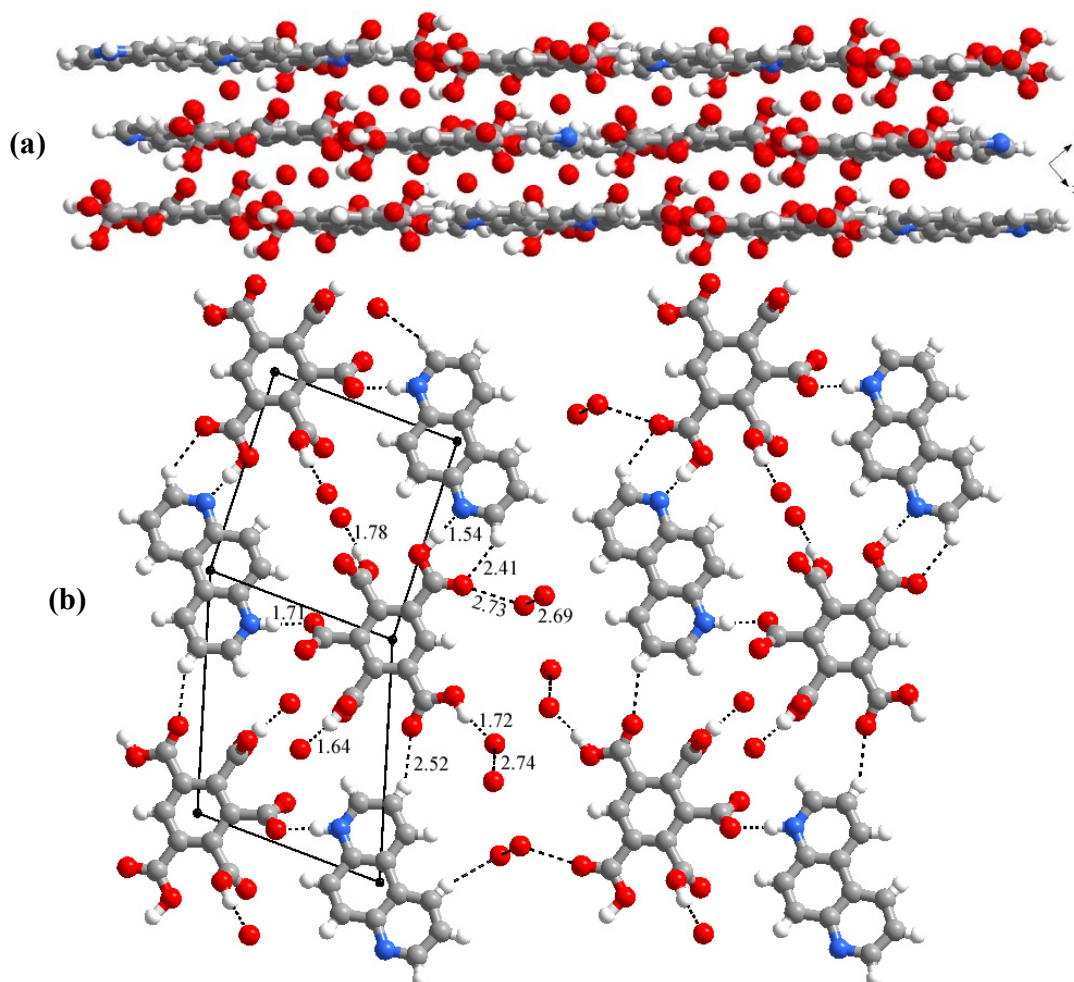


Figure 2.25. (a) A fused tetramer unit formed by acid, **BPC** and **47phe**, in two-dimensional sheet structure observed in complex **1h**. (b) The three-dimensional layer structure formed by the stacking of the sheets along Y-axis.

It is apparent from the structural features that the complex **1h** also may show thermal features like **1a-1f** due to the involvement of water molecules in the stabilization of structure **1h**.

The thermal analysis represented in Figure 2.26 indeed shows that the complex is very much unstable with the continuous weight loss throughout the temperature range.

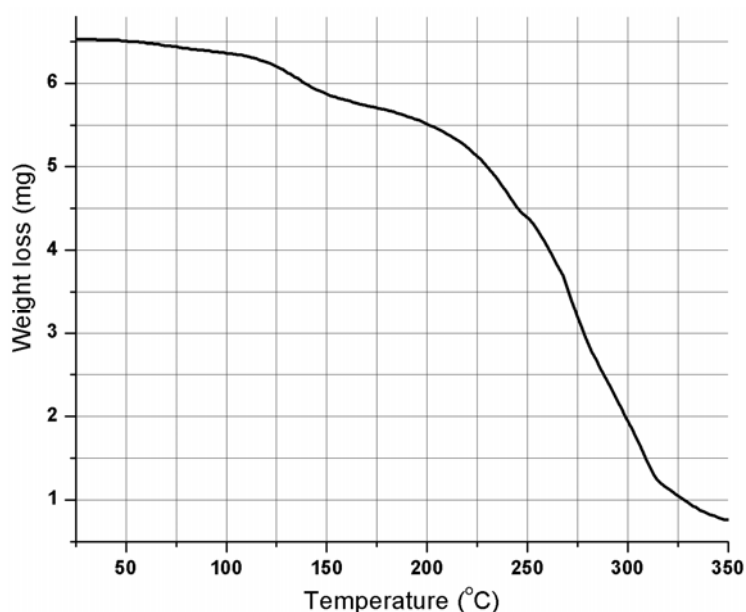


Figure 2.26. TGA plots of complex of **1h**.

Although, the hydrothermal method of crystallization gave different exotic assemblies only in the case of complexes formed by **BPC** with *bpy* and *47phe*, since the characterization is done based on just a single crystal analysis of a bulk material is not essential to rule out the formation of concomitant co-crystals of different types. To ensure that the different forms are due to the variation of crystallization conditions, the structures discussed in the above reactions are true representation of the bulk, powder

X-ray diffraction studies of all the samples have been carried out. The powder patterns, thus, obtained experimentally are compared with the simulated patterns. The patterns are shown in the Figure 2.27. It is well established from Figure 2.27 that in all the complexes, high degree of correlation is found between the simulated and experimental recorded patterns. Thus, confirming the authenticity of the structures done by the single crystal X-ray diffraction methods.

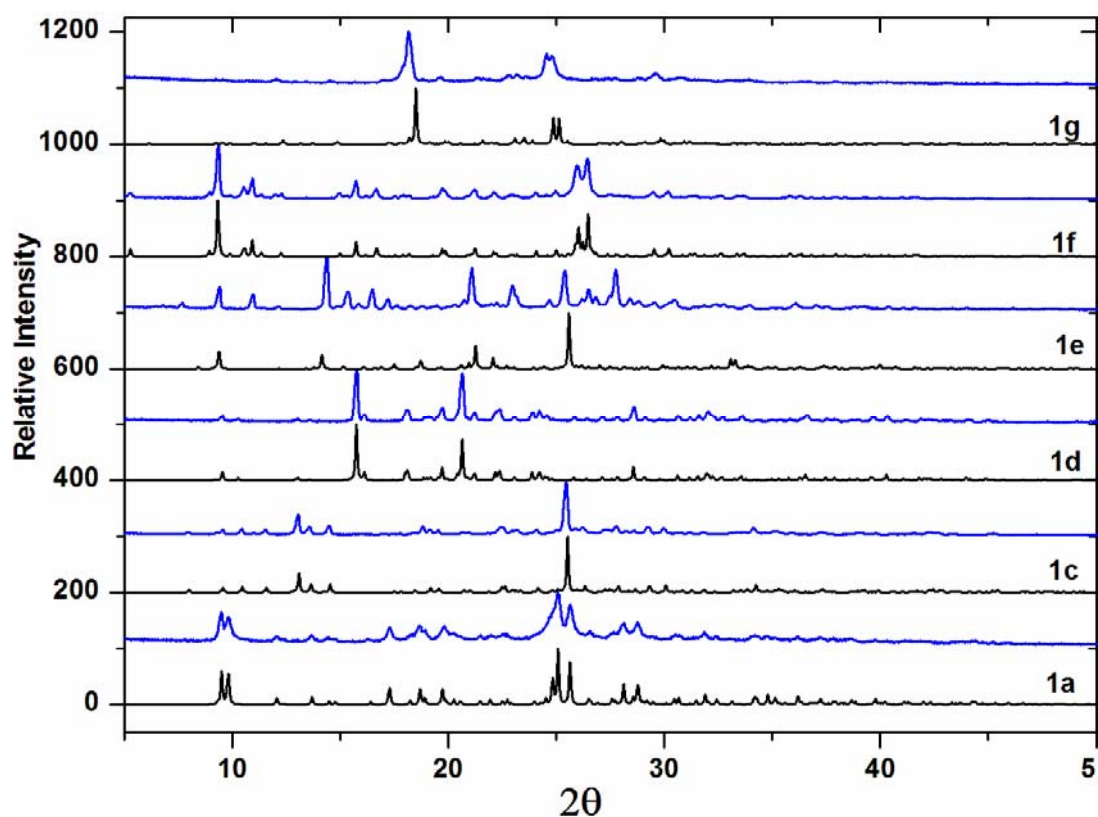


Figure 2.27. XRPD plots shows comparison between simulated XRPD patterns (black) with recorded XRPD patterns (blue) of complexes **1a**, **1c-1h**.

2.3. Conclusions

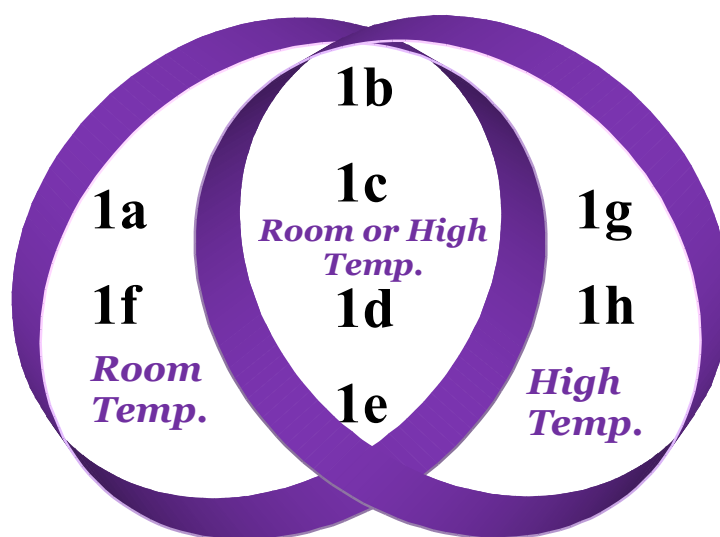
The synthesis and analysis of supramolecular assemblies formed by 1,2,3,4,5-benzenepentacarboxylic acid, **BPC** with various aza-donor compounds, 4,4'-bipyridine (*bpy*), 1,2-bis(4-pyridyl)ethane (*bpyea*), 1,2-bis(4-pyridyl)ethene (*bpyee*), 1,4-diazabicyclo[2.2.2]octane (*dabco*) and 4,7-phenanthroline (*47phe*), 1,10-phenanthroline (*110phe*) have been discussed.

The study has demonstrated the ability of **BPC** to form various supramolecular networks such as zeolite-type network, host guest assemblies, ladders, planar sheets, etc., depending upon the nature of aza-donor compounds in terms of dimensionality, geometrical flexibility etc., thus, demonstrating the significance of polycarboxylic acids in the synthesis of exotic supramolecular assemblies, which were exemplified in earlier studies with trimesic acid and 1,2,4,5-benzenetetracarboxylic acid. In all these assemblies, **1a-1h**, two-dimensional sheets are observed but differ in the mode of stacking. Additionally, the relative orientation of acid and base subunits, within co-crystals, also showed a significant effect in the formation of ultimate three dimensional packing.

It is noteworthy to mention that all the complexes, except **1g**, are hydrated with a variable quantity of water molecules. Significantly, the stability of the complex is directed by the interaction of the water molecules with its co-crystal formers. Further it has been noted that while in the complex **1a**, **BPC** established interaction with aza-donors through water molecules, in the complexes of **1f** and **1h**, **BPC** and the corresponding aza-donor form *heteromeric* hydrogen bonding patterns directly.

However, in the complex, **1e** and **1g**, **BPC** exclusively forms only *homomeric* hydrogen bonding patterns through C–H···O/C–H···O and O–H···O/C–H···O. The complexes **1a**, **1b**, **1e** and **1f** gave zeolite type three dimensional structures of variable channel dimensions, with the host network is being formed exclusively by **BPC** molecules through water molecules, except in **1f**.

It has also been shown that following different crystallization methods, different structures could be obtained but it does not apply universally to all the systems. Thus, **BPC** has shown tendency to form different structure with *bpy* and *47phe* depending upon the temperature of crystallization. But recognition between **BPC** and other aza-donors remains constant irrespective of the conditions. These variations are illustrated in the scheme 2.1 to show the clear distinctions.



Scheme 2.1

Thus, the study has shed some light to further tune of the intermolecular interactions of –COOH group to obtain exotic architectures of supramolecular

assemblies. Also, it reveals the vital role of the intermolecular interactions in the formation of host-guest systems based on the strength and rigidity of the host framework.

2.4. Experimental Section

2.4.1. Synthesis of molecular complexes, **1a** – **1h**

All the chemicals, **BPC** and the aza-donor compounds (*bpy*, *bpyea*, *bpyee*, *dabco*, *4,7 phe* and *1,10 phe*) were purchased from commercial suppliers and used as such without any further purification. Crystallizations were carried out using spectroscopic grade solvents. For a typical crystallization, in a 25 mL conical flask, 74.5 mg (0.25 mmol) of acid, **BPC** and 39.0 mg (0.25 mmol) of *bpy*, were dissolved in hot water and then subsequently cooling to room temperature at ambient conditions. Colorless rectangular block type single crystals of good quality were obtained within 4 days, which were used for single-crystal structure determination studies by X-ray diffraction methods. Complexes, **1g** and **1h** were prepared by hydrothermal method. For example, complex **1g** was obtained by dissolving mg 29.8mg (0.1 mmol) of **BPC** and 15.6 mg (0.1 mmol) of *bpy*, in 15 mL of H₂O in a Teflon-line pressure vessel and heated at 140 °C in a furnace for 4 days. Cooling the apparatus to room temperature, gave single crystals of **1g** in a 1:2 ratio.

2.4.2. Crystal structure determination

Good quality single crystals of molecular complexes **1a** – **1h** were carefully chosen after viewing through a Leica microscope (polarized) supported by a rotatable

polarizing stage and a CCD camera. The crystals were glued to a thin glass fiber using an adhesive (acrylate cyano) and mounted on a diffractometer equipped with an APEX CCD area detector. The X-ray intensity data were collected with varying exposure time, depending upon the quality of the crystal(s). The data collection was smooth in all the cases, except **1b** and no additional precautionary methods have been employed, as the crystals were quite stable. However, data collection in the crystals of **1b** was carried out by smearing the crystals in paraffin oil due to its instability. The intensity data were processed using Bruker's suite of data processing programs (SAINT),²² and absorption corrections were applied using SADABS.²³ The structure solution of all the complexes have been carried out by direct methods, and refinements were performed by full matrix least squares on F^2 using the SHELXTL²⁴ suite of programs. All the structures converged to good R factors. All the non-hydrogen atoms were refined anisotropically, and the hydrogen atoms obtained from Fourier maps were refined isotropically. All the refinements were smooth in all the structures. All the intermolecular interactions were computed using PLATON.²⁰

2.4.3. Thermogravimetric measurements

Thermal gravimetric analyses (TGA) were performed on a Mettler Toledo TGA/SDTA 851e module. Crystals taken from the mother liquor were blotted dry on filter paper and placed in open alumina pans for TGA experiments. Sample size is in the range of 1-7 mg. The samples were heated in the temperature range 25 to 450 °C at a rate of 10 °C/min. The samples were purged with a flow of dry nitrogen at 150 mL/min.

2.4.4. X-ray powder diffraction measurements

X-ray powder diffraction (XPRD) data were collected on a PANalytical diffractometer with $\text{Cu}_{\text{K}\alpha}$ radiation ($\lambda = 1.5406 \text{ \AA}$). The power of the X-ray generator was set to 40 kV and 30 mA with step size of 0.017° (2θ) in a continuous scanning mode. A microcrystalline mixture of the solids was prepared by grinding the required ratio of the precursors with a mortar and pestle for 2–10 min. Diffraction patterns were collected in the 2θ range $5\text{--}50^\circ$, at ambient temperature. Prolonged grinding of the compounds did not alter the diffraction patterns at all.

Table 2.2. Crystallographic data of the molecular complexes **1a-1h**, formed by **BPC** with various aza-donors.

	1a	1b	1c	1d
Formula	2(C ₁₁ H ₄ O ₁₀) (C ₁₀ H ₁₀ N ₂) 7(H ₂ O)	(C ₁₁ H ₄ O ₁₀) (C ₁₂ H ₁₄ N ₂) 4(H ₂ O)	2(C ₁₁ H ₅ O ₁₀) (C ₁₂ H ₁₂ N ₂) 2(H ₂ O)	(C ₁₁ H ₄ O ₁₀) (C ₆ H ₁₄ N ₂) (H ₂ O)
Fw	876.60	554.46	425.30	427.34
Crystal shape	blocks	Plates	blocks	blocks
Crystal color	colorless	Colorless	colorless	colorless
Crystal system	triclinic	Triclinic	triclinic	monoclinic
Space group	<i>P</i> $\bar{1}$	<i>P</i> $\bar{1}$	<i>P</i> $\bar{1}$	<i>P</i> 2 ₁ / <i>c</i>
<i>a</i> (Å)	9.508(1)	9.613(1)	8.044(4)	9.609(2)
<i>b</i> (Å)	10.310(1)	10.645(1)	10.183(5)	17.204(4)
<i>c</i> (Å)	10.811(2)	12.525(1)	11.738(6)	11.020(2)
α (°)	116.94(2)	103.19(2)	70.56(8)	90.00
β (°)	96.52(2)	90.00(2)	80.66(9)	93.18(4)
γ (°)	95.79(2)	90.00(2)	72.14(9)	90.00
<i>V</i> (Å ³)	924.8(2)	1248(2)	861.1(7)	1819.0(6)
<i>Z</i>	1	2	2	4
D _{calc} (g cm ⁻³)	1.574	1.476	1.640	1.560
T(K)	293	100	273	273
Mo $\kappa\alpha$	0.71073	0.71073	0.71073	0.71073
μ (mm ⁻¹)	0.141	0.124	0.143	0.133
2 θ range (°)	50.06	50.78	56.62	50.00
F(000)	454	580	440	892
Total reflns	8976	11932	7401	9959
No. unique reflns [<i>R</i> (int)]	3251 [0.0310]	4492 [0.1318]	3864 [0.0451]	3210 [0.0342]
No. reflns used	2140	4151	2627	2518
No. parameters	333	352	307	309
GOF on <i>F</i> ²	1.014	2.645	1.074	1.087
<i>R</i> ₁ [<i>I</i> >2 σ (<i>I</i>)]	0.0436	0.1454	0.0747	0.0601
w <i>R</i> ₂	0.0988	0.3995	0.1453	0.1381

Table 2.2. *contd...*

	1e	1f	1g	1h
Formula	(C ₁₁ H ₄ O ₁₀) 2(C ₁₂ H ₉ N ₂) 5(H ₂ O)	(C ₁₁ H ₄ O ₁₀) 2(C ₁₂ H ₉ N ₂) 5(H ₂ O)	(C ₁₁ H ₅ O ₁₀) 2(C ₁₀ H ₈ N ₂)	(C ₁₁ H ₅ O ₁₀) (C ₁₂ H ₉ N ₂) 4(H ₂ O)
Fw	748.65	748.65	610.53	550.43
Crystal shape	Blocks	blocks	blocks	blocks
Crystal color	colorless	colorless	colorless	colorless
Crystal system	monoclinic	triclinic	triclinic	triclinic
Space group	<i>P</i> 2 ₁ / <i>n</i>	<i>P</i> $\bar{1}$	<i>P</i> $\bar{1}$	<i>P</i> $\bar{1}$
<i>a</i> (Å)	14.138(6)	9.813(2)	9.546(2)	10.367(2)
<i>b</i> (Å)	10.277(4)	11.121(2)	10.549(2)	10.907(2)
<i>c</i> (Å)	23.269(9)	17.376(3)	15.354(4)	12.880(2)
α (°)	90.00	74.58(2)	70.18(4)	72.38(3)
β (°)	100.55(7)	80.39(3)	76.71(6)	74.42(3)
γ (°)	90.00	65.72(2)	70.76(4)	61.86(3)
<i>V</i> (Å ³)	3324.0(2)	1662.9(4)	1361.3(5)	1210.3(4)
<i>Z</i>	4	2	2	2
<i>D</i> _{calc} (g cm ⁻³)	1.496	1.495	1.489	1.488
<i>T</i> (K)	100	293	273	298
Mo $\kappa\alpha$	0.71073	0.71073	0.71073	0.71073
μ (mm ⁻¹)	0.119	0.119	0.114	0.127
2 θ range (°)	50.10	50.06	50.48	50.04
<i>F</i> (000)	1560	780	632	556
Total reflns	23394	15994	10060	11663
No. unique reflns [<i>R</i> (int)]	5860 [0.0513]	5859 [0.0485]	4896 [0.0692]	4241 [0.0287]
No. reflns used	4733	4025	2958	3287
No. parameters	590	565	411	408
GOF on <i>F</i> ²	1.284	0.957	1.120	1.041
<i>R</i> ₁ [<i>I</i> >2 σ (<i>I</i>)]	0.0770	0.0456	0.1093	0.0626
<i>wR</i> ₂	0.1420	0.1277	0.2120	0.1697

Table 2.3. Characteristics of hydrogen bonds (D-H \cdots X) in the molecular complexes of **1a-1h** (distances/Å and angles/°)#.

Hydrogen bonds	1a			1b			1c			1d		
O-H\cdotsO	1.55	2.60	172	1.67	2.47	168	1.58	2.60	171	1.69	2.50	172
	1.69	2.59	177	1.82	2.61	162	1.59	2.55	171	1.74	2.55	172
	1.77	2.67	159	1.88	2.67	165	1.66	2.61	165	1.88	2.75	173
	1.91	2.80	161	2.01	2.76	150	1.80	2.62	153	2.11	2.90	161
	1.92	2.84	164	2.12	2.87	149	1.87	2.77	172			
	2.08	3.03	176				1.91	2.85	168			
	2.10	2.92	145				1.93	2.77	160			
	2.27	3.01	137				1.98	2.82	169			
N⁺-H\cdotsO⁻	1.64	2.62	168	1.90	2.73	164	1.98	2.77	145	1.68	2.62	179
				1.96	2.81	168	2.53	3.16	127	2.38	3.14	148
C-H\cdotsO	2.29	3.12	150	2.34	3.20	155				2.53	3.45	159
	2.38	3.33	172	2.34	3.22	156				2.55	3.42	149
	2.56	3.30	126	2.43	3.29	154						
				2.44	3.30	153						
				2.48	3.22	137						
				2.53	3.42	162						

Table 2.3. contd...

Hydrogen bonds	1e			1f			1g			1h		
O–H[⋯]O	1.71	2.52	174	1.58	2.58	176	1.76	2.53	157	1.78	2.69	170
	1.72	2.52	165	1.90	2.72	158				1.64	2.62	170
	1.73	2.43	143	1.91	2.70	161				1.72	2.63	164
	1.91	2.73	165	1.91	2.73	163						
	1.92	2.71	157	1.94	2.79	176						
	1.92	2.75	169	1.95	2.78	167						
	2.05	2.93	164	2.00	2.79	154						
	2.07	2.96	168	2.26	2.92	136						
	2.08	2.88	166									
	2.10	2.87	153									
	2.11	2.93	166									
	2.31	2.93	132									
2.43	3.06	132										
N⁺–H[⋯]O⁻	1.85	2.75	156	1.76	2.60	168	1.76	2.59	162	1.71	2.63	174
	1.96	2.78	145	1.77	2.63	175				2.56	3.22	129
O–H[⋯]N				1.80	2.62	173	1.83	2.56	147	1.54	2.59	169
							1.86	2.61	150			
							1.88	2.65	157			
C–H[⋯]O	2.29	3.22	155	2.49	3.23	136	2.40	3.31	166	2.41	3.19	131
	2.33	3.14	139	2.52	3.21	133	2.45	3.33	159	2.51	3.34	152
	2.40	3.30	162	2.59	3.35	139	2.46	3.36	161	2.55	3.24	133
	2.46	3.31	141				2.54	3.40	155			
	2.52	3.35	140				2.56	3.42	154			
	2.55	3.50	160									

For each structure, the three columns represent distances of H[⋯]X, D[⋯]X and angle D–H[⋯]X, respectively.

2.5. References

1. (a) Lehn, J. M. *Supramolecular Chemistry*; VCH: Weinheim, 1995. (b) Lehn, J. M. *Angew. Chem., Int. Ed.* **1988**, *27*, 89-112. (c) J. Steed and J. L. Atwood, *Supramolecular Chemistry*; Wiley, New York, 2000. (d) Moulton, B.; Zaworotko, M. J. *Chem. Rev.* **2001**, *101*, 1629-1658.
2. (a) Whitesides, G. M.; Simanek, E. E.; Mathias, J. P.; Seto, C. T.; Chin, D. N.; Mammen, M.; Gordon, D. M. *Acc. Chem. Res.* **1995**, *28*, 37. (b) Prins, L. J.; Reinhoudt, D. N.; Timmerman, P. *Angew. Chem., Int. Ed.* **2001**, *40*, 2382-2426.
3. (a) Metrangolo, P.; Neukirch, H.; Pilati, T.; Resnati, G. *Acc. Chem. Res.* **2005**, *38*, 386-395. (b) Meyer, E. A.; Castellano, R. K.; Diederich, F. *Angew. Chem., Int. Ed.* **2003**, *115*, 1244-1287. (c) Lommerse, J. P. M.; Stone, A. J.; Taylor, R.; Allen, F. H. *J. Am. Chem. Soc.* **1996**, *118*, 3108-3116. (d) Shimpi, M. R.; SeethaLekshmi, N.; Pedireddi, V. R. *Cryst. Growth Des.* **2007**, *7*, 1958-1963.
4. (a) Fournier, J. H.; Maris, T.; Wuest, J. D. *J. Org. Chem.* **2004**, *69*, 1762-1775. (b) Malek, N.; Maris, T.; Simard, M.; Wuest, J. D. *J. Am. Chem. Soc.* **2005**, *127*, 5910-5916. (c) Demers, E.; Maris, T.; Wuest, J. D. *Cryst. Growth Des.* **2005**, *5*, 1227-1235. (d) Laliberté, D.; Maris, T.; Sirois, A.; Wuest, J. D. *Org. Lett.* **2003**, *5*, 4787-4790.
5. Desiraju, G. R. *Angew. Chem., Int. Ed.* **1995**, *34*, 2311-2327.
6. (a) McManus, G. J.; Wang, Z.; Zaworotko, M. J. *Cryst. Growth Des.* **2004**, *4*, 11-13. (b) Eddaoudi, M.; Moler, D. B.; Li, H.; Chen, B.; Reineke, T. M.; O'Keeffe, M.; Yaghi, O. M. *Acc. Chem. Res.* **2001**, *34*, 319-330. (c) Russell, V. A.; Etter, M. C.; Ward, M. D. *Chem. Mater.* **1994**, *6*, 1206-1217.

7. (a) Plass, K. E.; Kim, K.; Matzger, A. J. *J. Am. Chem. Soc.* **2004**, *126*, 9042-9053. (b) Varughese, S.; Pedireddi, V. R. *Chem. Eur. J.* **2006**, *12*, 1597-1609. (c) Brown, S. P.; Spiess, H. W. *Chem. Rev.* **2001**, *12*, 4125-4155.
8. (a) Bernstein, J.; Davis, R. E.; Shimoni, L.; Chang, N. L. *Angew. Chem., Int. Ed.* **1995**, *34*, 1555-1573 (b) Whitesides, G. M.; Mathias, J. P.; Seto, C. T. *Science* **1991**, *254*, 1312-1319. (c) Zeng, F. W.; Zimmerman, S. C. *Chem. Rev.* **1997**, *97*, 1681-1712. (d) Meyer, E. A.; Castellano, R. K.; Diederich, F. *Angew. Chem., Int. Ed.* **2003**, *42*, 1210-1250. (e) Rudkevich, D. M. *Angew. Chem., Int. Ed.* **2004**, *43*, 558-571. (f) Hosseini, M. W. *Coord. Chem. Rev.* **2003**, *240*, 157-166. (g) Sessler, J. L.; Jayawickramarajah, J. *Chem. Soc. Rev.* **2007**, *36*, 314-325.
9. (a) Lehn, J. M. *Angew. Chem., Int. Ed.* **1990**, *29*, 1304-1319. (b) Blake, A. J.; Champness, N. R.; Hubberstey, P.; Li, W.-S.; Withersby, M. A.; Schröder, M. *Coord. Chem. Rev.* **1999**, *183*, 117-138. (c) Stang, P. J.; Olenyuk, B. *Acc. Chem. Res.* **1997**, *30*, 502-518. (d) Philp, D.; Fraser Stoddart, J. *Angew. Chem., Int. Ed.* **1996**, *35*, 1154-1196. (e) Aakeröy, C. B.; Beatty, A. M.; Helfrich, B. A. *J. Am. Chem. Soc.* **2002**, *124*, 14425-14432. (f) Mathias, J. P.; Simanek, E. E.; Zerkowski, J. A.; Seto, C. T.; Whitesides, G. M. *J. Am. Chem. Soc.* **1994**, *116*, 4316-4325 (g) Batten, S. R.; Robson, R. *Angew. Chem., Int. Ed.* **1998**, *37*, 1461-1494. (h) Gillard, R. E.; Raymo, F. M.; Stoddart, J. F. *Chem. Eur. J.* **1997**, *3*, 1933-1940.
10. (a) Desiraju, G. R. *Acc. Chem. Res.* **1996**, *29*, 441-449. (b) Görbitz, C. H.; Etter, M. C. *J. Am. Chem. Soc.* **1992**, *114*, 627-631. (c) Bernstein, J.; Davis, R. E.; Shimoni, L.; Chang, N. L. *Angew. Chem., Int. Ed.* **1995**, *34*, 1555-1573. (d)

- Perumalla, S. R.; Suresh, E.; Pedireddi, V. R. *Angew. Chem., Int. Ed.* **2005**, *44*, 7752-7757. (e) Braga, D.; Grepioni, F. *Angew. Chem., Int. Ed.* **2004**, *43*, 4002-4011. (f) Seddon, K. R. *Cryst. Growth Des.* **2004**, *4*, 1087. (g) Dunitz, J. D.; Gavezzotti, A. *Angew. Chem., Int. Ed.* **2005**, *44*, 1766-1787.
11. (a) Steiner, T. *Angew. Chem., Int. Ed.* **2002**, *41*, 48-76. (b) Etter, M. C. *Acc. Chem. Res.* **1990**, *23*, 120-126. (c) Moulton, B.; Zaworotko, M. J. *Chem. Rev.* **2001**, *101*, 1629-1658. (d) Aakeröy, C. B. *Acta Crystogr.* **1997**, *B53*, 569-586.
12. (a) Frankenbach, G. M.; Etter, M. C. *Chem. Mater.* **1992**, *4*, 272-278. (b) Leiserowitz, L. *Acta Crystogr.* **1976**, *B32*, 775-802. (c) Biradha, K.; Zaworotko, M. J. *Cryst. Eng.* **1998**, *1*, 67. (d) Kuduva, S. S.; Craig, D. C.; Nangia, A.; Desiraju, G. R. *J. Am. Chem. Soc.* **1999**, *121*, 1936-1944. (e) Ermer, O.; Lex, J. *Angew. Chem., Int. Ed.* **1997**, *26*, 447-449. (f) Fabelo, O.; Cañadillas-Delgado, L.; Delgado, F. S.; Lorenzo-Luis, P.; Laz, M. M.; Julve, M.; Ruiz-Prez, C. *Cryst. Growth Des.* **2005**, *5*, 1163-1167. (g) Inabe, T. *J. Mater. Chem.* **2005**, *15*, 1317-1328. (h) Bhogala, B. R.; Nangia, A. *Cryst. Growth Des.* **2003**, *3*, 547-554. (i) Ishi, I. T.; Crego-Calama, M.; Timmerman, P.; Reinhoudt, D. N.; Shinkai, S. *Angew. Chem., Int. Ed.* **2002**, *41*, 1924-1929. (j) Cowan, J. A.; Howard, J. A. K.; McIntyre, G. J.; Lo, S. M. F.; Williams, I. D. *Acta Crystogr.* **2003**, *B59*, 794-801. (k) Dale, S. H.; Elsegood, M. R. J.; Hemmings, M.; Wilkinson, A. L. *CrystEngComm* **2004**, 207-214. .
13. (a) Vishweshwar, P.; Beauchamp, D. A.; Zaworotko, M. J. *Cryst. Growth Des.* **2006**, *6*, 2429-2431. (b) Arora, K. K.; Talwelkar, M.; Pedireddi, V. R. *New. J. Chem.* **2009**, *33*, 57-63. (c) Dang, H.; Maris, T.; Yi, J. H.; Rosei, F.; Nanci, A.;

- Wuest, J. D. *Langmuir*. **2007**, *23*, 11980-11985. (d) Aakeröy, C. B.; Seddon, K. R. *Chem. Soc. Rev.* **1993**, *22*, 397-407. (e) Ducharme, Y.; Wuest, J. D. *J. Org. Chem.* **1988**, *53*, 5787-5789.
14. (a) Shan, N.; Bond, A. D.; Jones, W. *New J. Chem.* **2003**, *27*, 365. (b) Almarsson, Ö.; Zaworotko, M. J. *Chem. Commun.* **2004**, *10*, 1889-1896. (c) Aakeröy, C. B.; Salmon, D. J. *CrystEngComm* **2005**, *7*, 439-448. (d) Etter, M. C.; Reutzel, S. M. *J. Am. Chem. Soc.* **1991**, *113*, 2586-2598.
15. Duchamp, D. J.; Marsh, R. E. *Acta Crystogr.* **1969**, *B25*, 5-19.
16. Shattock, T. R.; Vishweshwar, P.; Wang, Z.; Zaworotko, M. J. *Cryst. Growth Des.* **2005**, *5*, 2046-2049.
17. Arora, K. K.; Pedireddi, V. R. *J. Org. Chem.* **2003**, *68*, 9177-9185.
18. Allen, F. H.; Kennard, O. *Chem. Des. Automat. News* **1993**, *8*, 31-37.
19. Barrio, C.; Granda, S. G.; Beltran, F. G. *Acta Crystogr.* **1990**, *C46*, 2399-2401.
20. A. L. Spek, PLATON, molecular geometry program, University of Utrecht, The Netherlands, 1995.
21. Ranganathan, A.; Pedireddi, V. R.; Rao, C. N. R. *J. Am. Chem. Soc.* **1999**, *121*, 1752-1753.
22. *SAINT*, Version 6.02; Bruker AXS, Inc., Analytical X-ray Systems, 5465 East Cheryl Parkway, Madison, WI 53711-5373, 2000.
23. *SADABS* [Area-Detector Absorption Correction]; Siemens Industrial Automation, Inc.: Madison, WI, 1996.
24. G. M. Sheldrick, *SHELXTL*, University of Göttingen, Göttingen, Germany, 1997.

CHAPTER
3

**MOLECULAR ADDUCTS OF
BENZENEHEXACARBOXYLIC
ACID (MELLITIC ACID) WITH
VARIOUS AZA-DONOR
COMPOUNDS**

3.1. Introduction

Synthesis of molecular adducts,¹ particularly, employing organic substrates, by co-crystallization of the reactants from a suitable solvent or a mixture of solvents, is a widely used procedure for the creation of supramolecular assemblies, which is also discussed in the previous chapter with respect to the complexes of benzenepentacarboxylic acid.² Thus, co-crystallization is a powerful tool for the development of targeted assemblies of desired architectures with tailor-made properties that can be utilized in different applications. For example, synthesis of non-centrosymmetric materials for non-linear optical properties,³ host-guest type lattices for catalytical studies,⁴ preparation of pharmaceutical co-crystals⁵ for the evaluation in different types of formulations, for altering physical properties etc.

In addition to the examples discussed in the previous chapters, the following illustrations indeed further represent the efficiency of $-\text{COOH}$ and in particular as part of the polycarboxylic moiety.

Ermer demonstrated a infinite diamondoid network of adamantane-1,3,5,7-tetracarboxylic acid (**ATC**), in which $-\text{COOH}$ groups are tetrahedrally oriented as shown in Figure 3.1a.⁸ **ATC** is a particularly favorable example considering the rigidity of its carbon skeleton and almost the perfect tetrahedral alignment of the carboxylic groups; hence they self-assemble via hydrogen bonded carboxylic acid dimer to afford diamondoid networks, with large cavities of roughly 12 Å in diameter, as shown in Figure 3.1b. However, these cavities are filled by five independent

networks that interpenetrate to form five-fold diamondoid networks as shown in Figure 3.1c.

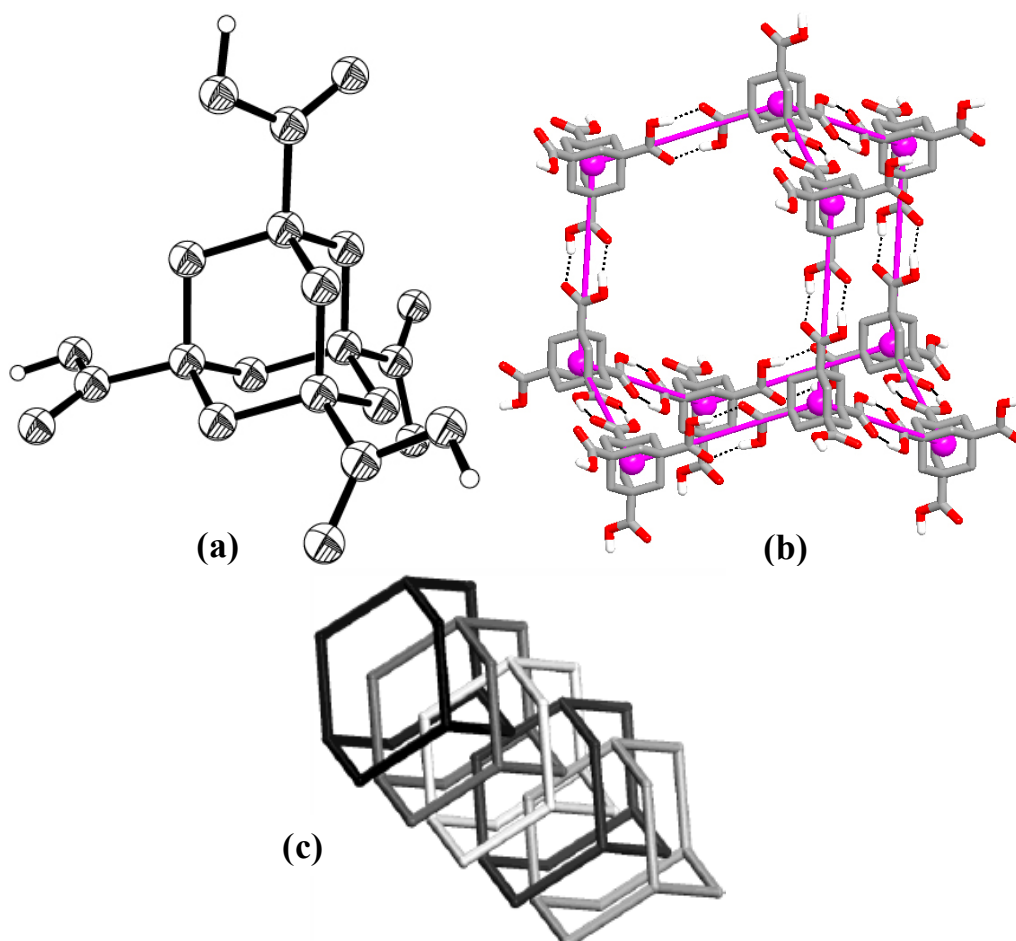


Figure 3.1. (a) Tetrahedrally directed four carboxylic groups of adamantane-1,3,5,7-tetracarboxylic acid (ATC). (b) Hydrogen-bonded diamondoid framework with a cavity. (c) Five-fold interpenetrating hydrogen-bonded diamondoid networks.

Zaworotko and co-workers⁹ exercised a paradigm based on modular design in which co-crystal former can be exploited for their ability to form supramolecular interactions with active pharmaceutical ingredients (APIs). In this regard, co-crystallization that was carried out in a 1:1 ratio of carbamazepine and ATC, from either methanol or ethanol, has been shown to give crystals contains only *heteromeric*

interactions. The two carboxylic acid groups of the ATC generate *heteromeric* interactions with two different carbamazepine molecules, and the exterior hydrogen-bond acceptor/donor sites of the carbamazepine molecules interact with the remaining acid groups by means of catemeric N—H···O and O—H···O hydrogen bonds. In this fashion, all the hydrogen-bonding donor/acceptor sites of carbamazepine molecule and ATC are satisfied as shown in Figure 3.2a. Further, the acid moiety interacts with four different carbamazepine molecules via two dimeric and two catemeric hydrogen bonds, as shown in Figure 3.2b.

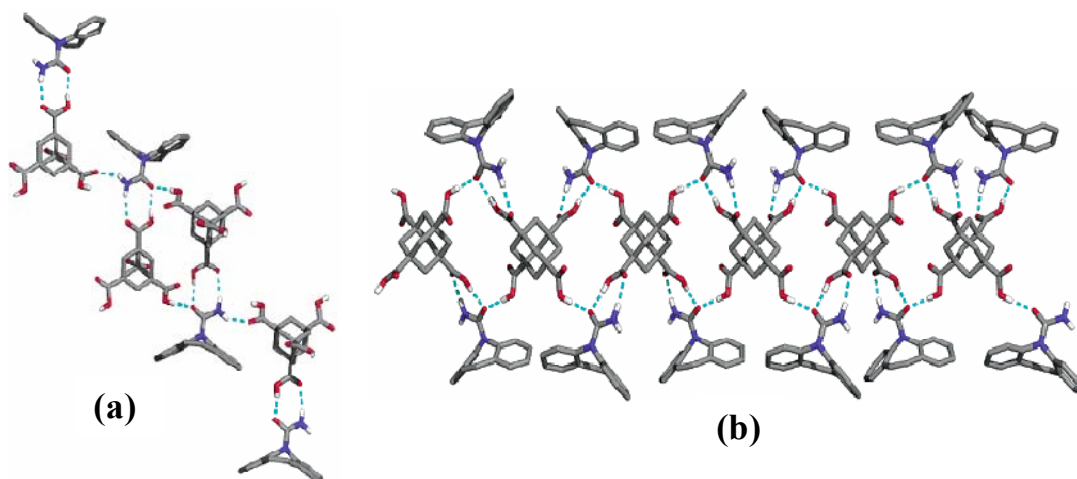


Figure 3.2. (a) Interaction of an amide group of carbamazepine with three different molecules of acid, ATC. (b) *Heteromeric* interactions present in the co-crystals of carbamazepine and ATC.

Price and co-workers¹⁰ have shown the formation of large cavities in two dimensional network, by self assembly process, in the crystal structure of biphenyl-3,3',5,5'-tetracarboxylic acid, which is like an extended tetracarboxylic acid, as shown in Figure 3.3a. As known for many organic structures with void space, herein also the

cavities are filled by 2-fold interpenetration of three independent networks as shown in Figure 3.3b.

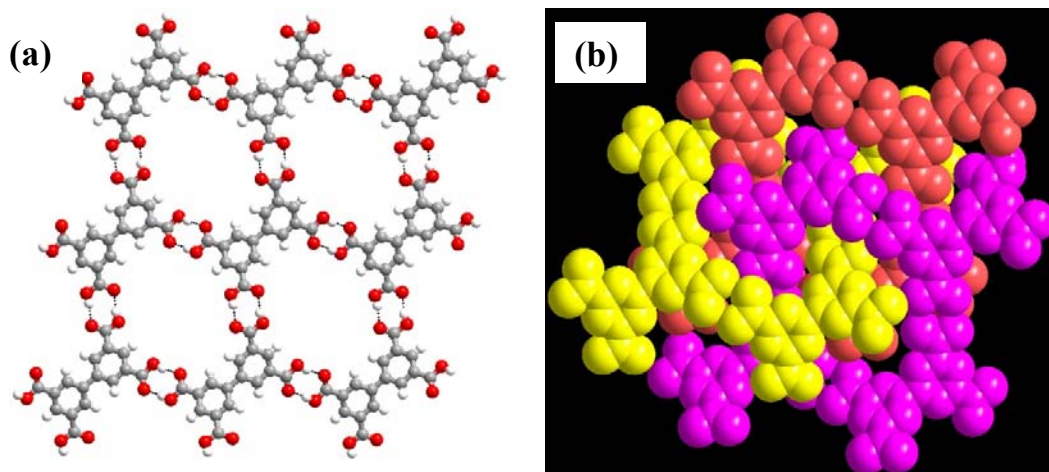


Figure 3.3. (a) Self-assembly of biphenyl-3,3',5,5'-tetracarboxylic acid molecules, through dimeric hydrogen bonds. (b) Hydrogen-bonded interpenetrating networks represented by space-filling model.

Taken into account the elegant and exotic assemblies of the polycarboxylic acids known in the literature and also knowledge gained from the studies of benzenepentacarboxylic acid in the supramolecular synthesis, as vividly described in chapter 2, exploration is continued for the utilization of other polycarboxylic acids available, like 1,2,3,4,5,6-benzenehexacarboxylic acid (**MA**).

3.2. Supramolecular Assemblies of Mellitic acid, MA

A review of the chemical literature and the crystallographic database [Cambridge Structural Database (CSD)] show a few reports of structures of mellitic acid (**MA**) with organic bases.¹¹ In addition, even the crystal structure of **MA**, known in the literature, was reported with an *R*-factor as high as 11.7%. Hence, prior to the co-crystallization of **MA** with other substrates, crystallization studies of **MA** has been

carried out using different methods such as slow evaporation, hydrothermal, solvothermal methods etc., in which hydrothermal methods gave good quality single crystals suitable for the structure determination by X-ray diffraction methods. In fact, the unit cell obtained (Table 3.1) is similar to the corresponding parameters reported by Darlow¹² but refined to a good *R*-factor of 4.35%. Crystal structure analysis of **MA** shows that asymmetric unit has two symmetry independent molecules (Figure 3.4). Further, it has been noted that, carboxyl groups are tilted significantly from the plane of the benzene ring, and linked to each other by O—H···O hydrogen bonds,¹³ in the form of the eight-member hydrogen bond rings ($R_2^2(8)$ pattern), well known for the —COOH groups.

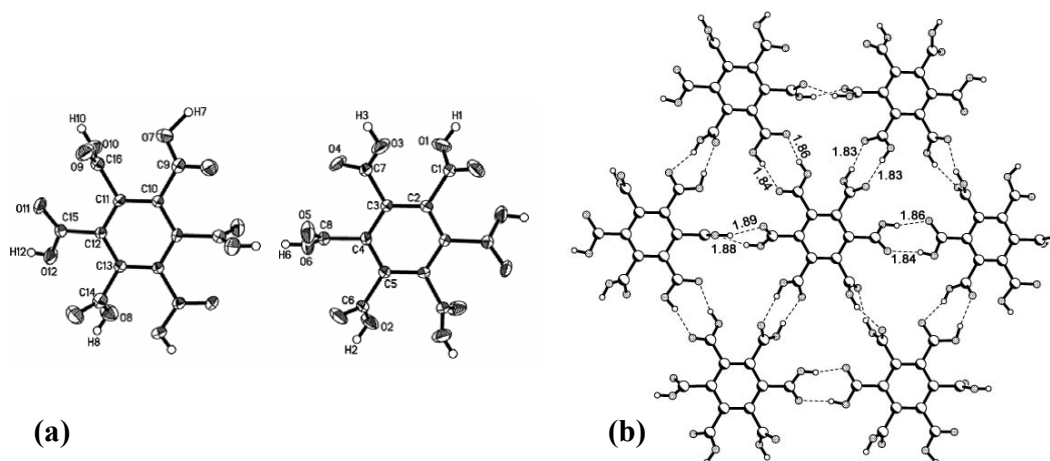


Figure 3.4. (a) ORTEP of asymmetric unit with two molecules of mellitic acid (**MA**) and (b) Arrangement of **MA** molecules in a typical layer found in its crystal structure.

The arrangement of **MA** molecules within a typical layer, as shown in Figure 3.4b, illustrates that all the six —COOH groups are indeed involved in the formation of O—H···O hydrogen bonds with adjacent moieties. The characteristics of the hydrogen bonds are given in Table 3.2.

Observing the effective utilization of all the functional groups in the self assembly process, in the native structure of **MA**, it may be possible to tailor the structure into supermolecules by inserting spacer molecules like aza-donors, by which the ultimate assembly give architecture for utilization in some application studies.

3.3. Molecular adducts of Mellitic acid, MA

Co-crystallization of **MA** with various aza-donor molecules has been carried out, as illustrate in Chart I, anticipating supramolecular assemblies with exotic architectures.

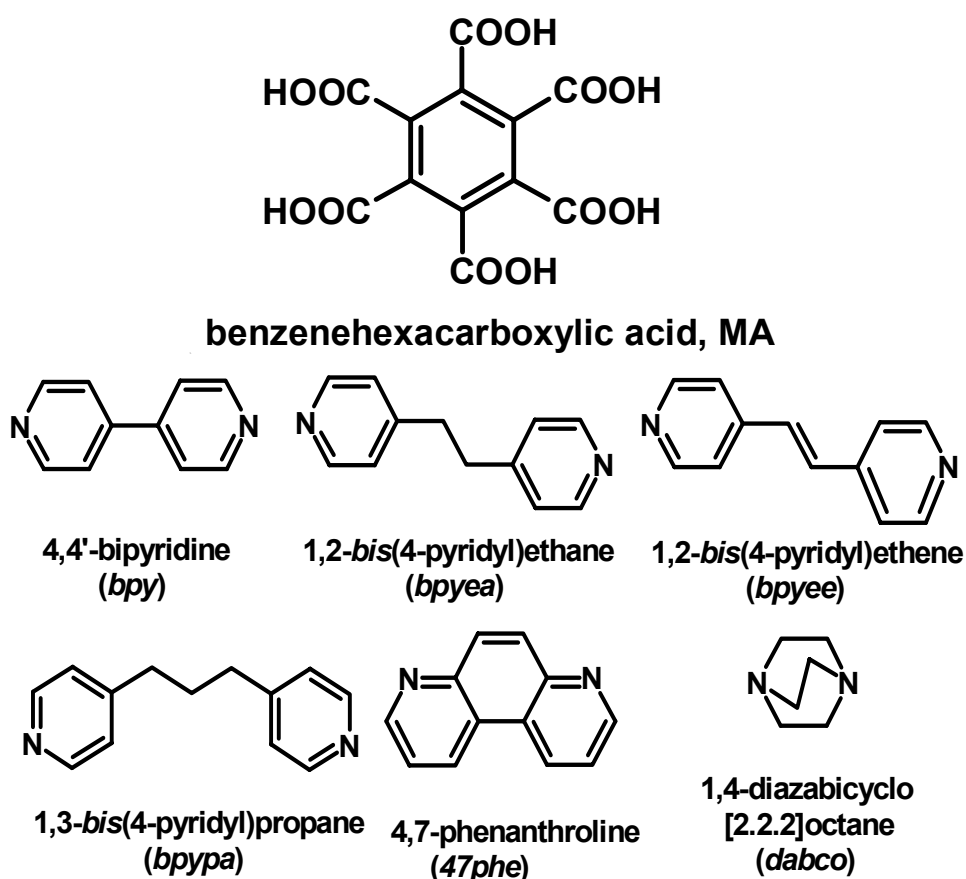


Chart I

Co-crystallization experiments yielded good quality single crystals of molecular complexes of **MA** with the aza-donor compounds, either by slow evaporation at room temperature or by hydrothermal method. The resulting molecular complexes along with crystallization conditions are given in Chart II and detailed discussion of the structural features is presented in the following sections.

Organic ligands	Crystallization conditions	Composition including solvent (H ₂ O) molecules	Molecular complexes
MA + <i>bpy</i>	RT ^a	1:2	1a
MA + <i>bpyea</i>	RT/HT ^b	1:1:5	1b
MA + <i>bpyee</i>	RT/HT	1:2:2	1c
MA + <i>bpyya</i>	RT/HT	1:1:1	1d
MA + <i>dabco</i>	RT/HT	1:1:5	1e
MA + <i>47phe</i>	RT/HT	1:2:2	1f
MA + <i>bpy</i>	HT	1:1:3	1g

RT^a = Room temperature, 28 °C, 4 days; HT^b = Hydrothermal, 180 °C, 2 days.

Chart II

3.3.1. Solid state structure of **MA** and *bpy*, **1a**

Dissolving **MA** and *bpy* together either in methanol or ethanol and subsequent evaporation at room temperature always gave a precipitate, irrespective of composition of the reactants. However, single crystals of **MA** and *bpy* were finally obtained from water as a solvent, in a 1:2 ratio (Figure 3.5), as confirmed by single

crystal data. The crystals, thus, obtained are labeled as **1a**. Pertinent crystallographic details are given in Table 3.1. Indeed, there are two crystallographically symmetry independent molecules, as observed in the native structure of **MA**. Further analysis reveals that crystal lattice is stabilized in the form of stacked layers in its three dimensional arrangement, as shown in Figure 3.6a. In fact, each layer is constituted by the molecules of **MA** and *bpy* corresponding to a specific symmetry. Arrangement of molecules in the typical layers is shown in Figure 3.6b and c.

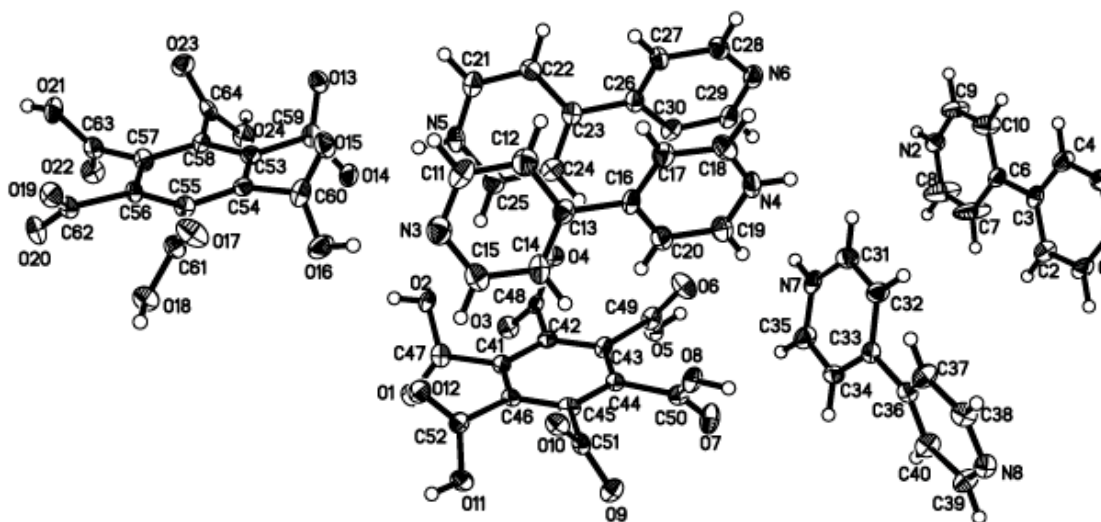


Figure 3.5. ORTEP of the asymmetric unit in the crystal structure of complex **1a**.

In a typical layer, the adjacent **MA** molecules are held together by O—H \cdots O (H \cdots O, 1.72, 1.74, 1.77 Å) hydrogen bonds in the form of one-dimensional chains, utilizing —COOH at 1,2,4,5-positions (Figure 3.8b,c). Such adjacent chains are connected together by *bpy* molecules through O—H \cdots N (H \cdots N, 1.81, 1.82, 1.91 Å) and N⁺—H \cdots O⁻ (H \cdots N, 1.72, 1.74, 1.76, 1.79 Å) hydrogen bonds. Thus, a ladder type structure is formed in both the types of layers. Further, such ladders in the adjacent layers are skewed at angle of 60° with each other, as shown in Figure 3.8d.

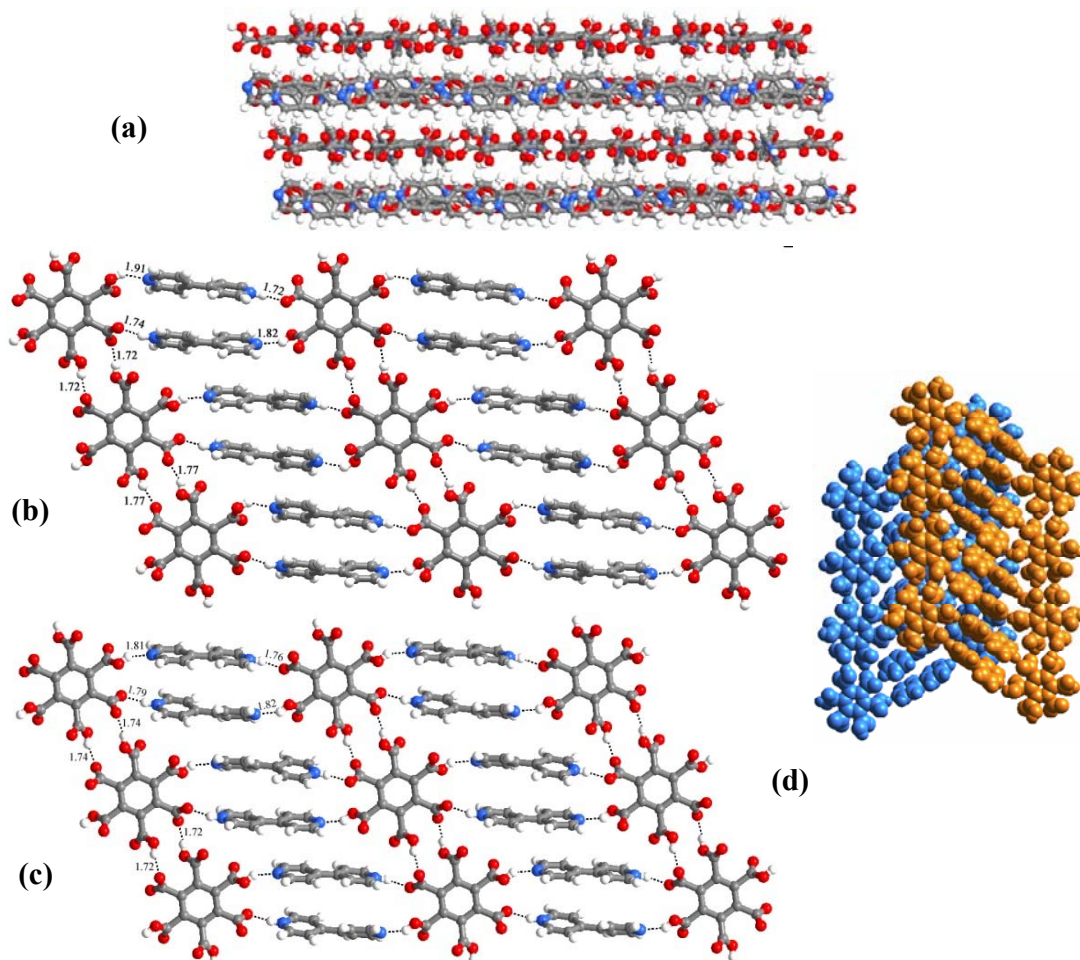


Figure 3.6. (a) Three-dimensional arrangement, in the form of stacked layers, in the crystal structure of **1a**. (b) and (c) Formation of ladders by **MA** and *bpy* in **1a**. (d) Overlap of ladders from the adjacent layers skewed by an angle of 60°.

3.3.2. Molecular complex of **MA** and *bpyea*, **1b**

Co-crystallization of **MA** and 1,2-*bis*(4-pyridyl)ethane (*bpyea*), by slow evaporation, at room temperature, gave single crystals, in a 1:1:5 ratio, including water molecules, which are labeled as **1b**. The asymmetric unit of **1b** also has two symmetry independent molecules of **MA** and *bpyea*. The ORTEP is shown in the Figure 3.7 and the complete crystallographic details are given in Table 3.2.

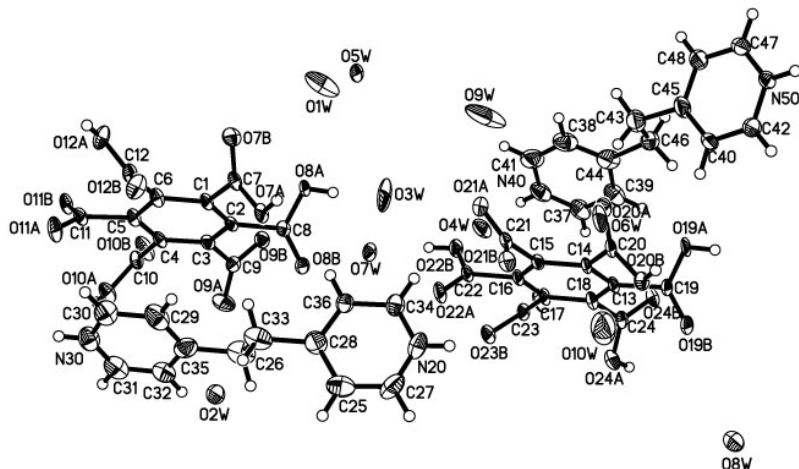


Figure 3.7. ORTEP (50% probability level) of the molecular complex, **1b**, of **MA** and *bpyea*.

In this structure, the carboxylic groups present at 1,3-positions of the both the symmetry independent molecules of **MA** are deprotonated and correspondingly symmetry independent molecules of *bpyea* get protonated at both the ends.

In an overall topological sense, the structural arrangement in three dimensions is the same in both **1a** and **1b**, in the form of stacked layers. In complex **1b**, the alternately stacked layers are due to either **MA** molecules or *bpyea* molecules, exclusively. In a typical layer, both the symmetry independent molecules of **MA**, labeled as **A** and **B**, form separate chains utilizing catemeric O—H···O[−] (H···O[−] 1.68, 1.68 Å) hydrogen bonds, as highlighted in Figure 3.8b. The adjacent chains of **A** and **B** molecules are further held together by different catemeric O—H···O[−] (H···O[−] 1.68, 1.72 Å) hydrogen bonds, as shown in Figure 3.8b. The characteristics of hydrogen bonds are tabulated in Table 3.2. Thus, a quartet of acid molecules of **A** and **B** together, is formed with void space, which is being occupied by two water molecules as guest entities.

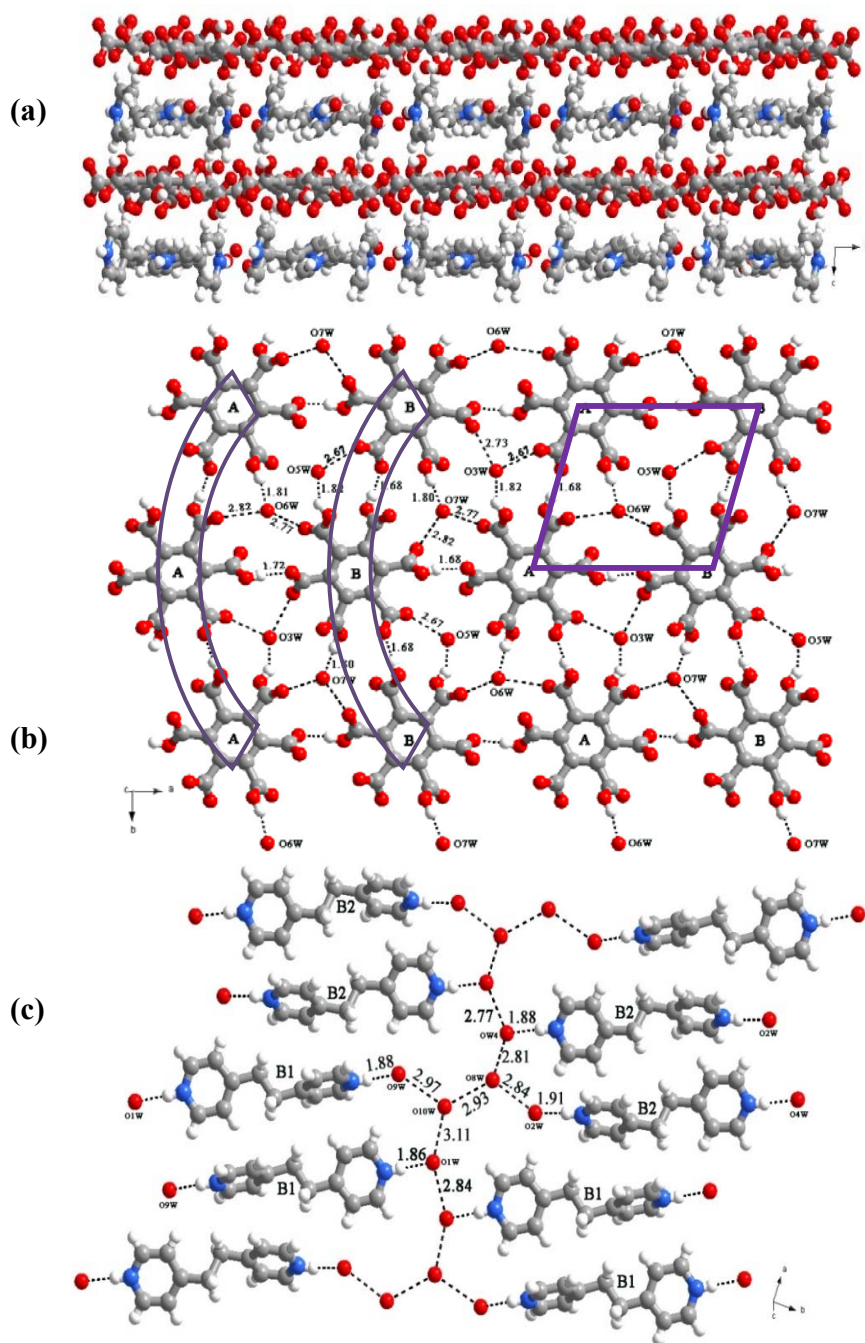


Figure 3.8. (a) Stacked layer structure in the crystal lattice of complex **1b**. (b) Arrangement of MA and water molecules in a layer, in complex **1b**. (c) Interaction of *bpyea* with water molecules and aggregation of symmetry independent molecules of *bpyea*.

In a typical layer of aza-donor molecules, both the symmetry independent molecules of *bpyea*, that are labeled as **B1** and **B2**, interact with water molecules through $N^+—H\cdots O$ ($H\cdots O$; 1.86, 1.88, 1.88, 1.91 Å) hydrogen bonds. Such an aggregation is shown in Figure 3.8c. A close view of the layers reflects that, as if chains of water molecules, held together by $O—H\cdots O$ hydrogen bonds, separate the adjacent *bpyea* molecules.

3.3.3. Molecular complex of MA and *bpyee*, **1c**

Co-crystallization of MA with 1,2-bis(4-pyridyl)ethene (*bpyee*), from water gave plate-like colorless crystals, suitable for X-ray diffraction study. The structure determination reveals that the MA forms a hydrated molecular complex, **1c** with *bpyee*, in a 1:2:2 ratio. Unlike in the structures **1a** and **1b**, there are no symmetry independent molecules in the structure of **1c**. ORTEP of the asymmetric unit is shown in Figure 3.9a. The complete crystallographic details are given in Table 3.2.

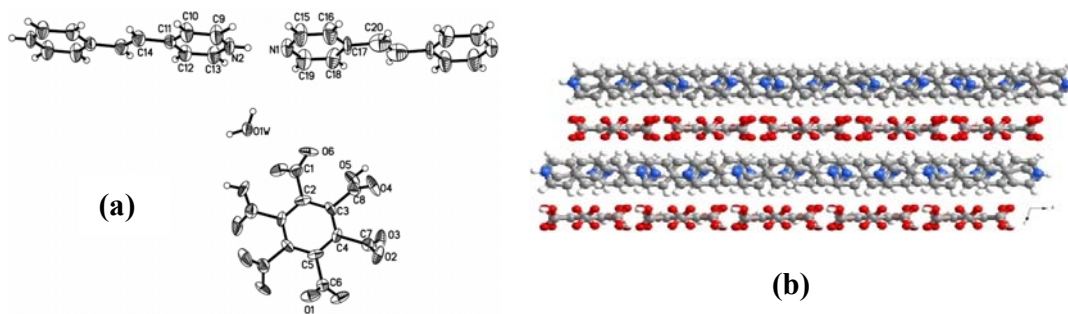


Figure 3.9. (a) ORTEP of the asymmetric unit in complex **1c**. (b) Arrangement of layers in the crystal lattice of **1c**.

In the crystal structure of **1c** also, the three dimensional arrangement is due to the stacking of layers almost in the same manner as that of structure **1b**. The packing arrangement is shown in Figure 3.9b. Along the stacking direction, the alternate layers

possess only either **MA** molecules or aza-donor molecules. In a typical layer of **MA**, molecules of **MA** form a quartet ensemble through catemeric $\text{O}-\text{H}\cdots\text{O}^-$ ($\text{H}\cdots\text{O}^-$; 1.72 Å) hydrogen bonds, with a void space, which is being occupied by two water molecules as shown in Figure 3.10a. These ensembles expand to form infinite sheets, as depicted in Figure 3.10a.

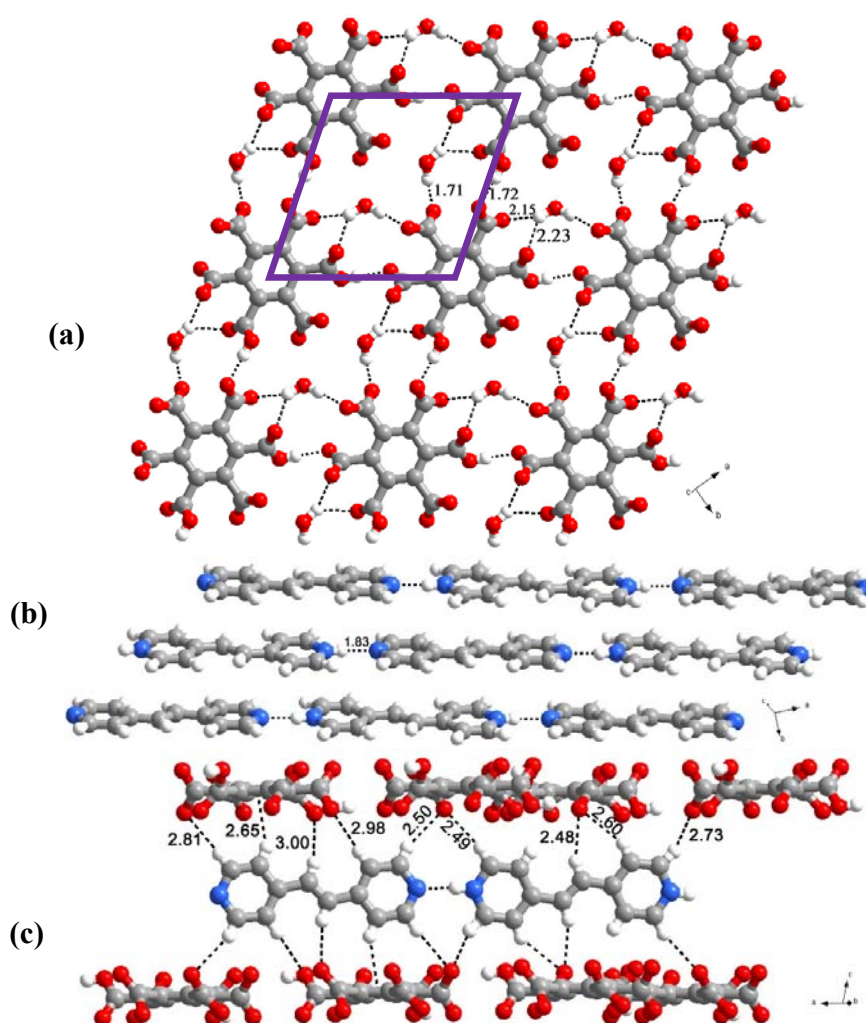


Figure 3.10. (a) Arrangement of **MA** molecules within a sheet, in the complex **1c**. (b) *Homomeric* interactions between molecules of *bpyee*. (c) Stabilization of layers through $\text{C}-\text{H}\cdots\text{O}$ hydrogen bonds.

In a typical layer of aza donor molecules, the neutral and protonated *bpyee* molecules are held together by $N^+ - H \cdots N$ ($H \cdots N$; 1.83 Å) hydrogen bonds, as shown in Figure 3.10b. It is noteworthy to mention that the aza-donor molecules are tilted with respect to the plane of the sheet, thus, enabling a strong interaction through multiple $C - H \cdots O$ hydrogen bonds, with the acid layers lie above and below in three dimensional arrangement. The corresponding $H \cdots O$ distances are in the range 2.48-3.00 Å.

3.3.4. Molecular complex of MA and *bpyea*, **1d**

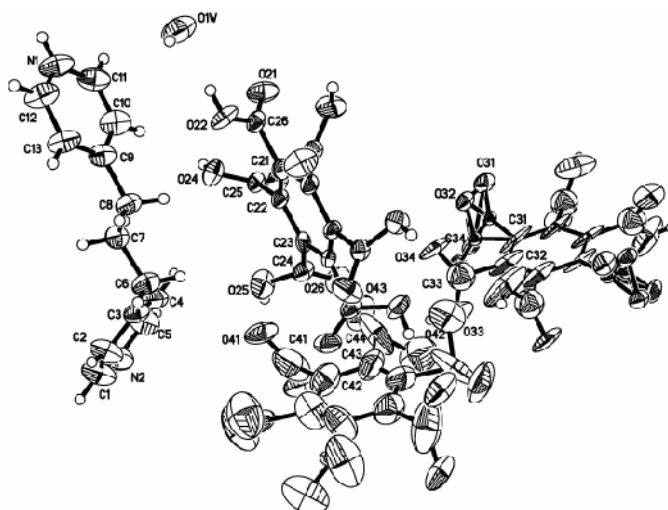


Figure 3.11. ORTEP of the asymmetric unit in the crystal structure of **1d**.

Co-crystallization of **MA** with 1,3-*bis*(4-pyridyl)propane, *bpyea* yielded complex **1d**, which has entirely different molecular arrangement in the crystal lattice than in the complexes **1a-1c**. The asymmetric unit of complex **1d** contains the co-crystal formers in a 3:1 ratio of **MA** and *bpyea*, along with a water molecule. ORTEP of the asymmetric unit is shown in Figure 3.11. Crystallography details are given in Table 3.1.

Packing analysis reveals that, in complex **1d**, molecules aggregate in the form of a host-guest type of network, with host network is being formed by **MA** molecules, in the form of rectangular blocks, along with four water molecules (See Figure 3.12a). The ensemble is created through a series of hydrogen bonds formed between the **MA** molecules as well as between **MA** and water. The characteristics of the hydrogen bonds are given in Table 3.2. Such a network invariably created void space, which is being occupied by *bpypa* molecules, as guest species, as shown in Figure 3.12b.

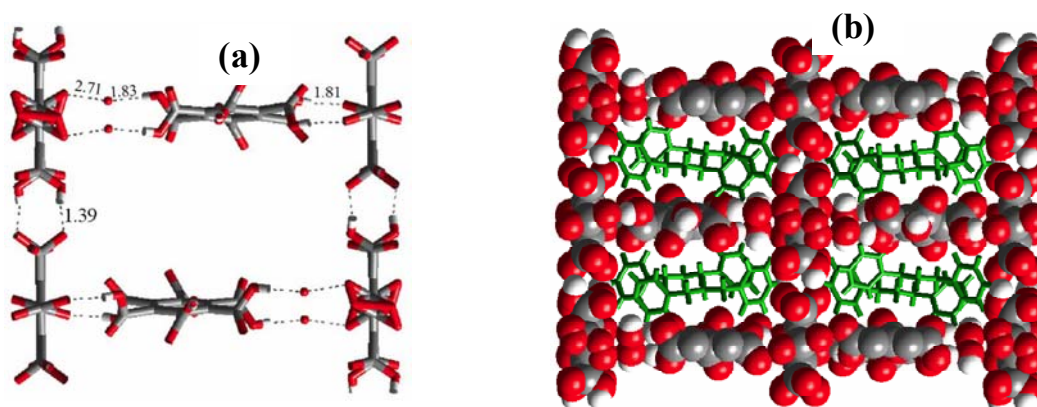


Figure 3.12. (a) A rectangular host network formed by molecules of **MA** and two water molecules in complex **1d**. (b) Representation of host-guest structure with *bpypa* molecules (green) in the channels as guest.

It is apparent from the structure of **1a-1d** that **MA** also form co-crystals with various aza-donor compounds at ease, like other aromatic polycarboxylic acids do, well known in the literature and in particular the complexes of **BPC** discussed in chapter 2. Further, a significant summation could be as the dimension of the aza-donor increases from *bpv* to *bpypa*, a three dimensional sheet structures are turned in to host-guest type networks. If ligands of suitable geometry of the channels are used, it may

even possible to obtain host-guest complexes. Thus, co-crystallizations of **MA** with some rigid aza-donor compounds have been carried out.

For this purpose, co-crystallization of **MA** with 1,4-diazabicyclo[2.2.2]octane (*dabco*), 4,7-phenanthroline (*47phe*), 1,7-phenanthroline (*17phe*) and 1,10-phenanthroline (*110phe*) have been carried out. However, the single crystals of **MA** with 1,10-phenanthroline and 1,7-phenanthroline are not of good quality to establish the structure by X-ray diffraction method. But, in other cases, the structures are easily obtained with the availability of good quality crystals. The salient features of the structures are discussed in following sections.

3.3.5. Molecular complex of MA and *dabco*, **1e**

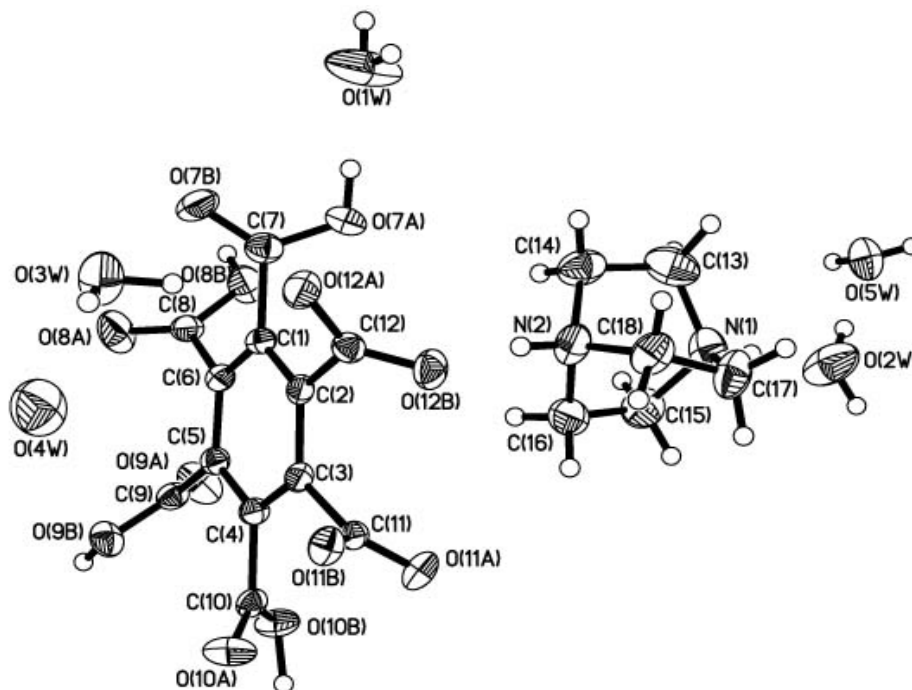


Figure 3.13. ORTEP of asymmetric unit of the complex **1e**.

MA and 1,4-diazabicyclo[2.2.2]octane, *dabco*, in water, gave colorless crystals suitable for single crystal structure determination study. Structure analysis of **1e** reveals that **MA** and *dabco* crystallizes in a chiral space group, $P2_12_12_1$. The ratio of the complex found in the asymmetric unit is 1:1, along with five water molecules. An ORTEP of the asymmetric unit is shown in Figure 3.13. The complete crystallographic details are given in Table 3.1.

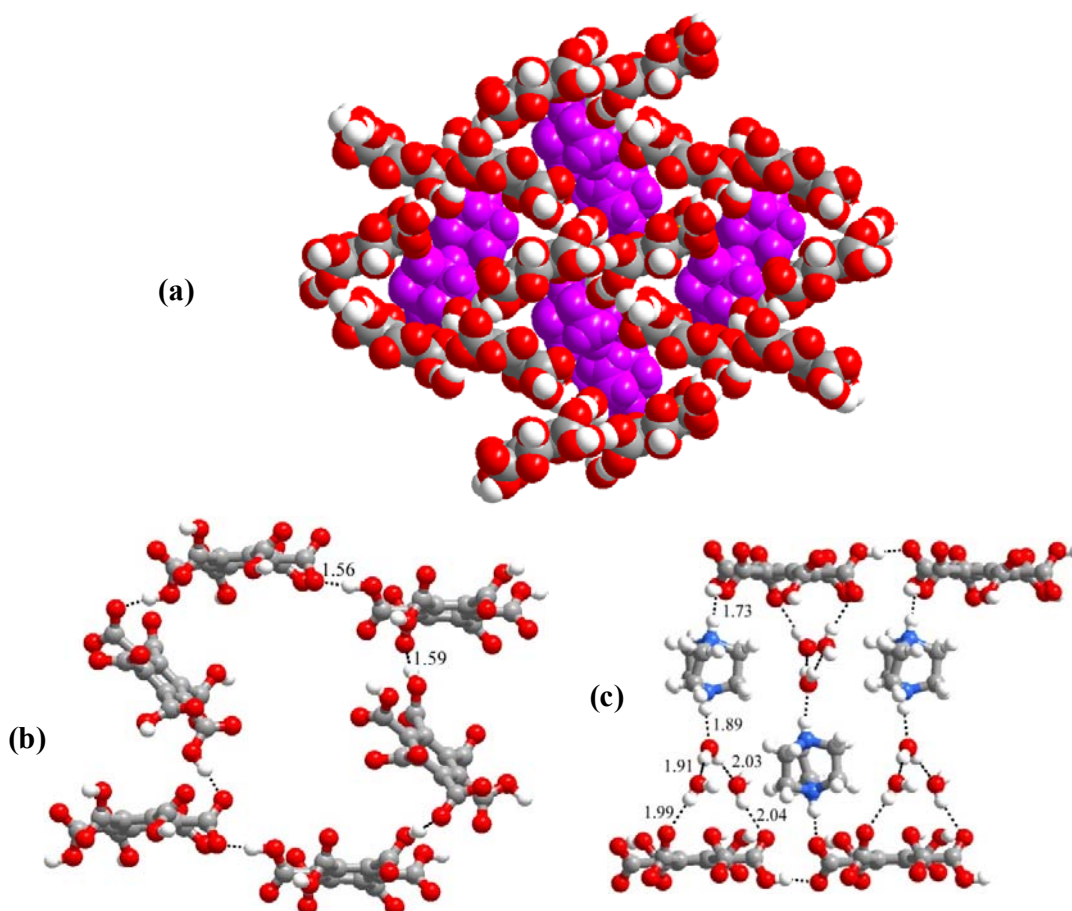


Figure 3.14. (a) Zeolite-type network structure observed in complex, **1e** with *dabco* and water molecules in the channels formed by the molecules of **MA**. (b) Representation of hydrogen bonded host network formed by **MA**. (c) Interaction of **MA** and *dabco* with water molecules in crystal structure of complex **1e**.

Further, the structural analysis reveals a facile conversion of two carboxyl groups of **MA** to carboxylate. Thus, the nitrogen atoms of *dabco* molecules are protonated at both the ends. In the three-dimensional arrangement, as observed in the complex **1d**, a zeolite-type network is realized. Such a network structure is shown in Figure 3.14a. In this structure, while the host network is being formed by **MA** molecules, in the form of rectangular blocks with void space, *dabco* and water remain as guest molecules in the channels. Analysis of self-assembly of molecules around the void space reveals that, in the host network, each **MA** molecule connected via catemeric $\text{O}-\text{H}\cdots\text{O}^-$ ($\text{H}\cdots\text{O}^-$, 1.56 and 1.59 Å) hydrogen bonds, creating cavities of $8.9 \times 14.7 \text{ \AA}^2$ in dimension, as shown in Figure 3.14b. The characteristics of hydrogen bonds are listed in Table 3.2. Further, the host network interacts with the guest species *dabco* molecules, through $\text{N}^+-\text{H}\cdots\text{O}$ ($\text{H}\cdots\text{O}$; 1.73 Å) hydrogen bonds and also with water molecules via $\text{N}^+-\text{H}\cdots\text{O}$ ($\text{H}\cdots\text{O}$; 1.89 Å) hydrogen bonds, as shown in Figure 3.14c.

3.3.6. Molecular complex of MA and 47phe, 1f

A reaction of **MA** and 4,7-phenanthroline (*47phe*) in a 1:1 ratio, at room temperature by slow evaporation method, gave good quality single crystals, which were characterized by X-ray diffraction method. Structures analysis reveals that, it is a hydrate of 1:2:2 complex of **MA** and *47phe*, **1f**. The contents of the asymmetric unit are shown in Figure 3.15.

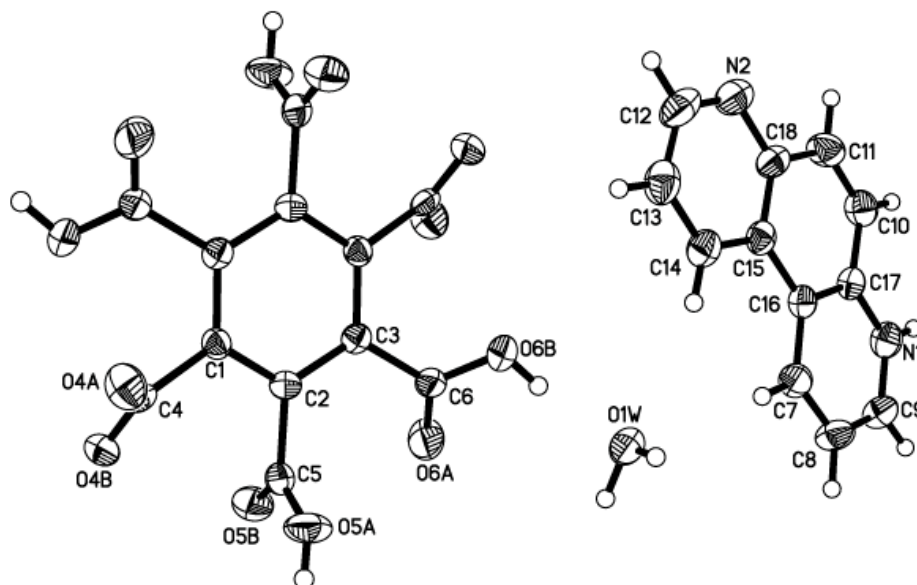


Figure 3.15. (a) ORTEP (50% probability level) of the molecular complex, **1f**, of **MA** and **47phe**.

Packing analysis and molecular arrangement in the crystal lattice reveals that, in the complex **1f** also, a zeolite type network is observed as found in **1e**. Such an assembly is shown in Figure 3.16a. It is apparent that while **MA** molecules along with water form a host network, the aza-donor moieties occupy the voids as guests. Further, the host network is due to the self assembly of **MA** molecules, with adjacent molecules are being held together by series of hydrogen bonds. In a microanalysis, it may be described that, by utilizing either 1, 2 or 4, 5 positioned carboxylic/carboxylate moieties, the molecules of **MA** form chains through O—H \cdots O (H \cdots O; 1.82 Å) hydrogen bonds. Such adjacent chains are further connected to each other through water molecules by O—H \cdots O hydrogen bonds (H \cdots O, 1.78 and 1.96 Å), as shown in Figure 3.16b.

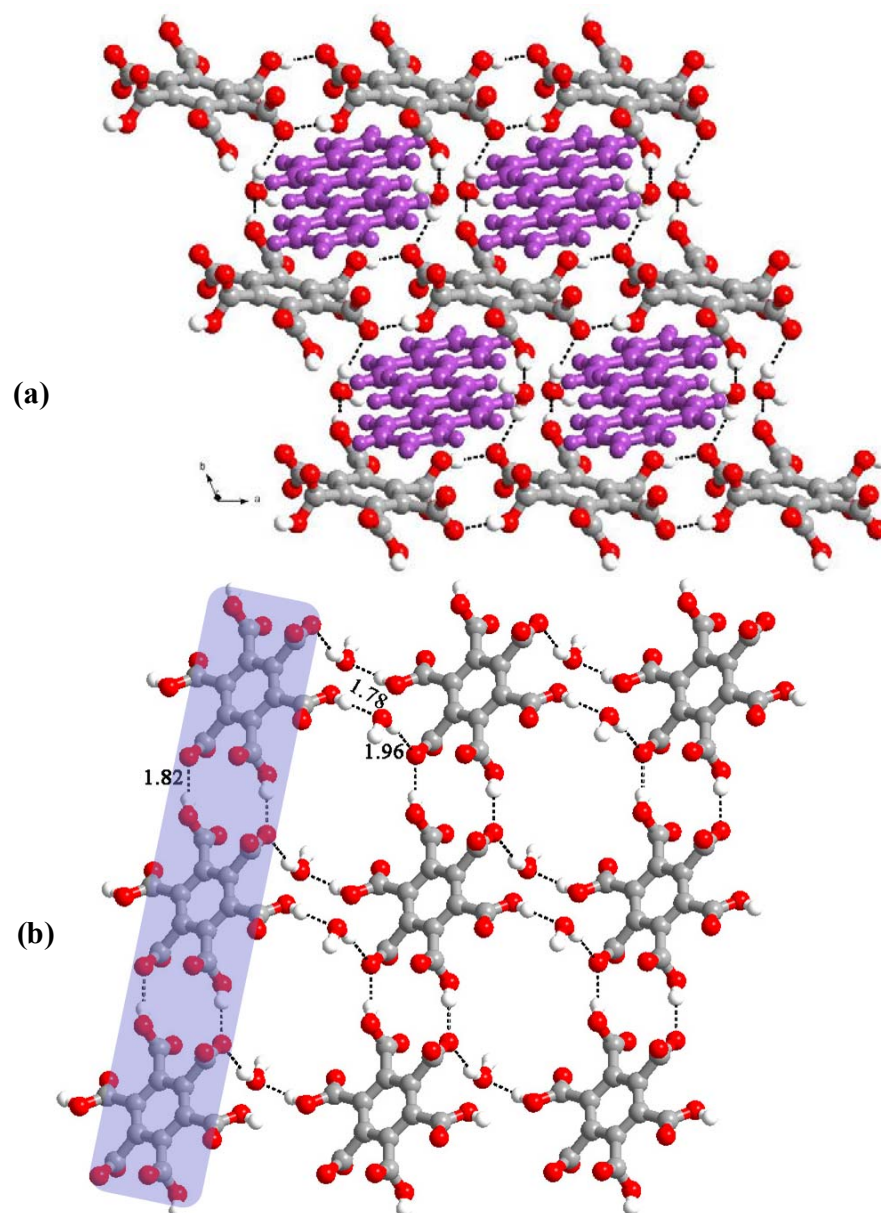


Figure 3.16. (a) Host-guest type arrangement of MA and *47phe* molecules in complex **1f**. (b) Self-assembly of MA molecules in the form of host network.

At this stage, focus was directed towards varying experimental conditions of crystallization, as we observed **BPC** showed variations in the formation of ultimate assemblies involves **BPC**, in particular with *bpy* and *47phe*. Hence, co-crystallization of MA and the aza-donor compounds, 4,4'-bipyridine (*bpy*), 1,2-bis(4-pyridyl)ethane

(*bpyea*), 1,2-bis(4-pyridyl)ethene (*bpyee*), 1,3-bis(4-pyridyl)propane (*bpyppa*), 1,4-diazabicyclo[2.2.2]octane (*dabco*), 1,10-phenanthroline (*110phe*), and 4,7-phenanthroline (*47phe*), etc. by hydrothermal methods have been carried out. It was found that **MA** also gave crystals of the same assemblies as observed at room temperature crystallization with all the aza-donors employed, except with *bpy*. The structural details of the complex are discussed below.

3.3.7. Molecular complex of MA and *bpy*, 1g

Co-crystallization of **MA** and *bpy*, by hydrothermal route (160 °C for 2days) gave single crystals with composition as a hydrate of 1:1 complex of the co-crystal formers, as determined by single crystal X-ray diffraction methods. Crystallographic details are given in Table 3.1. The contents of the asymmetric unit are shown in Figure 3.17.

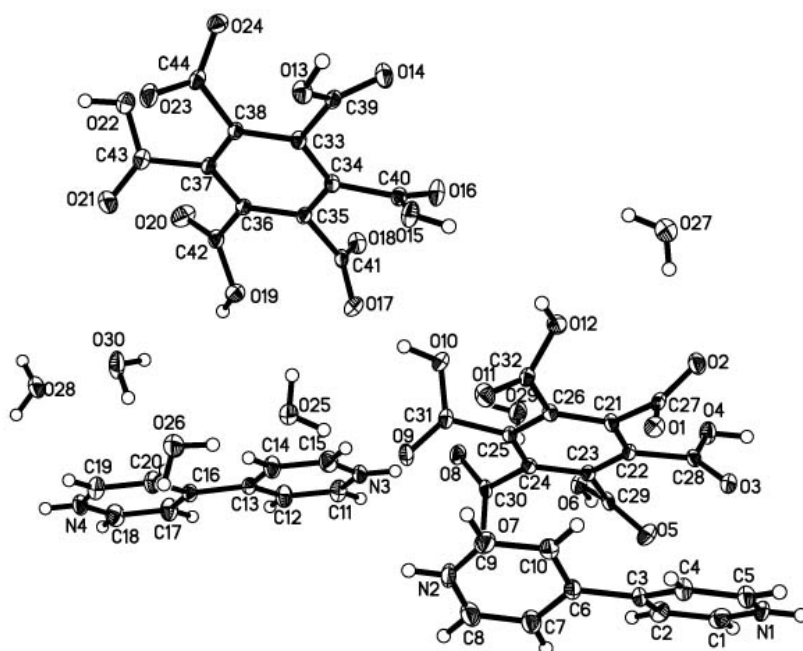


Figure 3.17. ORTEP of hydrated 1:1 complex of **MA** and *bpy*, 1g. .

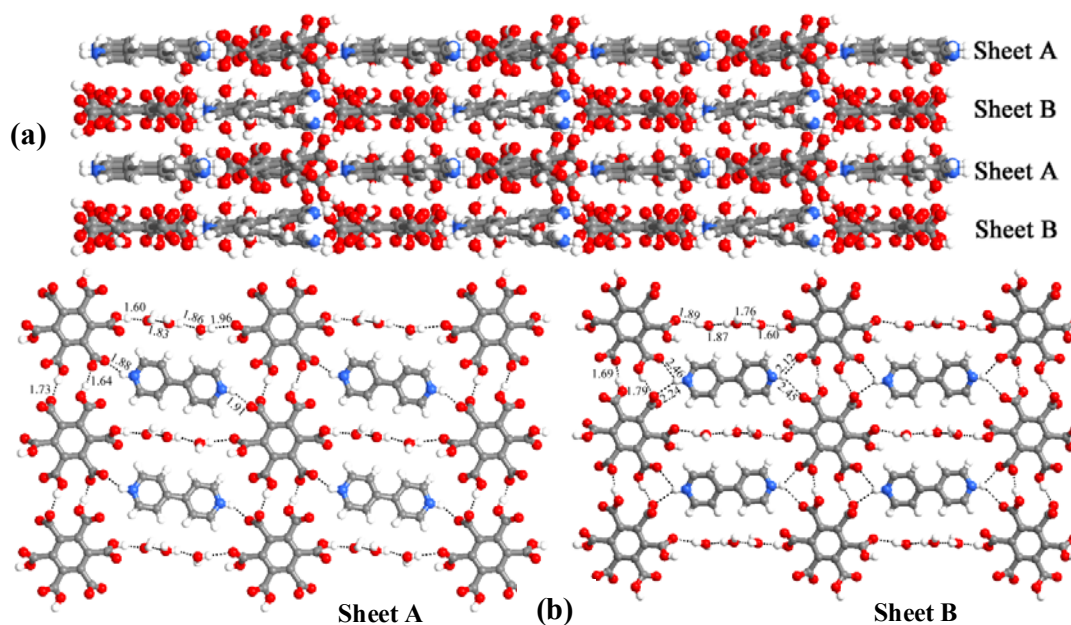


Figure 3.18. (a) Arrangement of molecules in the form of stacked layers, in the crystal structure of **1g**. (b) Molecules of **MA** and **bpy** within the layers, corresponding to two symmetry independent molecules (Sheet **A** and Sheet **B**).

The gross structure has several similarities with complex, **1a**. In the crystal lattice, two symmetry independent molecules are present. The arrangement of molecules in the crystal lattice is shown in Figure 3.18. The structure adopts stacked layers, comprising of molecules of one of the symmetry independent molecules in the alternate layers, labeled as sheet **A** and sheet **B**, (corresponding to two symmetry independent molecules, respectively), as shown in Figure 3.18, the arrangement is almost similar. The molecules of **MA**, form chains by catemeric type $\text{O}-\text{H}\cdots\text{O}^-$ ($\text{H}\cdots\text{O}^-$, 1.64, 1.73 and 1.69, 1.79 Å) hydrogen bonds (Table 3.2) formed by carboxyl and carboxylates via $R_2^2(14)$. Such adjacent chains are further held together by three water molecules, through $\text{O}-\text{H}\cdots\text{O}^-$ ($\text{H}\cdots\text{O}^-$, 1.89 and 1.96 Å) and $\text{O}-\text{H}\cdots\text{O}$ ($\text{H}\cdots\text{O}$, 1.60, 1.76, 1.83, 1.86 and 1.87 Å) hydrogen bonds (Figure 3.18).

Such an arrangement in both the sheets created cavities of dimension, $\sim 12 \times 9 \text{ \AA}^2$, which are being occupied by *bpy* molecules through the formation of $\text{N}^+ - \text{H} \cdots \text{O}^-$ ($\text{H} \cdots \text{O}^-$, 1.51, 1.56, 2.12, 2.24, 2.40, 2.45 \AA) hydrogen bonds. However, the sheets **A** and **B** did not stack via translation symmetry; thus, the cavities failed to constitute channels along a crystallographic direction

Since, at least in the case of **MA** and *bpy*, two different types of assemblies are observed by varying the crystallization parameters, analysis of all the co-crystals discussed have been analyzed by powder X-ray diffraction method also to ensure that no formation of concomitant crystals in either of the procedures. The experimental powder patterns are then compared with the simulated powder patterns obtained from the three dimensional structures established by single crystal X-ray diffraction method. The results are shown in Figure 3.19.

It has been observed that in all the cases, the patterns (simulated & experimental) match well indicating that during the co-crystallization process, only one type of the assembly is formed and three dimensional structures established are the representation of the bulk sample also.

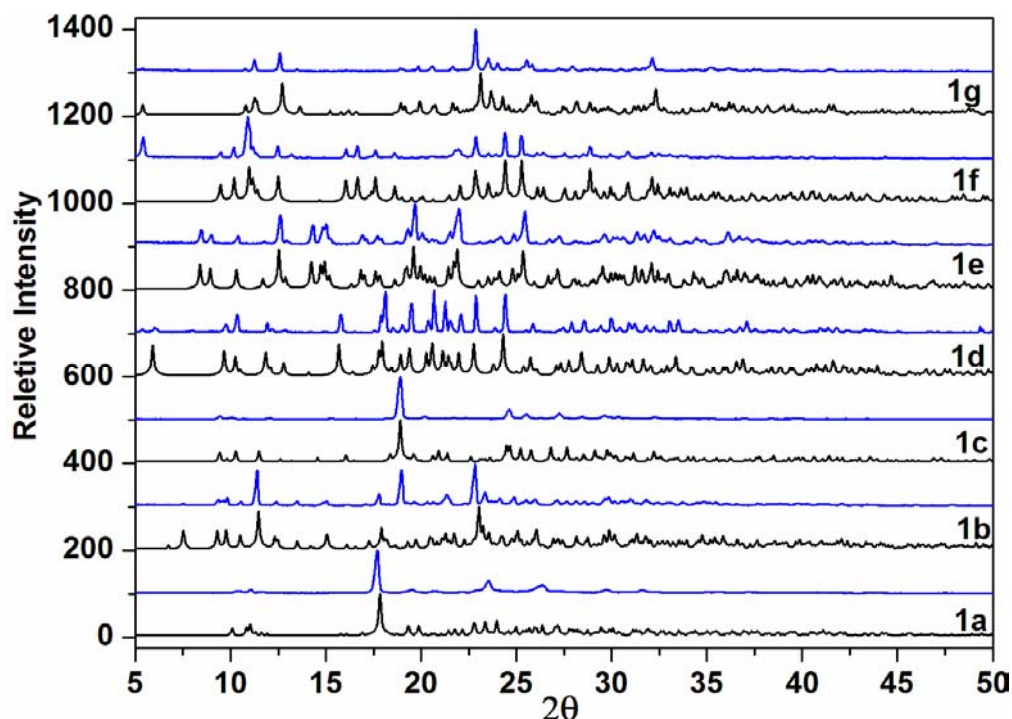


Figure 3.19. XRPD plots shows comparison between simulated XRPD patterns (black) and experimentally observed XRPD patterns (blue) of complexes **1a-1g**.

3.4. Conclusions

The synthesis and analysis of supramolecular assemblies formed by mellitic acid, **MA** with various aza-donor compounds such as 4,4'-bipyridine (*bpy*), 1,2-*bis*(4-pyridyl)ethane (*bpyea*), 1,2-*bis*(4-pyridyl)ethene (*bpyee*), 1,3-*bis*(4-pyridyl)propane (*bpyppa*), 1,4-diazabicyclo[2.2.2]octane (*dabco*) and 4,7-phenanthroline (*47phe*) have been reported.

In this study, the three complexes **1d**, **1e** and **1f**, has been found to form exotic host-guest networks by formation of various sizes of void space. The host network is primarily built by **MA** molecules, while aza-donor molecules play a role of guest species. Further, in majority of the structures, three dimensional structures is due to

the stacking of layers. In addition, a noteworthy observation is that except the complexes formed between **MA** and *bpy* (**1a** and **1g**), the aza-donor molecules are sandwiched between the layers of acids.

3.5. Experimental Section

3.5.1. Synthesis of molecular complexes, 1a–1g.

All the chemicals, **MA** and aza-donor compounds (*bpy*, *bpyea*, *bpyee*, *bpyya*, *dabco*, *47 phe* and *110 phe*) were purchased from commercial suppliers and used as such without any further purification. Crystallization experiments were carried out using spectroscopic grade solvents. For a typical crystallization, in a 25 mL conical flask, 74.5 mg (0.25 mmol) of **MA** and 39.0 mg (0.25 mmol) of *bpy* were dissolved in water by heating water to the boiling temperature and then subsequently cooling to room temperature at ambient conditions. Colorless rectangular block type single crystals of good quality were obtained within 4 days, which were used for single-crystal structure determination studies by X-ray diffraction methods. Complex, **1g** was prepared by hydrothermal method dissolving 34.2 mg (0.1 mmol) of **MA** and 15.6 mg of *bpy*, in 15 mL of H₂O and heated at 160 °C in a Teflon-line pressure vessel for 2 days. Cooling the apparatus to room temperature, gave single crystals of a complex of **MA** and *bpy* in a 1:1:3 ratio.

3.5.2. Crystal structure determination

Good quality single crystals of molecular complexes of acid **1a–1g** were carefully chosen after viewing through a Leica microscope (polarized) supported by a rotatable polarizing stage and a CCD camera. The crystals were glued to a thin

glass fiber using an adhesive (cyano acrylate) and mounted on a diffractometer equipped with an APEX CCD area detector. The X-ray intensity data were collected with varying exposure time depending upon the quality of the crystal(s). The data collection was smooth in all the cases, and no extraordinary methods have been employed, as the crystals were quite stable. The intensity data were processed using Bruker's suite of data processing programs (SAINT),¹⁵ and absorption corrections were applied using SADABS.¹⁶ The structure solution of all the complexes have been carried out by direct methods, and refinements were performed by full matrix least squares on F^2 using the SHELXTL-PLUS¹⁷ suite of programs. All the structures converged to good R -factors. All the non-hydrogen atoms were refined anisotropically, and the hydrogen atoms obtained from Fourier maps were refined isotropically. All the refinements were smooth in all the structures. All the intermolecular interactions were computed using PLATON.¹⁸

3.5.3. X-ray powder diffraction measurements

XPRD data were collected on a PANalytical diffractometer with $\text{CuK}\alpha$ radiation ($\lambda = 1.5406 \text{ \AA}$). The power of the X-ray generator was set to 40 kV and 30 mA with step size of 0.017° (2θ) in a continuous scanning mode. A microcrystalline mixture of the solids was prepared by grinding an required ratio of the precursors with a mortar and pestle for 2–10 min. Diffraction patterns were collected in the 2θ range $5\text{--}50^\circ$ at ambient temperature. Prolonged grinding of the compounds did not alter the diffraction patterns significantly.

Table 3.1. Crystallographic data of **MA** and the molecular complexes, **1a-1g**.

	MA	1a	1b	1c
Formula	C ₁₂ H ₆ O ₁₂	(C ₁₂ H ₄ O ₁₂) 2(C ₁₀ H ₉ N ₂)	(C ₁₂ H ₄ O ₁₂) (C ₁₂ H ₁₄ N ₂) 5(H ₂ O)	(C ₁₂ H ₄ O ₁₂) 2(C ₁₂ H ₁₁ N ₂) 2(H ₂ O)
Fw	342.17	654.54	606.40	742.64
Crystal shape	blocks	blocks	blocks	blocks
Crystal color	colorless	colorless	colorless	colorless
Crystal system	orthorhombic	triclinic	monoclinic	monoclinic
Space group	<i>Pccn</i>	<i>P</i> $\bar{1}$	<i>P2</i> ₁ / <i>c</i>	<i>C2/c</i>
<i>a</i> (Å)	8.127(1)	10.523(2)	19.056(5)	15.508(2)
<i>b</i> (Å)	16.544(2)	17.673(3)	18.099(4)	11.228(2)
<i>c</i> (Å)	19.114(3)	18.375(3)	15.482(4)	19.325(3)
α (°)	90.00	111.11(5)	90.00	90.00
β (°)	90.00	102.75(6)	94.45(4)	103.82(4)
γ (°)	90.00	105.71(6)	90.00	90.00
<i>V</i> (Å ³)	2569.9 (6)	2869.9 (1)	5324.0 (2)	3267.4(7)
<i>Z</i>	8	4	8	4
<i>D</i> _{calc} (g cm ⁻³)	1.769	1.515	1.513	1.510
<i>T</i> (K)	293(2)	120(2)	100(2)	278(2)
Mo <i>k</i> _α	0.71073	0.71073	0.71073	0.71073
μ (mm ⁻¹)	0.166	0.118	0.132	0.118
<i>2</i> θ _{max} (°)	46.54	50.00	50.02	41.82
<i>F</i> (000)	1392	1352	2496	1544
Total reflns	10262	13942	37544	19711
No. unique reflns [<i>R</i> (int)]	1850 [0.0382]	9515 [0.0653]	9348 [0.0378]	1734 [0.0683]
No. reflns used	1324	5044	6895	1422
No. parameters	228	865	783	263
GOF on <i>F</i> ²	1.041	0.975	1.682	2.020
<i>R</i> ₁ [<i>I</i> >2 σ (<i>I</i>)]	0.0435	0.0741	0.0933	0.0793
w <i>R</i> ₂	0.1227	0.1659	0.2542	0.2362

Table 3.1. Contd...

	1d	1e	1f	1g
Formula	(C ₁₂ H ₄ O ₁₂) (C ₁₃ H ₁₆ N ₂) H ₂ O	(C ₁₂ H ₄ O ₁₂) (C ₆ H ₁₄ N ₂) 5(H ₂ O)	(C ₁₂ H ₄ O ₁₂) 2(C ₁₂ H ₉ N ₂) 2(H ₂ O)	(C ₁₂ H ₄ O ₁₂) (C ₁₀ H ₁₀ N ₂) 3(H ₂ O)
Fw	556.43	542.41	738.61	552.40
Crystal shape	blocks	blocks	plates	blocks
Crystal color	colorless	colorless	colorless	colorless
Crystal system	orthorhombic	orthorhombic	triclinic	monoclinic
Space group	<i>I</i> 222	<i>P</i> 2 ₁ 2 ₁ 2 ₁	<i>P</i> $\bar{1}$	<i>P</i> c
<i>a</i> (Å)	9.613(2)	9.519(1)	9.031(1)	16.39(3)
<i>b</i> (Å)	17.251(4)	12.434(1)	9.390(1)	7.688(1)
<i>c</i> (Å)	29.900(7)	19.808(2)	10.681(1)	17.800(3)
α (°)	90.00	90.00	102.70(2)	90
β (°)	90.00	90.00	112.31(3)	90.71(1)
γ (°)	90.00	90.00	101.76(2)	90
<i>V</i> (Å ³)	4958.4 (1)	2344.0 (3)	775.0 (2)	2243.6
<i>Z</i>	8	4	1	4
<i>D</i> _{calc} (g cm ⁻³)	1.493	1.537	1.583	1.635
<i>T</i> (K)	293(2)	293(2)	293(2)	120(2)
Mo <i>k</i> _α	0.71073	0.71073	0.71073	0.71073
μ (mm ⁻¹)	0.123	0.139	0.124	0.141
2 θ _{max} (°)	46.70	50.08	46.54	61.02
<i>F</i> (000)	2304	1136	382	1144
Total reflns	15328	15571	6484	20404
No. unique reflns [<i>R</i> (int)]	3595 [0.0315]	4117 [0.0306]	2217 [0.0494]	13171 [0.0253]
No. reflns used	2473	3645	1602	11150
No. parameters	374	438	281	783
GOF on <i>F</i> ²	1.060	0.966	1.075	1.037
<i>R</i> ₁ [<i>I</i> >2 σ (<i>I</i>)]	0.0723	0.0280	0.0516	0.0437
w <i>R</i> ₂	0.2060	0.0609	0.0978	0.1077

Table 3.2. Characteristics of hydrogen bonds in **MA** and its molecular complexes with aza donors (distances/Å and angles/°)#.

Hydrogen bonds	MA			1a			1b			1c		
O–H···O	1.83	2.64	169	1.72	2.55	168	1.68	2.47	161	1.71	2.62	165
	1.84	2.66	165	1.72	2.55	170	1.68	2.48	164	1.72	2.53	171
	1.84	2.68	175	1.74	2.56	163	1.68	2.49	168	2.15	2.92	140
	1.86	2.65	162	1.77	2.55	154	1.72	2.53	170	2.23	2.94	133
	1.88	2.67	160				1.80	2.61	174			
	1.89	2.68	159				1.82	2.50	140			
	1.89	2.68	163				1.82	2.51	142			
							1.88	2.69	157			
N ⁺ –H···N										1.83	2.68	173
N ⁺ –H···O ⁻				1.72	2.58	166	1.86	2.71	172	1.86	2.69	163
				1.74	2.61	168	1.88	2.69	157			
				1.76	2.63	167	1.88	2.74	174			
				1.79	2.66	169	1.91	2.72	156			
O–H···N				1.81	2.54	145						
				1.82	2.57	147						
				1.91	2.61	140						

Table 3.2. *Contd...*

Hydrogen bonds	1d			1e			1f			1g		
O-H...O	1.39	2.10	141	1.56	2.58	174	1.78	2.62	163	1.60	2.52	176
	1.65	2.46	172	1.59	2.54	173	1.82	2.62	163	1.62	2.45	151
	1.81	2.62	171	1.62	2.55	171	1.96	2.80	167	1.64	2.56	168
	1.83	2.65	177	1.75	2.57	163				1.69	2.57	169
				1.82	2.80	164				1.73	2.62	169
				1.90	2.76	173				1.75	2.61	171
				1.91	2.79	171				1.76	2.65	164
				1.99	2.79	165				1.79	2.66	175
				1.99	2.83	177				1.83	2.67	156
				2.03	2.89	174				1.84	2.70	158
				2.04	2.89	166				1.86	2.70	159
				2.35	3.19	154				1.87	2.74	167
				2.49	3.11	126				1.89	2.76	165
O-H...N							1.87	2.82	156			
N ⁺ -H...O ⁻	2.15	2.78	128	1.73	2.64	167				1.88	2.70	152
	2.23	2.84	127	1.89	2.70	169				1.91	2.69	147
										2.12	2.81	135
										2.24	3.02	148
										2.45	3.11	132
N-H...N	2.35	3.08	134									

For each structure, the three columns correspond to distances of H...X, D...X and angle D-H...X, respectively.

3.6. References

- (a) Ling, A.R.; Baker, J. L. *J. Chem. Soc.* **1893**, *63*, 1314–1327. (b) Delori, A.; Suresh, E.; Pedireddi, V. R. *Chem. Eur. J.* **2008**, *14*, 6967–6977. (c) Braga, D.; Giaffreda, S. L.; Grepioni, F.; Palladino, G.; Polito, M. *New. J. Chem.* **2008**, *32*, 820–828. (d) Perumalla, S. R.; Suresh, E.; Pedireddi, V. R. *Angew. Chem., Int. Ed.* **2005**, *44*, 7752–7757. (e) Anderson, J. S. *Nature* **1937**, *140*, 583–584. (f) Bhogala, B. R.; Basavoju, S.; Nangia, A. *CrystEngComm* **2005**, *7*, 551–562. (g) Braga, D.; Polito, M.; Grepioni, F. *Cryst. Growth Des.* **2004**, *4*, 769–774.
- (a) McKinlay, R. M.; Thallapally, P. K.; Cave, G. W. V.; Atwood, J. L. *Angew. Chem., Int. Ed.* **2005**, *44*, 5733–5736. (b) Ikeda, M.; Nobori, T.; Schmutz, M.; Lehn, J. M. *Chem. Eur. J.* **2005**, *11*, 662–668. (c) Pedireddi, V. R.; Seethalekshmi, N. *Tetrahedron Lett.* **2004**, *45*, 1903–1906. (d) Ziener, U.; Lehn, J. M.; Mourran, A.; Moller, M. *Chem. Eur. J.* **2002**, *8*, 951–957. (e) Timmerman, P.; Jolliffe, K. A.; Calama, M. C.; Weidmann, J. L.; Prins, L. J.; Cardullo, F.; Snellink-Ruel, B. H. M.; Fokkens, R. H.; Nibbering, N. M. M.; Shinkai, S.; Reinhoudt, D. N. *Chem. Eur. J.* **2000**, *6*, 4104–4115.
- (a) Huang K.; Britton, D.; Etter, M. C.; Byrn, S. R. *J. Mater. Chem.* **1997**, *7*, 713–720. (b) Matulkova, I.; Nemeč, I.; Teubner, K.; Nemeč, P.; Micka, Z. *J. Mol. Struct.* **2008**, *873*, 46–60. (c) Wei, Y. L.; Zhu, Y.; Song, Y. L.; Hou, H. W.; Fan, Y. T. *Inorg. Chem. Commun.* **2002**, *5*, 166–170. (d) Matulkova, I.; Nemeč, I.; Teubner, K.; Nemeč, P.; Micka, Z. *J. Mol. Struct.* **2008**, *873*, 46–60. (e) Yufit, D. S.; Chetina, O. V.; Howard, J. A. K. *J. Mol. Struct.* **2006**, *784*, 214–221. (f) Cole,

- J. M.; Wilson, C. C.; Howard, J. A. K.; Cruickshank, F. R. *Acta Crystallogr.* **2000**, *B56*, 1085–1093.
4. (a) Kang, J. M.; Rebek, J. J. *Nature*, **1997**, *385*, 50–51. (b) Ziegler, M.; Brumaghim, J. L.; Raymond, K. N. *Angew. Chem., Int. Ed.* **2000**, *112*, 4285. (c) Yoshizawa, M.; Takeyama, Y.; Okano, T.; Fujita, M. *J. Am. Chem. Soc.* **2003**, *125*, 3243. (d) Fujita, M.; Umemoto, K.; Yoshizawa, M.; Fujita, N.; Kusukawa, T. *Chem. Commun.* **2001**, 509–210. (e) Hu, A.; Ngo, H. L.; Lin, W. *Angew. Chem., Int. Ed.* **2003**, *42*, 6000. (f) Wu, C. D.; Hu, A.; Zhang, L.; Lin, W. B. *J. Am. Chem. Soc.* **2005**, *127*, 8940. (g) Cho, S. H.; Ma, B. Q.; Nguyen, S. T.; Hupp, J. T.; Albrecht–Schmitt, T. E. *Chem. Commun.* **2006**, 2563. (h) Dybtsev, D. N.; Nuzhdin, A. L.; Chun, H.; Bryliakov, K. P.; Talsi, E. P.; Fedin, V. P.; Kim, K. *Angew. Chem., Int. Ed.* **2006**, *45*, 916. (i) Hasegawa, S.; Horike, S.; Matsuda, R.; Furukawa, S.; Mochizuki, K.; Kinoshita, Y.; Kitagawa, S. *J. Am. Chem. Soc.* **2007**, *129*, 2607. (j) Horcajada, P.; Surble, S.; Serre, C.; Hong, D. Y.; Seo, Y. K.; Chang, J. S.; Greneche, J. M.; Margiolaki, I.; Ferey, G. *Chem. Commun.* **2007**, 2820. (k) Fujita, M.; Kwon, Y. J.; Washizu, S.; Ogura, K. *J. Am. Chem. Soc.* **1994**, *116*, 1151. (l) Evans, O. R.; Ngo, H. L.; Lin, W. B. *J. Am. Chem. Soc.* **2001**, *123*, 10395.
5. (a) Almarsson, O.; Zaworotko, M. J. *Chem. Commun.* **2004**, 1889–1896. (b) Datta, S.; Grant, D. J. W. *Nat. Rev. Drug Discovery* **2004**, *3*, 42–57. (c) Rodriguez-Spong, B.; Price, C. P.; Jayasankar, A.; Matzger, A. J.; Rodriguez-Horenedo, N. *Adv. Drug Delivery Res.* **2004**, *56*, 241–274. (d) Morissette, S. L.; Almarsson, O.; Peterson, M. L.; Remenar, J. F.; Read, M. J.; Lemmo, A. V.; Ellis,

S.; Cima, M. J.; Gardner, C. R. *Adv. Drug Delivery Res.* **2004**, *56*, 275–300. (e) Gardner, C. R.; Walsh, C. T.; Almarsson, O. *Nat. Rev. Drug Discovery* **2004**, *3*, 926–934. (f) Remenar, J. F.; MacPhee, J. M.; Larson, B. K.; Tyagi, V. A.; Ho, J. H.; McIlroy, D. A.; Hickey, M. B.; Shaw, P. B.; Almarsson, O. *Org. Process Res. Dev.* **2003**, *7*, 990–996. (g) Huang, L. F.; Tong, W. Q. *Adv. Drug Delivery Res.* **2004**, *56*, 321–334. (h) Walsh, R. B.; Bradner, M. W.; Fleischman, S. G.; Morales, L. A.; Moulton, B.; Rodriguez-Horenedo, N.; Zaworotko, M. J. *Chem. Commun.* **2003**, 186–187. (i) Cheney, M. L.; Shan, N.; Healey, E. R.; Hanna, M.; Wojtas, L.; Zaworotko, M. J.; Sava, V.; Song, S. J.; Sanchez-Ramos, J. R. *Cryst. Growth Des.* **2010**, *10*, 394–405. (j) Roy, S.; Mahata, G.; Biradha, K. *Cryst. Growth Des.* **2009**, *9*, 5006–5008. (k) Karki, S.; Friscic, T.; Jones, W. *CrystEngComm* **2009**, *11*, 470–481. (l) Weyna, D. R.; Shattock, T.; Vishweshwar, P.; Zaworotko, M. J. *Cryst. Growth Des.* **2009**, *9*, 1106–1123. (m) Cooke, C. L.; Davey, R. J. *Cryst. Growth Des.* **2008**, *8*, 3483–3485. (n) Aakeroy, C. B.; Fasulo, M. E.; Desper, J. *Molecular Pharmaceutics* **2007**, *4*, 317–322. (o) Childs, S. L.; Stahly, G. P.; Park, A. *Molecular Pharmaceutics* **2007**, *4*, 323–338. (p) Ma, Z. B.; Moulton, B. *Molecular Pharmaceutics* **2007**, *4*, 373–385. (q) Rodriguez-Hornedo, N.; Nehru, S. J.; Seefeldt, K. F.; Pagan-Torres, Y.; Falkiewicz, C. *J. Pharma. Sci.* **2006**, *3*, 362–367. (r) Banerjee, R.; Bhatt, P. M.; Ravindra, N. V.; Desiraju, G. R. *Cryst. Growth Des.* **2005**, *5*, 2299–2309. (s) Childs, S. L.; Chyall, L. J.; Dunlap, J. T.; Smolenskaya, V. N.; Stahly, B. C.; Stahly, G. P. *J. Am. Chem. Soc.* **2004**, *126*, 13335–13342. (t) Vishweshwar, P.; McMahon, J. A.; Bis, J. A.; Zaworotko, M. J. *J. Pharma. Sci.* **2006**, *95*, 499–516.

6. (a) Duchamp, D. J.; Marsh, R. E. *Acta Crystallogr.* **1969**, *B25*, 5–19. (b) Sim, G. A.; Robertson, J. M.; Goodwin, T. H. *Acta Crystallogr.* **1955**, *8*, 157–164. (c) Ermer, O. *Helv. Chim. Acta*, **1981**, *64*, 1902–1909. (d) Colapietro, M.; Domenicano, A.; Marciante, C.; Portalone, G. *Acta Crystallogr.* **1984**, *A40*, C98–C99. (e) Bhogala, B.R.; Vishweshwar, P.; Nangia A. *Cryst. Growth Des.* **2002**, *2*, 325. (f) Takusagawa, F.; Hirotsu, K.; Srmada, A. *Bull. Chem. Soc. Jpn.* **1971**, *44*, 1274–1278. (g) Takusagawa, F.; Hirotsu, K.; Shimada, A. *Bull. Chem. Soc. Jpn.* **1973**, *46*, 2960–2965. (h) Benedetti, E.; Corradini, P.; Pedone C. *J. Am. Chem. Soc.* **1969**, *91*, 4075–4076. (i) Koningsveld, H. V. *Acta Crystallogr.* **1984**, *C40*, 1857.
7. (a) Aakeroy, C. B.; Schultheiss, N. C.; Rajbanshi, A.; Desper, J.; Moore, C. *Cryst. Growth Des.* **2009**, *9*, 432–441. (b) Pedireddi, V. R.; Arora, K. K. *J. Org. Chem.* **2003**, *44*, 9177–9185. (c) Sudhakar, P.; Srivijaya, R.; Sreekanth, B. R.; Jayanthi, P. K.; Vishweshwar, P.; Babu, M. J.; Vyas, K.; Iqbal, J. *J. Mol. Struct.* **2008**, *885*, 45–49. (d) Bhogala, B. R.; Nangia, A. *New. J. Chem.* **2008**, *32*, 800–807. (e) Aakeroy, C. B.; Schultheiss, N.; Desper, J.; Moore, C. *New. J. Chem.* **2006**, *30*, 1452–1460. (f) Babu, N. J.; Nangia, A. *Cryst. Growth Des.* **2006**, *6*, 1995–1999. (g) Vishweshwar, P.; Nangia, A.; Lynch, V. M. *Cryst. Growth Des.* **2003**, *3*, 783–790. (g) Aakeroy, C. B.; Beatty, A. M.; Helfrich, B. A. *J. Am. Chem. Soc.* **2002**, *124*, 14425–14432. (h) Vishweshwar, P.; Nangia, A.; Lynch, V. M. *J. Org. Chem.* **2002**, *67*, 556–565. (i) Shattock, T. R.; Arora, K. K.; Vishweshwar, P.; Zaworotko, M. J. *Cryst. Growth Des.* **2008**, *8*, 4533–4545.
8. Ermer, O. *J. Am. Chem. Soc.* **1988**, *110*, 3747–3754.

9. Fleischman, S. G.; Kuduva, S. S.; McMahon, J. A.; Moulton, B.; Bailey Walsh, R. D.; Rodríguez-Hornedo, N.; Zaworotko, M. J. *Cryst. Growth Des.* **2003**, *3*, 909–919.
10. Coles, S. J.; Holmes, R.; Hursthouse, M. B.; Price, D. J. *Acta Crystallogr.* **2002**, *E58*, O626–O628.
11. (a) Karle, I.; Gilardi, R. D.; Rao, C. C.; Muraleedharan, K. M.; Ranganthan, S. J. *Chem. Cryst.* **2003**, *33*, 727–749. (b) Inabe, T.; Kobayashi, N.; Naito, T. *Bull. Chem. Soc. Jpn.* **2003**, *76*, 1351. (c) Kobayashi, N.; Naito, T.; Inabe T. *CrystEngComm.* **2004**, *6*, 189.
12. Darlow, S. F. *Acta Crystallogr.* **1961**, *14*, 159.
13. (a) Feed, R.; Lehmann, M. S.; Muir, K. W.; Speakman, J. C. Z. *Kristallogr.* **1981**, *157*, 215–231. (b) Sim, G. A.; Robertson, J. M.; Goodwin, T. H. *Acta Cryst.* **1955**, *8*, 157–164. (c) Bruno, G.; Randaccio, T. *Acta Cryst.* **1980**, *B36*, 1711–1712.
14. Allen, F. H.; Kennard, O. *Chem. Des. Automat. News* **1993**, *8*, 31–37.
15. *SAINTE*, Version 6.02; Bruker AXS, Inc., Analytical X-ray Systems, 5465 East Cheryl Parkway, Madison, WI 53711–5373, 2000.
16. *SADABS* [Area-Detector Absorption Correction]; Siemens Industrial Automation, Inc.: Madison, WI, 1996.
17. G. M. Sheldrick, *SHELXTL*, University of Göttingen, Göttingen, Germany, 1997.
18. A. L. Spek, *PLATON*, molecular geometry program, University of Utrecht, The Netherlands, 1995.

**CHAPTER
4**

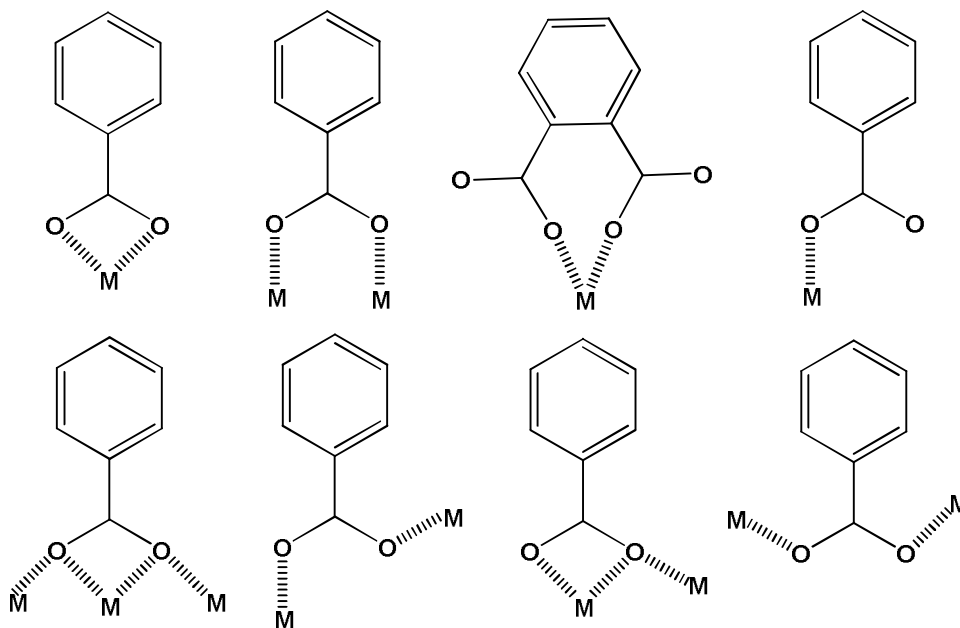
**Coordination Polymers
of Benzene Penta and
Hexa Carboxylic Acids**

4.1 Introduction

In recent times, coordination compounds are extensively being studied as metal-organic open framework network structures, considering metals ions as nodes and organic ligands as linkers.¹ The key to success of such networks is the ability of coordination spheres to be structure directing units, which direct the formation of the assemblies of desired architectural, chemical and physical properties. Synthesis of metal coordination polymers²⁻⁴ has attracted much attention not only due to their intriguing structural topologies and novel properties for potential applications, but also for bridging different branches of science, in particular, chemistry and physics. Thus, applications of these materials are multidimensional that include, for example, studies related to magnetism (long-range ordering, spin crossover), porosity (gas storage, ion and guest exchange), non-linear optical activity, chiral networks, reactive networks, heterogeneous catalysis, luminescence, multifunctional materials etc.⁵⁻⁷

Transition-metal ions are well utilized as versatile connectors in the construction of coordination complexes, because their chemistry such as, predictable nature of the coordination geometry is well documented and they can be conveniently incorporated into the network assemblies. In this direction, first-row transition elements along with Cd, Hg, Ag etc., are well explored in the construction of metal-organic frameworks and depending upon the metal ion and its oxidation state, coordination numbers can vary from 2 to 8, leading to various geometries, for example, linear, T- or Y-shaped, tetrahedral, square-planar, square-pyramidal, trigonal-bipyramidal, octahedral etc., thus, enabling the formation of a variety of architecture at ease.⁸

Among the organic ligands, the carboxylate mediated ligands are well documented in the literature, especially due to the formation of a wide range of bridging modes possible, as shown in Scheme 4.1, expanding the horizon of formation of numerous extended framework structures.



Scheme 4.1

In this direction, aromatic polycarboxylates, with substitution at various positions have been employed exclusively, with notable and exotic architectures reported in the literature, being the acids with substitutions at 1,2,3-;⁹ 1,3,5-;^{10,11} and 1,2,4,5-^{12,13} positions. However, to the best of our knowledge, penta substituted, 1,2,3,4,5-benzenepentacarboxylic acid (**BPC**) and hexa substituted, mellitic acid (**MA**), are not been well explored in the area of metal-organic frameworks, except for a few reports of Inabe and co-workers,¹⁴ Tong and co-workers¹⁵ etc. In fact, **BPC** and **MA** possess several interesting characteristics for the creation of myriad of exotic

supramolecular assemblies as specified herein: (a) availability of maximum carboxylic groups, whose deprotonation (partial or total) leads to extensive coordination to the metal ions; (b) ability to form not only coordination bonds but also hydrogen bonds, depending upon the degree of deprotonation; (c) conformational flexibility of the carboxylic groups and connectivity to the metal ion in different directions.

Hence, **BPC** and **MA** also apparently can yield open-frame structures in conjunction with metal ions, as any other polycarboxylic acids studied so far. Thus, we are interested to explore coordination polymers that contain transition metal ions and the polycarboxylic acids **BPC** and **MA**. In this chapter, structural features of the assemblies formed by M(II) [M = Co(II), Cu(II) and Cd(II)] species with **BPC** and **MA**, in the presence of some bipyridyl ligands like 4,4'-bipyridine (*bpy*), 1,2-bis(4-pyridyl)ethane (*bpyea*), and 1,3-bis(4-pyridyl)propane (*bpypa*) etc., as shown in Chart I, are discussed in detail.

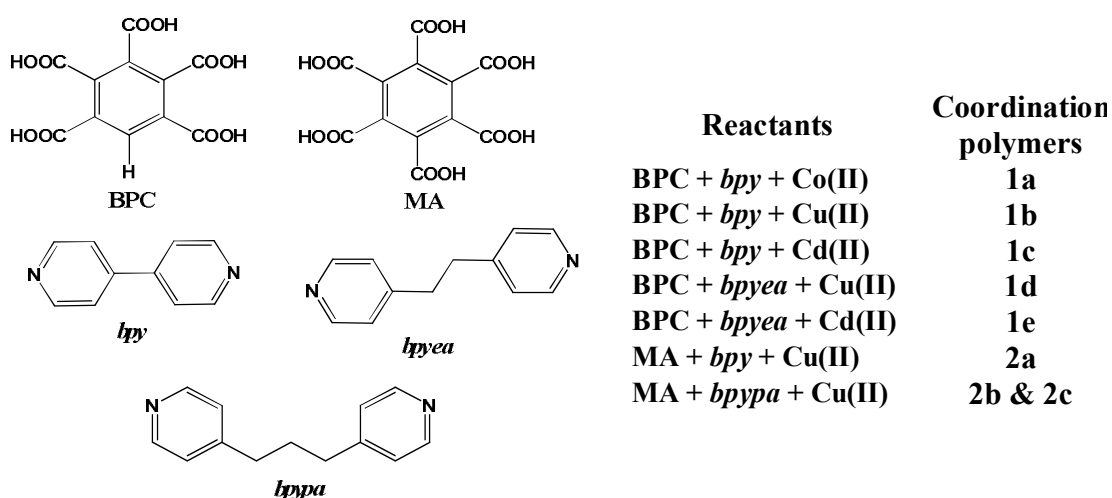


Chart I

4.2.1 Coordination complex of Co(II) with BPC and *bpy*-1a

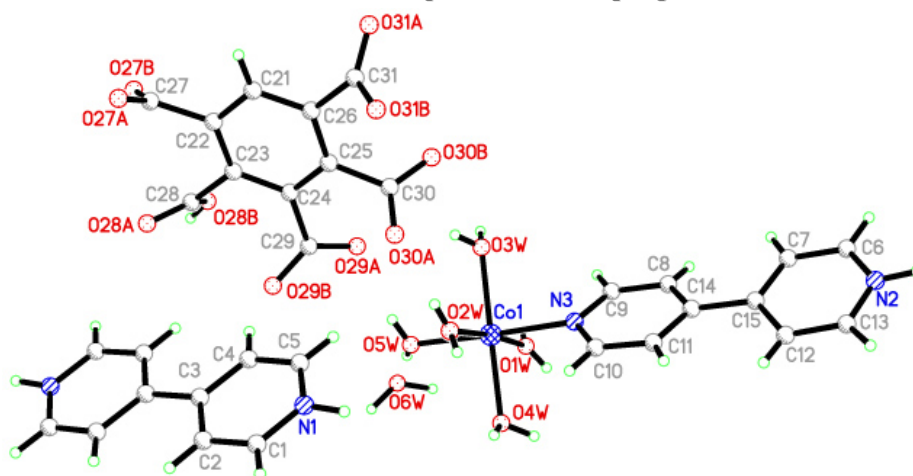


Figure 4.1. Asymmetric unit of complex 1a.

Hydrothermal reaction of cobalt nitrate hexahydrate and **BPC** with 4,4'-bipyridine, *bpy*, at 140 °C for four days and subsequent slow evaporation of the resultant solution, over a period of ten days, at ambient conditions, yielded well grown single crystals suitable for the structure determination by X-ray diffraction methods. The crystal structure determination reveals that the complex has a structural moiety $[\text{Co}(\text{C}_{10}\text{H}_9\text{N}_2)(\text{H}_2\text{O})_5](\text{C}_{11}\text{H}_2\text{O}_{10})0.5(\text{C}_{10}\text{H}_{10}\text{N}_2)(\text{H}_2\text{O})$ and crystallizes in triclinic space group, *P*1. Complete details, pertain to crystal structure determination are given in the Table 4.1. In the asymmetric unit, Co(II) is coordinated to a *bpy* molecule forming Co–N bond with a distance of 2.15 Å. All the other bonding parameters are listed in Table 4.2. Further, five water molecules are bonded to Co(II) with Co–O (2.07, 2.08, 2.09, 2.11, 2.11 Å, Table 4.2) bonds, leading to an octahedral geometry around the Co (II) species. Thus, there is no dative bond formed between Co(II) and **BPC**. However, in the crystal lattice, **BPC** molecules present as

uncoordinated species. Similarly, another uncoordinated *bpy* and water molecules are also present in the crystal lattice as illustrated in Figure 4.1.

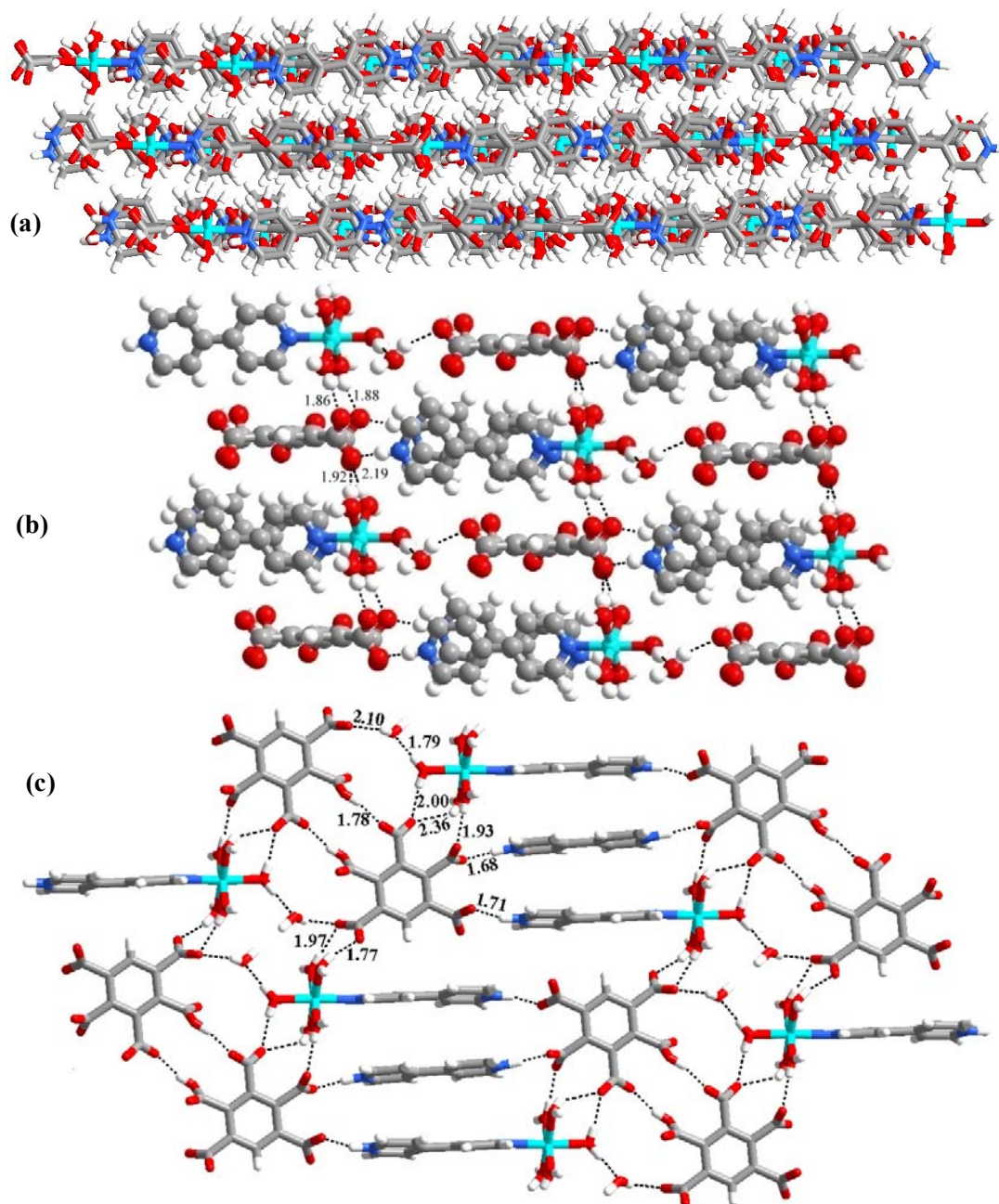


Figure 4.2. (a) Arrangement of stacked layers in complex **1a**. (b) Projection of interlayer hydrogen bonds (Dashed lines in black) (c) Packing of molecules, in two-dimensional arrangement, held together by hydrogen bonds.

In three-dimensional arrangement, molecules are arranged in stacked layers, as shown in Figure 4.2a. These stacked layers are held together by O–H \cdots O $^-$ (H \cdots O $^-$, 1.86, 1.88, 1.92 and 2.19 Å) hydrogen bonds formed between coordinated water molecules and **BPC** moieties, as shown in Figure 4.2b. In each sheet, as represented in Figure 4.2c, the **BPC** molecules form dimeric units, in the form of R $_2^2(14)$ topology through O–H \cdots O $^-$ (H \cdots O $^-$, 1.78 Å) hydrogen bonds formed between carboxyl and carboxylate groups. Such adjacent dimeric units are held together by uncoordinated *bpy* molecules as well as by *bpy* molecules that are connected to Co(II), with the aid of hydrogen bonds. While uncoordinated *bpy* molecules form N–H \cdots O $^-$ (H \cdots O $^-$, 1.68 Å) hydrogen bonds, the coordinated species are connected by N–H \cdots O as well as O–H \cdots O $^-$ hydrogen bonds. The characteristics of hydrogen bonds are listed in the Table 4.3. Thus, observing preferential formation of coordinate bond with only *bpy* molecules, we further intended to study the recurrence of such situations by varying the metal species as well as organic entities. For this purpose, to begin with preparation of coordinated complexes of **BPC** in the presence of *bpy* has been carried out, by replacing the metal ion. In this process, experiments with Ni(II) and Zn(II) salts did not yield appropriate good quality single crystals to elucidate three-dimensional structures, but, we were able to obtain desired quality single crystals from the reaction of Cu(II) and Cd(II) salts with **BPC** and *bpy* molecules, as discussed below.

4.2.2 Coordination polymer of Cu(II) with BPC and *bpy*-1b

Hydrothermal reaction of **BPC**, 4,4'-bipyridine, *bpy* and copper nitrate, at 140 °C for four days, yielded complex **1b**, with the composition as [Cu $_2$ (C $_{11}$ H $_1$ O $_{10}$)

(C₁₀H₈N₂)]4(H₂O). The crystal structure was established by single crystal X-ray diffraction method. The complete details of the crystallographic information are given in Table 4.1.

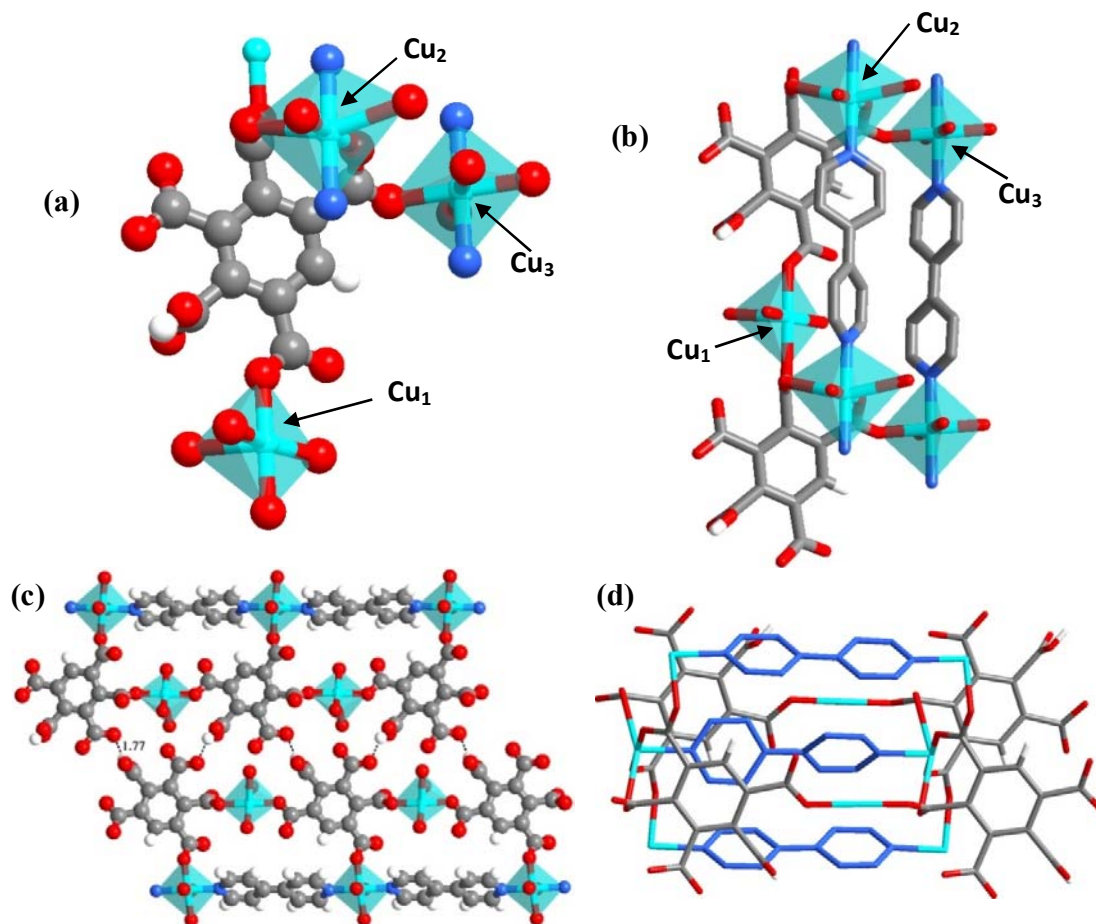


Figure 4.3. (a) Representation of dative bonds formed between **BPC** and Cu(II) in the structure **1b**. (b) Different coordination spheres of Cu(II) in the crystal structure of complex, **1b**, square pyramidal and octahedral geometry. (c) Packing of coordination polymers in two dimensions, held together by hydrogen bonds. (d) Presentation of double grid networks due to the interactions of **BPC** and *bpy* with Cu centre.

The structure analysis reveals that complex **1b** shows totally a different structural arrangement than observed in the complex **1a**. In the structure of complex

1b, the Cu(II) forms coordinate bond with **BPC** as well as *bpy* molecules. In the complex **1b**, Cu(II) exists in three different coordination environments, one is in square pyramidal (Cu_1) and two are in octahedral geometry (Cu_2 and Cu_3), as shown in Figure 4.3a. The details of coordination environment of the metal center are listed in Table 4.2. Thus, square pyramidal geometry around Cu_1 is due to the coordination of two **BPC** and three water molecules, where as the octahedral environment is formed at Cu_2 and Cu_3 through the dative bonds formed by both **BPC** and *bpy* molecules, as shown in Figure 4.3b. In specific, a carboxylate group from each of two **BPC** units is bound to Cu_2 centre by chelated mode and also two twisted *bpy* units through monodentate fashion, yielding a hexa coordination environment. However, around Cu_3 , two **BPC** and *bpy* units are bound monodentately, creating an octahedral environment with the remaining sites being occupied by water molecules through Cu–O dative bonds. In fact, such moieties are further held together the remaining uncoordinated carboxylic/carboxylate groups by $\text{O}-\text{H}\cdots\text{O}^-$ ($\text{H}\cdots\text{O}^-$, 1.77 Å) hydrogen bonds, as shown in Figure 4.3c. Ultimately, the ensembles yield a double grid network of Cu(II), two **BPC** molecules and three *bpy* molecules as shown in Figure 4.3d. For clarity purpose coordinated water molecules and hydrogen atoms on *bpy* molecules are removed.

4.2.3 Coordination polymer of Cd(II) with BPC and *bpy*-1c

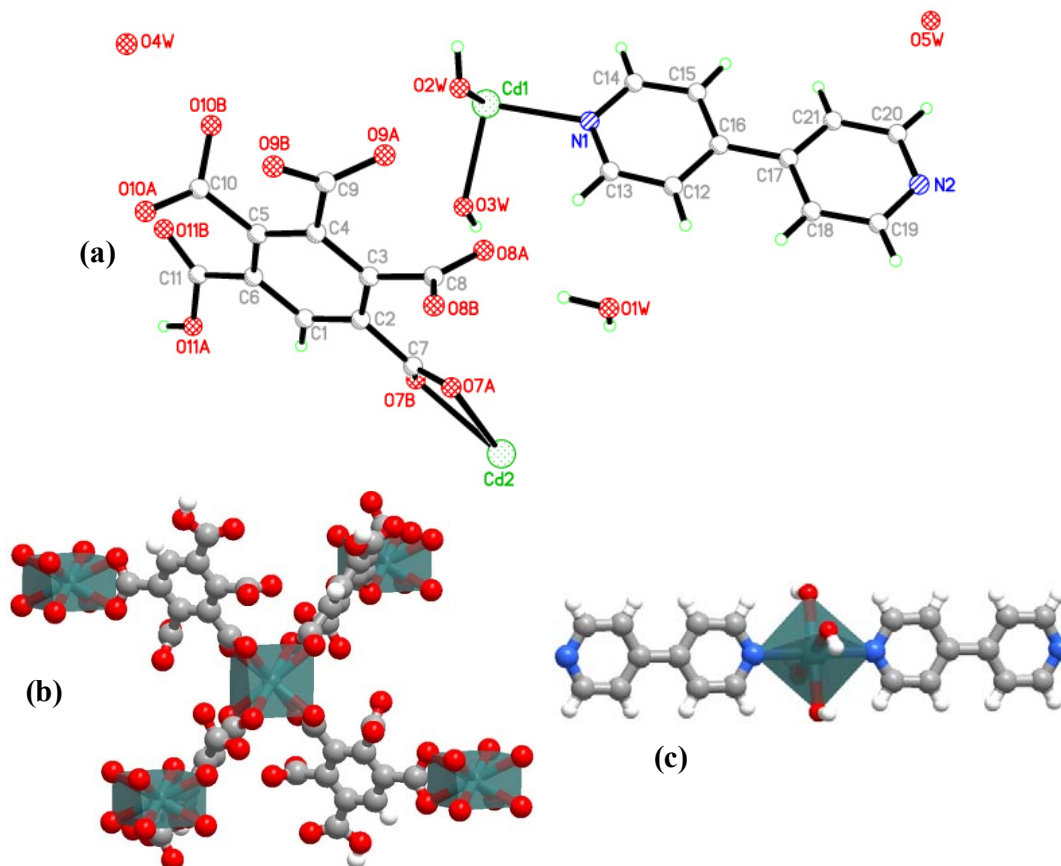


Figure 4.4. (a) ORTEP of asymmetric unit observed in complex **1c** (thermal ellipsoids are at 50% probability). Representation of dative bonds formed by (b) **BPC** and (c) *bpy* with Cd(II) in the complex **1c**.

Cocrystallization of **BPC** and cadmium acetate along with 4,4'-bipyridine, *bpy*, by hydrothermal methods, yielded colorless crystals, which is labeled as complex **1c**. The complex **1c** crystallizes in the monoclinic system, $P2_1/c$ space group, with a formula unit, $[\text{Cd}(\text{C}_{11}\text{H}_2\text{O}_{10})_2][\text{Cd}(\text{C}_{10}\text{H}_9\text{N}_2)_2(\text{H}_2\text{O})_4]6(\text{H}_2\text{O})$. The asymmetric unit of the complex is shown in Figure 4.4a. The crystallographic information is given in Table 4.1.

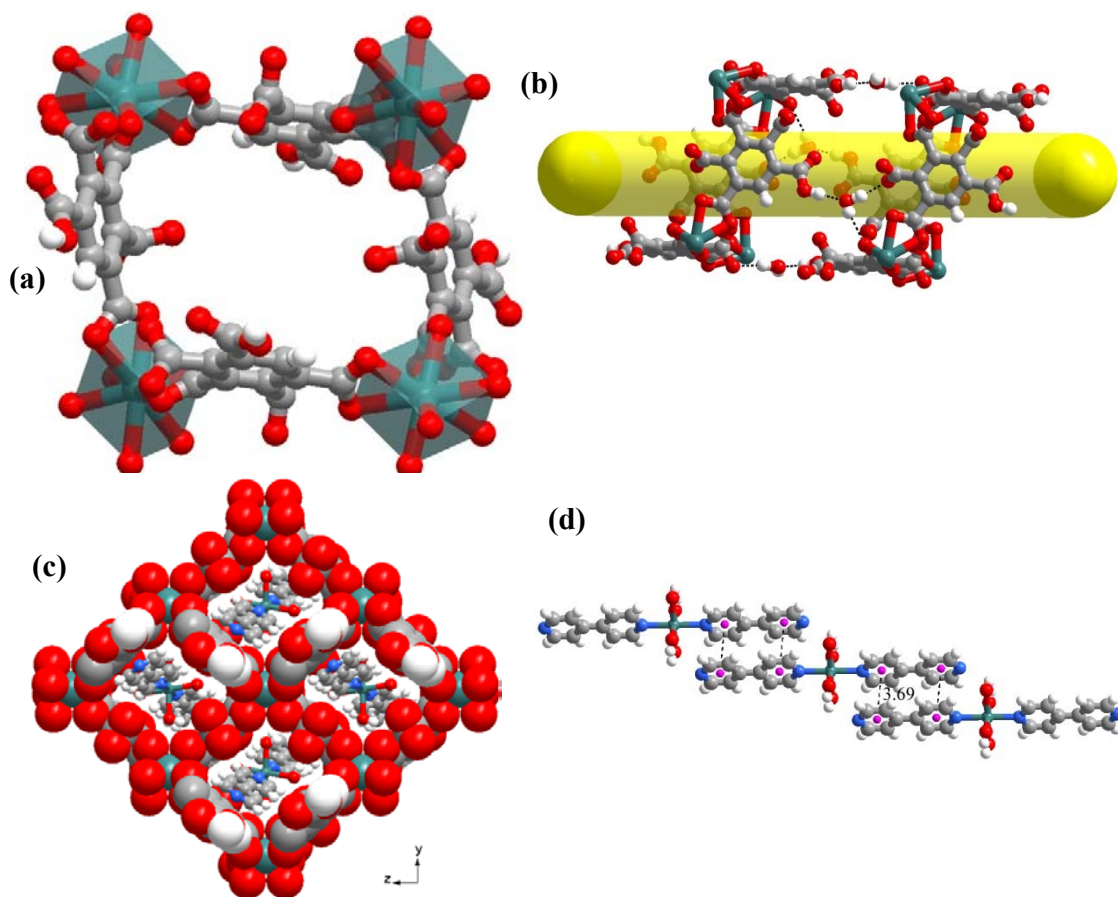


Figure 4.5. (a) A typical square-grid formed between **BPC** and Cd(II) by dative bonds. (b) Aggregation of square-grid networks held together by water molecules (c) Representation of filling of void space within the square grid network by two linear *bpy*-Cd polymer chains (d) Interaction between the guest moieties through π - π interactions.

In the crystal structure of **1c** Cd(II) exists in two octahedral and dodecahedral environments, through six and eight coordinate bonds, respectively, formed with **BPC** and *bpy* moieties, as shown in Figure 4.4. In fact, the coordination complex **1c**, in terms of formation of distinct coordination sphere as well as three-dimensional architecture is intriguing as compare to complex **1a** and **1b**. For example, in complex

1b also, metal ions are in different coordination environment but all together forms single polymeric network in three-dimensional arrangement. But in complex **1c**, which also shows two different coordination environments around metal centers, the molecular packing in three dimensional arrangements is such that dodecahedral coordination sphere exclusively present in the host network, while the octahedral coordination units are associated with guest species, as illustrated below.

One carboxylate group from each of four **BPC** moieties bound to Cd(II) centre through chelating mode and adopts a dodecahedral arrangement (See Figure 4.4b) with Cd–O distances in the range of 2.41–2.47 Å. The Cd(II) in an octahedral environment, as shown in Figure 4.4c, is due to the Cd–N bonds with a distance of 2.29 Å, formed by the *bpy* moieties, in a monodentate fashion and four Cd–O dative bonds observed in the range 2.29–2.33 Å are due to water molecules.

In three-dimensional arrangement, the moieties in the complex **1c** form a host-guest type polymeric network, as shown in Figure 4.5. The host polymer network is based on the aggregation of square grid ensemble of four **BPC** moieties and Cd(II) in dodecahedral coordination with voids of dimension 20 X 20 Å², as shown in Figure 4.5a. And the adjacent ensembles are held together by water molecules through O–H···O (1.71 Å) and O–H···O⁻ (1.86, 2.17 Å) hydrogen bonds (Figure 4.5b). In this arrangement, the voids within the square grid networks are also aligned, creating channels, which are being occupied by polymer chains of Cd(II) in octahedral coordination, as shown in Figure 4.5c. Within the channels, pyridine moieties from the adjacent coordination spheres are stacked through $\pi\cdots\pi$ interaction with a distance of 3.69 Å (See Figure 4.5d). In addition, the uncoordinated N-atom of *bpy* in the

coordination sphere interact with host framework through O–H \cdots N (1.71 Å) hydrogen bonds. Thus, the structure of **1c** exemplifies the significance of intermolecular interaction such as O–H \cdots O hydrogen bonds in the creation of exotic assemblies of coordination moieties, as both the host networks as well as guest species are exclusively stabilized by an extensive hydrogen bonding.

Encouraged by the exotic structural features of the complexes formed by **BPC** with different metal species, in the presence of 4,4'-bipyridine, attention has been directed to explore the influence of other aza-donor compounds, in the formation of coordination assemblies of **BPC** with the metal species. Hence, reactions of **BPC** with 1,2-bis(4-pyridyl)ethene (*bpyee*), 1,2-bis(4-pyridyl)ethane (*bpyea*) and 1,3-bis(4-pyridyl)propane (*bpypa*) were carried out in presence of Co(II), Cu(II) and Cd(II) that were employed in the preparation of the assemblies, **1a-1c**. However, we were not successful to obtain good quality single crystals with 1,2-bis(4-pyridyl)ethene (*bpyee*) with either of the metal species and **BPC**. Also, the single crystals obtained with Co(II) are so unstable that three dimensional structure could not be established by single crystal X-ray diffraction methods. Similarly, the case with the experiments with *bpypa* and Cu(II) and Co(II). Thus, in the following sections, the structural features of assemblies formed by Cu(II), Cd(II) with *bpyea* are discussed.

4.2.4 Coordination polymer of Cu(II) with BPC and *bpyea* - **1d.**

A mixture of **BPC**, 1,2-bis(4-pyridyl)ethane (*bpyea*) and copper nitrate in an autoclave heated up to 140 °C and subsequently cooling to room temperature gave light blue crystals. The crystal structure determination reveals that complex **1d**

crystallizes in the space group, $P2_1$ with a molecular formula, $[\text{Cu}(\text{BPC})(\text{bpy})]2(\text{H}_2\text{O})$ and the asymmetric unit contents are shown in Figure 4.6a. The complete details of the crystallographic information are given in Table 4.1.

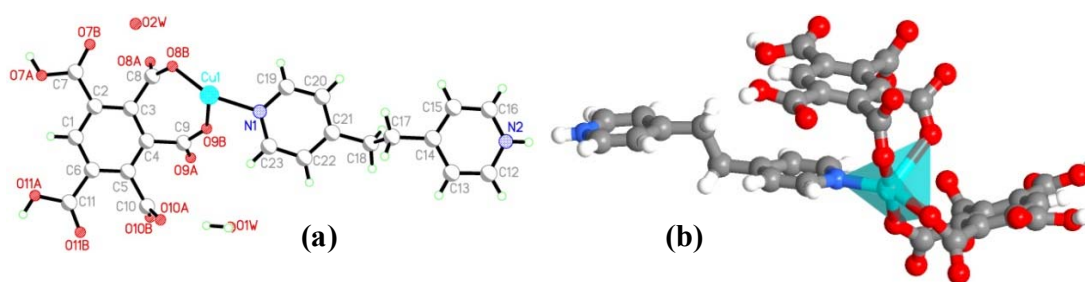


Figure 4.6. (a) ORTEP at the 50% probability thermal ellipsoids of complex **1d**. (b) Coordination environment of Cu(II) in the complex **1d**.

In complex **1d**, one carboxylate group of each of two **BPC** moieties interacts with Cu(II) by chelation process, forming Cu–O coordinate bonds in the range 1.946–2.450 Å. Further, the **bpy** unit also interact with the Cu(II) species, through Cu–N dative bond with a distance of 1.993 Å, creating a penta-coordination around Cu(II). The discrete **BPC-Cu-bpy** coordinated unit is shown in Figure 4.6b. The details of coordination environment are given in Table 4.2. The structure of **1d**, in three dimensional arrangement, is due to the stacking of layers contributed by the coordination polymer chains formed by **BPC-Cu-bpy** moieties. Such a packing is shown in Figure 4.7a. The sheets are, indeed, stabilized by water molecules through O–H \cdots O hydrogen bonds.

Further analysis reveals that within a sheet, the polymer chains are held together by N–H \cdots O (H \cdots O, 2.09 Å) hydrogen bonds as shown in Figure 4.7a, as well as C–H \cdots O (H \cdots O, 2.80, 2.84 Å) hydrogen bonds. In such an arrangement, the adjacent

aromatic moieties along a columnar direction form $\pi\cdots\pi$ interactions with pyridine \cdots pyridine distance being 3.51, while pyridine \cdots BPC distance is 3.53 Å.

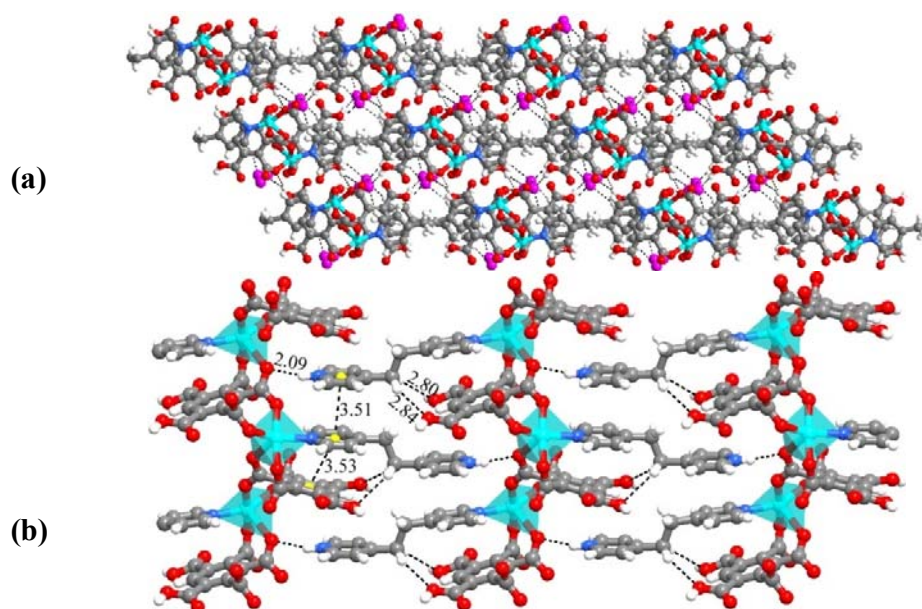


Figure 4.7. (a) Stacked layers structure in three-dimensional arrangement observed in complex **1d**. (b) Perspective view of two dimensional arrangements of coordination polymer chains held together by hydrogen bonds in complex **1d**.

4.2.5 Coordination polymer of Cd(II) with BPC and *bpyea* - 1e.

Red transparent crystals were formed within five days, by slow evaporation of an aqueous solution separated from an autoclave that was previously heated at 140 °C, containing the mixture of equimolar amount of BPC, Cd(II) and 1,2-bis(4-pyridyl)ethane, *bpyea*. The crystal structure was established by single crystal X-ray diffraction method. The complete details of the crystallographic information are given in Table 4.1.

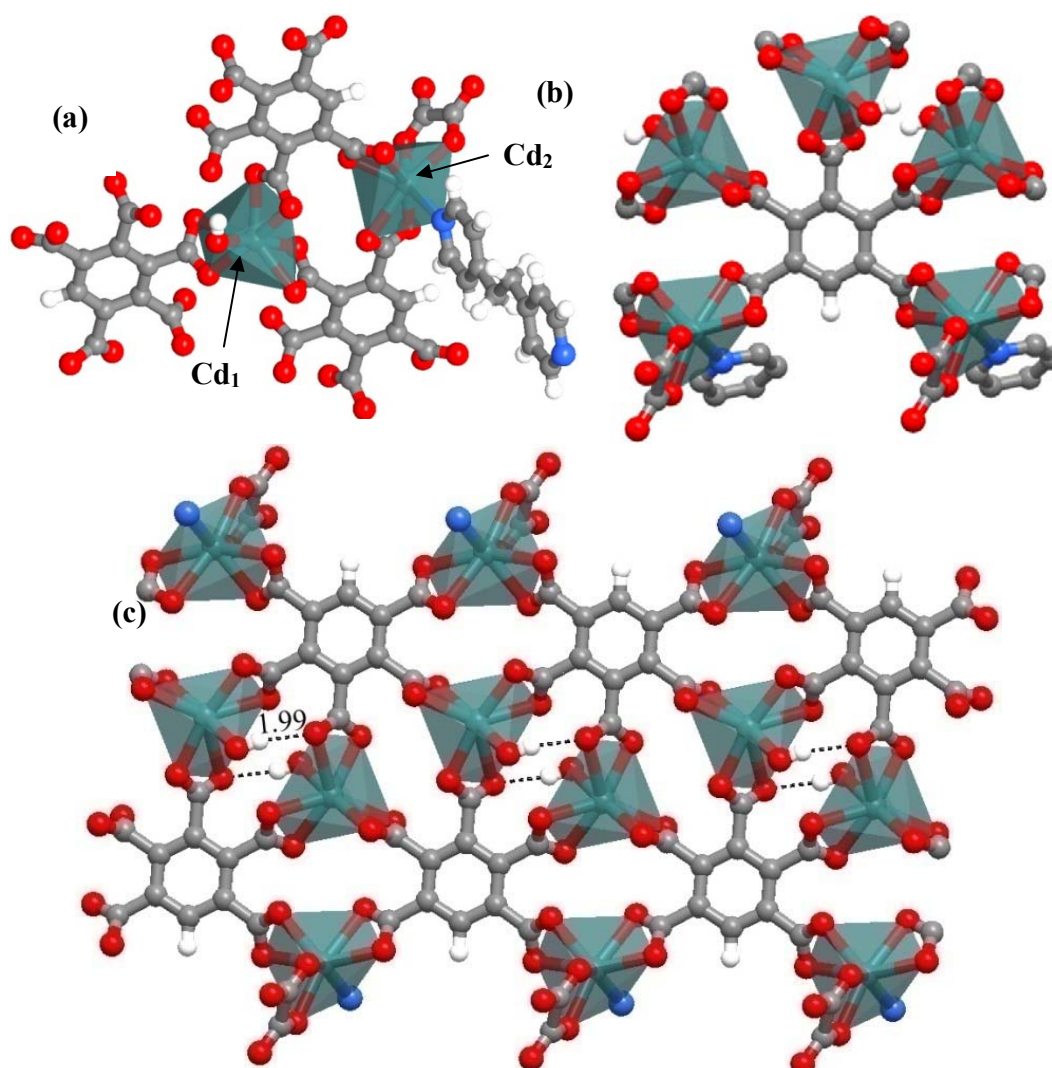


Figure 4.8. (a) A perspective of view of the coordination environments of Cd(II) in complex **1e**. (b) Representation of dative bonds formed by all the carboxylate moieties of **BPC** molecule. (c) Two-dimensional network of Cd-**BPC**.

A noteworthy observation is that unlike in the other structures, **1a-1d**, it appears that part of acetate ions turned into oxalate moieties, which are also present in the asymmetric unit.

In the crystal structure of **1e**, two kinds of Cd(II) are present in the asymmetric unit. Cd₁ is hepta-coordinated with one carboxylate group of each of the three **BPC**

moieties form dative bonds in a chelating mode, with the remaining sites being fulfilled by the dative bonds formed by water molecules. The Cd₁–O bond distances occur in the complex **1e** are in the range 2.26–2.39 Å. Cd₂ also shows similar hepta coordination environment but bounded by six oxygen atoms with one carboxylate of each of two **BPC**, and an oxalate (in situ generated from acetate anion), forming dative bonds through chelating mode and one nitrogen atom of *bp_{yea}* moiety, as shown in Figure 4.8a. The six Cd₂–O distances are in the range of 2.29–2.54 Å, while Cd–N distance is 2.38 Å. Also, it is noteworthy to mention here, that all the carboxylate groups on **BPC** interact with metal as shown in Figure 4.8b. Further, in two-dimensional arrangement, **BPC**–Cd₁ molecules form sheet structure, as shown in Figure 4.8c. However in the three dimensional arrangement, the two dimensional coordination networks construct a square grid network, with cavities of dimension 19.7 X 20 Å², as shown in Figure 4.9a. But the void space is further diminished into 19.7 X 10 Å², with effective interpenetration of the adjacent sheets, as shown in Figure 4.9b. Such voids are occupied by uncoordinated guest *bp_{yea}* and water molecules (See Figure 4.9c). Within the channels, the guest molecules (*bp_{yea}*) are protonated and interact with molecules of water through N⁺–H⁺···O (H⁺···O, 1.90, 1.92 Å) hydrogen bonds. The characteristics of hydrogen bonds are listed in Table 4.3. The interaction between, *bp_{yea}* and water molecules in the channels is shown in Figure 4.9d. The water molecules in the channels are further connected to host framework through O–H⁺···O (H⁺···O, 1.94, 1.98 Å) hydrogen bonds.

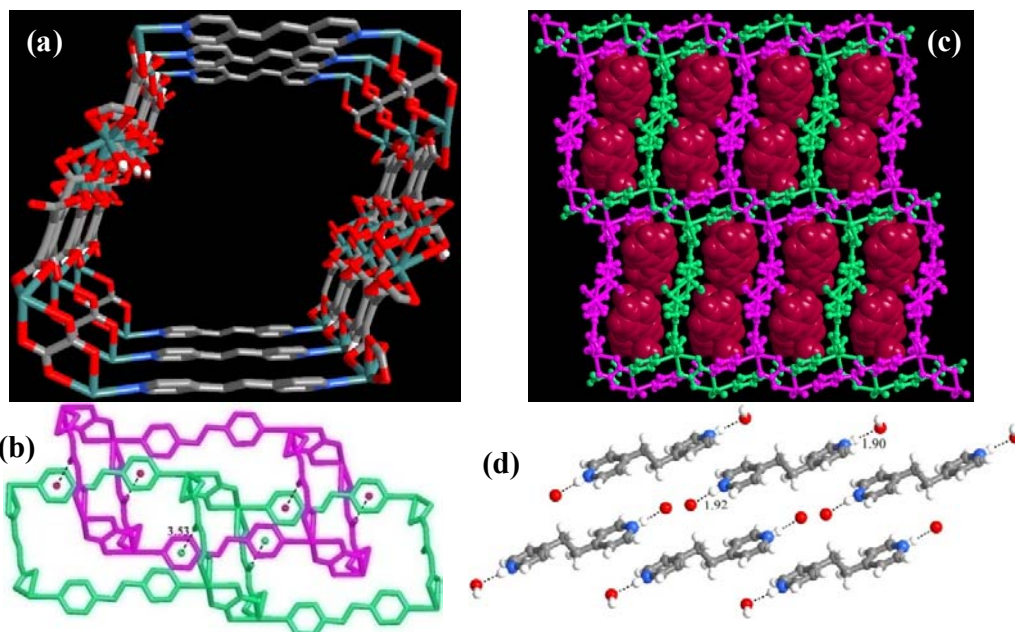


Figure 4.9. (a) A typical square-grid unit observed in complex **1e**. (b) Illustration of 2-fold interpenetration in the complex **1e**. (c) Encapsulation of *bpyea* and water as guest in the channels created after in interpenetration. The interpenetrated networks are shown in different colors. (d) Representation of interaction between *bpyea* and water molecules in the channels.

4.3 Coordination assemblies of mellitic acid, MA.

In combination of metal coordination studies of polycarboxylic acids, further experiment were carried out replacing **BPC** with 1,2,3,4,5,6-benzenehexacarboxylic acid (mellitic acid, **MA**). In this process, the metal salts and organic ligands that have been used for the studies with **BPC** have been retained. Thus, co-crystallization of **MA** with *bpy*, *bpyee*, *bpyea* independently with Co(II), Cu(II) and Cd(II) have been carried out. However, we were successful in obtaining only the complex of Cu(II) and **MA** with *bpy*. The structural feature of this assembly is discussed in detail in the following section.

4.3.1 Coordination polymer of Cu(II) with MA and *bpy*-2a

Treatment of MA and *bpy* with Cu(II) under hydrothermal condition at 160 °C for 48 h, gave blue crystals of coordination complex, **2a**. The structure determination reveals that complex **2a** is a 2:1:1 coordination complex of Cu(II), MA and *bpy* along with two molecules of water (solvent of crystallization). Complete details of the crystallographic information are given in Table 4.1

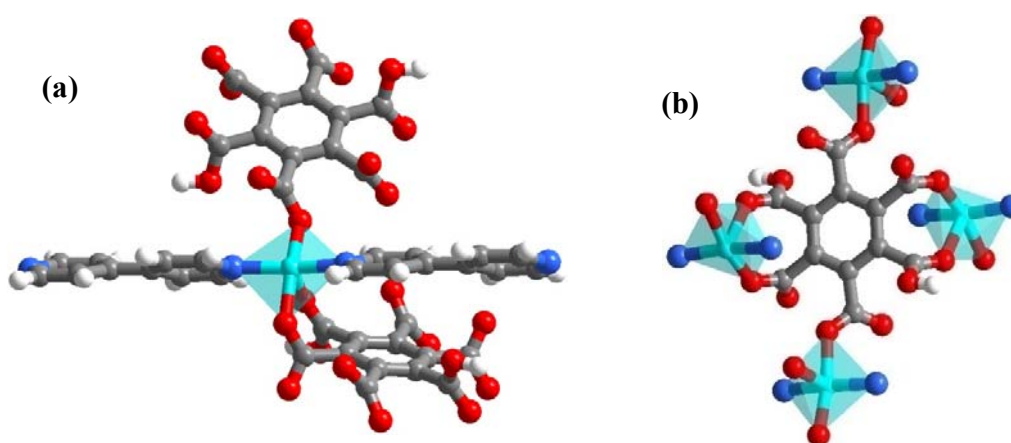


Figure 4.11. (a) Coordination sphere of Cu(II) in the crystal structure of complex, **2a**, in a square pyramidal geometry. (b) Representation of dative bonds formed by carboxylic groups of MA with Cu(II) in the structure of **2a**.

In complex **2a**, metal species form dative bonds with MA as well as *bpy* molecule. Structure analysis reveals a penta coordination around Cu(II), with bonds formed by two molecules of each MA and *bpy* in a square pyramidal geometry, as shown in Figure 4.11a. While *bpy* molecules form single dative bonds with Cu–N bonds, MA interacts with Cu(II) through monodentate as well as chelating mode. The three Cu–O distances are 1.95, 1.97 and 2.40 Å, while Cu–N distances being 1.99 and 2.02 Å. Further complete details of coordination environment are given in Table 4.2.

Also, it is noteworthy to mention that all the carboxylic groups on **MA** did interact with metal, as shown in Figure 4.11b.

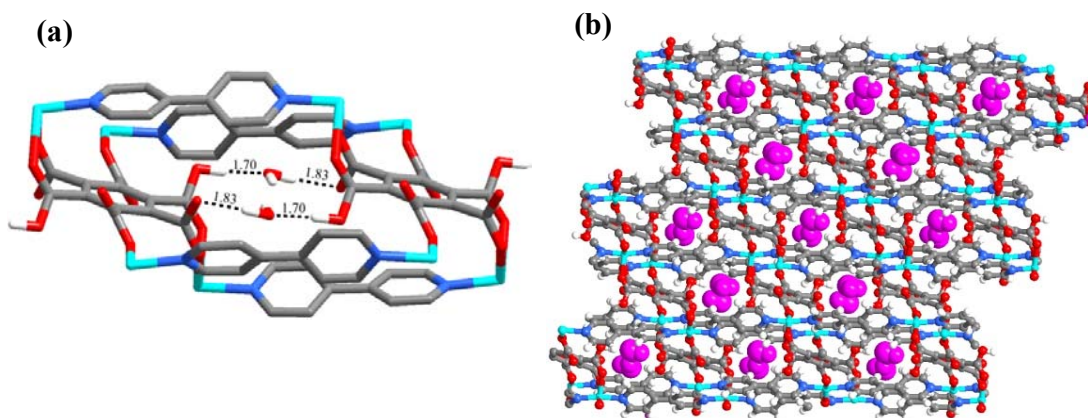


Figure 4.12. (a) Formation of cavities (being filled by water molecules) that are being created due to the interaction of **MA** and *bpy* with Cu(II) ion in the complex **2a**. (b) Three-dimensional arrangement of molecules, with channels filled by water molecules.

Such coordination spheres form a double square network comprising of two **MA** molecules and four *bpy* molecules, with cavities which are filled by water molecules, as shown in Figure 4.12a. Such a cavity network ultimately constitutes channels in three-dimensional arrangement (see Figure 4.12b). The water molecules within the channels interact with the host network through O–H \cdots O (H \cdots O, 1.70, 1.83 Å) and O–H \cdots O $^-$ (H \cdots O $^-$, 1.83 Å) hydrogen bonds. The characteristics of hydrogen bonds are listed in Table 4.2.

In continuation of the experiments with other aza-donor ligands, in order to prepare complexes of **MA** with Cu(II) and *bpypa*, under hydrothermal condition, the chemical entities were dissolved in water at room temperature and the aqueous solution of the mixture was transferred into an autoclave. However, we were unable to

obtain suitable crystals for single crystal X-ray diffraction analysis. Interestingly, we observed small good quality crystals from the solution remained in the conical flask after transferring into autoclave. Surprisingly, the crystals were formed in two colors, Prussian and Royal Blue and also with different morphology. Image of the different types of crystals observed is shown in Figure 4.13. Also by scanning electron microscopy (SEM), it has been confirmed that both the types of crystals are metal (copper) complexes. The two types of crystals, Prussian and Royal blue are labeled as **2b** and **2c**, respectively.

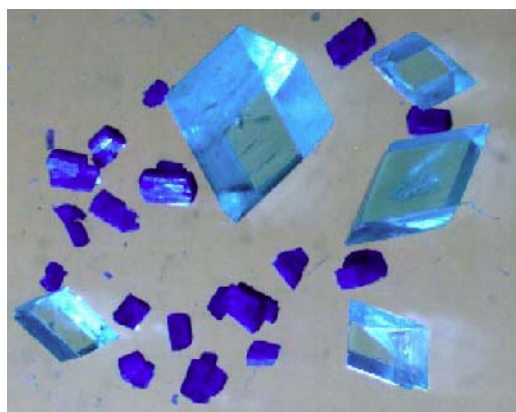


Figure 4.13. Morphology and color of the two different types of crystals of assemblies of Cu(II), MA and *bpypa*.

4.3.2 Coordination Assemblies of Cu(II) with MA and *bpypa*, **2b and **2c**.**

The structure analysis based on the asymmetric unit as shown in Figure 4.14a reveals that in the crystals **2b**, around each Cu(II), hexa coordination is prevailed due to the Cu–O dative bonds formed by two MA molecules with the corresponding distance being 1.93 Å in monodanted way and four water molecules with Cu–O dative bonds distance of 2.03 and 2.38 Å. Thus, an octahedral complex is observed in the

crystals of **2b**. In addition, *bpypa* molecules remain in the crystal lattice as uncoordinated ligands. Such entities are self-assembled further such that coordinated and uncoordinated moieties expand in the form of layers, which are in turns stacked in three-dimensional arrangement, as shown in Figure 4.14c. It is interesting to note that each layer is, indeed, stabilized by different types of hydrogen bonds. The detail of molecular arrangement in a typical layer is shown in Figure 4.15.

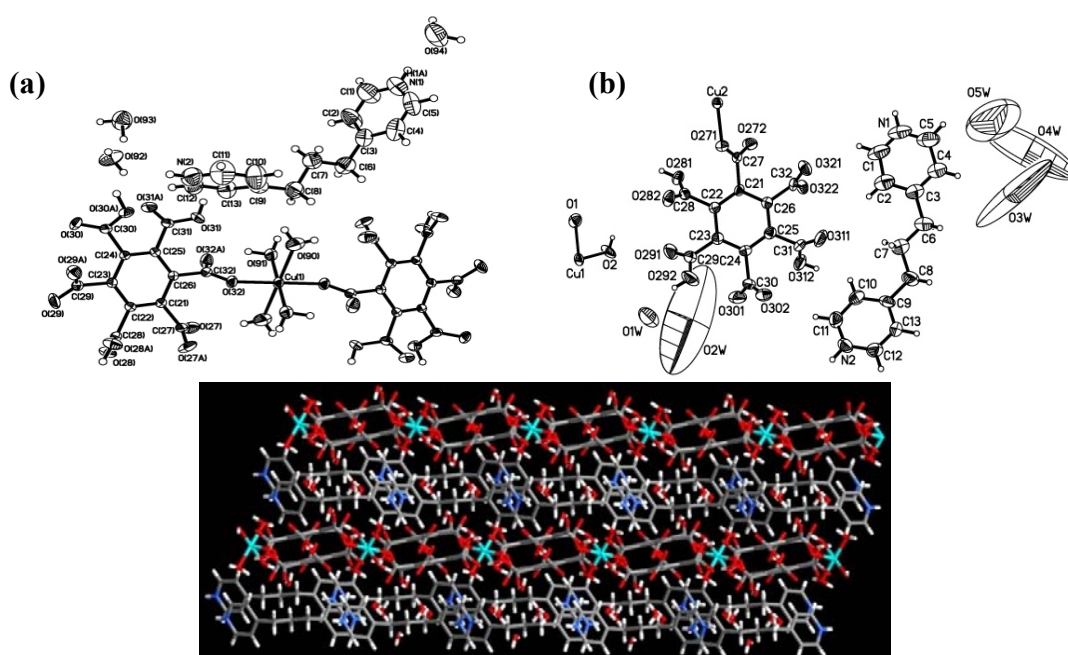


Figure 4.14. ORTEP of asymmetric units in the crystal structures of (a) **2b** and (b) **2c**. (c) Three-dimensional arrangement of coordination sheets of **MA** and Cu(II) separated by sheets of *bpypa* molecules.

Thus, in each coordination sheet, the adjacent moieties are held together by intramolecular hydrogen bonds (Figure 4.15a), constituting a quartet network. The characteristics of hydrogen bonds are listed in Table 4.3. In the layers of aza-donor molecules, *bpypa* molecules, are connected to each other through three water molecules by $N^+ - H \cdots O$ ($H \cdots O$, 1.87, 1.92 Å), as shown in Figure 4.15b.

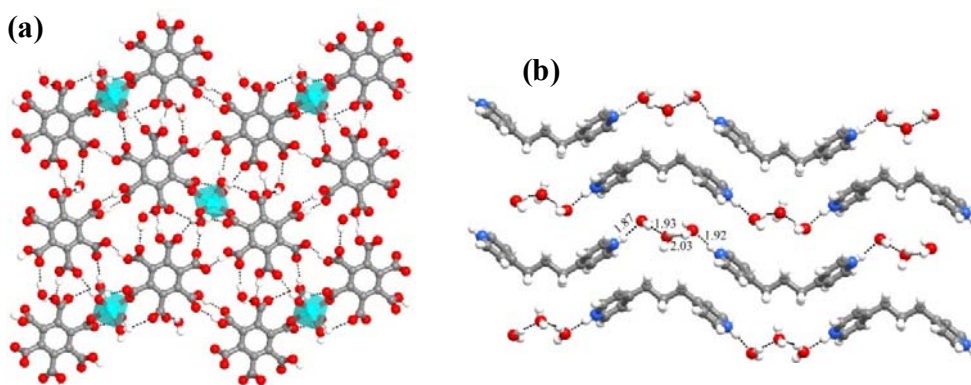


Figure 4.15. (a) Packing of coordination spheres held together by hydrogen bonds, in a typical layered structure in the crystals **2b**. (b) Arrangement of *bpypa* molecules within a sheet through the interactions established with water molecules.

Structural analysis on Prussian blue crystals, **2c**, shows quite intriguing features. ORTEP of an asymmetric unit is shown in Figure 4.14b. Interestingly, in the crystals of **2c** also *bpypa* molecules did not coordinate to Cu(II). In the complex **2c**, Cu(II) exists in two different coordination environments, octahedral and square-planar through hexa and tetra coordination to **MA** moieties, as shown in Figure 4.16.

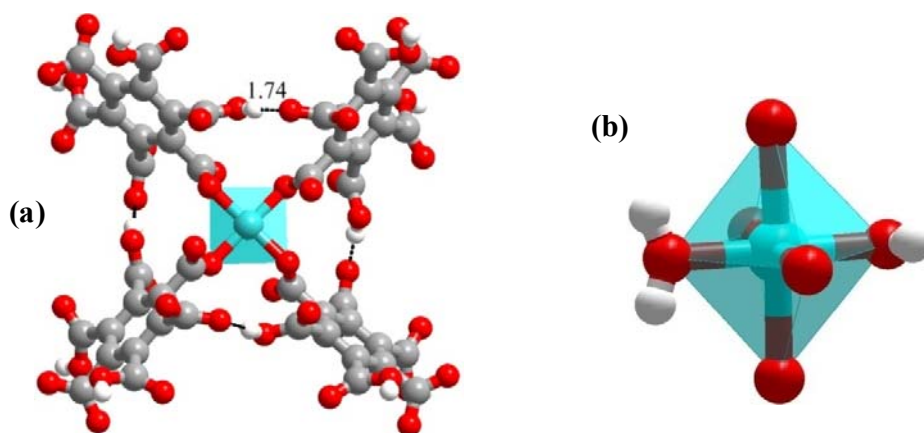


Figure 4.16. (a) Square-planar geometry with four **MA** molecules connected to Cu(II) in monodentate mode in the crystals of **2c**. (b) Cu(II) in octahedral geometry, with the coordination of six water molecules.

While octahedral geometry around Cu(II) is due to the coordination sphere formed with six water molecules by Cu–O bonds of distances of 1.89 and 2.18 Å, the square planar geometry is due to the interaction of four MA molecules through the formation of Cu–O bonds in monodentate fashion, with distances of 1.927 Å. Further, those four MA molecules are also held together by single intermolecular O–H···O hydrogen bonds, as shown in Figure 4.16a, with a H···O distance of 1.74 Å.

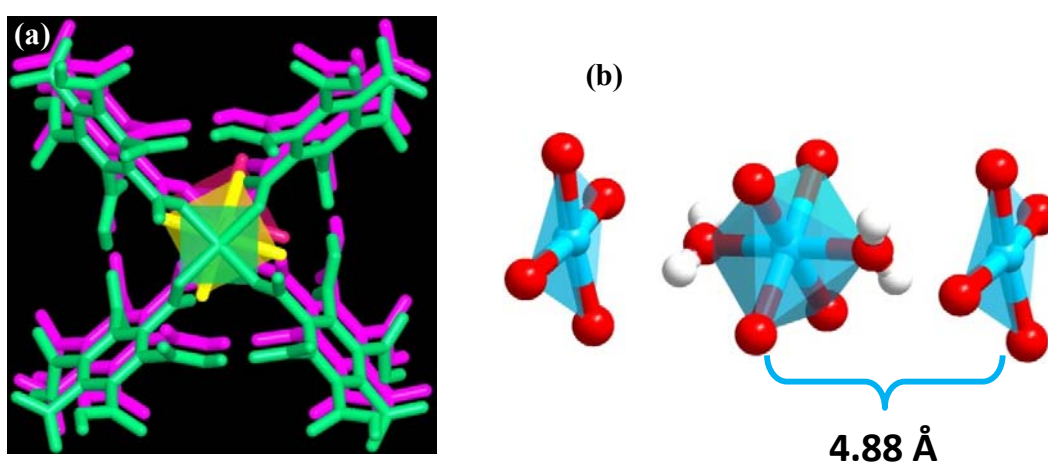


Figure 4.17. Packing and interaction between square-planar and octahedral coordination spheres in the crystal structure of **2c**. (a) Top view (b) lateral view.

Further, the two different coordination spheres lie in three-dimensional arrangement, in alternate layers such that each of Cu(II) hexahydrate (Figure 4.16b) indeed joins the tetra coordinated sheets, through O–H···O hydrogen bonds, as shown in Figure 4.17a. The distance between the two different types of coordination spheres is 4.88 Å (see Figure 4.17b).

Further, in each layer, ensembles of square planner moieties interact with each other through O–H···O hydrogen bonds creating cavities (Figure 4.18a), which are in

turn align to yield channels of dimension $16 \times 30 \text{ \AA}^2$, as shown in Figure 4.18b. Such channels are occupied by *bpypa* molecules and a cluster of water molecules.

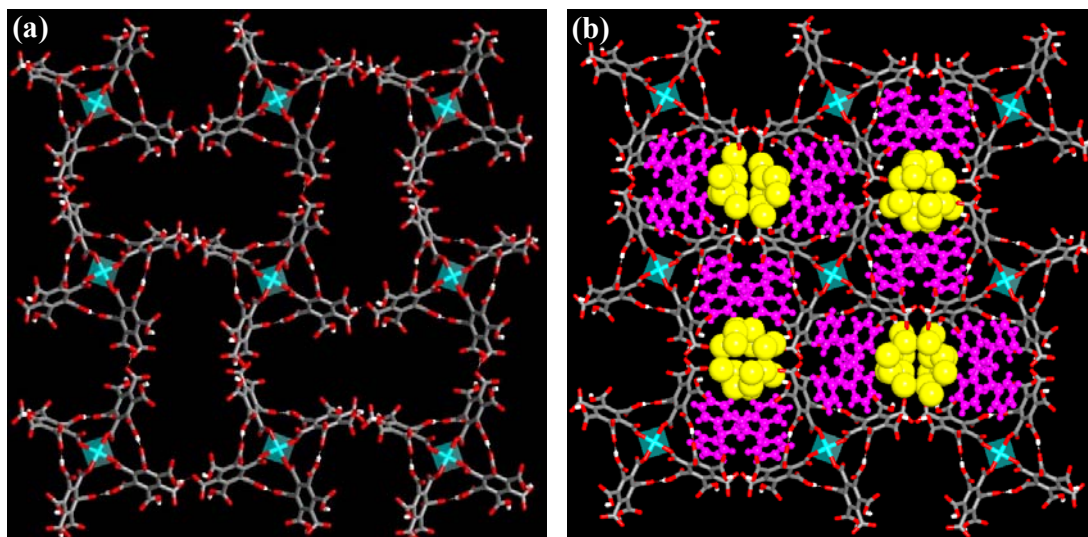


Figure 4.18. (a) Interaction between ensembles of square-planar moieties in two-dimensional arrangement, in the crystal structure of **2c**. (b) Arrangement of guest species, *bpypa* and water molecules within the channels observed in **2c**.

4.4 Conclusion

The coordination polymers resulting from two aromatic polycarboxylic acids, 1,2,3,4,5-benzenepentacarboxylic acid and 1,2,3,4,5,6-benzenehexacarboxylic acid with transition metal ions (Co(II), Cu(II) and Cd(II)) in the presence of flexible bipyridyl ligands (4,4'-bipyridine, 1,2-*bis*(4-pyridyl)ethane and 1,3-*bis*(4-pyridyl)propane) have been reported. The polycarboxylic acids employed in this work **BPC** and **MA** display their characteristic distinct coordination modes as represented in Figure 4.19.

A noteworthy feature in this study is that both the acid moieties and aza-donor

ligands remain uncoordinated in some complexes, perhaps need to be carefully modeled further to explore the factors influencing such distinct feature.

The carboxylate groups on **BPC** show no coordination features towards metal species in the complex **1a**, whereas maximum coordinated bonds are observed in the complex **1e**. Also, the carboxylate interact with metal ions either by monodentate mode or chelating mode.

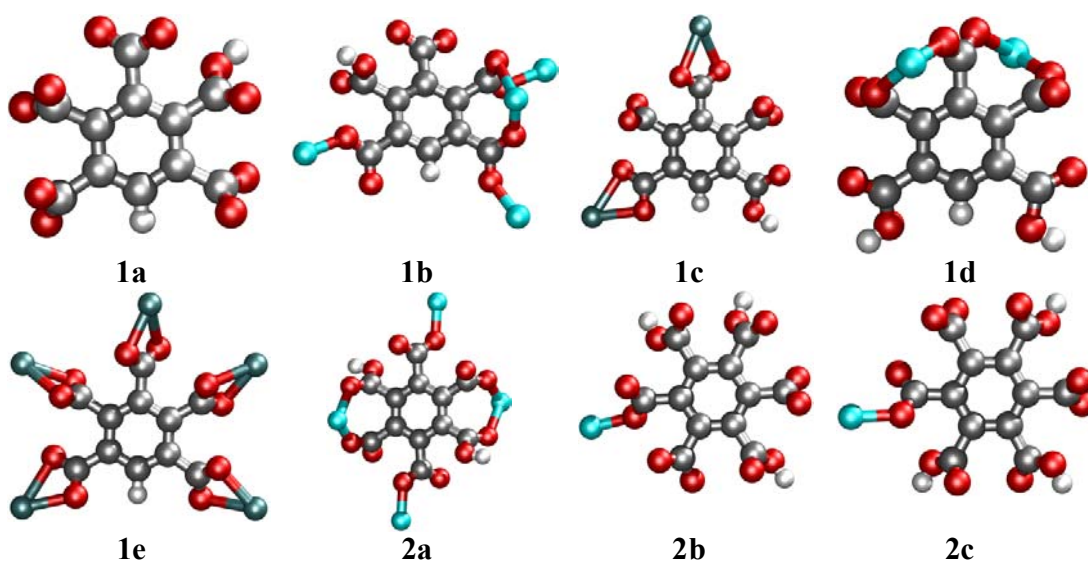


Figure 4.19. Acid metal coordination environment in the complexes of **1a-1e** and **2a-2c**.

The study demonstrates the utilization of both coordinate bond as well as hydrogen bonds in the preparation of coordination assemblies. The structural evaluation reveals that the conditions like, flexibility of polycarboxylic groups, coordination modes of spacer ligands, coordination geometry at metal centre and solvent of crystallization bring about notable variation in the formation of coordination complexes.

4.5 Experimental Section

4.5.1 Preparation of coordination polymers

All the chemicals, benzenepentacarboxylic acid (**BPC**), mellitic acid (**MA**), aza-donor compounds (*bpy*, *bpyea* and *bpypa*) and metal salts (copper nitrate hexahydrate, cobalt nitrate hexahydrate and cadmium acetate) were purchased from commercial suppliers and used as such without any further purification.

Synthesis of complexes 1a-1e and 2a.

To an aqueous solution (15 mL) of metal salt (0.1 mmol), was added the acid under consideration (0.1 mmol), and the respective aza donor compound (0.1 mmol), with stirring. After stirring for 15 minutes at room temperature, the mixture was transferred and sealed in a Teflon-lined stainless-steel autoclave of 23 mL capacity under autogenic pressure and heated to 140 °C-160 °C for 24 hour. The crystals obtained were washed with distilled water and dried at room temperature, which were used for structure determination studies by X-ray diffraction methods.

Synthesis of complexes 2b and 2c.

For a typical crystallization, in a 25 mL conical flask, 0.25 mmol of the **MA**, 0.25 mmol of metal salt and 0.25 mmol of *bpypa* were dissolved in water by heating water to the boiling temperature and then subsequently cooling to room temperature at ambient conditions. Block type single crystals of good quality were obtained within 15 minutes, which were used for structure determination by X-ray diffraction methods.

4.5.2 Crystal Structure Determination

Good quality single crystals of molecular complexes of **1a-1f** and **2a-2c** were carefully chosen after viewing through a Leica microscope (polarized) supported by a rotatable polarizing stage and CCD camera. The crystals were glued to a thin glass fiber using an adhesive (acrylate cyano) and mounted on a diffractometer equipped with the APEX CCD area detector. The X-ray intensity data were collected with varying exposure time depending upon the quality of the crystal(s). The data collection was smooth in all the cases, and no extraordinary methods have been employed, as the crystals were quite stable. The intensity data were processed using Bruker's suite of data processing programs (SAINT),¹⁶ and absorption corrections were applied using SADABS.¹⁷ The structure solution of all the complexes have been carried out by direct methods, and refinements were performed by full matrix least squares on F^2 using the SHELXTL-PLUS¹⁸ suite of programs. All the structures converged to good R-factors. All the non-hydrogen atoms were refined anisotropically, and the hydrogen atoms obtained from Fourier maps were refined isotropically. All the refinements were smooth in all the structures. All the intermolecular interactions were computed using PLATON.¹⁹

Table 4.1. Crystallographic data for the coordination complexes **1a-1e** and **2a-2c**.

	1a	1b	1c
Formula	[Co(C ₁₀ H ₉ N ₂)(H ₂ O) ₅] (C ₁₁ H ₂ O ₁₀)0.5(C ₁₀ H ₁₀ N ₂) (H ₂ O)	[Cu ₂ (C ₁₁ H ₁ O ₁₀) (C ₁₀ H ₈ N ₂)] 4(H ₂ O)	[Cd(C ₁₁ H ₂ O ₁₀) ₂] [Cd(C ₁₀ H ₉ N ₂) ₂ (H ₂ O) ₄] 6 (H ₂ O)
Fw	697.44	641.39	1293.48
Crystal shape	blocks	blocks	blocks
Crystal color	colorless	blue	colorless
Crystal system	triclinic	monoclinic	monoclinic
Space group	<i>P</i> $\bar{1}$	<i>C</i> 2/c	<i>P</i> 2 ₁ /c
<i>a</i> (Å)	9.898(2)	22.739(5)	11.880(3)
<i>b</i> (Å)	12.287(2)	11.151(3)	12.956(3)
<i>c</i> (Å)	13.646(3)	19.259(3)	15.057(3)
α (°)	65.17(3)	90.00	90.00
β (°)	75.79(3)	119.59(1)	90.00(4)
γ (°)	77.20(3)	90.00	90.00
<i>V</i> (Å ³)	1446.8(5)	4246.2(2)	2317.5(9)
<i>Z</i>	2	8	2
<i>D</i> _{calc} (g cm ⁻³)	1.601	2.007	1.854
<i>T</i> (K)	100	293	100
Mo <i>k</i> _α	0.71073	0.71073	0.71073
μ (mm ⁻¹)	0.678	2.092	1.028
2 θ range (°)	50.58	50.20	50.08
<i>F</i> (000)	720	2560	1288
Total reflns	14281	19992	11469
No. unique reflns [<i>R</i> (int)]	5234 [0.0273]	3747 [0.1311]	4092 [0.0893]
No. reflns used	4363	3136	3053
No. parameters	527	357	367
GOF on <i>F</i> ²	1.030	1.525	1.063
<i>R</i> ₁ [<i>I</i> >2 σ (<i>I</i>)]	0.0392	0.0758	0.0702
<i>wR</i> ₂	0.0930	0.2228	0.1839

Table 4.1. contd...

	1d	1e
Formula	[Cu(C ₁₁ H ₃ O ₁₀) (C ₁₂ H ₁₂ N ₂) 2(H ₂ O)]	[Cd ₂ (C ₁₁ H ₀ O ₁₀) 0.5(C ₁₂ H ₁₂ N ₂)0.5(C ₂ O ₂) (2H ₂ O)] (C ₁₂ H ₁₄ N ₂) 3(H ₂ O)
Fw	577.93	891.34
Crystal shape	blocks	blocks
Crystal color	blue	colorless
Crystal system	monoclinic	triclinic
Space group	<i>P</i> 2 ₁	<i>P</i> $\bar{1}$
<i>a</i> (Å)	9.601(2)	9.303(1)
<i>b</i> (Å)	10.074(2)	9.573(2)
<i>c</i> (Å)	11.625(2)	18.669(3)
α (°)	90.00	82.06(3)
β (°)	90.26(4)	79.15(3)
γ (°)	90.00	72.69(3)
<i>V</i> (Å ³)	1124.4(3)	1553.1(4)
<i>Z</i>	2	2
<i>D</i> _{calc} (g cm ⁻³)	1.707	1.906
<i>T</i> (K)	293(2)	293(2)
Mo <i>k</i> _α	0.71073	0.71073
μ (mm ⁻¹)	1.047	1.451
2 θ range (°)	50.06	46.54
<i>F</i> (000)	590	882
Total reflns	5725	13054
No. unique reflns [<i>R</i> (int)]	3782 [0.0444]	4479 [0.0414]
No. reflns used	3254	3663
No. parameters	356	473
GOF on <i>F</i> ²	1.175	1.109
<i>R</i> ₁ [<i>I</i> >2 σ (<i>I</i>)]	0.0581	0.0432
<i>wR</i> ₂	0.1203	0.0802

Table 4.1. *contd...*

	2a	2b	2c
Formula	[Cu ₂ (C ₁₂ H ₂ O ₁₂)(C ₁₀ H ₈ N ₂) ₂] 2(H ₂ O)	[Cu ₁ (C ₁₂ H ₃ O ₁₂) ₂ (H ₂ O) ₄] 2(C ₁₃ H ₁₆ N ₂) 6(H ₂ O)	[Cu ₁ (C ₁₂ H ₃ O ₁₂) ₄] [Cu ₁ (H ₂ O) ₆] 4(C ₁₃ H ₁₆ N ₂)18(H ₂ O)
Fw	406.81	1322.55	2885.66
Crystal shape	blocks	blocks	blocks
Crystal color	blue	blue	dark blue
Crystal system	monoclinic	monoclinic	tetragonal
Space group	<i>P</i> 2 ₁ / <i>n</i>	<i>P</i> 2 ₁ / <i>n</i>	<i>P</i> $\bar{4}$ 2 ₁ / <i>c</i>
<i>a</i> (Å)	11.80(3)	9.641(6)	24.505(10)
<i>b</i> (Å)	10.967(3)	18.443(11)	24.505(10)
<i>c</i> (Å)	12.351(3)	16.577(10)	9.766(6)
α (°)	90	90	90
β (°)	111.36(1)	102.88(1)	90
γ (°)	90	90	90
<i>V</i> (Å ³)	1397.7(2)	2873(3)	5864(5)
<i>Z</i>	4	2	2
<i>D</i> _{calc} (g cm ⁻³)	1.933	1.529	1.521
<i>T</i> (K)	120(2)	293(2)	293(1)
Mo <i>k</i> _α	0.71073	0.71073	0.71073
μ (mm ⁻¹)	1.613	0.485	0.480
2 θ range (°)	55.00	46.70	50.44
<i>F</i> (000)	824	1374	2751
Total reflns	10446	17744	11569
No. unique reflns [<i>R</i> (int)]	3204 [0.0205]	4755 [0.0255]	5236 [0.0555]
No. reflns used	2857	3458	4363
No. parameters	247	451	419
GOF on <i>F</i> ²	1.073	0.775	1.228
<i>R</i> ₁ [<i>I</i> >2 σ (<i>I</i>)]	0.0266	0.0331	0.0701
w <i>R</i> ₂	0.0710	0.0969	0.1766

Table 4.2. Coordination environment of the metal centres in the complexes **1a -1f** and **2a – 2c** (distance/Å and angles/°).

1a		1b		1c	
Co1-O1W	2.067	Cu1-O8A	1.927	Cd1-O3W	2.290
Co1-O5W	2.079	Cu1-O11A	1.928	Cd1- N1	2.294
Co1-O2W	2.092	Cu1-O4W	1.995	Cd1-O2W	2.331
Co1-O4W	2.107	Cu1-O3W	2.000	Cd2-O9A	2.415
Co1-O3W	2.107	Cu1-O2W	2.350	Cd2-O7B	2.455
Co1-N3	2.152	Cu2-O9B	1.945	Cd2-O7A	2.471
O5W- Co1 -O2W	85.11	Cu3-O9A	2.007	Cd2-O9B	2.479
O1W -Co1 -O4W	86.30	Cu3-N2	2.024	O3W-Cd1- O2W	85.14
O2W -Co1- O4W	88.84	Cu2-N1	2.057	N1-Cd1-O2W	88.46
O5W -Co1- O3W	88.99	Cu1-N3	2.016	O3W- Cd1-N1	89.29
O4W- Co1- N3	89.01	O8A-Cu1-O3W	84.90	O3W-Cd1-N1	90.71
O3W- Co1- N3	89.59	O11A-Cu1-O2W	85.90	N1-Cd1-O2W	91.54
O2W -Co1 -O3W	89.75	O9A-Cu3-N2	86.50	N1-Cd1- N1	180.00
O1W- Co1- N3	90.20	O4W-Cu1-O2W	87.10	O3W- Cd -O3W	180.00
O2W -Co1- N3	92.14	O11A-Cu1-O4W	87.40	O2W-Cd1-O2W	180.00
O5W -Co1- O4W	92.34	O9B-Cu2-N1	89.68	O3W-Cd1- O2W	85.14
O1W -Co1 -O5W	92.67	O9B-Cu2-N3	90.32	O7B Cd2 O7A	53.29
O1W -Co1- O3W	95.17	O8A-Cu1-O2W	92.00	O9A Cd2 O9B	53.69
O1W -Co1 -O2W	174.57	O11A-Cu1-O3W	93.20	O9A Cd2 O7A	73.48
O5W- Co1- N3	176.91	O9A-Cu3-N2	93.50	O9A Cd2 O7B	78.63
O4W -Co1 -O3W	177.97	O8A-Cu1-O4W	95.30	O7A Cd2 O9B	78.70
		O3W-Cu1-O2W	110.7	O7B Cd2 O9B	82.84
		O4W-Cu1-O3W	162.1	O7B Cd2 O9B	97.16
		O8A-Cu1-O11A	176.5	O7A Cd2 O9B	101.30
		O9B-Cu2-O9B	179.4	O9A Cd2 O7B	101.37
		N2-Cu3-N2	180.0	O9A Cd2 O7A	106.52
		O9A-Cu3-O9A	180.0	O9A Cd2 O9B	126.31
		N3-Cu2-N1	180.0	O7B Cd2 O7A	126.71
				O7A Cd2 O7A	180.00
				O7B Cd2 O7B	180.00
				O9A Cd2 O9A	180.00

Table 4.2. contd...

1d		1e	
Cu1-O10B	1.946	Cd1- O7B	2.291
Cu1-O9B	1.958	Cd1- O31B	2.312
Cu1-O8B	1.985	Cd1- O11B	2.327
Cu1-O8A	2.450	Cd1- N3	2.384
Cu1-N1	1.993	Cd1- O31A	2.412
O9B-Cu1-N1	87.60	Cd1- O11A	2.497
O10B-Cu1-O8B	88.28	Cd1- O7A	2.536
O9B-Cu1-O8B	89.60	Cd2- O9B	2.263
O10B-Cu1-N1	92.50	Cd2- O8A	2.303
O8B-Cu1-N1	153.80	Cd2- O3W	2.363
O10B-Cu1-O9B	175.40	Cd2 -O10B	2.371
		Cd2 -O10A	2.386
		Cd2- O8B	2.444
		O11B- Cd1 -O11A	53.87
		O7B -Cd1 -O7A	53.91
		O31B- Cd1- O31A	69.03
		O11B- Cd1- O31A	79.51
		O11B -Cd1- O7A	79.73
		N3- Cd1 -O7A	82.53
		O7B- Cd1- O31A	83.77
		O31B- Cd1 -O11A	85.86
		O7B- Cd1 -N3	89.20
		O31B- Cd1- N3	86.76
		N3- Cd1 -O11A	86.97
		O11A- Cd1- O7A	101.41
		O31A -Cd1- O11A	111.77
		O31B- Cd1 -O11B	113.45
		O7B- Cd1- O11B	114.32
		O31A- Cd1- O7A	117.34
		O7B- Cd1- O31B	118.27
		O11B- Cd1- N3	131.79
		N3 -Cd1- O31A	147.31
		O7B- Cd1 -O11A	155.32
		O31B -Cd1-O7A	166.67
		O8A- Cd2-O8B	55.23
		O10B- Cd2- O10A	55.28
		O3W- Cd2- O10A	78.21
		O9B -Cd2 -O3W	78.56
		O3W -Cd2 -O10B	87.23
		O9B- Cd2 -O8B	88.09
		O10A- Cd2 -O8B	96.63
		O9B -Cd2 -O8A	100.44
		O8A -Cd2 -O10A	101.34
		O8A -Cd2 -O10B	102.01
		O3W Cd2- O8B	113.32
		O9B- Cd2 -O10B	128.16
		O10B -Cd2 -O8B	142.27
		O9B -Cd2 -O10A	156.26
		O8A- Cd2 -O3W	168.53

Table 4.2. *contd...*

2a		2b		2c	
Cu1-O2	1.947	Cu1-O32	1.932	Cu1-O1	2.183
Cu1-O4	1.970	Cu1-O90	2.384	Cu1-O2	1.890
Cu1-O5	2.402	Cu1-O91	2.028	Cu2-O271	1.927
Cu1-N1	2.017	O32-Cu1-O32	180.00	O1-Cu1-O1	90.02
Cu1-N2	1.989	O32-Cu1-O90	86.35	O1-Cu1-O1	177.70
O2-Cu1-O4	162.74	O32-Cu1-O90	93.65	O2-Cu1-O1	88.83
O2-Cu1-O5	81.93	O32-Cu1-O91	92.91	O2-Cu1-O1	91.17
O2-Cu1-N1	91.96	O32-Cu1-O91	87.09	O2-Cu1-O2	178.00
O2-Cu1-N2	90.22	O90-Cu1-O90	180.00	O271-Cu2-O271	90.35
O4-Cu1-O5	80.80	O91-Cu1-O90	87.04	O271-Cu2-O271	171.10
O4-Cu1-N1	88.09	O91-Cu1-O90	92.96		
O4-Cu1-N2	93.00	O91-Cu1-O91	180.00		
N1-Cu1-O5	90.48				
N2-Cu1-O5	100.45				
N2-Cu1-N1	169.04				

Table 4.3. Characteristics of hydrogen bonds in the coordination complexes of **BPC** and **MA** (distances/Å and angles/°).[#]

Hydrogen Bonds	1a			1b			1c		
O-H...O	1.77	2.60	166.0	1.77	2.56	160	1.71	2.60	175
	1.78	2.54	167.0				1.83	2.66	170
	1.79	2.66	174.0				1.86	2.77	163
	1.86	2.71	176.0				2.17	2.82	165
	1.88	2.73	166.0				2.35	3.12	153
	1.92	2.73	173.0						
	1.93	2.66	178.0						
	1.97	2.72	176.0						
	2.00	2.74	170.0						
	2.10	2.96	152.0						
	2.19	2.84	135.0						
	2.36	3.01	134.0						
	2.36	2.96	141.0						
2.50	3.06	134.0							
N-H...O	1.68	2.64	176.0						
	1.71	2.62	165.0						
C-H...O	2.29	3.12	160.0	2.36	3.29	175	2.39	3.19	142
	2.32	3.28	161.0	2.39	3.29	163	2.41	3.35	171
	2.46	3.33	156.0	2.49	3.38	159	2.48	3.18	131
	2.55	3.46	165.0				2.49	3.40	162
	2.57	3.37	159.0				2.57	3.40	145
	2.57	3.40	148.0				2.58	3.49	175

Table 4.3. contd...

Hydrogen Bonds	1d			1e		
O-H...O	1.78	2.61	171	1.94	2.79	168
	1.80	2.77	168	1.98	2.81	159
	1.81	2.62	174	1.99	2.79	163
	1.87	2.81	176			
N-H...O	2.09	2.94	171	1.90	2.74	165
				1.92	2.75	161
C-H...O	2.48	3.38	164	2.31	3.01	132
	2.49	3.34	151	2.43	3.19	139
				2.48	3.24	139
				2.52	3.25	135

Table 4.3. contd...

Hydrogen Bonds	2a			2b			2c		
O-H...O	1.83	2.62	160	1.50	2.76	164	1.76	2.57	178
	2.01	2.75	159	1.61	2.42	171	1.79	2.58	162
				1.81	2.71	174	1.88	2.73	169
				1.89	2.74	126	2.92	3.51	130
				1.95	2.82	151			
				2.05	2.83	168			
				2.06	2.81	172			
				2.15	2.94	169			
				2.22	3.05	160			
				2.46	3.10	123			
				2.82	3.83	145			
N-H...O				1.87	2.69	160	1.88	2.73	169
				1.92	2.75	161	1.88	2.74	176
				2.79	3.39	128	2.87	3.52	133
C-H...O	2.36	3.14	139	2.26	3.17	166	2.45	3.35	163
	2.39	3.25	149	2.27	3.16	162	2.48	3.24	139
	2.46	3.18	136	2.52	3.26	133	2.50	3.30	143
	2.53	3.36	145	2.56	3.45	158	2.60	3.51	165
	2.62	3.24	122	2.57	3.34	137	2.66	3.29	125
	2.70	3.29	12	2.60	3.52	169	2.66	3.35	129
	2.83	3.55	133	2.64	3.42	141	2.70	3.38	130
	2.88	3.22	102	2.71	3.49	136	2.74	3.57	148
	2.88	3.50	124	2.72	3.41	132	2.45	3.35	163

For each structure, the three columns corresponds to distance of H...X, D...X and angle D-H...X, respectively.

4.6 References

1. (a) Moulton, B.; Zaworotko, M. J. *Chem. Rev.* **2001**, *101*, 1629-1658. (b) Batten, S. R.; Robson, R. *Angew. Chem., Int. Ed.* **1998**, *37*, 1460-1494. (c) Hagrman, P. J.; Hagrman, D.; Zubieta, J. *Angew. Chem., Int. Ed.* **1999**, *38*, 2638-2684. (d) Aakeroy, C. B.; Beatty, A. M. *Aust. J. Chem.* **2001**, *54*, 409-421. (e) Khlobystov, A. N.; Blake, A. J.; Champness, N. R.; Lemenovskii, D. A.; Majouga, A. G.; Zyk, N. V.; Schroder, M. *Coord. Chem. Rev.* **2001**, *222*, 155-192. (f) Zaworotko, M. J. *Chem. Commun.* **2001**, 1-9. (g) Matsuda, R.; Kitaura, R.; Kitagawa, S.; Kubota, Y.; Belosludov, R. V.; Kobayashi, T. C.; Sakamoto, H.; Chiba, T.; Takata, M.; Kawazoe, Y.; Mita, Y. *Nature* **2005**, *436*, 238-241. (h) Kitaura, R.; Kitagawa, S.; Kubota, Y.; Kobayashi, T. C.; Kindo, K.; Mita, Y.; Matsuo, A.; Kobayashi, M.; Chang, H. C.; Ozawa, T. C.; Suzuki, M.; Sakata, M.; Takata, M. *Science* **2002**, *298*, 2358-2361.
2. (a) Reviews for coordination polymers: (a) Bradshaw, D.; Claridge, J. B.; Cussen, E. J.; Prior, T. J.; Rosseinsky, M. J. *Acc. Chem. Res.* **2005**, *38*, 273-282. (b) Kitagawa, S.; Uemura, K. *Chem. Soc. Rev.* **2005**, *34*, 109-119. (c) Eddaoudi, M.; Moler, D. B.; Li, H.; Chen, B.; Reineke, T. M.; O'Keeffe, M.; Yaghi, O. M. *Acc. Chem. Res.* **2001**, *34*, 319-330. (d) Papaefstathiou, G. S.; MacGillivray, L. R. *Coord. Chem. Rev.* **2003**, *246*, 169-184. (e) Moulton, B.; Zaworotko, M. J. *Curr. Opin. Solid St. Mater. Sci.* **2002**, *6*, 117. (f) Uemura, T.; Yanai, N.; Kitagawa, S. *Chem. Soc. Rev.* **2009**, *38*, 1228-1236. (g) Zaworotko, M. J. *Chem. Soc. Rev.* **1994**, *23*, 283-288.

3. (a) Makinen, S. K.; Melcer, N. J.; Parvez, M.; Shimizu, G. K. H. *Chem. Eur. J.* **2001**, *7*, 5176-5182. (b) Uemura, K.; Kitagawa, S.; Fukui, K.; Saito, K. *J. Am. Chem. Soc.* **2004**, *126*, 3817- 3828 (c) Soldatov, D. V.; Enright, G. D.; Ripmeester, J. A. *Chem. Mater.* **2002**, *14*, 348-356. (d) Cussen, E. J.; Claridge, J. B.; Rosseinsky, M. J.; Kepert, C. J. *J. Am. Chem. Soc.* **2002**, *124*, 9574-9581. (e) Takamizawa, S.; Nakata, E.-i.; Yokoyama, H.; Mochizuki, K.; Mori, W. *Angew. Chem., Int. Ed.* **2003**, *42*, 4331-4334. (f) Maji, T. K.; Uemura, K.; Chang, H. C.; Matsuda, R.; Kitagawa, S. *Angew. Chem., Int. Ed.* **2004**, *43*, 3269-3272. (g) Lee, E. Y.; Suh, M. P. *Angew. Chem., Int. Ed.* **2004**, *43*, 2798-2801. (h) Choi, H. J.; Suh, M. P. *J. Am. Chem. Soc.* **2004**, *126*, 15844-15851. (i) Zeng, M. H.; Feng, X. L.; Chen, X. M. *Dalton Trans.* **2004**, 2217-2223. (j) Kondo, M.; Irie, Y.; Shimizu, Y.; Miyazawa, M.; Kawaguchi, H.; Nakamura, A.; Naito, T.; Maeda, K.; Uchida, F. *Inorg. Chem.* **2004**, *43*, 6139-6141.
4. (a) Wu, C. D.; Lin, W. *Angew. Chem., Int. Ed.* **2005**, *44*, 1958-1961. (b) Soldatov, D. V.; Ripmeester, J. A. *Chem. Eur. J.* **2001**, *7*, 2979-2994. (c) Takaoka, K.; Kawano, M.; Tominaga, M.; Fujita, M. *Angew. Chem., Int. Ed.* **2005**, *44*, 2151-2154. (d) Halder, G. J.; Kepert, C. J. *J. Am. Chem. Soc.* **2005**, *127*, 7891-7900. (e) Uemura, K.; Kitagawa, S.; Kondo, M.; Fukui, K.; Kitaura, R.; Chang, H. C.; Mizutani, T. *Chem. Eur. J.* **2002**, *8*, 3586-3600. (f) Uemura, K.; Kitagawa, S.; Saito, K.; Fukui, K.; Matsumoto, K. *J. Therm. Anal. Calorim.* **2005**, *81*, 529-532.
5. (a) Férey, G. *Chem. Soc. Rev.* **2008**, *37*, 191. (b) Cheetham, A. K.; Rao, C. N. R.; Feller, R. K. *Chem. Commun.* **2006**, 4780. (c) Cheetham, A. K.; Rao, C. N.

- R. *Science* **2007**, *318*, 58. (d) Tan, J. C.; Merrill, C. A.; Orton, J. B.; Cheetham, A. K. *Acta Mater.* **2009**, *57*, 3481. (e) Rowsell, J. L. C.; Yaghi, O. M. *Microporous Mesoporous Mater.* **2004**, *73*, 3. (f) Terpin, A. J.; Ziegler, M.; Johnson, D. W.; Raymond, K. N. *Angew. Chem., Int. Ed.* **2001**, *40*, 157-160. (g) Eddaoudi, M.; Moler, D. B.; Li, H.; Chen, B.; Reineke, T. M.; O'Keeffe, M.; Yaghi, O. M. *Acc. Chem. Res.* **2001**, *34*, 319-330. (h) Chen, B.; Ockwig, N. W.; Millward, A. R.; Contreras, D. S.; Yaghi, O. M. *Angew. Chem., Int. Ed.* **2005**, *44*, 4745-4749.
6. (a) Jun, Y. L.; Sung, J. H.; Kim, C.; Kim, S. J.; Kim, Y. *Inorg. Chem. Commun.* **2005**, *8*, 692-696. (b) Janiak, C. *Dalton Trans.* **2003**, 2781-2804. (c) Amabilino, D. B.; Veciana, J. *Top. Curr. Chem.* **2006**, *265*, 253-302. (d) Armaroli, N.; Accorsi, G.; Holler, M.; Moudam, O.; Nierengarten, J.; Zhou, Z.; Wegh, R. T.; Welter, R. *Adv. Mater.* **2006**, *18*, 1313-1316. (e) Langley, P. J.; Hulliger, J. *Chem. Soc. Rev.* **1999**, *28*, 279-291. (f) Ohmori, O.; Fujita, M. *Chem. Commun.* **2004**, 1586-1587. (g) Uemura, T.; Horike, S.; Kitagawa, S. *Chem. Asian J.* **2006**, *1*, 36-44. (h) Brammer, L. *Chem. Soc. Rev.* **2004**, *33*, 476-489. (l) Wu, C. D.; Hu, A.; Zhang, L.; Lin, W. *J. Am. Chem. Soc.*, **2005**, *127*, 8940-8941.
7. (a) Pan, L.; Olson, D. H.; Ciemnomolonski, L. R.; Heddy, R.; Li, J. *Angew. Chem., Int. Ed.* **2006**, *45*, 616-619. (b) Hermes, S.; Schrter, M.; Schmid, R.; Khodeir, L.; Muhler, M.; Tissler, A.; Fischer, R. W.; Fischer, R. A. *Angew. Chem., Int. Ed.* **2005**, *44*, 6237-6241. (c) Kepert, C. J. *Chem. Commun.* **2006**, 695-700 and references within. (d) Gaspar, A.B., Ksenofontov, V.; Seredyuk, M.; Gütllich, P. *Coord. Chem. Rev.* **2005**, *249*, 2661-2676.

8. Kitagawa, S.; Kitaura, R.; Noro, S. *Angew. Chem., Int. Ed.* **2004**, *43*, 2334-2375.
9. (a) Akhbari, K.; Morsali, A. *Inorg. Chim. Acta* **2009**, *362*, 1692-1700. (b) Bai, H. Y.; Ma, J. F.; Yang, J.; Liu, Y. Y.; Hua, W.; Ma, J. C. *Cryst. Growth Des.* **2010**, *10*, 995-1016. (c) Liu, B.; Xu, L. *Inorg. Chem. Commun.* **2006**, *9*, 364-366. (d) Liu, Y. Y.; Ma, J. C.; Xie, Y. P.; Ma, J. F. *J. Coord. Chem.* **2008**, *61*, 3450-3457. (e) Ma, L. F.; Li, C. P.; Wang, L. Y.; Du, M. *Cryst. Growth Des.* **2010**, *10*, 2641-2649. (f) Ma, L. F.; Liu, B.; Wang, L. Y.; Hu, J. L.; Du, M. *CrystEngComm* **2010**, *12*, 1439-1449. (g) Xu, L.; Liu, B.; Guo, G.; Huang, J. S. *Inorg. Chem. Commun.* **2006**, *9*, 220-222. (h) Zhang, Z. J.; Liu, H. Y.; Zhang, S. Y.; Shi, W.; Cheng, P. *Inorg. Chem. Commun.* **2009**, *12*, 223-226. (i) Zheng, Y. Z.; Tong, M. L.; Chen, X. M. *New J. Chem.* **2004**, *28*, 1412-1415. (j) Zheng, Y. Z.; Zhang, Y. B.; Tong, M. L.; Xue, W.; Chen, X. M. *Dalton Trans.* **2009**, 1396-1406.
10. (a) Shi, X.; Zhu, G.; Fang, Q.; Wu, G.; Tian, G.; Wang, R.; Zhang, D.; Xue, M.; Qiu, S. *Eur. J. Inorg. Chem.* **2004**, 185-191. (b) Che, G. B.; Liu, C. B.; Liu, B.; Wang, Q. W.; Xu, Z. L. *CrystEngComm* **2008**, *10*, 184-191. (c) Luo, F.; Zheng, J. M.; Batten, S. R. *Chem. Commun.* **2007**, 3744-3746. (d) Zhou, Y. F.; Lou, B. Y.; Yuan, D. Q.; Xu, Y. Q.; Jiang, F. L.; Hong, M. C. *Inorg. Chim. Acta* **2005**, *358*, 3057-3064. (e) Cheng, D.; Khan, M. A.; Houser, R. P. *Cryst. Growth Des.* **2004**, *4*, 599-604. (f) Zhang, W.; Bruda, S.; Landee, C. P.; Parent, J. L.; Turnbull, M. M. *Inorg. Chim. Acta* **2003**, *342*, 193-201. (g) Fang, Q.; Zhu, G.; Shi, X.; Wu, G.; Tian, G.; Wang, R.; Qiu, S. *J. Solid State Chem.* **2004**, *177*, 1060-1066. (h) Braverman, M. A.; Supkowski, R. M.; LaDuca, R. L. *J. Solid*

- State Chem.* **2007**, *180*, 1852-1862. (i) Choi, E. Y.; Kwon, Y. U. *Inorg. Chem.* **2005**, *44*, 538-545. (j) Ding, B.; Yi, L.; Liu, Y.; Cheng, P.; Dong, Y. B.; Ma, J. P. *Inorg. Chem. Commun.* **2005**, *8*, 38-40. (k) Konar, S.; Mukherjee, P. S.; Zangrando, E.; Drew, M. G. B.; Diaz, C.; Ribas, J.; Chaudhuri, N. R. *Inorg. Chim. Acta* **2005**, *358*, 29-35. (l) Wang, Y.; Cao, R.; Sun, D.; Bi, W.; Li, X.; Li, X. *J. Mol. Struct.* **2003**, *657*, 301-309.
11. (a) Lin, Z.; Chen, L.; Yue, C.; Yuan, D.; Jiang, F.; Hong, M. *J. Solid State Chem.* **2006**, *179*, 1154-1160. (b) Wang, J.; Lin, Z. J.; Ou, Y. C.; Shen, Y.; Herchel, R.; Tong, M. L. *Chem. A Eur. J.* **2008**, *14*, 7218-7235. (c) Choi, E. Y.; Kwon, Y. U. *Inorg. Chem. Commun.* **2004**, *7*, 942-945. (d) Yang, Y. Y.; Huang, Z. Q.; Szeto, L.; Wong, W. T. *App. Organometallic Chem.* **2004**, *18*, 97-98. (e) Liu, G. X.; Zhu, K.; Chen, H.; Huang, R. Y.; Xu, H.; Ren, X. M. *Inorg. Chim. Acta* **2009**, *362*, 1605-1610. (f) Krishnamurthy, D.; Murugavel, R. *Indian J. Chem. A* **2003**, *42*, 2267-2276. (g) Xu, L.; Choi, E. Y.; Kwon, Y. U. *Inorg. Chem. Commun.* **2008**, *11*, 150-154. (h) Shi, J.; Ye, J. W.; Song, T. Y.; Zhang, D. J.; Ma, K. R.; Ha, J.; Xu, J. N.; Zhang, P. *Inorg. Chem. Commun.* **2007**, *10*, 1534-1536. (i) Xu, Y. H.; Lan, Y. Q.; Shao, K. Z.; Su, Z. M.; Liao, Y. *J. Solid State Chem.* **2010**, *183*, 849-857. (j) Bai, H. Y.; Ma, J. F.; Yang, J.; Liu, Y. Y.; Hua, W.; Ma, J. C. *Cryst. Growth Des.* **2010**, *10*, 995-1016. (k) Xie, L. H.; Lin, J. B.; Liu, X. M.; Wang, Y.; Zhang, W. X.; Zhang, J. P.; Chen, X. M. *Inorg. Chem.* **2010**, *49*, 1158-1165. (l) Zhou, H.; Lin, J. D.; Du, S. W. *J. Mol. Struct.* **2009**, *930*, 49-54.

12. (a) Zhao, L. M.; Li, H. H.; Wu, Y.; Zhang, S. Y.; Zhang, Z. J.; Shi, W.; Cheng, P.; Liao, D. Z.; Yan, S. P. *Eur. J. Inorg. Chem.* **2010**, 1983-1990. (b) Li, X.; Wang, Y.; Ma, Z.; Zhang, R.; Zhao, J. *J. Coord. Chem.* **2010**, *6*, 1029-1037. (c) Zhang, N.; Li, M. X.; Wang, Z. X.; Shao, M.; Zhu, S. R. *Inorg. Chim. Acta* **2010**, *363*, 8-14. (c) Huang, R. Y.; Xu, H. M.; Zhu, K.; Liu, G. X.; Ren, X. M. *Jiegou Huaxue* **2009**, *28*, 1661-1665. (d) Fabelo, O.; Pasín, J.; Cadillas-Delgado, L.; Delgado, F. S.; Yuste, C.; Lloret, F.; Julve, M.; Ruiz-Prez, C. *CrystEngComm* **2009**, *11*, 2169-2179. (e) Liu, H. K.; Tsao, T. H.; Zhang, Y. T.; Lin, C. H. *CrystEngComm* **2009**, *11*, 1462-1468. (f) Majumder, A.; Gramlich, V.; Rosair, G. M.; Batten, S. R.; Masuda, J. D.; El Fallah, M. S.; Ribas, J.; Sutter, J. P.; Desplanches, C.; Mitra, S. *Cryst. Growth Des.* **2006**, *6*, 2355-2368.
13. (a) Ghosh, S. K.; Bharadwaj, P. K. *Inorg. Chem.* **2004**, *43*, 5180-5182. (b) Shi, X.; Zhu, G.; Wang, X.; Li, G.; Fang, Q.; Wu, G.; Tian, G.; Xue, M.; Zhao, X.; Wang, R.; Qiu, S. *Cryst. Growth Des.* **2005**, *5*, 207-213. (c) Sun, Y. Q.; Zhang, J.; Yang, G. Y. *J. Coord. Chem.* **2004**, *57*, 1299-1308. (d) Ruiz-Prez, C.; Lorenzo-Luis, P.; Hernandez-Molina, M.; Laz, M. M.; Delgado, F. S.; Gili, P.; Julve, M. *Eur. J. Inorg. Chem.* **2004**, 3873-3879. (e) Wang, Y. B.; Zhuang, W. J.; Jin, L. P.; Lu, S. Z. *J. Mol. Struct.* **2005**, *737*, 165-172. (e) Hu, M. L.; Zhu, N. W.; Li, X. H.; Chen, F. *Cryst. Res. Tech.* **2004**, *39*, 505-510. (e) Cho, J.; Lough, A. J.; Kim, J. C. *Inorg. Chim. Acta* **2003**, *342*, 305-310. (f) Cao, R.; Shi, Q.; Sun, D.; Hong, M.; Bi, W.; Zhao, Y. *Inorg. Chem.* **2002**, *41*, 6161-

6168. (g) Murugavel, R.; Krishnamurthy, D.; Sathiyendiran, M. *J. Chem. Soc., Dalton Trans.* **2002**, 2, 34-39.
14. Kobayashi, N.; Naito, T.; Inabe, T. *Bull. Chem. Soc. Jpn.* **2003**, 76, 1351-1362.
15. Wang, J.; Lin, Z.; Ou, Y. C.; Yang, N.; Zhang, Y. H.; Tong, M. L. *Inorg. Chem.* **2008**, 47, 190-199.
16. *SAINT*, Version 6.02; Bruker AXS, Inc., Analytical X-ray Systems, 5465 East Cheryl Parkway, Madison, WI 53711-5373, 2000.
17. *SADABS* [Area-Detector Absorption Correction]; Siemens Industrial Automation, Inc.: Madison, WI, 1996.
18. G. M. Sheldrick, *SHELXTL*, University of Göttingen, Göttingen, Germany, 1997.
19. A. L. Spek, *PLATON*, molecular geometry program, University of Utrecht, The Netherlands, 1995.

Publications:

1. Room-Temperature Ionic Liquids: For a Difference in the Supramolecular Synthesis.
Pedireddi, V. R.; **Shimpi M. R.**; Yakhani, J.V.
Macromol. Symp., **2006**, *241*, 83–87.
2. Novel Supramolecular Assemblies of Coordination Polymers of Zn(II) and Bis (4-nitrophenyl) phosphoric Acid with Some Aza-Donor Compounds.
Samipillai, M.; **Shimpi, M. R.**; Pedireddi, V. R.
Cryst. Growth Des. **2007**, *7*, 1791–1796.
3. Supramolecular Architecture in Some 4-Halophenylboronic Acid.
Shimpi, M. R.; Nanappan, S.; Pedireddi, V. R.
Cryst. Growth Des. **2007**, *7*, 1958–1963.
4. Variants in the Molecular Adducts of Benzenhexacarboxylic Acid (Mellitic Acid) with Aza– donor Compounds.
Shimpi, M. R.; Turner, M. Howard, J. A. K.; Pedireddi, V. R. (Manuscript under preparation).
5. A facile route for the synthesis of Gold nanoplates and nanoparticles.
Arora, K. K.; **Shimpi, M. R.**; Pedireddi, V. R. (Manuscript under preparation).
6. Novel Supramolecular Assemblies of Benzenepentacarboxylic acid : A case study of synthesis at low and high temperature molecular assemblies.
Shimpi, M. R.; Pedireddi, V. R. (Manuscript under preparation).

Symposia/Poster presentation:

- RSC-Student Symposium, West India Section, 24–25 September 2004, Bombay, INDIA.
- 35th National Seminar on Crystallography, 22–24 February 2006, National Physical Laboratory, New Delhi–110012, INDIA.
- 36th National Seminar on Crystallography, 22–24 January 2007, University Of Madras, Chennai– 600 025, INDIA.
- 11th BCA/CCG Intensive Course in X-ray Structure Analysis 24th March–2nd April 2007, Trevelyan College, Durham, UK.
- RSC–Student Symposium, West India Section, 19–20 October 2007, Goa University, Goa, INDIA.
- 38th National Seminar on Crystallography, 11–13 February 2009, University of Mysore, Mysore – 570 006, INDIA.
- Indo-US Bilateral Workshop on Pharmaceutical Cocrystals and Polymorphs, 8–11 February 2009, Hotel Regaalis, Mysore–570 006, INDIA.